

# **For Reference**

---


**NOT TO BE TAKEN FROM THIS ROOM**



Ex libris  
UNIVERSITATIS  
ALBERTAEASIS







Digitized by the Internet Archive  
in 2022 with funding from  
University of Alberta Library

<https://archive.org/details/Havskov1978>





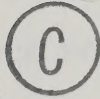




THE UNIVERSITY OF ALBERTA

PLATE TECTONICS AND SEISMIC EVIDENCE FOR MANTLE  
INHOMOGENEITIES

by



JENS HAVSKOV

A THESIS

SUBMITTED TO THE FACULTY OF GRADUATE STUDIES AND RESEARCH  
IN PARTIAL FULFILMENT OF THE REQUIREMENTS FOR THE DEGREE  
OF DOCTOR OF PHILOSOPHY

IN

PHYSICS

DEPARTMENT OF PHYSICS

EDMONTON, ALBERTA

SPRING 78





## ABSTRACT

Paleomagnetic observations, oceanic magnetic lineations and the present continental margins are combined in an interactive computer program to generate maps for seven periods in the Phanerozoic Era . On an azimuthal-equidistant map projection with origin on the centroid of the continental lithosphere the boundaries are seen to display a high degree of symmetry and order. By using geological evidence an attempt is made to model a reconstruction of major plate boundaries in the past. During the Cambrian and Ordovician periods the continental segments were as widely dispersed as at the present and formed a ring of plates on the paleo-equator but with North Africa and South America contiguous and close to the south pole. In these, as in other periods, there is symmetry about the spin axis. Extensive plate motion occurred at about the time of the Caledonian Orogeny when the continental segments evolved toward the formation of a single large group called Pangaea by Wegener . This evolution occupied much of the upper Paleozoic and Mesozoic Eras. Toward the end of the Cretaceous period a more dispersed form began to develop yielding the present pattern of two antipodal quasi-circular plates separated by a ring of more irregular quasi-





elliptical plates. The results suggest the presence of a slowly evolving mantle-wide convection system which is symmetric about the earth's spin axis.

If mantle-wide convection is occurring at the present time then evidence for this should be present in the form of seismic velocity heterogeneities. Seismic observations from many sources have been examined in an attempt to find such effects. The use of differential core reflected travel time residuals is shown to be of value in such studies and was used here. The technique is extended also to include differential values of slowness and azimuth residuals of core reflected phases. The world wide results from this study clearly indicates the presence of lateral inhomogeneities throughout the mantle. A detailed study was possible for rays passing underneath the Caribbean and the Southeast Pacific. Under the eastern part of the Caribbean the upper and middle mantle is dominated by a high velocity zone which changes laterally into a low velocity zone under Central America. There is evidence for anomalous regions extending well below the Benioff zones near Fiji and the New Hebrides Islands. This may be interpreted in terms of subduction continuing into the lower mantle.

In the process of obtaining the best possible slowness and azimuth values, a new method, using only the available array data, was developed to determine the dip and the





strike of the Mohorovicic discontinuity under the array. The method employs the coherencies of body waves in the P coda from both the vertical and horizontal detectors to obtain the slowness and azimuth of the direct and converted wave at the Mohorovicic discontinuity.



## ACKNOWLEDGEMENTS

First of all I wish to thank my supervisor Dr E.R. Kanasewich who originally interested me in the topic of this thesis and provided much help and guidance. He was actively involved in the work resulting in chapter one. The same is the case with Dr M.E. Evans who provided all the paleomagnetic data and did much of the work related to paleomagnetism.

C. McCloughan was a constant help in practical matters, mainly related to computing. He provided several of the programs used.

I would also like to acknowledge my appreciation of the financial support provided by the Department of Physics, the University of Alberta.





## TABLE OF CONTENTS

CHAPTER	PAGE
1. PLATE TECTONICS IN THE PHANEROZOIC .....	1
Introduction .....	1
Basic data and plate tectonic models .....	9
Tertiary period .....	13
Cretaceous period .....	20
Triassic period .....	25
Permo-Carboniferous period .....	31
Devonian period .....	37
Ordovician period .....	41
Cambrian period .....	45
Interpretation .....	49
2. REVIEW OF SEISMIC EVIDENCE FOR LATERAL INHOMOGENEITIES IN THE MANTLE .....	64
Travel times .....	65
Comparison of travel time curves .....	66
P-wave residuals as a function of azimuth .....	67
Inversion of travel time curves in terms of velocity	68
Inversion of travel time residuals in terms of velocity perturbations on a 3 dimensional mantle ...	68
The ray parameter $p$ .....	77
Interpretation of anomalous $p$ -Az values .....	78
$p$ residuals .....	79
3. SEISMIC DATA PROCESSING .....	92
Methods selected for this study .....	92





# TABLE OF CONTENTS

CHAPTER	PAGE
Data base and area studied .....	93
Calculation of p-Az .....	97
Testing and using the covespa program .....	105
4. DETERMINATION OF THE DIP OF THE MOHO BY COVESPA ANALYSIS .....	110
5. MANTLE INHOMOGENEITIES .....	123
Analysis of travel time and p-Az data .....	126
Interpretation of the residuals .....	142
Data from other parts of the world .....	145
Conclusion .....	160
REFERENCES .....	163
APPENDIX 1 .....	176
APPENDIX 2 .....	191
APPENDIX 3 .....	197
APPENDIX 4 .....	201
APPENDIX 5 .....	202



## LIST OF TABLES

Table	Description	Page
2.1	References to lateral inhomogeneities in the mantle. ....	89
3.1	An example of the two cards giving the relevant travel time data. ....	95
3.2	Typical covespagrams for the PcP and P phases. ....	104
3.3	An example of the array response for the 1974 and 1970 arrays. ....	108
3.4	Comparison between a symmetric and an elongated array. ....	109
4.1	An example of covespagrams for P and PS. ....	113
4.2	The array response for a single and a mixture of two phases. ....	115
4.3	The array response for a single and a mixture of two phases. ....	116
5.1	Comparison between differential travel times. ....	127
5.2	The world wide data. ....	148
5.3	Average travel time residuals for the world wide data. ....	150
5.4	Average travel time residuals for data from the southeast Pacific. ....	153
5.5	Maximum scatter in ScS-S travel time residuals for data from the southeast Pacific. ....	156
A1.1	Rotation data and average unrotated paleomagnetic poles. ....	176
A1.2	Comparable statistics for all solutions using paleomagnetic data. ....	181
A1.3	Paleomagnetic data used in reconstructions. ....	183
A2.1	Tables giving the change in the ray parameter as a function of dip and strike. ....	191





## LIST OF FIGURES

Figure	Page
1.1 Azimuthal equidistant projections of the world. ...	3
1.2 An Eckert projection of the world. ....	5
1.3 Model of the continents for the Tertiary period. ..	15
1.4 Tertiary geology. ....	16
1.5 Model of the continents for the Cretaceous period. 21	21
1.6 Cretaceous geology. ....	22
1.7 Model of the continents according to Bullard. ....	26
1.8 Model of the continents for the Triassic period. ..	28
1.9 Triassic geology. ....	29
1.10 Model of the continents at the Permo-Carboniferous boundary. ....	33
1.11 An alternate model for the Permo-Carboniferous. ...	34
1.12 Permo-Carboniferous geology. ....	35
1.13 Model of the continents for the Devonian period. ..	39
1.14 Devonian geology. ....	40
1.15 Model of the continents for the Ordovician period. 43	43
1.16 Ordovician geology. ....	44
1.17 Model of the continents for the Cambrian period. ..	46
1.18 Cambrian geology. ....	47
1.19 The position of the continents in different geological periods. ....	53
1.20 Variation of the latitude of the mean paleomagnetic south pole. ....	54





## LIST OF FIGURES

Figure	Page
1.21 A model of the plate tectonic pattern in the Cambrian period on an Eckert projection. ....	57
1.22 Cross sections of the Earth. ....	61
2.1 ScS and S rays. ....	71
2.2 The ScS and double reflected ScS2 rays. ....	74
2.3 An azimuthal anomaly as seen by the array. ....	80
2.4 An example of an array diagram. ....	82
3.1 Some seismic phases. ....	96
3.2 The locations of the VASA arrays in Alberta. ....	98
3.3 A covespagram showing the arrival of both P and PcP phases. ....	102
4.1 Crustal thickness in Western Canada. ....	112
4.2 The observed differences in slowness and azimuth between the P and PS arrivals. ....	117
4.3 The coordinate system in which the ray vector <u>B</u> is defined. ....	118
4.4 Dipping interface coordiante system. ....	120
5.1 Comparison of differential travel times. ....	125
5.2 Difference in the travel time residuals of ScS-S between the radially polarized componenets and the transversely polarized componenets. ....	128
5.3 All the travel time data used in this study. ....	129
5.4 All the observed differential travel time residuals from the Caribbean area. ....	131
5.5 The array data for rays passing under the Caribbean. ....	132
5.6 Velocity anomalies along the reflected rays. ....	135



## LIST OF FIGURES

Figure	Page
5.7 Velocity anomalies along the direct rays. ....	136
5.8 Correlation plots for the southern Caribbean area.	138
5.9 Correlation plots of shear wave residuals. ....	139
5.10 Correlation plots for the southern United States. .	140
5.11 A summery of all the velocity anomalies along the direct rays. ....	143
5.12 A summery of all the velocity amomalies along the reflected rays. ....	146
5.13 All the rays from the world wide travel time data.	149
5.14 The anomalous world wide ray paths. ....	152
5.15 All the rays originating in the South Pacific. ....	154
5.16 SCS-S travel time residuals for events from the South Pacific. ....	159





## CHAPTER 1

### PLATE TECTONICS IN THE PHANEROZOIC

#### INTRODUCTION

Plate tectonic models of oceanic lithosphere for the Tertiary and Cretaceous periods have been made for the Atlantic ( Pitman and Talwani ,1972), Pacific ( Herron, 1972; Larson and Pitman, 1972; Atwater and Molnar, 1973; Molnar et al, 1975, Cooper et al, 1976), Indian ( Fisher et al, 1971; McKenzie and Sclater, 1971), and Arctic ( Lambert, 1974 ) oceanic areas. These reconstructions using magnetic lineations cannot be continued beyond the Cretaceous - Jurassic boundary because of the youthfulness of oceanic basins and their destruction by subduction. Any further attempts at modelling in the Mesozoic and Paleozoic eras must rely on data from continental crust. However, purely geological evidence does not, in general, permit a unique solution. Some of the ambiguity would be reduced if it were possible to establish the properties of the plates as a function of time and to determine the global dynamic system, often referred to as the driving mechanism. A few properties and principles which may be of value in reconstructing a plate tectonic model at any time in the past have been pointed out by Kanasevich (1976) and these will be tested



and explored using paleomagnetic evidence.

A series of azimuthal-equidistant map projections, centered on each of the plates of lithosphere were used by Kanasewich (1976) to demonstrate a high degree of ordering and symmetry in the major plates at the present time. Major plates cover 9 to 20 % of the earth's surface and are clearly differentiated in size and shape from mini-plates or splinters which cover areas of 3 % or less ( Nasca - 3%: Phillipines - 1.6 %; Arabia - 1%; Cocos - 0.6 %). The lithosphere was shown to be highly organized with two antipodal quasi-circular plates ( African and Pacific ), 120 degrees in diameter, separated by a ring of quasi-elliptical plates ( Fig. 1.1 ). The semi-major and semi-minor axes are defined by triple junctions. The normal Mercator projection distorts the pattern in high latitudes but if the continental outlines are rotated so that the great circle path through the north and south poles and the center of the ring plates becomes the equator in an Eckert projection, the distortion becomes minimal ( Fig. 1.2 ). The Eckert ( Ortelius ) projection has equal spacing of parallels and displays the the entire earth with an approximation to an equal-area projection. The quasi-elliptical plates have their major axes all aligned at about the same angle to the "pseudo-equator". The symmetry inherent in the present pattern and the large dimensions of the major plates (120 degrees as a diameter or semi-major axis) is strong evidence



Figure 1.1 . Azimuthal equidistant projections centered on the African plate and its antipodes in the Pacific plate for the present time (0 my). Note that both quasi-circular plates have a radius of 60 degrees. A ring of quasi-elliptical plates lies at a distance of 90 degrees from the center of the African and Pacific plates.

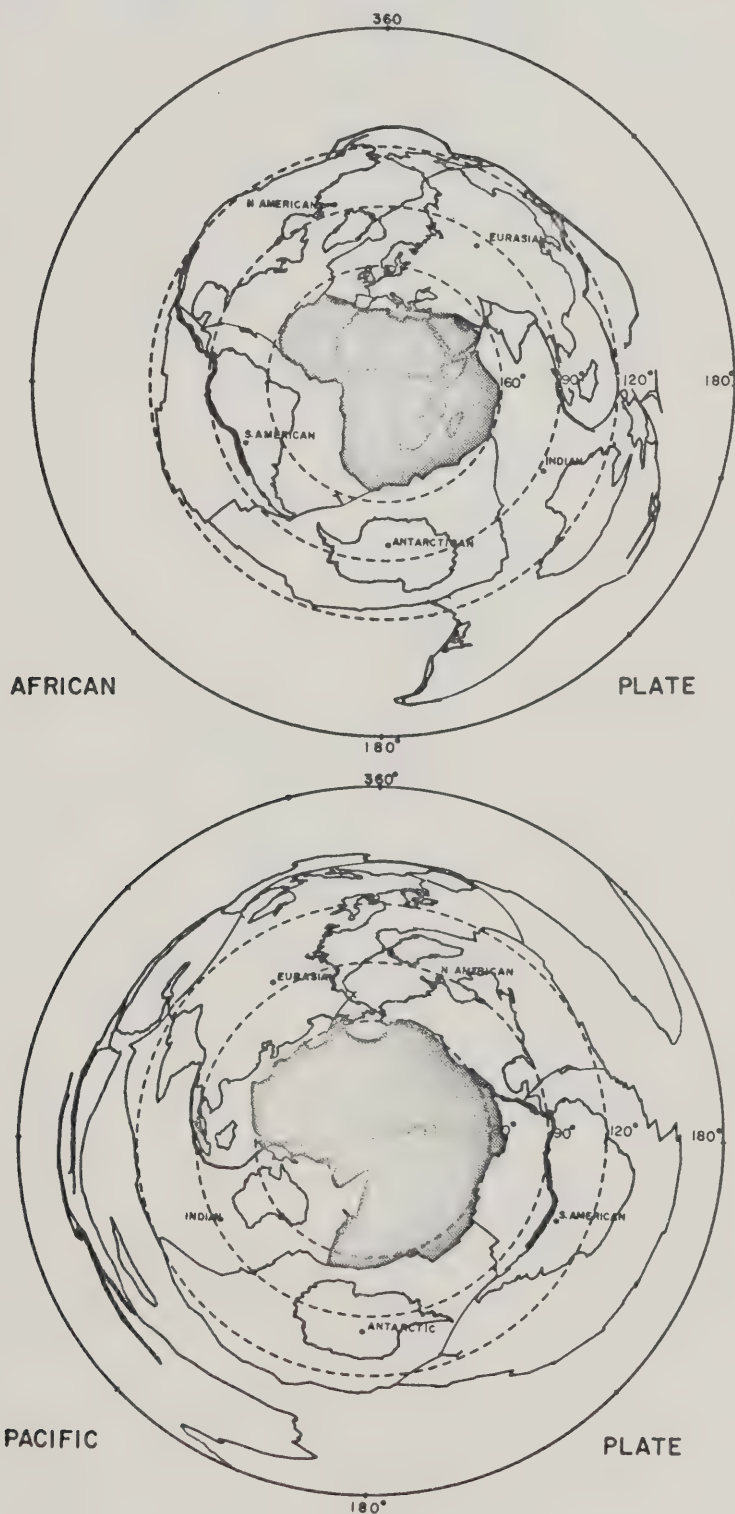
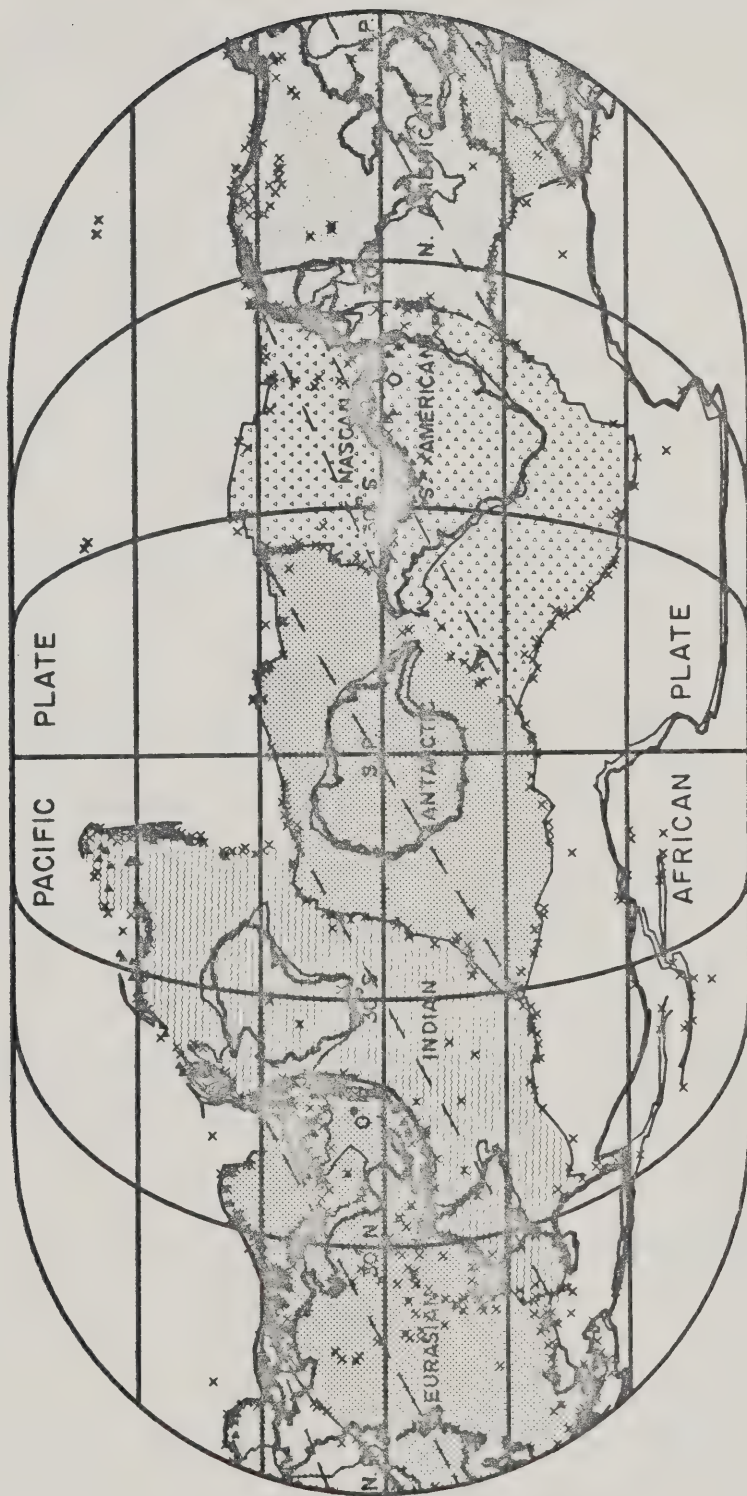








Figure 1.2 . The ring of quasi-elliptical plates at the present time displayed on an Eckert projection. The great circle path (at 90 degrees in figure 1.1) passing through the N and S poles and the center of the ring plates was rotated to form a pseudo-equator in this projection. The orientation of the quasi-elliptical plates is defined by the dashed lines from an African triple junction to a Pacific triple junction. Shallow earthquakes are shown as crosses.



PRESENT - 0 M. Y.





against dynamic systems which produce random plate distributions. The present evidence suggests that the physical properties of the earth may be described in terms of spherical harmonics with dominant terms of order three.

In reconstructing a plate tectonic model for any period some rules or principles should be established. Some of these are absolute and result from restrictions imposed by the geometry of plate motions on a spherical surface. Others are in the nature of postulates made from observations, particularly over the sea floor, at the present time and may not be universally applicable throughout the earth's history. For instance, it is assumed that the plates remain rigid when they interact even though it is known that considerable deformation occurs, particularly when two continental plates collide as along the Alpine and Himalayan mountain chains. These continental interactions, and others like the transcurrent motion along the San Andreas or Great Glen fault systems involve minor amounts of crust and are assumed to be second order effects when considering the global results of continental drift. The following principles will be observed as closely as possible in obtaining the models for each period.

1. The major tectonic features of the earth may be described by the interaction of six to nine uncoupled rigid plates of lithosphere with



dimensions 60 to 120 degrees (Elsasser, 1969; Le Pichon, 1968; Kanasewich, 1976).

2. The plates are created and destroyed along ridges and trenches respectively (Vine and Matthews, 1963; Hess, 1962; Oliver and Isacks, 1967; Isacks et al, 1968).

3. Transform faults conserve lithosphere and are lines of slip between two plates. They lie on small circles centered on the pole of relative motion between two plates (Wilson, 1965; McKenzie and Parker, 1967).

4. The poles of rotation between pairs of plates is relatively stable for long periods of time (Morgan, 1968; McKenzie and Parker, 1967).

5. An absolute reference frame for plate kinematics is defined, to a good approximation, by minimizing the translational motion of plate boundaries. The velocity of plates is inversely proportional to the amount of continental lithosphere they contain. Purely oceanic plates move about 5 times faster than purely continental plates which, at the present time move at about 1.5 cm./year (Minster et al, 1974; Kaula,



1975).

6. The continental lithosphere extends to the 500 fathom contour along coast lines ( Bullard et al, 1965).

7. Continental crust, by virtue of its buoyancy is not destroyed in any significant amount along plate margins ( McKenzie, 1969).

8. A eugeosyncline is direct evidence for a trench and a subduction zone. Miogeosynclines and zones of diastrophism are secondary lines of evidence for the near-by presence of a subduction zone ( Dewey and Bird, 1970).

9. The continuing presence of a seaway or an ocean throughout more than one geological period is taken as direct evidence for the occurrence of sea floor spreading and the presence of a ridge system.

10. The geomagnetic field has always been dominated by a dipole component and, when averaged over the order of  $10^6$  years, the axis of the dipole coincides with the rotation axis of the earth ( Torreson et al, 1949; McElhinny and





Merrill, 1975; Evans, 1976).

## BASIC DATA AND PLATE TECTONIC MODELS

Various reconstructions of the continents have been made previously using Euler's theorem which states that any line on the surface of a sphere may be moved to another position and orientation by a single rotation about an axis passing through the center of the sphere. Notable examples are by Bullard et al (1965) and Smith and Hallam (1970) who used the fit of the continental margins to obtain a Triassic model. Smith et al (1973) made extensive use of paleomagnetic data to model continental positions during several periods. We are able to draw upon much new paleomagnetic data and also the dating of magnetic lineations on the sea floor in obtaining new computer assisted reconstructions of the continental margins for seven periods. The paleomagnetic data used is that summarized by Irving (1960a,b, 1961, 1962a,b, 1965), Irving and Stott (1963) and McElhinny (1968a,b, 1969, 1970, 1972a,b) and summarized by McElhinny (1973). In addition, we used a computer file, referred to here as the Ottawa list, compiled under the direction of E. Irving at the Earth Physics Branch, Department of Energy, Mines and Resources, Ottawa . Data were also obtained from a recent compilation by



McElhinny and Cowley (1977). Finally , in some cases very recently reported data were taken directly from the publications involved.

All of the paleomagnetic data actually used is tabulated and commented upon when discussing the appropriate continental reconstruction. A standard format is employed for tabulating the data used in each of the seven reconstructions ( Tables 1 and 3, Appendix 1 ). For each continental segment Table 1 gives the number of poles available, their age range, the latitude and longitude of their mean, and the associated statistical parameters  $K$  and  $A_{95}$  ( Fisher , 1953). This latter parameter is the semi-angle of the cone within which the mean lies with 95% confidence. The precision parameter  $K$  is analagous to the invariance of a Gaussian distribution and thus increases as the poles are more tightly grouped. It is given by  $K = (N - 1)/(N - R)$ , where  $N$  is the number of poles involved (treated as unit vectors) and  $R$  is their vector resultant. As a rough guide values of  $K$  greater than 20 can be regarded as indicating "good" grouping.

The number of separate continental segments for which data is available ranges from 8 for the Devonian and Ordovician to 13 for the Tertiary and the Triassic . The number of poles involved ranges from 35 ( Cambrian ) to 94 ( Carboniferous ) with an overall total of 436. The magnetic





lineations were determined by digital sampling of maps produced by Pitman et al (1974). Data on zones of glaciation, paleontology, and lithology were used to establish that polar and equatorial regions for each period agreed with the geological interpretation.

An interactive computer program was developed to rotate the continental segments about any pole of rotation. The paleomagnetic results were used initially to position each continental segment on the appropriate latitude and in the correct orientation so that all averages of measured poles were exactly on the south pole. It was found to be most convenient , at this stage, to initiate an interactive routine which modified the positions to eliminate overlap of continental margins while monitoring the results on a display device. For the Tertiary and Cretaceous periods the magnetic lineations were used to establish relative longitude. For all periods the absolute longitude was obtained from an application of the fifth principle (see above).

The sum of the square of the velocities of equal area portions of all continental blocks was minimized in a least squares sense to determine longitude. When the relative longitude could not be obtained from magnetic lineations , the largest contiguous continental group was given priority since present evidence indicates that purely



continental plates have the lowest velocity. The velocity was determined along a small circle, centered on the pole of relative motion from one period to the next.

This procedure was applied, in order of area, to the remaining group of continental segments. The solution is not unique but is the most conservative estimate and is valuable in giving a quantitative estimate of the minimum velocity which satisfies the paleomagnetic observations.

The models for each period have been generated by a digital computer and a Calcomp plotter on a Mercator projection because of its familiarity. More specifically the projection is a Miller modified Mercator one in which the map ordinate is  $y = c \ln \tan (45 + 0.4 \text{ lat})$  where lat is the latitude in degrees and  $c$  is a scaling constant. This modification allows one to depict the earth from pole to pole. For purposes of interpretation an azimuthal-equidistant projection with the origin approximately on the centroid of the continental masses is more useful. This projection has the property that great circle paths from the origin to any point on the sphere transform into straight lines from the center of the projection. Regions at epicentral distances less than 90 degrees have minimal distortion. At greater distances the azimuthal distortion becomes serious, reaching a maximum at 180 degrees, where a point on the opposite side of the earth from the origin is



transformed into the bounding circumference. The distorted portion is, of course, conveniently placed on the ocean dominated portion of the earth.

### Tertiary Period - Anomaly 13 - 38 MY

Magnetic lineations for anomaly 13 ( Pitman et al, 1974) were matched to give the relative positions of the continental blocks for the Oligocene - Eocene boundary 38 my ago ( Heirtzler et al, 1968; Anonymous, 1964) ( Fig. 1.3 ). Paleomagnetic observations were not used to determine any of the relative rotations but the mean pole position ( for all observations listed in Table 1 of the Appendix 1 and shown on the diagrams ) was used to obtain the absolute position of the spin axis in the Tertiary. The absolute longitude for all continents was obtained simultaneously by minimizing the velocity of 3 by 3 degree equal area continental segments between the time of anomaly 13 and the present. This simple procedure gives a solution which compares very well with reconstructions of the east central Indian Ocean by Sclater and Fisher (1974); the North Pacific by Atwater (1970) and Atwater and Molnar (1973); the North Atlantic by Pitman and Talwani (1972 ). Note that the position of magnetic anomaly 13 off the coast of North America relies heavily on the superposition of a very short segment east of Cape Horn in South America.







Figure 1.3 . The position of the continents at the time of magnetic anomaly 13 ( Eocene - Oligocene boundary ) on an azimuthal equidistant projection and a Miller -modified Mercator projection. Arrows indicate the trajectory of the plates between 38 my ago and the present on a minimum velocity assumption. The velocity vectors are placed at points where the continents have a minimum and a maximum plate velocity. Mean paleomagnetic poles and their 95% confidence circles are shown. N and S indicate the north and south poles.











The paleomagnetic data used is summarized in Tables 1 and 2 of the Appendix 1. A total of 66 poles from 13 continental segments is involved. For the most part, these data are summarized by McElhinny (1973), with updated results for India from Wensink (1975), and data for Siberia from the Ottawa list. In this latter case only the most reliable results, that is those awarded two stars by Irving et al, have been considered. The poles from within any given continental segment are generally well grouped, with values of Fisher's precision parameter (  $K$  ) ranging from 26 to 84. Exact ages cannot be associated with all the poles in question and inevitably the paleomagnetic sampling represents a much broader time interval than that associated with the production of anomaly 13. Forty-three of the 52 poles lie in the interval Paleocene to Oligocene (65 - 23 my), but the overall range is from upper Cretaceous to Pleistocene ( see Tables 1 and 2 of the Appendix 1 for details).

Because the measured pole positions were not used in determining the relative position of the continental segments the paleomagnetic results are an independent verification of principle 10 for the Tertiary period. Fisher's precision parameter,  $K$ , may be used to quantify the agreement. If the continents are restrained to their present day geographic locations, the  $K$  value is 21. The precision parameter increases to 30 if the continents are



placed on the positions indicated by the magnetic anomalies on the sea floor. Despite the disparity in ages of the samples involved, the increase in precision passes the standard test for the ratio of the two K values ( McElhinny , 1964) at the 80% significance level.

Eocene and Oligocene global geology is summarized in figure 1.4 which shows the mid- Tertiary earth on an azimuthal-equidistant projection centered on the mean of the continental segments and also centered on the opposite side in the Pacific Ocean . The summary maps and world-wide correlation charts of rock formations by Kummel (1970) were the primary source of information but many other maps were consulted throughout this study. The mid-oceanic ridges were obtained from the position of anomaly 13, 38 my ago. The position of the subduction zones was inferred from the geologic evidence. Episodes of volcanism in western South America occurred in the Miocene and Pliocene ( Harrington, 1962) and it is possible that the Phoenix ( Larson and Chase , 1972) and South American plates were not separated by a subduction zone prior to the late Eocene. In post- Eocene times this plate separated into the slow moving, dominantly continental, South American plate and the fast moving, predominantly oceanic Nascan plate. The present remnants of the Farallon plate ( McKenzie and Morgan , 1969 ) are the Cocos and Juan de Fuca plates. The parts of continents having the maximum and minimum velocities for their small



circle paths between the Tertiary and the present time are shown on the figures. It must be emphasized that the velocities and paths are not unique and represent minimum estimates.

It was noted in figure 1.1 that the African and Pacific quasi-circular" plates are symmetrically located with respect to the geographic pole at the present time. This same symmetry of the African and Pacific plates is evident in the Tertiary period. The equator passes close to the center of these two plates and also the center, C , of the entire continental lithosphere. The diameters of the African and Pacific plates are 100 and 120 degrees respectively. The group of "ring" plates consists of (1) South America and Phoenix , (2) Antarctica , (3) Australia , (4) India , (5) Eurasia , and (6) North America . The maximum velocity of the continental plates, under the assumption that simultaneous minimization of all segments yields absolute longitude, varies from 8.6 to 0.4 cm/yr ( Table 1, Appendix 1 , and Figure 1.3 ). The Indian plate moves northward with a velocity of 5.9 to 8.6 cm/yr while the next most rapid plate is the Australian with a northward velocity of 4.5 to 6.6 cm/yr. This is in accord with present day observations that plates with a high ratio of oceanic to continental crust move most rapidly. Since Antarctica is almost surrounded by spreading centers it's movement is geometrically restricted to between 0.5 and 1.6 cm/yr.





Associated with the "ring" plates are minor segments in the Mediterranean and the Caribbean seas and the Kula and Juan de Fuca plates. These fragments are of great interest to studies of local geology but are unlikely to be a significant part of the boundary conditions which determine the dynamics of the global system. In summary the plate tectonic pattern in the Tertiary period was similar to what is seen at the present time.

#### Cretaceous Period - Anomaly M1 - 110 MY

Paleomagnetic observations were used to make a preliminary model of the continental arrangement at the base of the upper Cretaceous, 110 my ago. A minor separation of South America and Africa is necessary to satisfy the available magnetic lineations for anomaly M1. The solution in figure 1.5 is very similar to that of Smith et al (1974). The position of the magnetic lineations in the Pacific relative to the North and South American continents were taken from figure 1.7 of Larson and Pitman (1972). Their model used both paleomagnetic poles and the position of anomaly M1 from Larson and Chase (1972) to obtain a convincing demonstration for the existence of two stable triple junctions which separated the Pacific, Kula, Farallon and Phoenix plates. New Zealand, the Auckland Plateau and New Caledonia have been rotated toward Antarctica and south-east Australia in accordance with the magnetic lineations



Figure 1.5 . Model of the continents for the Cretaceous period at the time of magnetic anomaly M1 . The longitude is not absolutely determined but was obtained by a least squares minimization of continental velocities between the Cretaceous and Tertiary periods. The upper figure shows that the Laurasian poles form a separate group from the Gondwana poles.

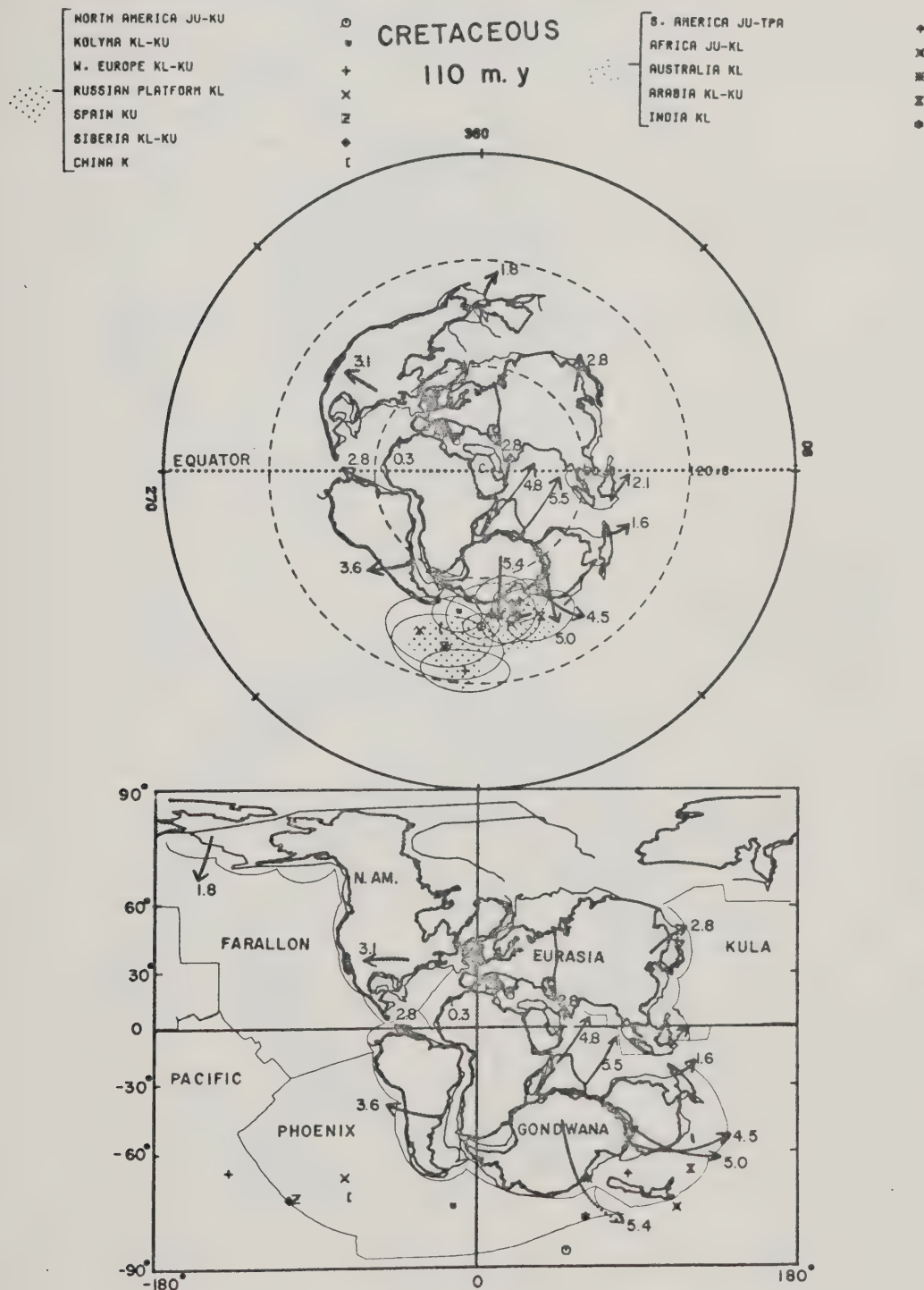
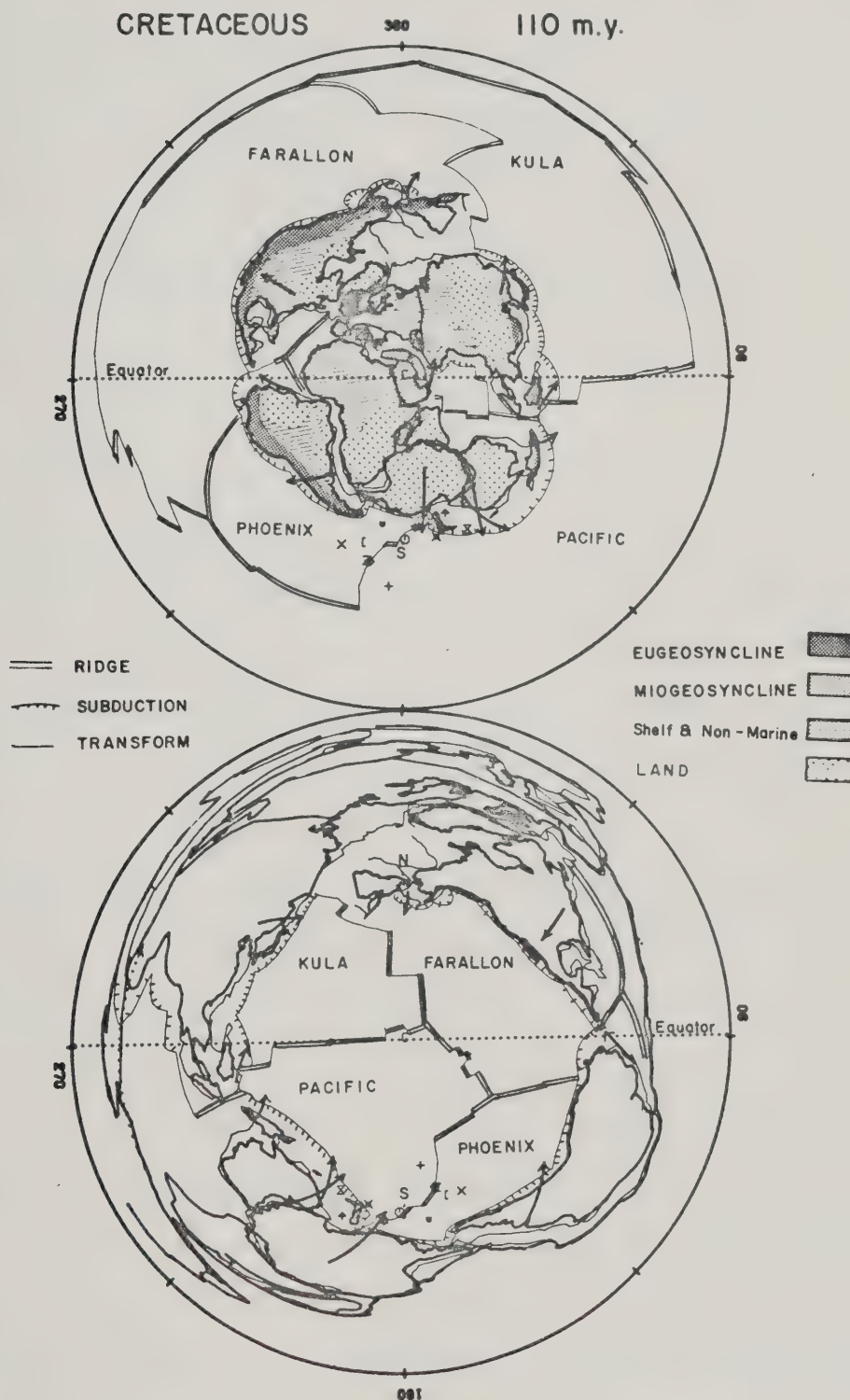




Figure 1.6 . Cretaceous geology and postulated plate boundaries on an azimuthal equidistant projection. The double set of triple junctions in the Pacific is shown with minimal distortion in the lower diagram.







which show the area starting to separate at the base of anomaly 32, 76 my ago. The Kolyma block has been detached from Siberia along the Chersky foldbelt following the geological evidence reported by Churkin, (1969,1972) although the paleomagnetic evidence is ambiguous for this period. The preservation of magnetic lineations M1 to M13 (about 110 to 130 my ago) in the Bering Sea basin (Cooper et al, 1976) is strong evidence that Alaska and the Kolyma block have remained a single block throughout this critical period.

Fifty-six paleomagnetic poles from 12 separate continental blocks were used and K values vary from 15 to 114 (table 1, Appendix 1). Fifty-two of these poles are Cretaceous in age, 3 are listed as Lower Cretaceous to Upper Jurassic and 1 has a quoted age range of Upper Jurassic to Paleocene. Most of the data is summarized by McElhinny (1973) with additions from lists XIII and XIV. Newly reported poles permit tighter temporal constraints to be placed on the African data, and the Australian data is that reported by Schmidt (1976).

Fisher's precision parameter increases from 7, for no continental drift between the present and the Cretaceous, to 21 for the model shown in figure 1.5. This increase is significant at the three standard deviation (99%) level. The distribution is not as concentrated as in the Tertiary and,



in fact, the poles for the northern group of continents ( Laurasia ) are clearly separated from the poles of the southern group ( Gondwanaland ) . Any attempt to superimpose the two sets of pole positions leads to substantial overlap of Africa and Eurasia . This pattern of pole clustering will be found to be present throughout the Mesozoic and Upper Paleozoic Eras. Its existence in the Permo - Triassic was reported by Briden et al (1970) . It can be accounted for by the presence of a small non-axial multipole component in the earth's magnetic field in addition to the dominant axial dipole component.

On an azimuthal-equidistant projection the continental lithosphere for the Cretaceous period displays a most remarkable symmetry. All the continental segments are within 90 degrees of their centroid which lies on the paleo-equator. The Tethyan sea lies opposite the opening in the North Atlantic Ocean forming the North American and Canary basins. Eugeosynclines form a rim nearly all the way around the block of continental lithosphere in figure 1.6 . It is apparent that the four oceanic plates ( Farallon, Phoenix, Kula and Pacific ) generated from the twin sets of ridge-type triple junctions produced active subduction zones around Pangaea . The spreading center which had created the Tethys sea was weak and beginning to change character towards the end of the Mesozoic Era . The geometric arrangement of the spreading centers and the symmetry of



the continental lithosphere is considerably different from that of the Tertiary and the present time. The velocity vectors showing continental velocity along small circle paths are dominantly outward from the African plate. The velocity of all continental segments are very uniform; excluding Africa, the minimum and maximum velocities vary from 2 to 5 cm/yr ( Table 1, Appendix 1 ). A spreading center between South America and Africa is starting to separate these two continents. Although more subdivisions are beginning to be apparent, there are basically only three large continental plates, Gondwanaland, North America and Eurasia opposite the four large oceanic plates.

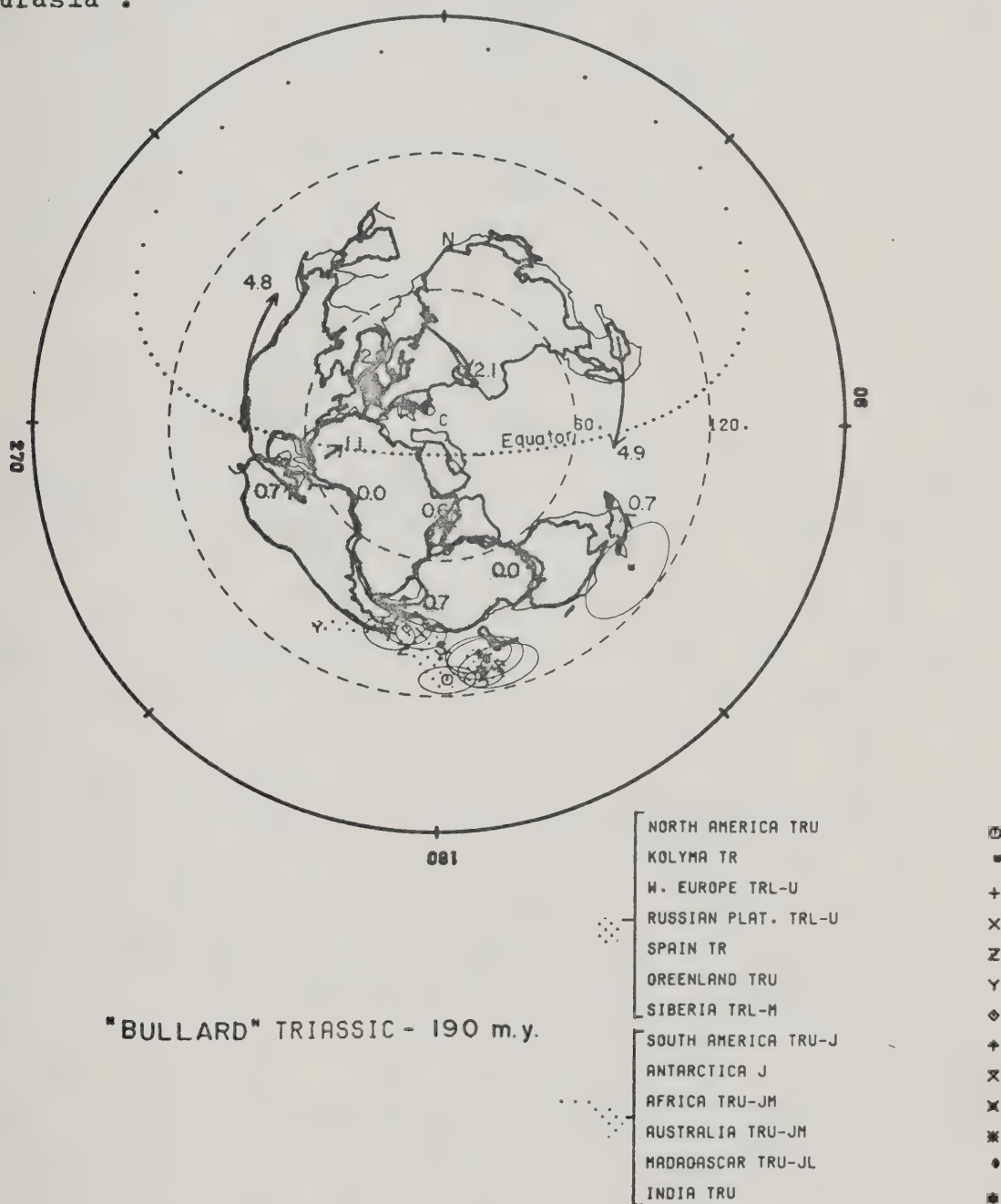
#### Triassic Period - 190 MY

As a standard for comparison the well-known reconstructions by Bullard et al (1965) and Smith and Hallam (1970) were used without modification to produce the supercontinent of Pangaea ( Wegener, 1929). Their solution minimizes the mean square misfit of the longitude, relative to the pole of rotation, of the continental margin. The mean position of the south pole was obtained from paleomagnetic data as shown in figure 1.7 and in Table 1 of the Appendix 1. The mean age of these data is 190 my on the Jurassic - Triassic boundary. The pole for Kolyma diverges widely from the mean and was not included. This problem will be discussed later. A total of 90 paleomagnetic poles from 13





Figure 1.7 . Model of the continents according to Bullard et al (1965) and Smith and Hallam (1970) on an azimuthal equidistant projection. The velocities in cm/yr are based on a least squares minimum velocity assumption between the Triassic and Cretaceous . The separate group of Laurasian and Gondwana poles are indicated. The Kolyma pole misfits as badly if Kolyma is included with North America or Eurasia .





continental segments is available and Fisher's precision parameters range from 31 to 111. For the northern continents the data are essentially that described by McElhinny (1973) but for Gondwanaland the recent summary by Schmidt (1976) has been used. In the former case only Triassic data are involved, but Schmidt includes some Jurassic poles in his compilation. Omitting Kolyma, Fisher's precision parameter increases from 4 for no continental drift between the present and the Triassic to 28 for the model shown in figure 1.7.

The reconstruction of Bullard and others has been criticized because it conflicts with geological evidence in the overlapped portion of Central America (McBirney and Bass, 1969; King, 1970; Ladd, 1976). Following the principles established in the introduction the interactive computer program allows one to arrive at a solution which does not overlap portions of Central America which have outcrops of Triassic or older rocks. The alternate Triassic model is shown in figure 1.8. Fisher's precision parameter increases from 4 for the case of no continental drift to only 21 for this model but the increase is still significant at the 99.9% level. A better fit of the paleomagnetic data can only be constructed by overlapping continents as was done in figure 1.7. Our solution is preferred to the one by Bullard et al (1965) not only because there are no objectionable overlapping portions but because our



Figure 1.8 . Our model of the continents for the Triassic period. The Kolyma pole (W) has a good fit if Kolyma and possibly Alaska are at the same latitude as Japan (shown dotted). W is the position of the Kolyma pole for the dashed outline. Note that Central America does not overlap South America as in figure 1.7.

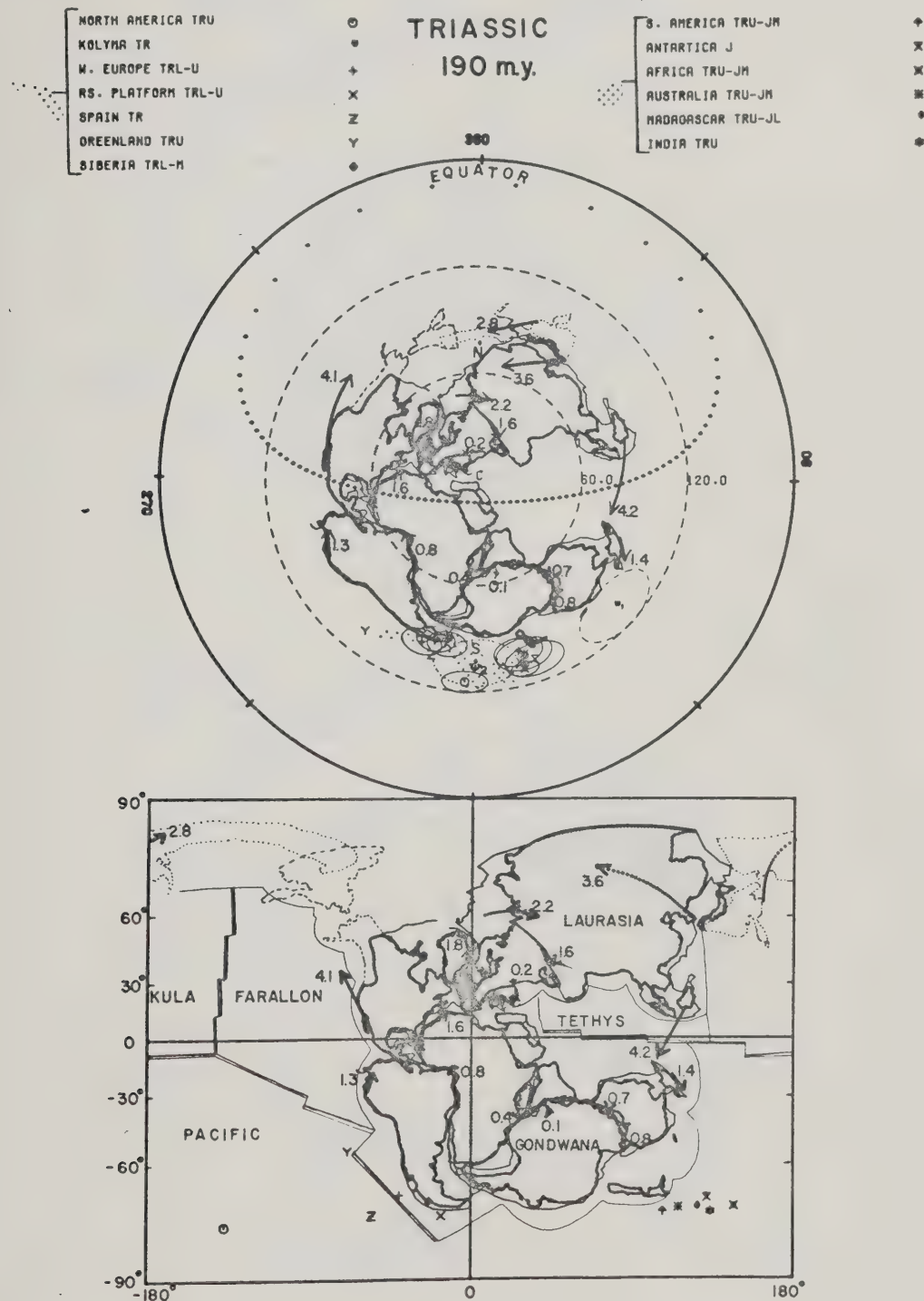
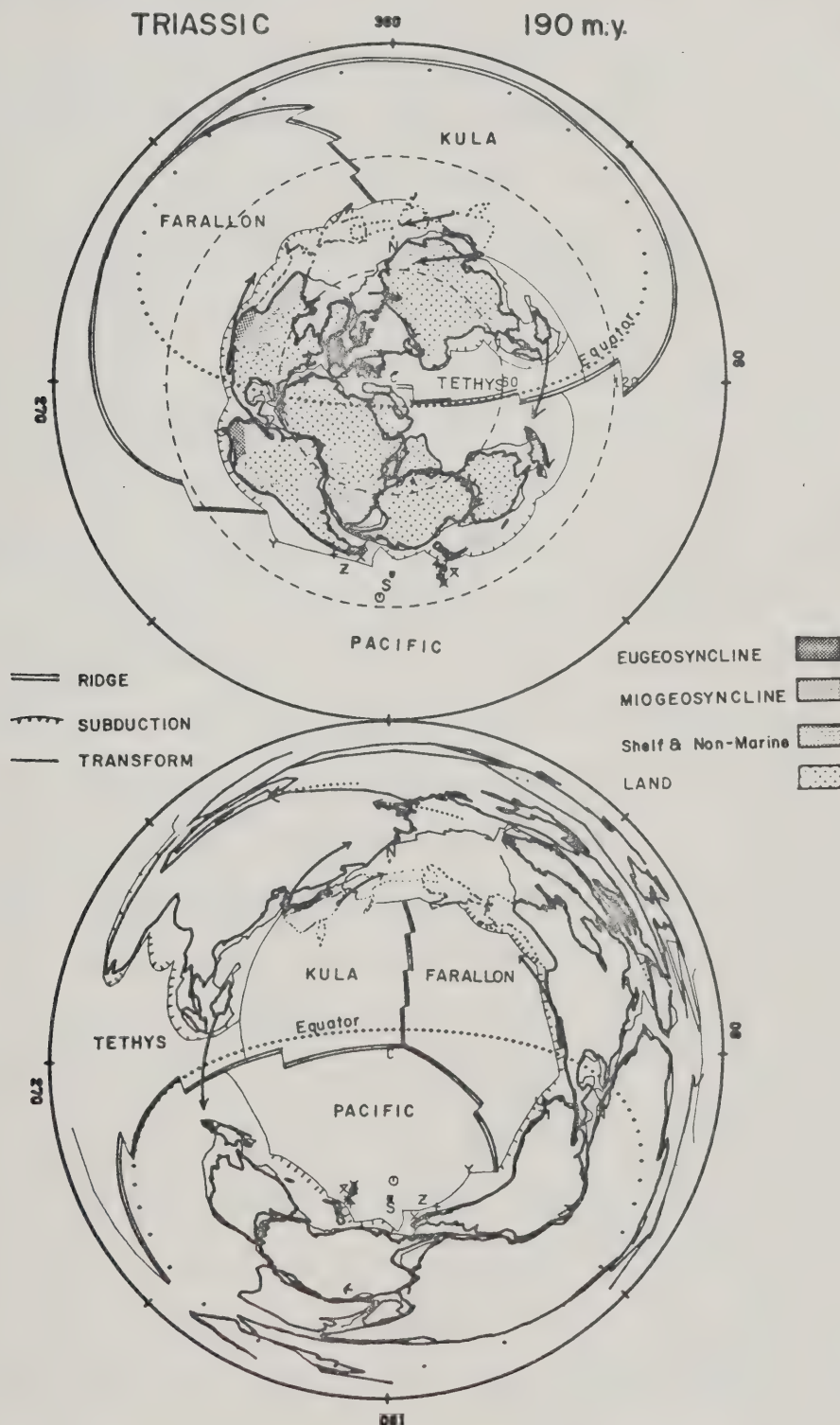






Figure 1.9 . Triassic geology and postulated plate boundaries on an azimuthal equidistant projection. The triple junction in the Pacific is hypothetical but reasonable on the basis of eugeosynclinal deposits, interpreted as due to subduction zones, around the periphery of the Pacific Ocean .





reconstructions for the Paleozoic Era indicate that Pangaea did not continue to exist but consisted of two or more continents that moved independently. There are two main changes over the previous solution. (1) North America and Eurasia have been shifted away from Africa to eliminate any overlap of Central America with Precambrian and Paleozoic outcrops. (2) Kolyma and Alaska have been detached from North America and rotated into a position in accord with the Triassic paleomagnetic data. This second alternative is the more uncertain. Not only is it difficult to know where Alaska and British Columbia should be separated from North America but also the longitude cannot be determined unambiguously. The geological evidence is also ambiguous. Kolyma and Alaska will be kept together with North America in producing models for more ancient periods because the modifications, if required, are easily visualized. Two of the possibilities for the Kolyma group are dotted in figure 1.8. The absolute longitude for Pangaea was obtained using the least square solution for velocity between 190 and 110 my years ago. The paths of finite rotation along small circles were similarly obtained non-unique minimum estimates. From the sparse data on M type magnetic lineations it is unlikely that there is a large longitudinal shift so the velocities given are probably close to their true value. It is seen that the large continent of Gondwana has a velocity less than 1 cm/yr between the Triassic and the Cretaceous periods. On the other hand, parts of Laurasia



have velocities of 2 to 5 cm/yr in the form of a rotation which opens up the Atlantic Ocean and closes the Tethys Sea . As in the Cretaceous period, the pole positions form two distinct populations and any attempt at superimposing them leads to a greater degree of continental overlap.

Geological information has been included on the new Triassic model in figure 1.9 and an attempt is made to sketch in the ridges and subduction zones. The continental grouping is not as symmetric as in the Cretaceous period but the same basic pattern is evident. The equator is close to the centroid of the two continental plates of Laurasia and Gondwana . Plates dominated by oceanic lithosphere are Kula, Farallon, Pacific and Tethys . The tectonic activity does not seem to demand more than 6 or 7 large plates. At least one ridge-type triple junction is required in the Pacific and one section of the ridge follows an equatorial path to produce the Tethys Sea . If the Pacific ridge-type triple junction is stable then the subduction zones that result on the periphery of the continental margins may effectively keep Pangaea as a stable entity for several geological periods.

#### Permo - Carboniferous Period - 280 MY

Ninety-four poles are available but these represent only 10 continental fragments. With the exception of India





the K values lie between 25 and 178, and all but one of the poles are Carboniferous or Permian (see Table 1, Appendix 1). The data is as summarized by McElhinny (1973), except for South America (Thompson, 1972), Australia (McElhinny and Embleton, 1974), and India (Wensink 1975). In this last case 5 poles are listed and they are poorly grouped ( $K = 9$ ). Rather than attempt any more or less arbitrary rejection of data we have chosen to simply average the poles and let the large error circle reflect the lack of precision for India during this time interval.

The arrangement of North America and Europe relative to Africa and South America must be different from that in the Triassic. Consequently it must be assumed that the "optimum" fit achieved by Bullard et al (1965) and Smith and Hallam (1970), in so far as it ever existed, was a transitory phenomenon. As in the Triassic, a limiting case for the absolute longitude was obtained by using a least squares solution on Pangaea as a whole for a minimum velocity between 280 and 190 million years ago. Much of the velocity is taken up by a general northward drift of Pangaea and is under 4 cm/yr for all continents. The Tethys sea was consistently wider as we proceed to earlier periods. The south pole is centered on the well-known zone of glacial deposits and erosional features of eastern South America, southern Africa, Antarctica, India and Australia. As in the Mesozoic Era the pole positions for Gondwana and Laurasia



Figure 1.10 . Model of the continents at the Permo - Carboniferous boundary. The Laurasian and Gondwana poles form two separate groups. The velocity vectors in cm/yr are minimum estimates from the Permo - Carboniferous to the Triassic periods.

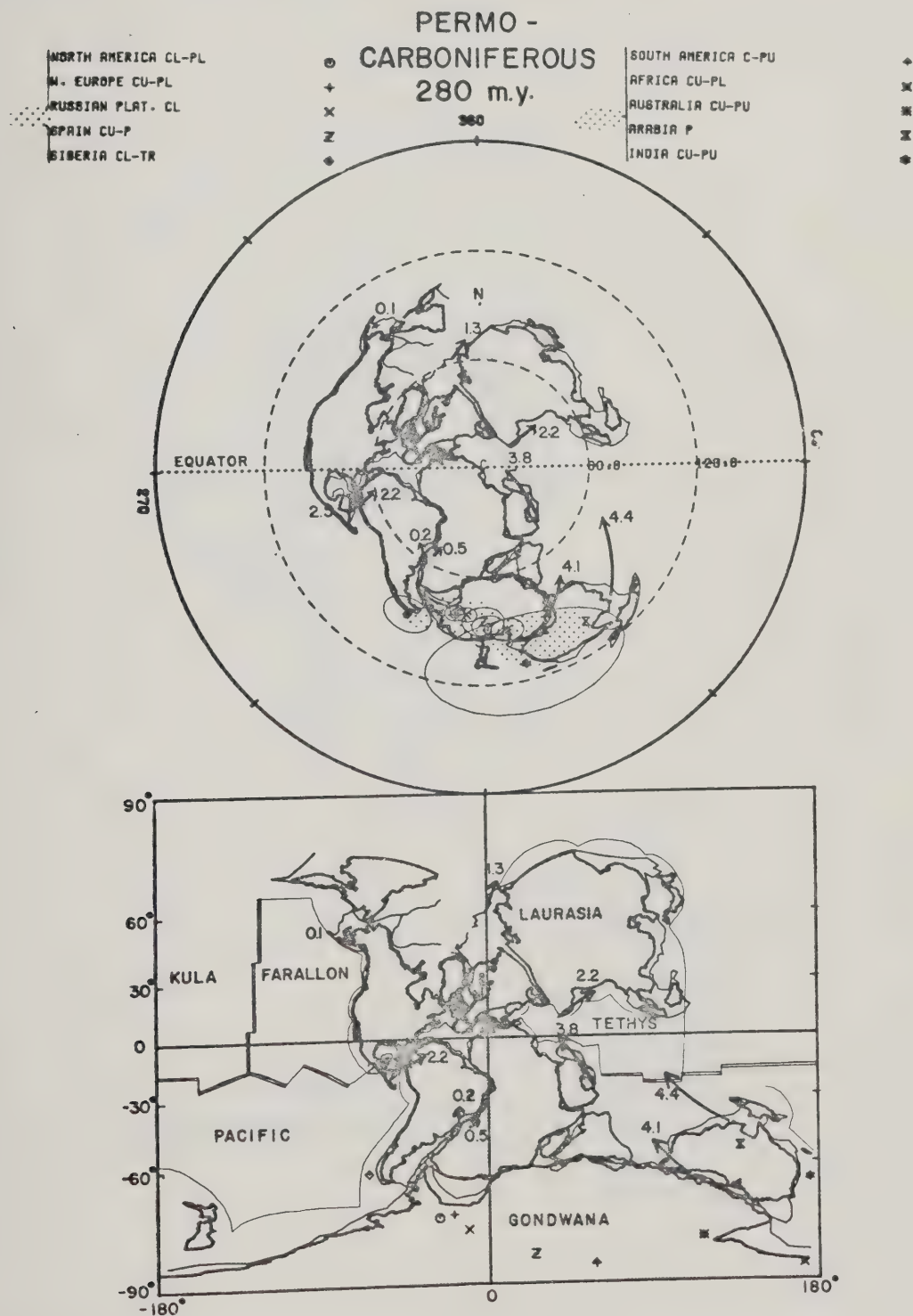




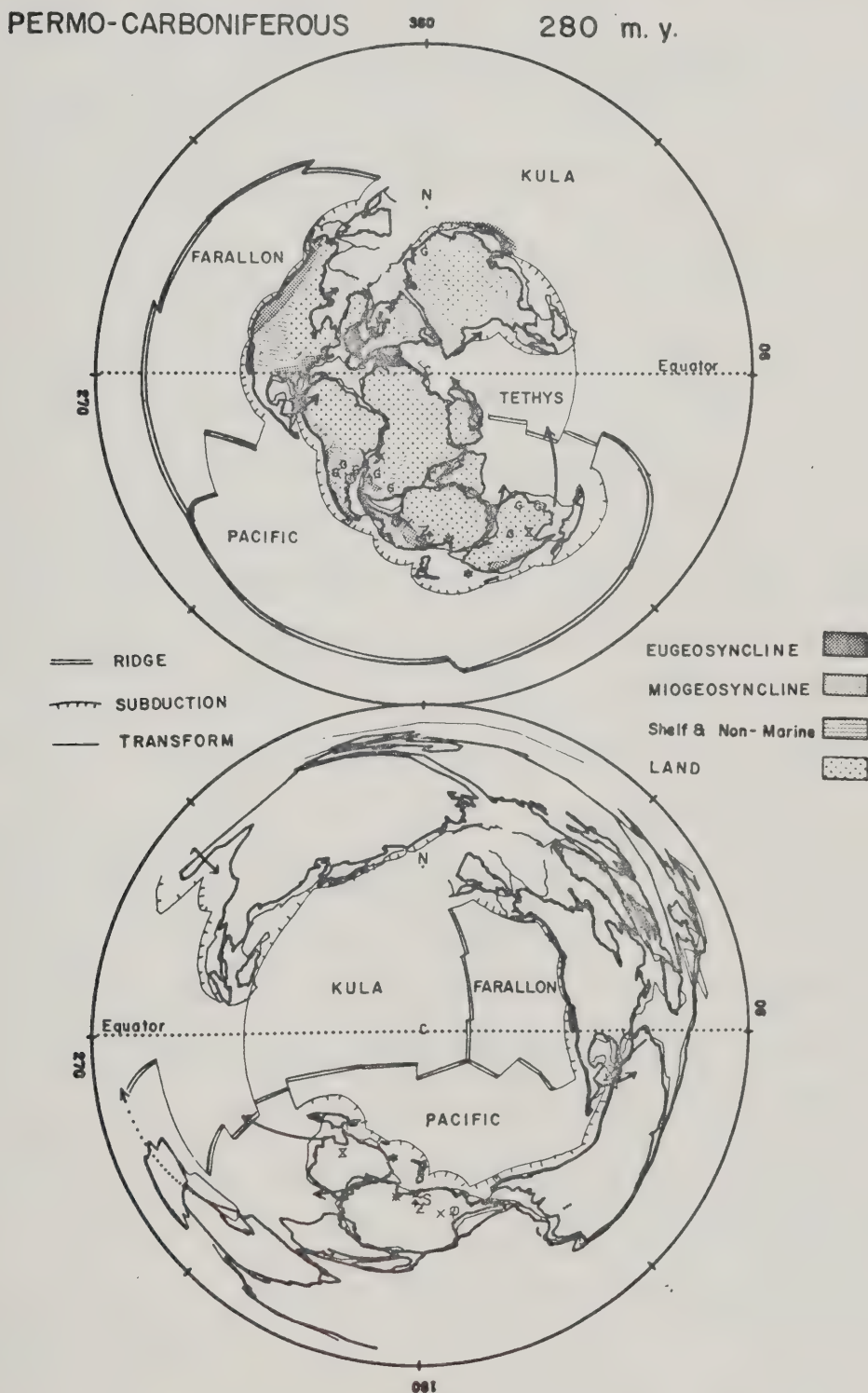
Figure 1.11 . An alternate computer model for the Permo - Carboniferous in which the Antarctic Peninsula is west of South America . Based solely on paleomagnetic data this model is equally probable in the Mesozoic Era but is less probable in the Devonian and older periods.







Figure 1.12 . Permo - Carboniferous geology and postulated plate boundaries on an azimuthal equidistant projection. The locations of glacial indicators are denoted by G .





form two distinct populations in the upper Paleozoic and they cannot be superimposed without a large amount of continental overlap ( Fig. 1.10 ). Fisher's precision parameter, (  $K$  ), increases from 3 for no continental drift between the present and the Permo - Carboniferous to 18 for the model shown in figures 1.13 and 1.14. This is significant at the 99.9% confidence level.

In the course of computerized modelling an alternate fit of Antarctica and South America against Africa was arrived at ( Fig. 1.11 ). Fisher's precision parameter increases from 3 for no continental drift between the present and the Permo - Carboniferous to 19 for this model. A similar reconstruction of Gondwanaland has been proposed by Barron et al, (1977) and it has a precision parameter of 16 ( Table 2, Appendix 1 ). However their model places Madagascar east of Mozambique and there is an oceanic gap between Africa and India . The basic reconstruction of South America, Antarctica and Africa in figure 1.11 was applied to paleomagnetic data from the Cretaceous to the Cambrian periods. The results are summarized in Table 2, Appendix 1 . In general one cannot favor the traditional Bullard or the alternate one because both are equally probable in a statistical test for the Mesozoic Era. However, for the major part of the Paleozoic Era the more traditional solutions we offer are significantly better at the 60 to 90% confidence level.



Global geological data is superimposed in figure 1.12 together with postulated subduction zones and ridges. The pattern is similar to that in the Triassic although the symmetry of the continental blocks is distorted by the widening of the Tethyan seaway. Continental collision is the dominant form of interaction and is assumed to be the cause of the final phases of the Appalachian Orogeny in North America, the Hercynian Orogeny in Europe and northwest Africa, and the Uralian Orogeny between the Baltic and the Angaran cratons. The continents of Laurasia and Gondwana must be treated as two or more interacting plates. Subduction of oceanic plates is assumed to be responsible for the Kanimblan Orogeny in Australia, and the Antler Orogeny in western North America.

#### Devonian Period - 370 MY

Paleomagnetic data is available for only 8 continental fragments, and although the total number of poles is 50, 4 of the 8 fragments are represented by less than 5 poles. Precision parameters range from 20 to 162 and ages cover a considerable span from Middle Silurian to Lower Carboniferous. The single African pole is that reported by Hailwood (1974), otherwise the data is that summarized by Mc Elhinny (1973) updated from lists XIII and XIV.





Paleomagnetic results require a wider dispersion of Laurasia and Gondwanaland in the Devonian . It is probable that the Tethys seaway was a continuous channel dividing the continental masses into two major parts. The precision parameter increases from 6 for no continental drift from the present to the Devonian to 41 with the reconstruction shown in figure 1.13. This is significant at the 99.9% confidence level. The longitude of Siberia , and therefore its position relative to Europe , is ambiguous but the formation of the Ural foldbelt in the Carboniferous places a constraint on the separation. All of the continental segments have a northward component of velocity close to 3 cm/yr. The distribution of continental lithosphere on an azimuthal-equidistant projection in figure 1.13 shows the same symmetry as in the Mesozoic and Upper Paleozoic despite the widening Tethyan gap.

Geological information has been added in figure 1.14. As has been pointed out many times ( Briden and Irving, 1964; McElhinny, 1967), the distribution of Devonian reefs compares well with the location of the paleomagnetic equator. Note also that the ' Old Red Continent ' in Europe straddles the equator, in agreement with the fossil fauna and continental rocks which are interpreted as having been deposited in a tropical and semi-arid climate. Since the distribution of continents and their associated geosynclines is similar to that in the Permo - Carboniferous , the same





Figure 1.13 . Model of the continents in the Devonian period. The relative position of Siberia is most uncertain and the longitude was determined by requiring the velocity from the Devonian to the Permo - Carboniferous to be a minimum.

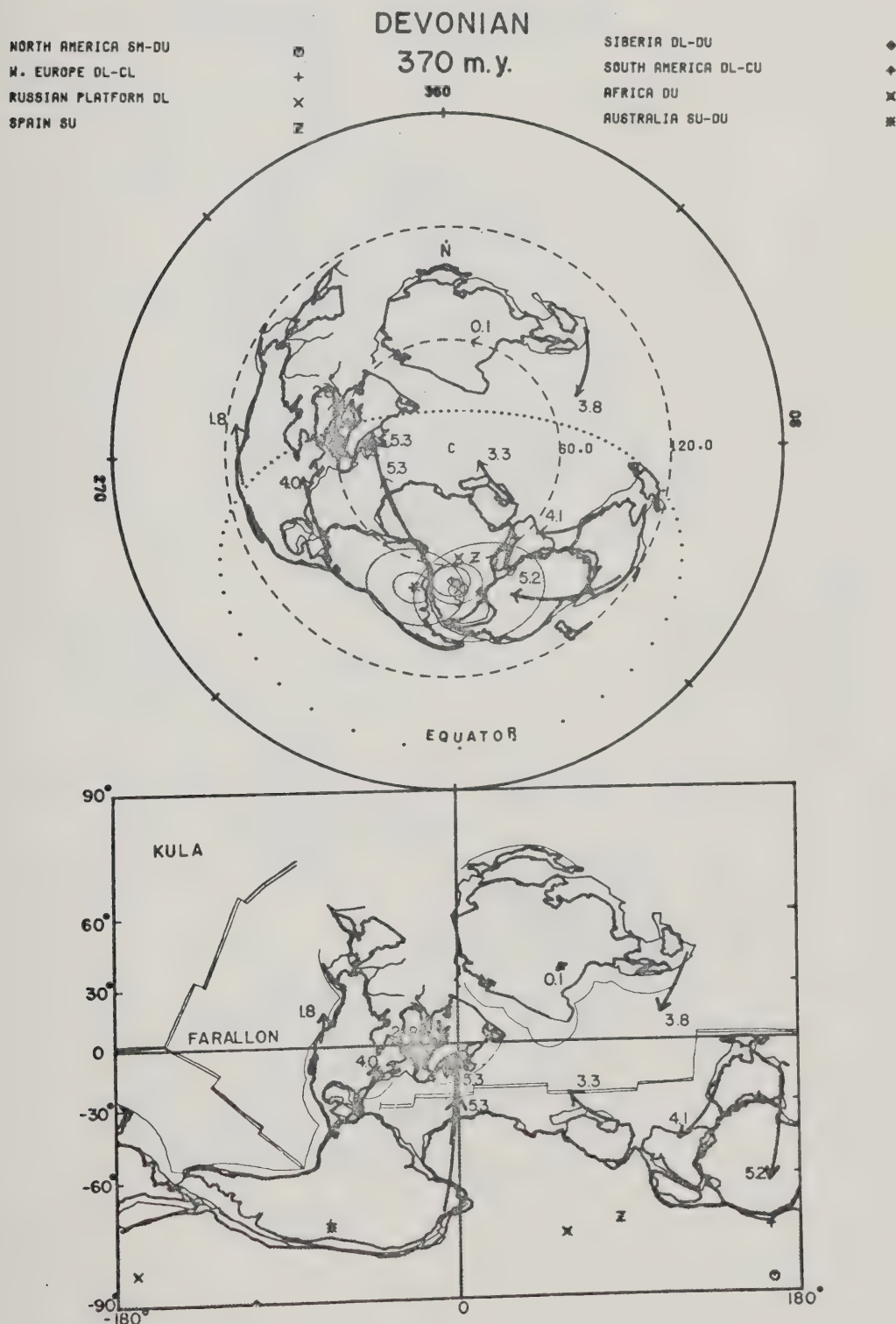
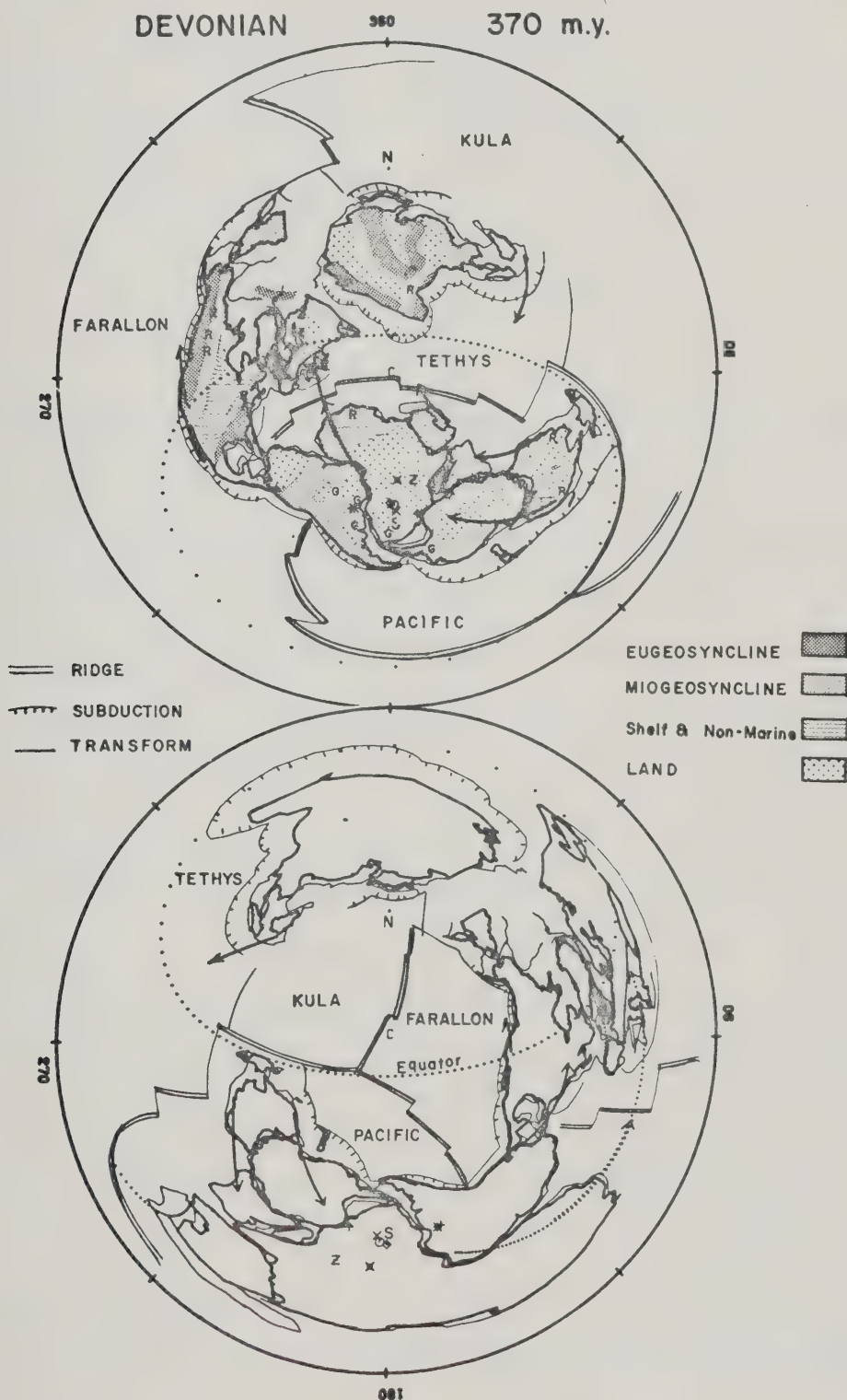




Figure 1.14 . Devonian geology and postulated plate boundaries on an azimuthal equidistant projection. The locations of reefs are indicated by the letter R .





oceanic ridge-type triple junction is assumed to be active still. One arm of the ridge system forms a near- globe encircling system around Gondwanaland . The complex pattern of diastrophism cutting across Siberia and China may be indicative of a collision of segments of the Asian landmass but the sparceness of the paleomagnetic observations does not justify any separation.

#### Ordovician Period - 470 MY

There is a considerable body of paleomagnetic data for the Lower Paleozoic to indicate a major reorganization of continental segments and some large scale continental drift. In an effort to analyze the changes as a function of time an Ordovician reconstruction has been attempted. The quantity and quality of the observational results are lower than for later periods but since the resultant model is similar to an independent one using Cambrian data, it is thought to have some validity. In order to obtain a meaningful Ordovician reconstruction we have restricted the temporal spread of suitable paleomagnetic poles as much as possible. This leads to a compilation of 45 poles from 8 continental segments, although only Siberia is represented by more than 10 poles. One pole from the North American compilation of Deutsch and Rao (1977) is listed as Cambro- Ordovician . The Western European summary is that of Faller et al (1977), in which all the sampling sites involved lie in the British Isles and





may not therefore yield a pole characteristic of Western Europe as a whole (see discussion in McElhinny, 1973, page 208). The South American poles we have listed are those reported by Thompson (1973).

The paleolatitude for all continental segments becomes quite low in the Ordovician and Cambrian periods. This places all the continental plates on or near the equator (figure 1.15) and to accomodate them the variation in longitude is highly constrained. Omitting the unrepresentative Western European pole, the precision parameter,  $K$ , increases from 3 for no continental drift between the present and the Ordovician to 33 for the reconstruction shown in figure 1.15. This is significant at the 99.9% confidence level.

Geological data is superimposed in figure 1.16. Africa has undergone a large amount of drift because the south pole now appears in the Tethyan Ocean north of this continent. The continental segments are arranged symmetrically along the equator. This configuration suggests a plate pattern similar to the one at the present time with the "ring" plates on the paleo-equator but with dominantly oceanic plates covering the poles. The individual plate boundaries cannot be established with any certainty because of the change in pattern and the imprecision of much of the data. The spreading center in the Tethyan Ocean must have been



Figure 1.15 . Model of the continents in the Ordovician period. The south pole is at the origin of the azimuthal equidistant projection.

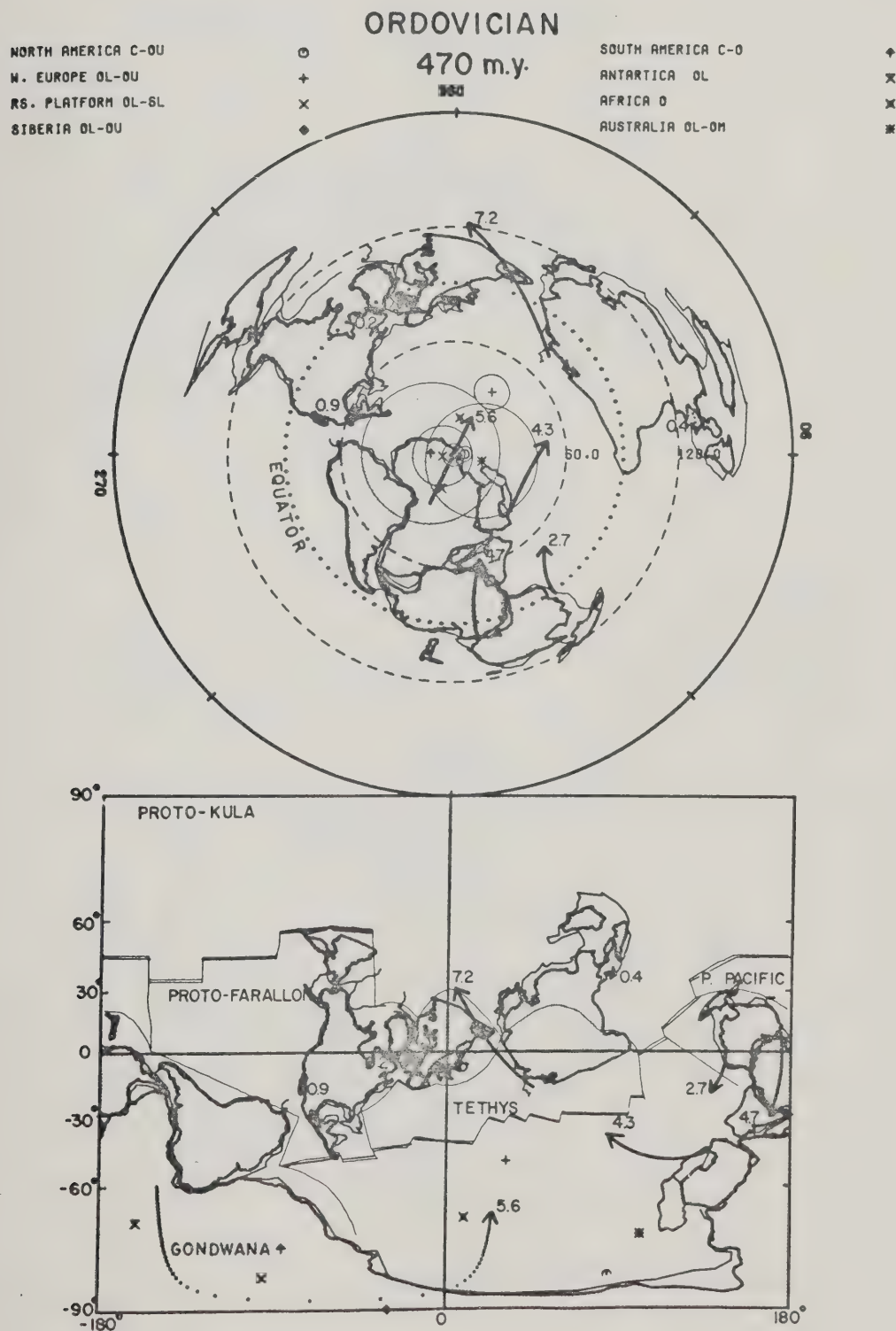
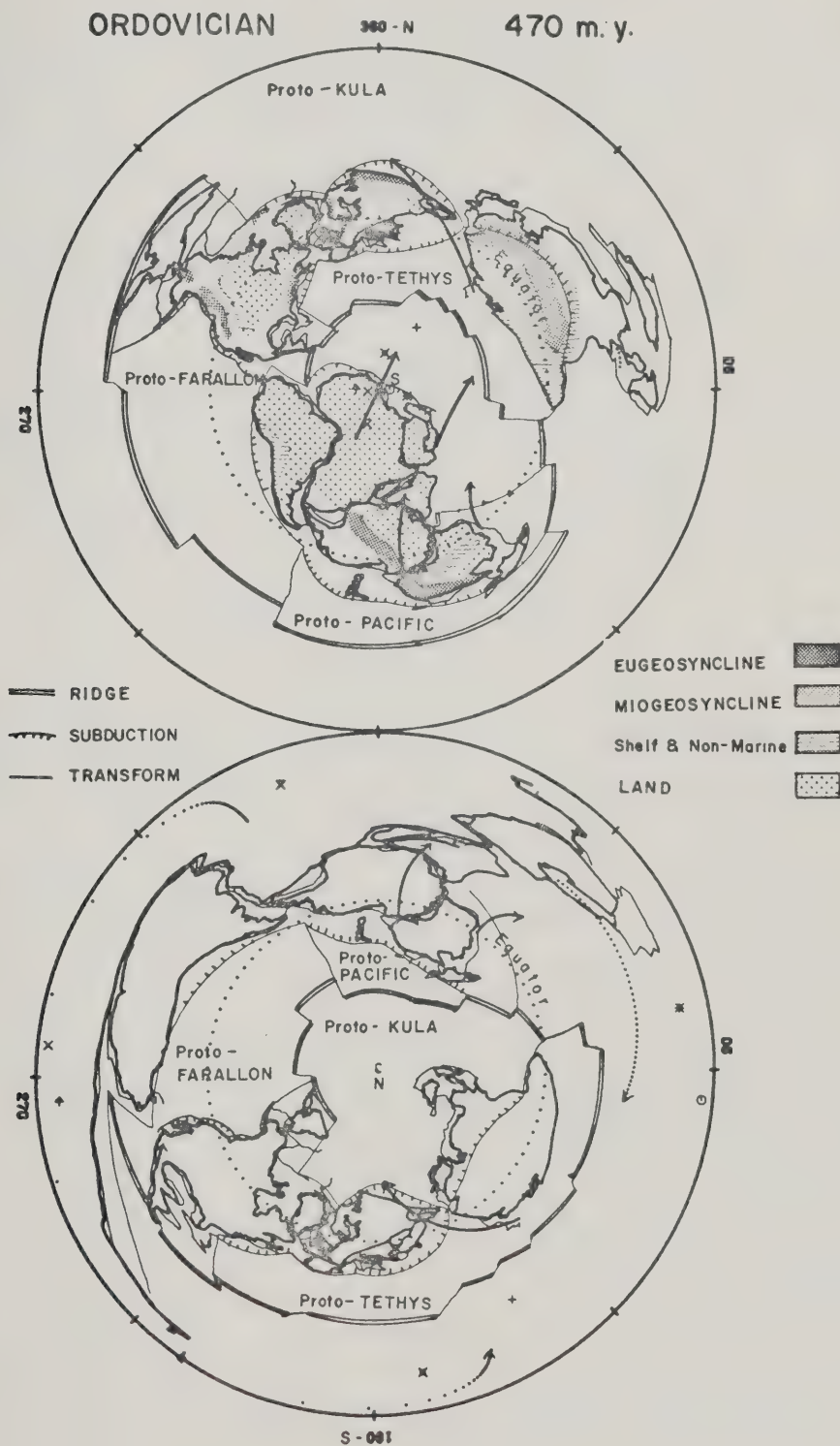




Figure 1.16 . Ordovician geology and postulated plate boundaries on an azimuthal equidistant projection centered on the south pole. In the lower figure the projection is centered on the north pole.







quite active to have created such a wide seaway and to have carried Gondwana to its indicated position. The "Pacific" plate, now centered on the north pole, must also have been very active to generate the Caledonian Orogeny, along the periphery of the "ring" plates. The Caledonian Orogeny was episodic from the Late Cambrian to the Middle Devonian and this appears to have reorganized the plate tectonic pattern drastically. Certainly, the velocity of the continental segments between the Ordovician and the Devonian is rather high, often with a northward component of 5 to 7 cm/yr but much more paleomagnetic data is necessary to document the precise position of the continental segments.

#### Cambrian Period - 550 MY

The continental fragments are represented by a total of only 35 poles, some of which are uppermost Precambrian and others Lower Ordovician. With the exception of South America, K values lie between 19 and 99. For North America we have followed Van der Voo et al (1976) and for India we have used the summary by Wensink (1975). The South American summary is that given by Thompson (1973) who lists 5 Cambrian poles; individually these poles are of poor quality (only 1 has an alpha 95 under 20 degrees) and as a group they are highly scattered (K = 4, A 95 = 41 degrees). If taken at face value they imply large amounts of polar wandering within the Cambrian. Whilst this may in fact be





Figure 1.17 . Model of the continents in the Cambrian period. The south pole is at the center of the azimuthal equidistant projection.

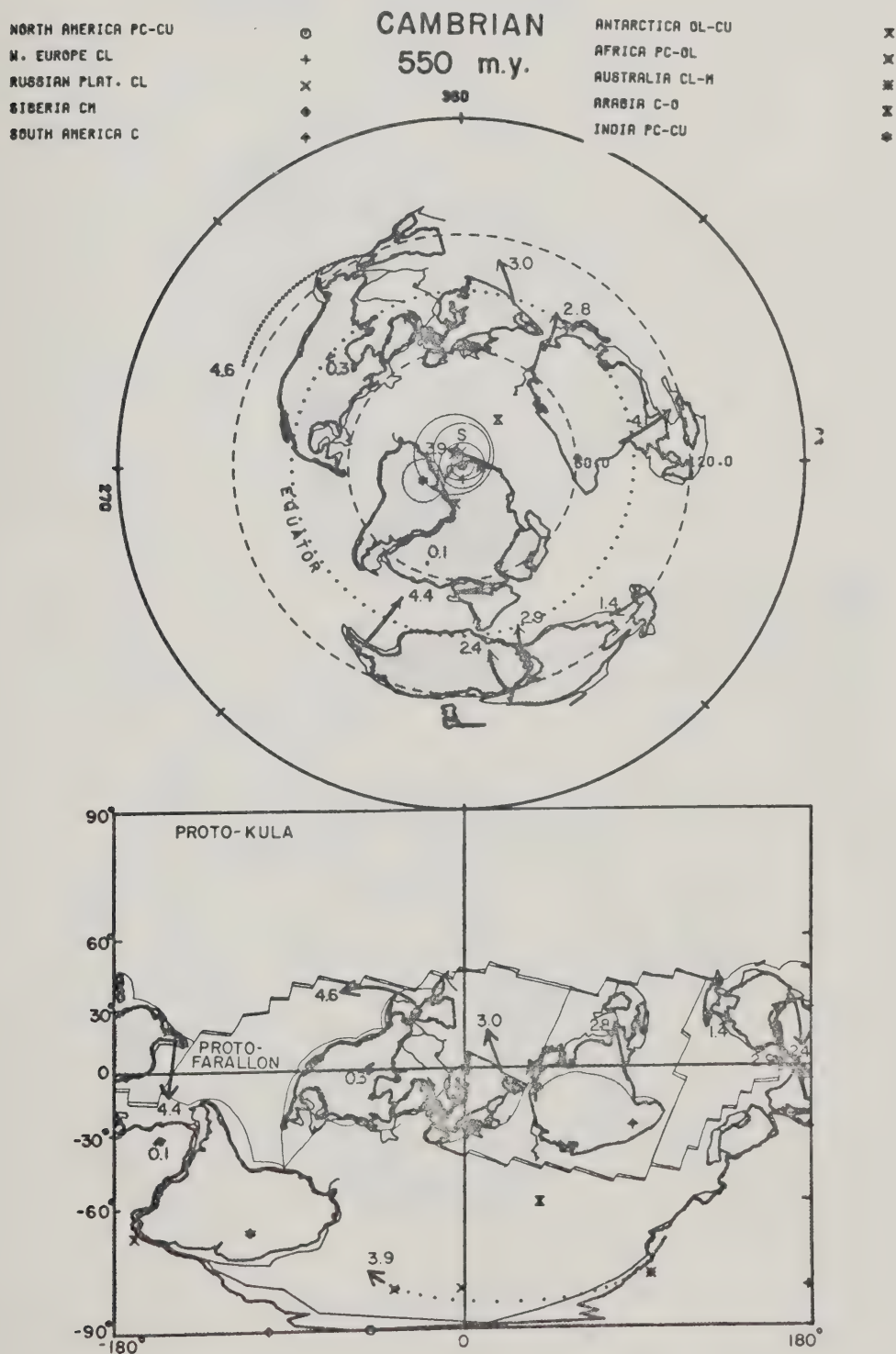
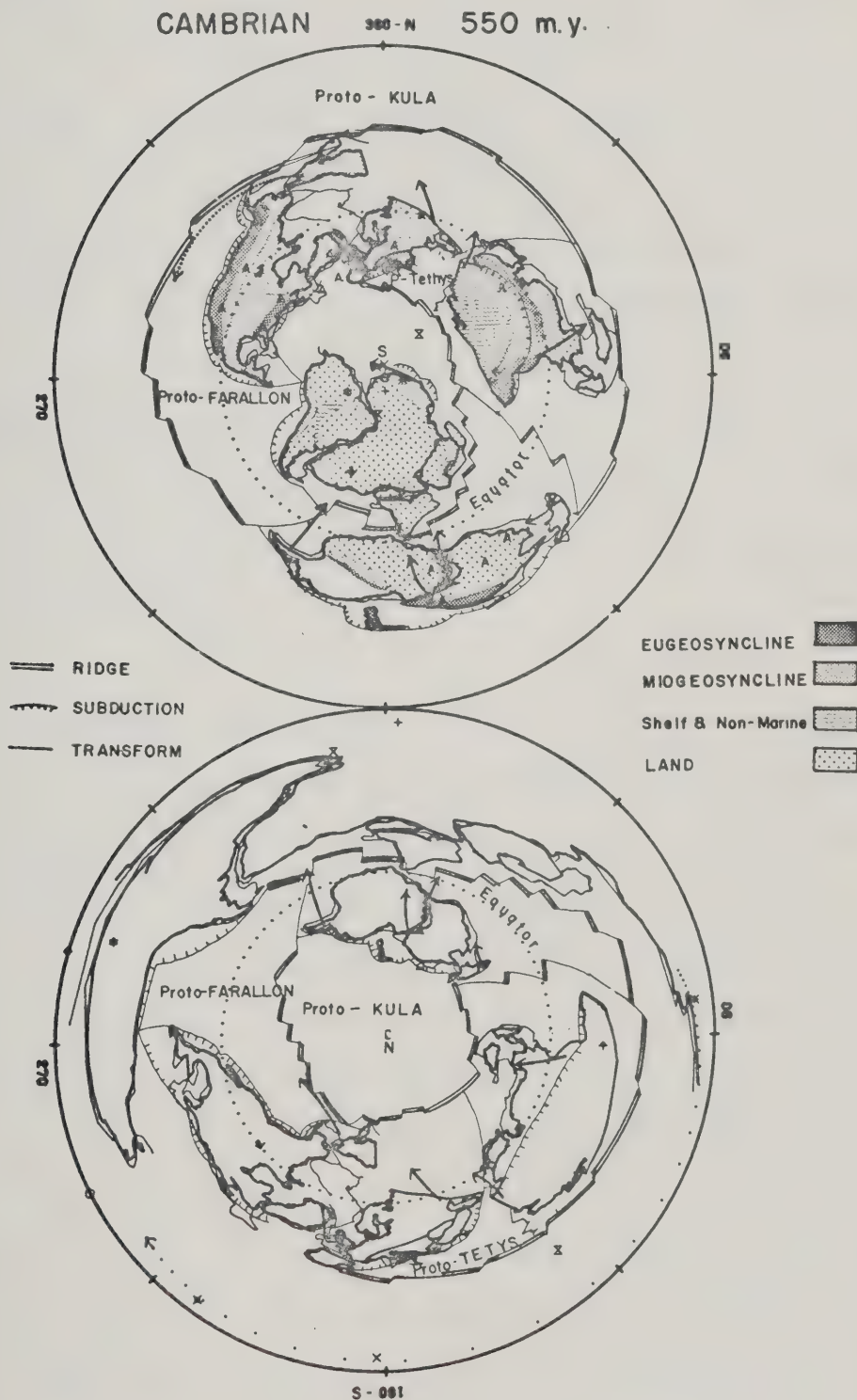




Figure 1.18 cambrian geology and postulated plate boundaries on an azimuthal equidistant projection centered on the south pole. Symbols A mark the location of *Archaeocyathus* fossils. In the lower figure the projection has its origin at the north pole.





true (see Hailwood , 1974, for example) we prefer to adopt the conservative approach of excluding these data until they are corroborated by studies from other continents. Consequently the South American pole is illustrated on figure 1.17 but is not used in the reconstruction and the associated statistics. Fisher's precision parameter increases from 5 for no continental drift between the present and the Cambrian to 26 for the model shown in figure 1.17. This is significant at the 99.5% confidence level. If Australia and Antarctica are kept together with Africa to maintain Gondwana the precision parameter increases to only 12, (table 2, Appendix 1) , even omitting the South American data. The pattern and polar symmetry is very similar to that in the Ordovician .

Geological data and the postulated plate boundaries are shown in figure 1.18. The position of the paleo-equator corresponds well to outcrops built from skeletons of the reef organism, *Archaeocyathus* . The proto - Atlantic between Europe and North America that was postulated by Wilson (1966) and by Dewey and Bird (1970) is required here by the paleomagnetic data although the longitudinal change is uncertain. The Tethyan and Australian spreading center must have been fairly intense to generate the rotation of North America, Europe and Asia with velocities of 3 to 4 cm/yr. The spreading center between Antarctica and Africa must have been dying out as Gondwanaland is a recognizable entity in





the Ordovician . All continental plates require a minimum velocity of between 2 and 4 cm/yr between the Cambrian and Ordovician periods.

## INTERPRETATION

Using paleomagnetic observations and a small number of principles based on plate tectonic data and concepts it has been possible to reconstruct continental fragments for six periods between the Cretaceous and the Cambrian in a statistically significant manner. The grouping of the paleomagnetic poles show an improvement in Fisher's precision parameter at the 99% or 3 standard deviation significance level. The model for the Tertiary period was made using magnetic lineations and is an independent test of the paleomagnetic method. An alternate reconstruction following the early work of Bullard et al (1965) and Smith and Hallam (1970), hereafter referred to as the " Bullard " model, for brevity, was also made. This " Bullard " model for Pangaea in the Permo - Triassic ( Fig. 1.7) was kept as a distinct unit, allowing polar wander but no continental separation, from the Triassic to the Cambrian. It has often been used, without justification, for displaying tectonic and paleontological data from the Lower Paleozoic Era . It must be emphasized that neither Bullard nor his coworkers have ever claimed any validity for this model over such an extended period of time . Indeed, Smith et al (1973) reached



a similar conclusion and have put forward a set of models, not using plate tectonic principles, but employing the paleomagnetic data available to them, in which Pangaea is broken apart in the Paleozoic . From Table 2, Appendix 1, it is seen that the Fisher's precision parameter,  $K$  , for the " Bullard " model, degenerates from 28 in the Triassic to 4 in the Cambrian . The improvement in our model over the " Bullard " one is significant at the one standard deviation level for the Permo - Carboniferous and Devonian periods and at the 3 standard deviation level for the Ordovician and Cambrian periods. Therefore we reject any reconstruction in which Pangaea existed for more than a brief time in the first half of the Mesozoic Era .

Models using paleomagnetic data contain ambiguities due to the uncertainty in the longitude. The minimization with respect to velocity of the plates to define the longitude, although non-unique, has proven to be of great value. Alternate positions of the continental segments can be readily visualized by consulting the Mercator projections and the increase in plate velocity can be estimated by the relative shift from the minimum velocity point . From the Devonian period to the present time the dated magnetic lineations and the reconstruction of Gondwana and Laurasia place severe restrictions on the longitude (unless one has reasons to believe in a shift of the earth's entire lithosphere along lines of latitude). In the Devonian period



the North American and Asian continents are restrained to the position shown by the geological evidence for the formation of the Urals . In the Cambrian and Ordovician periods the shift of all major segments to an equatorial position places very tight constraints on the longitude. In summary, unless the paleomagnetic evidence is missing, as in China , or in error, the relative longitude of all major continental segments is estimated to be restrained within 10 degrees . Their velocities are then within 1 cm/yr of their true values.

If we now accept the continental reconstruction as approximately correct, the azimuthal equidistant maps, with origin on the center of mass of the continental margins, are useful in examining various geometrical properties. In all periods there is present a single large ocean, similar to the present Pacific Ocean . In the early Paleozoic , up to the time of the Caledonian Orogeny , this ocean was centered on the North Pole . Subsequently it occupied an equatorial position antipodal to the Tethys sea north of Africa . At the end of the Mesozoic Era the center of the Pacific plate shifted to a position antipodal to the center of the African plate. The continental segments are grouped in a cluster which is related to the spin axis. The center of mass, C , is either on the South Pole , as in the Cambrian and Ordovician periods, or else near the equator.





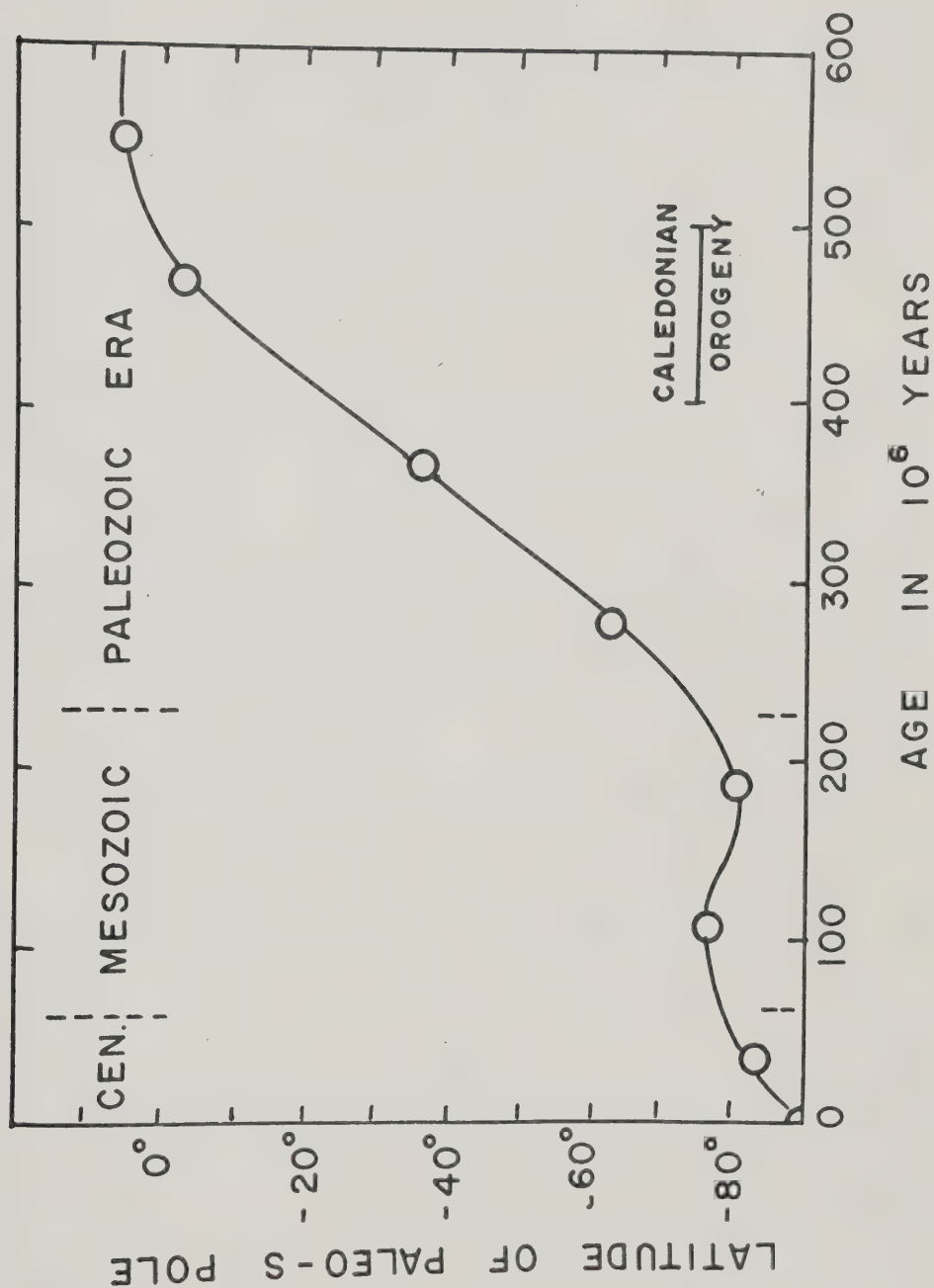


Figure 1.19 . The motion of four continents relative to the present position of Africa between 550 and 0 million years ago. An azimuthal equidistant projection is used and the reconstruction is based on a minimum velocity assumption for all continental segments. The total motion of the continents is approximately 90 degrees. Central North America and Siberia move from an equatorial position to one close to the north pole. Central Africa moves from a south polar position to an equatorial one. Eastern Australia moves from 30 N in the Cambrian to 60 S latitude in the Cretaceous as a part of Gondwana . Its subsequent motion is independent of that of Africa .





Figure 1.20 . Variation of the latitude of the mean paleomagnetic south pole in the present coordinate system as a function of time.





The drift of the continents in the Phanerozoic Era is illustrated in figure 1.19. A graph ( Fig. 1.20 ) using data listed under LAT in Table 2 of the Appendix 1 shows the change in latitude of the mean south paleomagnetic pole as a function of time. Samples from the Cambrian and Ordovician systems yield paleomagnetic south poles close to the present equator. A rapid shift in latitude occurred at the time of the Caledonian Orogeny which culminated toward the end of the Ordovician period. This was concurrent with a major reorganization of the continental segments and relatively rapid continental plate motion. The rest of the Paleozoic is represented by a uniform drift toward the present polar position accompanied by a reorganization of the continents into Gondwana and Laurasia . The Tethys sea closed uniformly from its oceanic proportions in the Lower Paleozoic . A high degree of symmetry occurred in the Mesozoic Era with Laurasia and Gondwana locked together to form the supercontinent of Pangaea . The latitude of the pole stabilized near 80 degrees in terms of present day coordinates. The end of the Mesozoic shows a very symmetric arrangement even though Gondwana and Laurasia are separating with the formation of a proto- Atlantic Ocean in a symmetric relation to the Tethys sea with respect to the map center ( Fig. 1.5 ) . In the Tertiary period the latitude in figure 1.20 begins to shift, once again, towards 90 degrees. The continental arrangement has the symmetry of the present day with the African and the Pacific quasi-circular plates



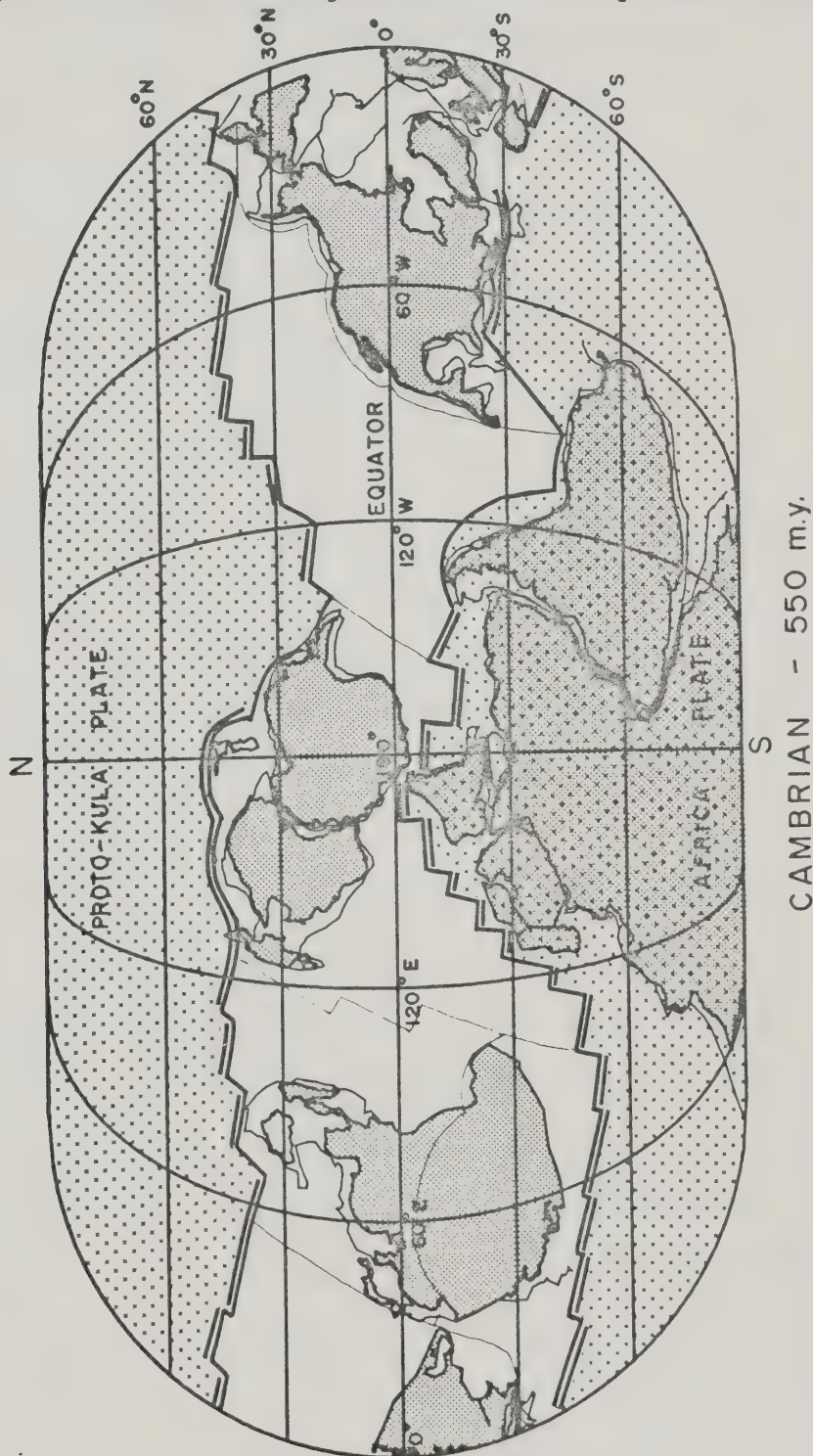


separated by a ring of quasi-elliptical plates ( Fig. 1.4 ) . It is significant that the variation in the latitude of the pole with time is not random but is a very regular and systematic function of time.

The reconstruction of plate boundaries in the past requires further assumptions as outlined in the principles in the introduction . The incompleteness of paleomagnetic observations is compounded by the gaps in the geological record. However, accepting that the reconstructions have some validity, it is seen that the number of plates varies from 6 to 8 or 9 . Small plates, such as the Indian in the Tertiary or the Nazca at the present time, have very rapid motions and disappear quickly as independent entities. There appears to have been 7 or 8 major plates in the Lower Paleozoic and Cenozoic Eras . There may have been as few as 6 in the Upper Paleozoic and Mesozoic Eras although the number occupying the enlarged Pacific Ocean is speculative. The plate arrangement also shows a certain symmetry during each period. The Cambrian and Ordovician periods have an equatorial ring of dominantly continental plates indicating a close similarity to the present situation. A south oceanic polar plate, containing Africa lies opposite the major north polar oceanic plate. The arrangement on an Eckert projection ( Fig. 1.21) should be compared to a similar one of the present plate system ( Fig. 1.2 ) except that the "ring" plates are rotated 90 degrees to the spin axis. The Upper



Figure 1.21 . A model of the plate tectonic pattern in the Cambrian period on an Eckert projection. This figure should be compared to the configuration at the present time in figure 1.2.





Paleozoic and Mesozoic plate arrangement is one in which the continental blocks have an equatorial position opposite the oceanic group of plates. Following principle 9, there must be a spreading center in the Tethys sea which is seen to follow the equator. As the Tethys seaway becomes smaller towards the Cretaceous period the continental and plate arrangement acquires greater symmetry. In conclusion, the arrangement of plates is neither random in space or time. On the contrary, the plate tectonic pattern appears to have an evolutionary development with a time scale of several hundred million years and a high degree of spatial organization whose physical properties should be described by low order spherical harmonics. Such an ordered kinematic and geometric system on the surface of the earth must be reflected also in the dynamic system within its interior.

The organization of the lithosphere with two antipodal quasi-circular plates separated by a ring of quasi-elliptical plates at the present time was considered by Kanasewich (1976) to be convincing evidence for a mantle-wide convective system. Theoretical studies by Chandrasekhar (1961) investigated three-dimensional convection in spherical shells of a uniform Newtonian incompressible fluid. A variational principle was used to determine the Rayleigh number for the onset of convection in cells with various sizes. Since the core is liquid with a small viscosity, compared to the mantle, the lower boundary





condition must have zero shear stress (free-slip) . The boundary condition at the lithosphere-asthenosphere contact is more complex but it is reasonable to assume that the lithosphere is free to move with the underlying mantle. More complex and irregular plate boundaries will result because this condition is only approximated when considering the broad pattern of convective motion. With upper and lower boundaries being free-slip and using the present size of the mantle it is found that a flow generated by internal sources distributed as a spherical harmonic of degree three is most readily excited ( Rayleigh number,  $R = 19,000$ ) . Those with degree 2 (  $R = 22,000$ ) and degree 4 (  $R = 21,000$ ) are only slightly larger and are probably easily excited. That with degree 6 has a Rayleigh number of 35,000. It has been found by Chamalaun and Roberts (1962) that axially symmetrical modes are excited more readily than unsymmetrical modes. A very detailed knowledge of the boundary conditions and the physical properties of the mantle would be necessary to make a theoretical prediction of the combination of modes excited and maintained in the flow pattern. However it seems reasonable to assume that, if mantle-wide convection occurs, the low order spherical harmonics will have the dominant amplitudes.

Two-dimensional models of convective flow can be used to solve more complex physical states. Thus Takeuchi and Sakata (1970) have made a theoretical computation on a two-



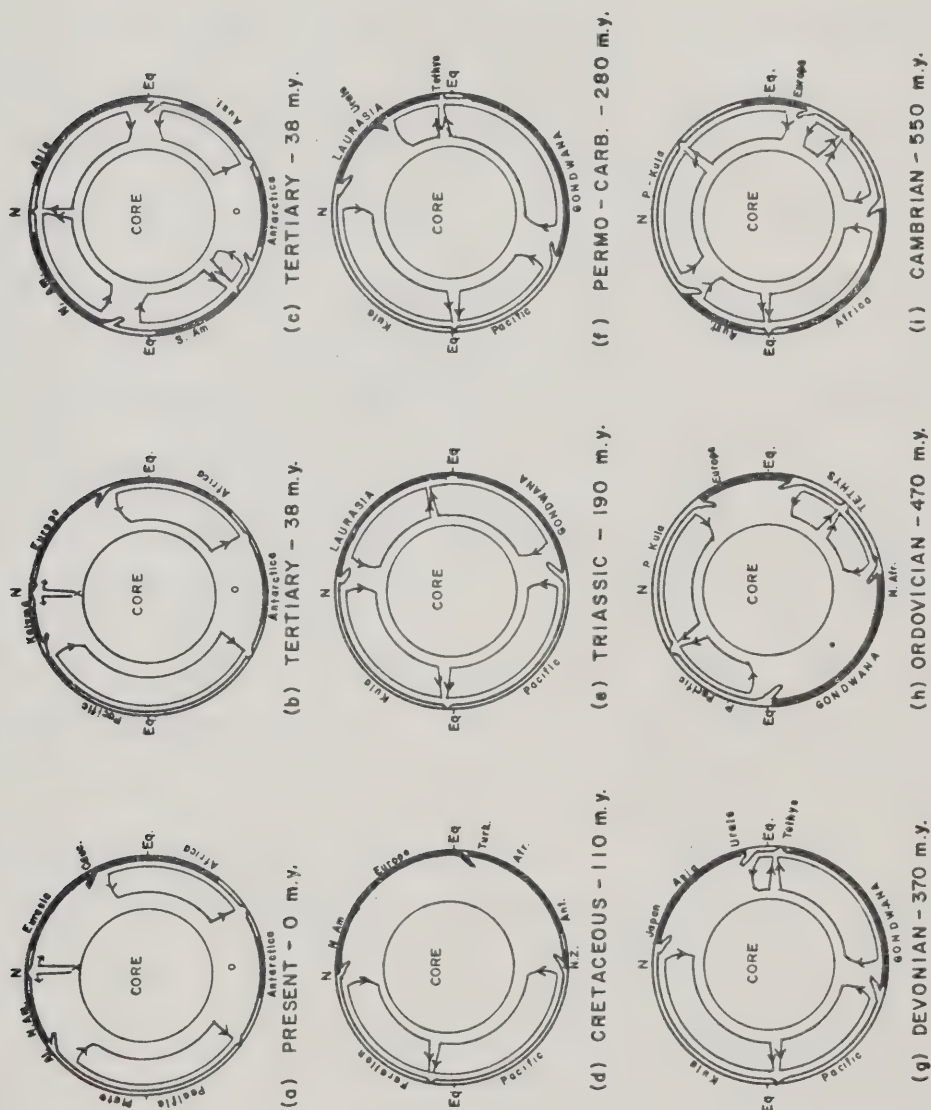


layered Newtonian fluid with two-dimensional rectilinear geometry. The boundary conditions were zero shear stress at the surface and a non-slipping (zero velocity) lower boundary which was being heated. The lower layer occupied 90% of the total thickness and was 1000 times more viscous than the upper (asthenospheric) layer. This model showed that there are larger horizontal velocities in the upper layer but that the return flow is in the lower, more viscous, layer. Studies by Peltier (1973 ) for heating distributed uniformly through a model with the same boundary conditions gave similar results. Davies (1977) studied a model similar to the one by Takeuchi and Sakata but with both boundary conditions being free-slipping and there was no heating. The upper layer was taken to be 700 km thick and the lower one was 2300 km. Davies found that 5 orders of magnitude contrast between the viscosity in the lower and upper layer are necessary to exclude flow from the more viscous layer. The contrast becomes even greater as the upper layer is made thinner. Although the models are simple and the boundary conditions not as complex as those encountered in the real earth, when theoretical studies have been carried out to include the entire mantle, the results indicate that the lower mantle must be involved in the dynamics of plate tectonics.

Assuming mantle-wide convection, a series of cross sections have been drawn up in figure 1.22 to illustrate



Figure 1.22 . Cross sections of the Earth along the great circle path 360 - C - 180 in the azimuthal equidistant projections of figures 1.1, 1.4, 1.6, 1.9, 1.12, 1.14, 1.16 and 1.18. The dimensions and directions of hypothetical mantle current systems are indicated.





hypothetical flow patterns for the 7 periods modelled with paleomagnetic data in figures 1.4 to 1.18. Most of the cross sections of the earth cut the azimuthal-equidistant projections along a great circle path between 360, C and 180 in figures 1.4 to 1.18. A polar cross section ( Fig. 1.22h,i) at any longitude for the Cambrian and Ordovician periods tends to show 6 cells or a convective pattern that can be described by a 3rd order spherical harmonic. The Devonian period ( Fig. 1.22g) has a 2nd order convective pattern which is somewhat irregular. The Ordovician pattern is also more irregular than the Cambrian one. Comparing the Devonian and Ordovician spreading centers on a Mercator projection (figures 1.13 and 1.15) it is seen that the change in convective order is evolutionary. The Ordovician Tethys spreading center moved toward the equator and broke through between Asia and Australia to join the Pacific spreading center which evolved, in the Devonian, into a triple junction. If the Pacific oceanic spreading centers were consistently more active than the Tethys one, the rapidly moving Kula, Farallon and Pacific plates would tend to concentrate the continental segments into the one large continent called Pangaea by Wegener . As the cross sections in figure 1.22 (d to g) show, the convection pattern remained stable as a 2nd order system until the Cretaceous period. A 2nd order system is still present in the Cretaceous but the Tethys spreading center has decayed away and as seen in figures 1.5 and 1.6, a transition is





occurring to a new order at the beginning of the Cenozoic Era . This is a more complex system which tended to split Gondwana and Laurasia apart. The Pacific system developed a double triple junction ( Fig. 1.6) with the four oceanic plates of Pacific, Kula, Farallon, and Phoenix . In the Tertiary period (figure 1.4) the spreading center between the Phoenix and Farallon plates began to dominate so that the Kula and Farallon plates were subducted out of existence underneath Asia and North America . The North Atlantic ridge, which first appeared in the Jurassic period, also became dominant and a spreading center formed three-quarters of the way around Africa . The Tertiary spreading centers, like the present ones, are complex, involving many axially symmetric modes of low order spherical harmonics. But the 3rd and 1st orders predominate. This produces two main spreading centers which drive the Pacific and African plates in a northward direction ( Fig. 1.22a,b ). The two cells have very different velocities and are decoupled by a ring of plates and minor spreading centers. These show the third order pattern more clearly ( Fig. 1.22c) if another cross section is made through the "ring" perpendicular to the one in figure 1.22b.



## CHAPTER 2

### REVIEW OF SEISMIC EVIDENCE FOR LATERAL INHOMOGENEITIES IN THE MANTLE

Over the last ten years lateral inhomogeneities in the mantle have received increased attention. There are several reasons. The increased quality of seismic data with the introduction of the seismic array and the World Wide Standard Seismic Network (WWSSN) has refined the spherically symmetric average earth models, with the result that the deviations from these models have become more evident. Also the theory of plate tectonics and the continuing debate about whole mantle convection has focused attention on possible lateral inhomogeneities in the mantle. This review attempts to present the most important seismic methods for detection of lateral inhomogeneities in the mantle, and specifically in the deeper mantle. The much studied subject of crust and upper mantle inhomogeneities, particular those related to plate boundaries will not get much attention, since acceptable models already exist. Different methods of studying the seismic data and some of the results are examined. A summary of the evidence for lateral inhomogeneities is given in table 2.1.



## TRAVEL TIMES

Travel times of seismic phases, especially for the P and S phases, have been the tool most often used for determining mantle structure. Other seismic phases have been used in more specific studies, for example PcP travel times are used to determine the radius of the core.

A travel time residual,  $T_{res}$ , can be written as

$$T_{res} = T - C + A + E + R + S + M \quad (2.1)$$

- T: The observed travel time.
- C: The calculated travel time as a function of distance and focal depth for a radially homogenous earth.
- A: Correction for the station altitude above sea level.
- E: Correction for earth ellipticity, usually corrected as suggested by Bullen (1965).

R: Station regional correction which can be written

$$R = A + B \sin (Az + D) \quad (2.2)$$

A, B and D are constants for a certain station and Az is the azimuth measured from the station towards the event. A is the azimuth independent correction and B and E the azimuth dependent terms. Herrin and Taggart (1968) have tabulated A, B, and D for a large number of stations in the WWSSN network. The corrections clearly show the existence of regional lateral inhomogeneities in the crust and uppermost mantle.

S: Since earthquakes occur in tectonically active areas





with large inhomogeneities, source related travel time anomalies,  $S$ , are to be expected. Attempts have been made to make general corrections, as expressed in 2.2, (Herrin and Taggart (1968a)) or corrections are calculated for special cases (Engdahl and Johnson (1974)). Most results are not corrected for source effects and source related anomalies are often used as evidence for lateral inhomogeneities in the source region either close to the source (Engdahl and Johnson (1968), Jacob (1972)) or well below the source (Engdahl (1975)).

M: Errors which arise from event mislocation, or mistakes in determining the event origin time.

From this discussion of the terms in (2.1) it is seen that residuals can have several explanations. Several methods are discussed below for identifying residuals due to the deeper part of the ray path.

#### Comparison of travel time curves.

Travel time anomalies,  $T_{res}$ , plotted against epicentral distance,  $\Delta$ , will often show a systematic variation indicating that anomalies are not random. An improvement of the results can be obtained by using only deep earthquakes ( $h > 500$  km) thus eliminating or reducing source anomalies. Such a study was made by Julian and Sengupta (1973) who also used regional station corrections  $R$ . The conclusion of that





study was that the majority of lateral anomalies are below 2000 kms depth, as the travel time curves show much difference from region to region for  $\Delta > 85$  degrees. A large part of the deeper mantle was mapped as being either slow or fast relative to the J-B tables (Jeffreys and Bullen (1967)). Size of the anomalies was 1000 km or less. The approximate region of anomaly was arbitrarily defined to be that part of the ray covering the central  $30^\circ$  of the ray path. This is a reasonable assumption since 25% of the travel time is spent in the lower 10% of the ray path. A similar study was made by Au (1977) suggesting the existence of relative low velocity regions in the lower mantle under the Indian Ocean and the Himalayan mountains.

#### P-wave residuals as a function of azimuth

As mentioned earlier, the systematic variation of  $T_{res}$  with azimuth is usually interpreted as due to velocity anomalies in the upper mantle. Herrin and Taggart (1968) did not interpret their results in terms of velocity anomalies at any particular depth, but it is possible to make use of their tabulations to do so. An analysis was made by Brown (1973) for the stations in the Scandinavian network. It appears that seismic waves travel faster for paths which approach Scandinavia from the north than from the south. Several possible models were tried to explain the anomalies and the conclusion reached was that because of the extensive area showing the anomaly, the most likely explanation would



be a dipping structure under Scandinavia at depths of 600 to 700 km.

### Inversion of travel time curves in terms of velocity.

Several inversions using the Herglotz - Wiechert method have been presented using paths of world-wide data. If enough data is present it is possible to compare velocity models calculated from data from different regions. Niazi (1973) made such a study using S-waves and showed that below 2500 kms depth the mantle beneath Iceland and the North Pole differed significantly, the S-wave velocity being highest close to Iceland. This can possibly be correlated to Morgan's (1972) suggestion of a hotspot under Iceland.

### Inversion of travel time residuals in terms of velocity perturbations in a 3 dimensional mantle.

Two global inversions have been reported in the literature. Sengupta and Toksoz (1976) used 1490 P and PcP and 314 S and ScS travel times from deep events. The data were first fitted to an average radial velocity model. Then the anomalies for each station were averaged and used to correct the individual travel times. The remaining travel time anomalies were fitted through constant perturbations in 3-dimensional blocks of size 10 deg. in latitude, 10 deg. in longitude and 500 kms in depth. A method of successive approximations was used (Aki et al (1974)), which Sengupta



and Toksoz describe as follows. The  $r$ 'th approximation of the velocity perturbation for the  $m$ 'th block ( $= p_m^r$ ) is given by the weighted least squares solution to the system of  $n$  linear equations of the form

$$T_{ij} + C_{ij}^r = K_{ijm}^r * p_m^r \quad (2.3)$$

A summation convention is assumed to apply to subscripts in equation (2.3). The number of rays passing through the  $m$ 'th block is  $n$ ,  $T_{ij}$  is the observed travel time anomaly for the  $i$ 'th earthquake and  $j$ 'th station;  $C_{ij}^r$  is the  $r$ 'th approximation of the correction to  $T_{ij}$  from the perturbation of velocity in the remaining blocks and  $K_{ijm}^r$  is the  $r$ 'th approximation of the travel time in the  $m$ 'th block corresponding to  $T_{ij}$ . Strictly speaking, as Sengupta and Toksoz state, the problem is undetermined. However by using different sequences of sampling the blocks, some consistent results emerged. Lateral inhomogeneities were most prominent in the upper mantle and near the core-mantle boundary. The velocity perturbations were mapped for depths of 0-500 km and for 2500 km - 2900 km. The upper mantle anomalies corresponds well with surface features (high velocity under continents, low under oceans), while the lower mantle anomalies do not.

A similar, but much more extensive study was made by Dziewonski et al (1977). About 700000 arrival times were selected from the Bulletin of the International Seismological Center. Only the best data was used and only events with more than 100 stations reporting were selected.





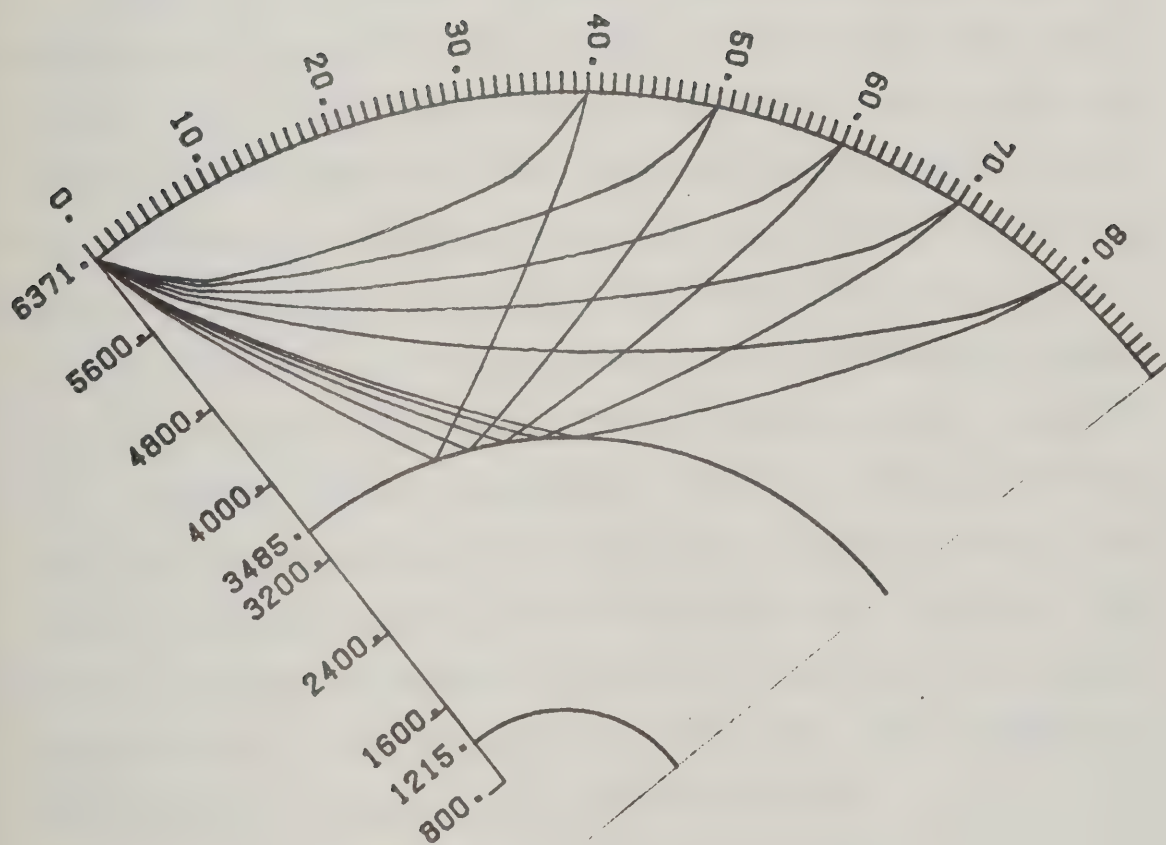
Residuals were calculated relative to velocity model PEM-C (Dziewonski et al (1975)). Regional station corrections were applied as described in equation 2.2 and the resulting residuals inverted in terms of velocity perturbations. The block size was 36 deg. latitude, 60 deg. longitude and the separation in depth at 0 - 670 - 1100 - 1500 - 2200 kms and the core-mantle boundary. The resulting perturbations in velocity were much smaller (0.5%) than those found by Sengupta and Toksoz (2%). This is probably due to the larger block size. The velocity perturbations were analyzed using spherical harmonic analysis for the 5 different depths regions. Results above 1500 kms depth were unstable indicating that the anomalies have dimensions smaller than the grid size. For the deeper mantle consistent results were obtained. No correlation with surface features was found but a correlation exists between large wavelength gravity anomalies, as observed at the surface, and those computed from velocity anomalies at depths greater than 1100 km.

In the study of lower mantle inhomogeneities the differential travel time of the phases PcP-P and ScS-S are especially useful since the ray paths are nearly identical in the upper mantle. It is seen in figure 2.1 that in the upper mantle the ray paths are very close for S and ScS or P and PcP. That is especially true for longer distances, ( $\Delta > 50$  degrees). Differential travel times reduce or eliminate errors in hypocenter and epicenter location, absolute time determination, event origin time and station anomalies. An



Figure 2.1

ScS and S rays in the distance range 40 to 80 degrees. The numbers to the left are distances in km from the earth's center.





anomaly in the differential travel time must then be located either along the S or ScS ray path below a depth where the two ray paths diverge a distance of at least one wavelength (100 km for a velocity of 5 km/s and a frequency of 0.05 Hz). For instance at an epicentral distance of 50 degrees the two rays separate about 200 km at depths of 500 km while at a distance of 70 degrees the same separation occurs at about 1000 km. So it is an advantage to use as large distances as possible, but the values much beyond 80 degrees are not practical as ScS arrives very close in time to S. The same arguments are true for PcP and P.

Hales and Roberts (1970) used ScS-S travel times to estimate the radius of the core. On plotting the ScS-S travel times residuals versus epicentral distance in the range 48 to 70 degrees it was noted that substantial scatter existed. Scatter as large as up to 8 seconds were noted, and Hales and Roberts suggested the existence of lateral inhomogeneities in the lower mantle, or alternatively bumps on the core-mantle boundary. Several studies (e.g. Engdahl and Johnson (1974), Buchbinder (1968)) using arrivals reflected off and within the core have shown that bumps on the core-mantle boundary cannot be larger than 5-10 km. This is not enough to explain the large scatter ( $V_s = 7.3$  km/s, time scatter =  $2 \times 10 / 7.3$  sec = 2.7 sec), so the suggestion about lateral inhomogeneities seems reasonable.

Mitchell and Helmberger (1973) used a much larger set





of long period ScS-S travel times in a study of the S velocities near the core-mantle boundary. They hoped that by using long period S waves (periods of 20s) the effect of lateral inhomogeneities could be minimized. The average ScS-S residuals from events in South America and the Sea of Okhotsk were quite different. This was interpreted in terms of lateral differences at the base of the mantle. Buchbinder and Popinet (1973) used short period PcP-P travel times and PcP amplitudes in a study of the core-mantle boundary. They found a distance independent scatter in the PcP-P travel times ( $\pm 2.5$  sec.) and noted that this probably was due to lateral inhomogeneities in the lower mantle.

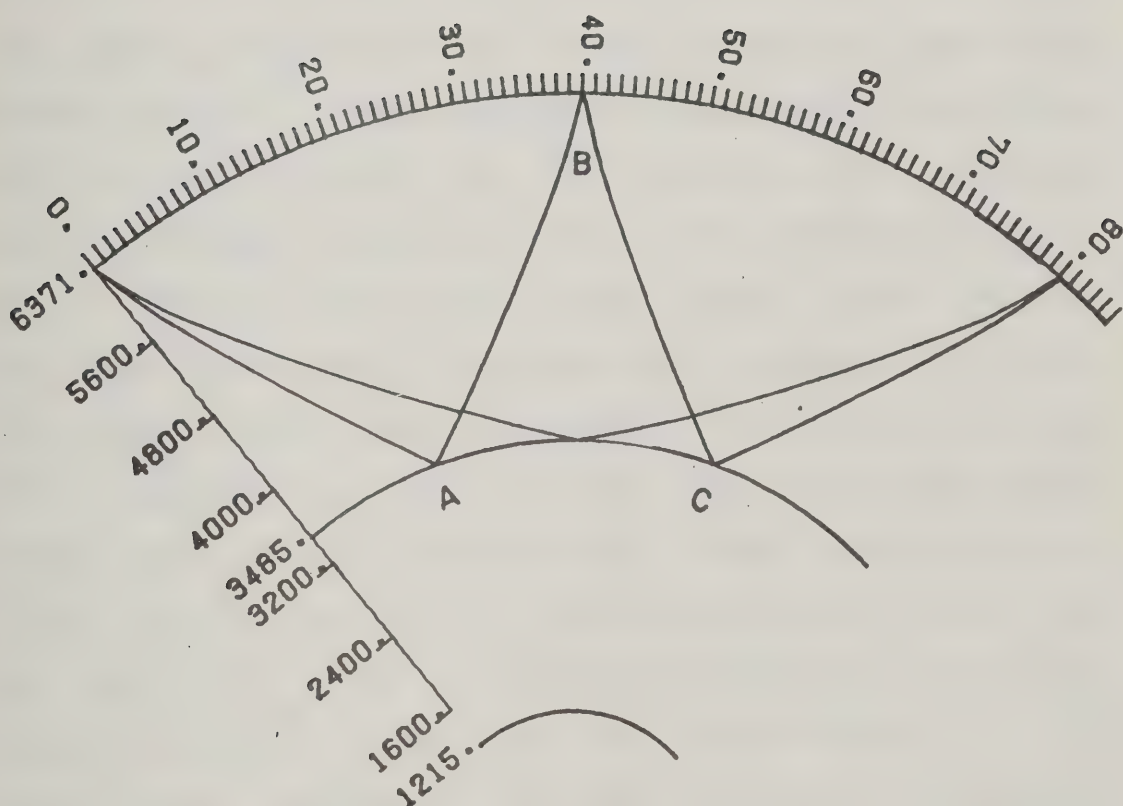
The studies mentioned so far did not use PcP-P or ScS-S travel times with the express purpose of studying lower mantle inhomogeneities, but the possibility was shown, and several studies followed using differential travel times for that purpose. Jordan and Lynn (1974) and Jordan (1975) used a set of PcP-P and ScS-S travel times with events from South America as recorded in North America. By correlating the ScS-S residuals with S residuals, they were able to show the existence of a high velocity region in the lower mantle below the Caribbean. Sipkin and Jordan (1975) studied world wide ScS-S travel times to show that the difference between oceanic and continental areas extends to a depth of 400 km. A similar study was done by Baumgardt (1976) using PcP-P travel times, and he, like Sipkin and Jordan, found that velocities under continents are higher than under oceans.





Figure 2.2

The ScS and double reflected ScS2 rays. The numbers to the left are distances in km from the earth's center.





Okal and Anderson (1975) criticize the work of Sipkin and Jordan arguing that the only 4 stations used to represent oceanic lithosphere are on oceanic islands less than 30 million years old, and are not a very typical representation of oceanic lithosphere. To overcome this problem Okal and Anderson used multiple ScS phases, that is, S waves reflected off the core and surface of the earth several times. For instance by taking the difference in travel time between the once core reflected ScS and the twice core reflected ScS<sub>2</sub> phase (see fig 2.2), station and source anomalies are eliminated and gross anomalies must be along the surface reflected ray A-B-C. By choosing rays having reflection point B under "normal" Pacific crust, the problem of having rays sampling the crust-mantle under anomalous oceanic islands should be avoided. Okal and Anderson claim that an anomaly in the differential travel time ScS<sub>2</sub>-ScS will be an indication of an anomaly in the upper part of the ray A-B-C. Clearly this interpretation is not unique and it seems likely that any part of the ray A-B-C could pass through the anomaly. Nevertheless, their results seem to indicate that the majority of inhomogeneities are found in the upper 200 km of the mantle. The one way travel time residuals in ray A-B vary from +5 over oceans to -3.5 seconds over continents and Okal and Anderson could show that there was a correlation between the size of the anomaly and the age of the plate. Younger parts of a plate (near ridges) have a more developed low velocity zone and thus



larger one way S-travel times, while the opposite is the case for the older parts of the plate. By comparing possible models with the travel time residuals, Okal and Anderson concluded, that their observations could be explained by a lateral changing velocity in the upper 200 km of the mantle.

Sipkin and Jordan (1976) also used multiple ScS phases and thereby confirmed their results from 1975, still claiming that ocean continent differences extends to depths exceeding 400 km.

The very special differential travel time ScS-P is used by Choudhury et al (1975) in a study of events from the South Pacific, recorded in Antarctica. In the distance range used (50-60 degrees), the ScS and P travel time curves have almost identical slope, making ScS-P times distance independent and thus eliminating errors arising from epicenter mislocations. On the other hand, ScS-P times are very sensitive to the depth of the earthquake and Choudhury et al use the ScS-P times to show the existence of lateral inhomogeneities in the source region.

Engdahl (1975) studied deep focus events from Fiji and Tonga as recorded at Alaskan stations. He calculated the difference in P travel times for two groups of stations, thereby eliminating errors due to event mislocation, near source inhomogeneities and wrong origin time. A large number of such differential travel times for different events were determined, and it became clear that the residuals differed





from events in the northern and southern region of Fiji - Tonga. Because of the proximity of the two groups of recording stations it was concluded that the difference in travel time most likely originated close to the earthquakes. Johnson showed that in the Fiji-Tonga region, there must be lateral differences in the mantle below a depth of 700 km depth, that is, lower than plates, as defined by earthquakes, are depicted. This could be an indication that plates are sinking well below the depth of the deepest earthquake.

#### THE\_RAY\_PARAMETER\_p

Since the introduction of the seismic array some of the problems related to travel time studies have been avoided. The array samples the wave front at several spatial locations and it is thus possible to directly determine the slowness,  $p = dT/ddel$ , by measuring the time difference in arrival time,  $dT$ , between sensors separated by  $ddel$ . The slowness can also be measured as the slope of a travel time curve, but errors in event location and origin time will then affect the value of  $p$ . An additional parameter measured by the array is the azimuth,  $Az$ , or the direction from which the waves arrive. The ray parameter can then be represented as a vector,  $p$ , with magnitude,  $p$ , and direction determined by  $Az$ . The azimuth measurement is very useful since deviations of the ray path from a great circle path indicate that lateral inhomogeneities exist somewhere along the ray.



Also the measurement of  $p$  is important since a small velocity anomaly can affect the value of  $p$  quite significantly without giving a travel time anomaly. Furthermore  $p$  is very sensitive to the velocity,  $v$ , at the bottom of the ray path where  $p = r/v$ ,  $r$  being the distance from the center of the earth to the bottom point of the ray.

Interpretation of anomalous p-Az values: An anomaly in  $p$  or  $Az$  can have its origin anywhere along the ray path, so, as in travel time studies, some method must be used to estimate where the anomaly is located. A lateral inhomogeneity in the crust under the array can severely change the observed value of  $p$ - $Az$  by introducing different delays in the travel time to the different sensors. A large scale inhomogeneity, larger than the array aperture, will give consistent changes in  $p$ - $Az$  for measurement from different events, and can therefore be corrected. Medium scale inhomogeneities (similar in size to the array aperture), will give fluctuating anomalies in  $p$ - $Az$  for different events and correction is difficult. Small scale anomalies will appear as random noise in an array with many detectors and may cancel out or be treated by time sequence analysis. Similar structural inhomogeneities at the source will affect the observed values of  $p$ - $Az$  much less than at the receiver. Since the ray bundle arriving at the array only spreads out 100-200 km, the individual rays at the source side will be very close together, and thus get about the same time delay



from any small scale anomalies there. Larger scale anomalies at the source can change the direction of the whole ray bundle, but from fig 2.3 it is seen that the effect is small at the receiver side. Davies and Sheppard (1972) estimated that the maximum error in  $p$  and  $Az$  to be expected from source anomalies would be 3% and 2 degrees respectively.

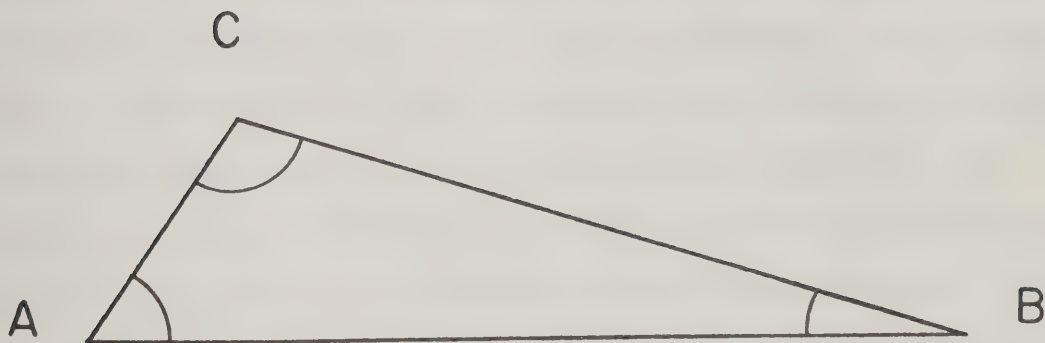
p-residuals: A large number of studies using the ray parameter have the objective of determining  $p$  as a function of distance since this relationship is used in the Herglotz - Wiechert inversion to calculate velocities in the earth. As a by-product of these studies, lateral inhomogeneities are often suggested to explain discrepancies between different studies, or differences between velocity models from different regions. Toksoz et al (1967) made a global study of inhomogeneities in the mantle using  $p$  values from LASA. On plotting  $p$  versus  $\Delta$  for results coming from 2 different directions ( $Az = 140$  and  $310$  degrees) it was found that the curves differed significantly in the distance range  $65-87$  degrees. Toksoz et al argued, that since the angle of incidence for the rays to LASA, in that distance range, only changes 6 degrees, this difference could not be a receiver effect and the most likely explanation would be a lateral difference in the velocity gradient at depths  $1800-2600$  km. This interpretation is made under the the assumption that the lateral difference is located at the deepest point of the ray. Chinnery (1969) used  $p$  data and travel times from





Figure 2.3

An azimuthal anomaly as seen by the array. The anomalous velocity gradient is located at C and it causes an azimuthal anomaly, angle A, as seen by the receiver and angle B at the source. If source and receiver were interchanged it is seen that the azimuthal deviation as observed by the receiver would be considerable less than in the first case. In general the observed azimuthal deviation for the same velocity anomaly decreases with the distance to the anomaly.







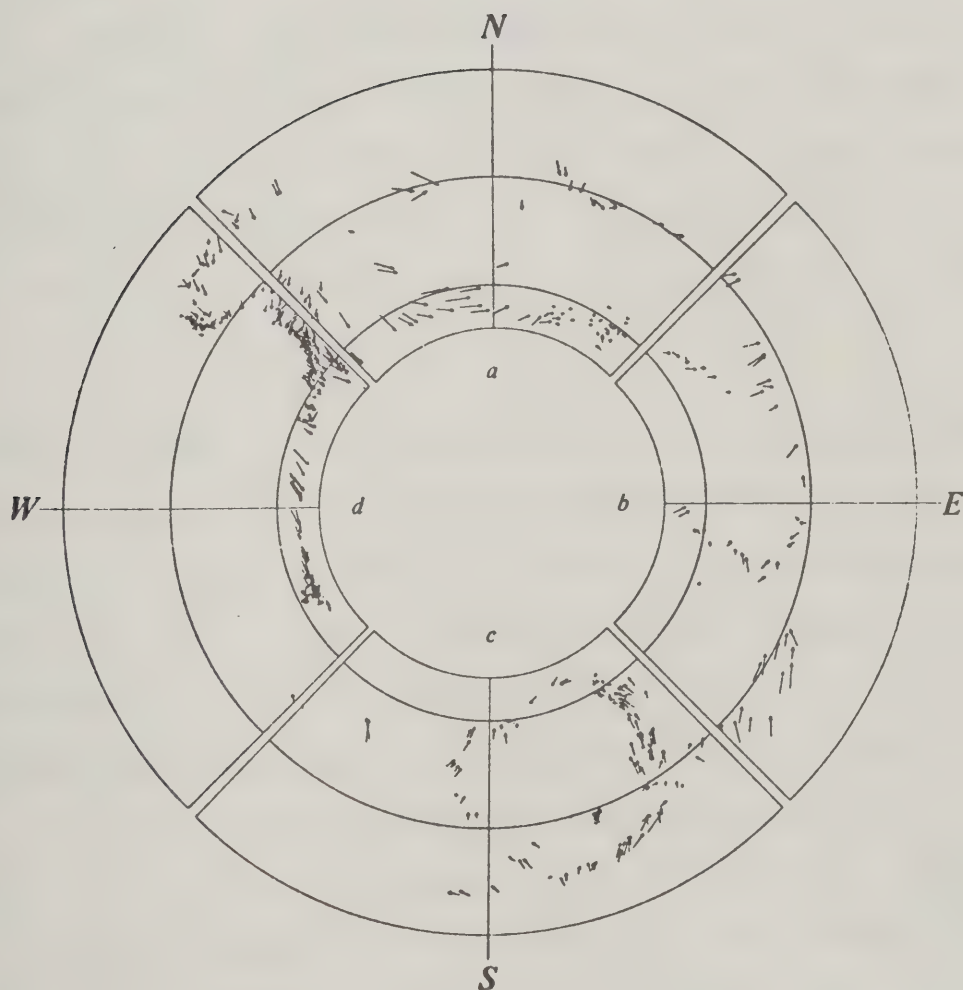
LASA, and also found inconsistent results for distances greater than 80 degrees. He also suggested lateral inhomogeneities in the deeper mantle as an explanation. Johnson (1967, 1969) inverted a large set of  $p$  observation into velocity models for the mantle. Comparing his results for the lower mantle with results from other studies he found different velocities at the same depth and therefore suggested that the lower mantle varied laterally. Several other studies using comparable techniques obtained similar results.

A common feature of many array studies is that the major objective is to get a slowness-distance curve so azimuth anomalies are not interpreted. With the accumulating evidence for lateral inhomogeneities in the mantle more attention has been given to the measurement of azimuth. Davies and Sheppard (1972) used the LASA array for a global study yielding both  $p$  and  $Az$ , which were combined into a vector  $p$ . They plotted the vector residual between the observed and calculated  $p$ -vector in an array diagram, (see fig 2.4). At a glance it is possible to see from which ray path the anomaly originate, and also the direction and magnitude of the anomaly. Davies and Sheppard found that part of the anomalies could be ascribed to crustal variation under the array but several variations in the  $p$ - $Az$  anomalies were fluctuating too fast with  $Az$  to be a station anomaly. It was concluded that lateral inhomogeneities probably can



Figure 2.4

An example of an array diagram. The figure is from Davies and Sheppard (1972) showing results from the LASA array. The outer circle represents a slowness value of 10 sec/deg while the inner circles are at 7.5, 5.0 and 4.0 sec/deg. Directions north (N), south (S), east (E) and west (W) are as seen from the center of the array.





be found at all levels of the mantle and only some of them are related to surface feature like hot spots and subduction zones.

Wiechert (1972) found azimuth anomalies for rays arriving at the Yellowknife array and bottoming under the Aleutians. To exclude structure near the array, as responsible for the anomalies, Wiechert looked at the p-Az anomalies at subarrays and found the same variation in the p-Az deviations, as using the whole array. Comparison of his observations with array measurements elsewhere showed similar results for rays bottoming in the same region, but having different origin. Source anomalies could therefore be excluded and Wiechert concluded that most likely lateral inhomogeneities exists near the bottoming points of the rays. Several other similar studies are mentioned in table 2.1.

The seismic array can be used to locate earthquakes. The epicenter can be located using the measured azimuth and a distance obtained from a p versus distance table. This method is not very accurate, since small scale inhomogeneities can give significant anomalies in p and Az and thus giving a mislocation the event. Knowing where the event is from conventional travel time determination, it is possible to use the anomalous array mislocation. Powell (1976) study patterns of mislocations for several deep events, using 3 seismic arrays, and interpreted the results





in terms of heterogeneities below the subduction zones at depths of at least 650 or 800 km. Kanasewich et al (1972, 1973) used the VASA and PEACE arrays for measuring p-Az rays bottoming in the deeper mantle at points having a surface projection at or close to Hawaii. Low values of  $p$  were found for these rays compared to rays from other parts of the world to VASA. Because of the consistency of results from the two arrays and from several different events, source anomalies were ruled out. Since the  $p$  measurements for other ray paths did not produce any large anomalies no significant station anomaly was expected. The low  $p$  values for rays under Hawaii were then ascribed to a velocity anomaly at the deepest point of the ray, where  $p = r/v$ , and thus interpreted in terms of a high velocity anomaly at depths between the core-mantle boundary and 500 km above. Kanasewich and Gutowski (1975) confirmed previous results by using the LASA and VASA array and making more use of the azimuth anomalies. The horizontal dimension of the high velocity region could be limited to 150 km.

Wright (1975) criticized Kanasewich et al's interpretation of the p-Az data and argued that anomalies, such as observed for the rays under Hawaii, are often seen without having any correlation with deeper mantle inhomogeneities. Also, the velocity anomaly does not have to be at the deepest point of the ray, but could originate somewhere between Hawaii and North America. Wright (1975, 1973) presented data from the Yellowknife array using rays



which bottom just north of the area sampled by Kanasewich et al, and found no anomaly. Wright also claimed that the argument for ruling out anomalies under VASA is not valid, since the UK type arrays show similar anomalies in  $p$ -Az arising from crustal structure under the array. Kanasewich et al (1975b) replied that these comparable anomalies were measured with small arrays which are much more sensitive to crustal variations, and that no comparable crust related fluctuations in  $p$ -Az have been found at the large aperture VASA array. Okal and Kuster (1975) used a 50 km aperture array on two island groups in French Polynesia and showed that large anomalies in  $p$ -Az could be found for rays bottoming under Hawaii if individual island arrays were used. However combining the two subsets into an oblong array, 350 km in length, the anomalies were found to cancel. They used this as an argument against the interpretation by Kanasewich et al, but according to their fig 4, only 4 rays in the vicinity of Hawaii were used, and it is difficult to see exactly where the rays bottom relative to the data given by Kanasewich et al. More questionable is their combination into an odd shaped array of seismic structures from two groups of Pacific Islands. Berteusson (1975) made a similar study with the LASA array and concludes that the LASA array is not big enough (similar in size to the VASA array), to rule out the effects of local small scale lateral inhomogeneities, and thus the Hawaii anomalies seen with VASA were probably generated under the array.



The previous discussion shows how ambiguous the interpretation of p-Az data is and additional information must be obtained somewhere. In the case of Hawaii additional information comes from a study by Best et al (1974). They used travel times of ScS3 with both earthquake and receiver on Hawaii, thus sampling only the mantle directly below Hawaii. Their results showed the two-way travel time was faster than normal, the anomaly being 0.7 sec. for a J-B model and 5.3 sec. for the Jordan model B1. So somewhere between the surface and the core-mantle boundary there is material with relatively high velocity and the interpretation by Kanasewich et al cannot be discarded.

P-waves diffracted around the core sample a large area of the core-mantle boundary. Alexander and Phinney (1966) and Phinney and Alexander (1968) used ratios of spectral amplitudes of diffracted P-waves around the core-mantle boundary and could thereby calculate the attenuation at the core-mantle boundary as a function of frequency. They found significant differences in attenuation for different regions, and in general, a difference between the core-mantle boundary under the Central Pacific and the Africa - North Atlantic area. Needham and Davies (1973) made an amplitude study of diffracted P-waves recorded at LASA and station BMO. They found significant differences in amplitude for different rays and could show that lateral inhomogeneities in the lowest 100 km of the mantle would most easily explain





the observations. Sacks and Snoke (1976) used amplitudes of core phases having near-grazing incidence at the core-mantle boundary (and thus high sensitivity to anomalies on the core-mantle boundary) and compared them with near vertical incident phases (low sensitivity to core-mantle boundary anomalies). The data was interpreted in terms of lateral inhomogeneities close to the core-mantle boundary.

Several studies have shown the possibility of scattering of short period P-waves at all levels in the mantle. Doornbos (1976) analyzed precursors to PKP at the NORSAR array. Combination of measurement of  $p$ ,  $A_z$ , travel times and spectral ratios of PKP and its precursors were most easily interpreted in terms of scattering in the lower mantle. Scale length of anomalies was thought to be 10-30 km. Wright (1975) also studied the precursor to PKP at the Yellowknife array and gets similar results. Husebye and King (1976) used precursors to PKIKP recorded at NORSAR and also show that they originate by a scattering process close to the core-mantle boundary.

A broad study by Toksoz et al (1969) made use of spherical harmonic analysis of various geophysical data such as seismic travel time residuals, heat flow, crustal thickness, and surface topography. The amount of correlation between the different geophysical parameters was calculated and it was found that at long wavelengths ( $n \leq 6$ ) gravitational, heat flow and seismic travel time variations





were not correlated with topography. It was also found that gravity and seismic travel time anomalies could not be compensated for in the crust and therefore large scale mantle inhomogeneities would have to exist. Dziewonski et al (1975) inverted free oscillation data, P-wave travel times and surface wave dispersion data in terms of velocities. Continent - ocean differences were found to exist to a depth of 400 km. Below that depth no velocity anomalies were found greater than 0.2% for P and 0.4% for S. These values correspond well with a more comprehensive global study by Dziewonski (1977) which was discussed previously.

Despite much ambiguity in the interpretation of seismic observations there is no doubt that lateral inhomogeneities do exist at all levels in the mantle. A problem exists with determining the exact location and the size and magnitude of the anomalies. The size seems to vary from 10 to several thousand kilometers and the magnitude of the anomalies is in general, larger for small scale anomalies than for larger ones. The maximum deviation reported is 10% in velocity. Most inhomogeneities seem to be located either in the upper mantle or in the lowest few hundred kilometers of the mantle.



Table 2.1

References to lateral inhomogeneities in the mantle. Depth and size is in kilometers, and magnitude is percentage of velocity, or the change in velocity in km/s, where P and S means P and S velocity respectively. The abbreviations are: p: The ray parameter; del: Epicentral distance; Az: Azimuth; CMB: The core mantle boundary; h: Depth; har. an.: harmonic analysis; vs: Versus.

METHOD	LOCATION	DEPTH SIZE, MAGNETUDE	AUTHOR
P travel times	-	lower mantle - , P 0.1	Hales et al 1970
P travel times	Central Asia	h<400 - , -	Bugayevskiy et al. 1970
travel times and wave shape	-	- 100-1000, -	Nersesov et al. 1972
P-travel times	N. Hemisphere	h>2000 1000, -	Julian and Sengupta 1973
S travel times	North Pole - Iceland	h=2500 , 1%	Niazi 1973
P-travel times and azimuth	Scandinavia	h>600 1000, -	Brown 1973
P, S, PcP, ScS 3-D inversion	World	h>2500, h<500 500, 2%	Sengupta and Toksoz 1976
P-travel times 3-D inversion	World	h>2500 >1000, 0.5%	Dziewonski et al. 1977
P-travel times WWSSN library	Indian Ocean Himalaya	h>2000 2000, -	Ou 1977
ScS-S travel times	-	lower mantle - , -	Hales and Roberts 1970
ScS-S travel times	Caribbean N. Pac., Alas.	close to CMB - , -	Mitchel et al. 1973
PcP-P times PcP/P amplit.	North of 60. parallel	lower mantle - , -	Buchbinder and Popinnet 1973



PcP-P, ScS-S travel times	Caribbean	600<h<1400 2000, -	Jordan and Lynn 1974
ScS-S travel times	World	0<h<400 Cont. vs Ocean	Sipkin and Jordan 1975
PcP-P travel times	N. Hemisphere	lower mantle Cont. vs Ocean	Baumgardt 1976
PcP-P travel times	NW. Atlantic	close to CMB	Stewart 1977 1000, >2%
multiple ScS travel times	World	h<200 Cont. vs Ocean	Okal and Anderson 1975
multiple ScS travel times	World	h<400 Cont. vs Ocean	Sipkin and Jordan 1976
multiple ScS travel times	Hawaii	lower mantle - , -	Best and Johnson 1974
relative P travel times	Fiji Tonga	h>700 500, >10%	Engdahl 1975
difference in P p-del curves	N. Pacific Cen. America	1800<h<2600 - , -	Toksoz et al. 1967
scatter in p, P travel times	-	lower mantle - , -	Chinnery 1969
P wave p-del inversion	-	lower mantle - , -	Johnson 1969
p anomalies, P travel times	Atlantic Central Asia	1750<h<2300 - , P 0.1	Husebye et al. 1971
P p-del curves	SE. Asia	lower mantle 1000, P 0.1	Vinnik et al. 1972
S p-del curves	N. America Pacific	h<1000 Ct.vs.Oc, P 0.1	Robinson and Kovach 1972
P p-del curves P travel times	N. Asia	1700<h<2300 - , p 0.3	Kulhanek and Brown 1974
p and Az anomalies	World	500<h<CMB 200-1000, -	Davies and Sheppard 1972
p and Az anomalies	Aleutian	800<h<950 - , 2.5%	Wiechert 1972
P, pP, PcP, PnKP p-Az anomalies	N. Hemisphere	h>2500 - , -	Wright 1973





P, pP, PCP, PnKP	N. Hemisphere	$h > 1850$	Wright 1975
p-Az anomalies		- , -	
p-Az anomalies	Fennoscandia	$h < 1000$	Noponen 1974
P travel times		1500 , -	
p and Az anomalies	Hawaii	$2500 < h < \text{CMB}$	Kanasewich et al. 1975, 73, 72
		150 , -	
p and Az anomalies	Caribbean	$1900 < h < 2600$	Bates 1976
		- , -	
event mislocation patterns	S. Pacific	$h > 650$ , $h > 850$	Powell 1976
		500, -	
travel times	-	close to CMB	Sacks 1967
diff. P waves			
spectra of	Pacific, Atlantic, Africa	close to CMB	Phinney and Alexander 1969
diff. P waves		- , -	
amplitude of	Pacific	close to CMB	Needham and Davies 1973
diff. P waves		200 , -	
amplitude of	-	close to CMB	Sacks and Snoke 1976
core phases		- , -	
scattering of	-	close to CMB	Wright 1975
PKP waves		small, -	
scattering of	-	$2300 < h < \text{CMB}$	Doornbos 1976
PKP waves		10-30, 3%	
scattering of	-	close to CMB	Husebye and King 1976
PKIKP waves		small, -	
spherical har.	World	-	Toksoz et al 1969
an. geop. data		large , -	
free osc. and	World	-	Dziewonski et al. 1975
travel times		large, 0.2-0.4%	



## CHAPTER 3

### SEISMIC DATA PROCESSING

#### Methods selected for this study:

From the previous discussion of ways to detect lateral inhomogeneities, two techniques seem specially suitable. One is the use of differential travel times, PcP-P and ScS-S, and the other measurement of the seismic ray parameter. Since inhomogeneities of any dimension are to be expected, short period data will be preferred to avoid averaging out smaller scale anomalies. Specifically the short period ScS-S residuals will be investigated, since other studies have used only long period ScS-S.

The parameters p-Az will be measured for both P and PcP phases. By subtracting the p-Az values of P from those of PcP, it is hoped that these differential values will have a reduced bias due to source and station heterogeneities in much the same way as the differential travel times. Furthermore, whenever possible, a combination of travel time residuals and p-Az residuals will be used, thus hopefully eliminating some of the ambiguities in interpretation.



Data base and area studied:

The main source of travel time data was from earthquakes recorded with the WWSSN and Canadian network. Seismogram copies on microfilm from these stations were obtained from the World Data Center, National Oceanic and Atmospheric Administration, Boulder Colorado. A minor source was seismograms from the Edmonton station EDM, and digital recordings from the VASA array. Array data was exclusively from the VASA array from its operation in 1970 and 1974. All the data was for events in South and Central America as recorded in North America. Thus the projection of all the rays intersect in the vicinity the Caribbean and Central America. The reason for choosing this area is that North America has a dense network of seismic stations, and there are many earthquakes within an epicentral distance of  $80^\circ$  in South and Central America. The Caribbean is also tectonically complicated with some evidence for mantle inhomogeneities thus making it interesting to study. The theoretical travel times were calculated using the J-B seismological tables (Jeffreys and Bullen (1967)). Corrections were made for station elevation and ellipticity, the latter calculated using the Bullen (1965) formulation. Travel times for 18 phases were calculated for each event - station combination. For some of the phases travel time tables had to be constructed. For instance for the multiple reflection ScS<sub>2</sub>, travel times were derived from the ScS travel times. Also a routine had to be written for





calculating ellipticity corrections for phases such as PcP2, which are not in Bullen's tables. A program originally written by Dr. E.R. Kanasewich calculating travel times, distances and azimuths was extended to incorporate any combination of phases, stations and events. The input parameters only required the phase name, the station identifier and an assigned event identifier. The travel time tables and the station and event parameters are contained in separate files. All the output from the algorithm was printed on library cards, which are stored together with the corresponding seismograms on microfilm. Thus all the relevant information about any earthquake - station combination was available together with the seismograms on hand. An example of the two output cards is shown in table 3.1 and fig 3.1 shows some of the phases for which travel times were calculated.

About 3500 six component seismograms were searched for the phases ScS, ScS2 PcP and PcP2. With the aid of theoretical arrival times for all phases which are expected to have easily detectable amplitudes the phases were identified or rejected if no reliable identification could be made. Only high quality arrivals with a clear onset were used. If a core reflected phase was identified both the direct and reflected phase (for example S and ScS) were read on all seismograms if possible. Also the differential travel time from peak to peak was read, if the corresponding peaks could be identified. Finally the P arrival time on the short





Table 3.1

An example of the two cards giving all the relevant data for the event GT74 5 recorded at station JCT.

## Card 1

```

JCT                      GT74 5
JUNCTION CITY (WWNSS)    TEXAS
STATION DATA: LAT,LON(DEG),ELEV(KM)
  30.479 -99.802 0.591
EVENT DATA: ID AND LOCATION.
GT74 5    SOUTHERN PERU
LAT,LON(DEG):  -15.00 -72.20
DEPH(KM) AND MAG.  113.0  5.8
ORIGIN TIME:  27  4 74  6  1 47.30
DISTANCES AND AZIMUTHS:
SEISM DIST(DEG):  52.42
GEOC DIST(DEG):  52.45
GEOC DIST(KM):  5832.0
GEOC AZM(DEG) EV:  329.70
GEOC AZM(DEG) ST:  145.61
THE FOLLOWING CARD HAS PHASE ARR. TIME(HR,MIN,
SEC), RAY PARAMETER P(SEC/DEG), APPARENT VELOCITY
APPV(KM/SEC), ANGLE OF INCIDENCE AINC(DEG)
ELLIPTICITY CORRECTION CELL(SEC) AND STATION
ELEVATION CORRECTION          CSUR(SEC)

```

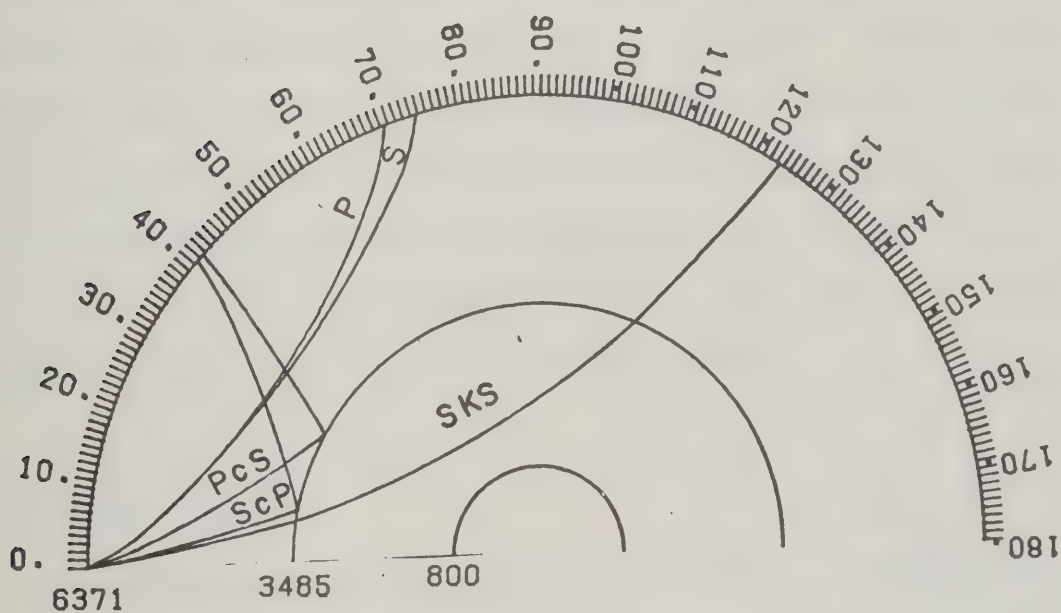
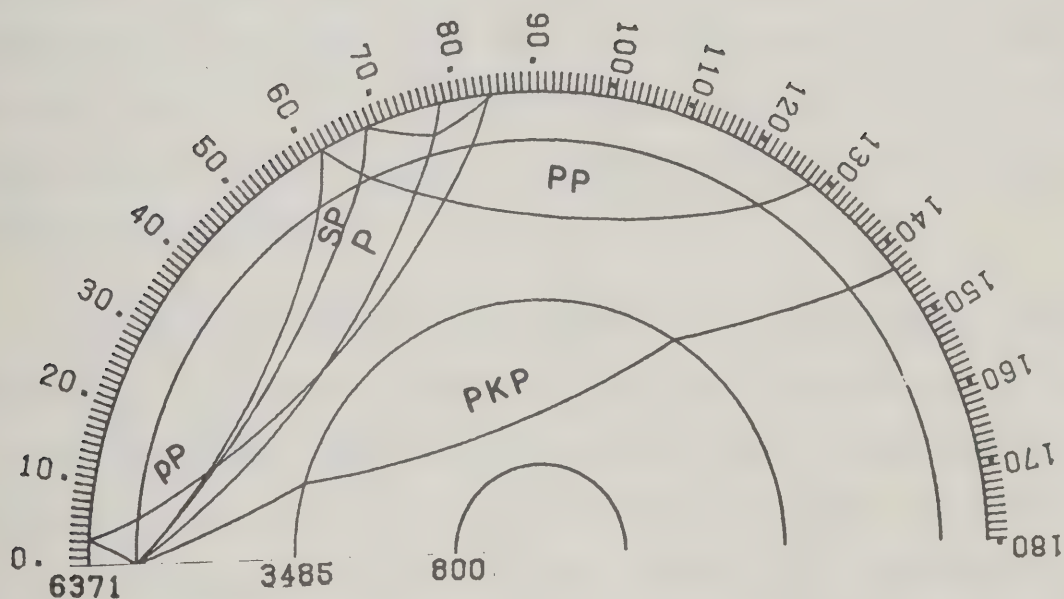
## Card 2

JCT	GT74 5							
PHA	ARR	TIME	P	APPV	AINC	CELL	CSUR	
P	6 10	50.71	7.44	14.9	15.5	0.35	0.15	
PKP	0 0	0.0	0.0	0.0	0.0	0.0	0.0	
S	6 18	6.64	13.59	8.2	16.3	0.62	0.27	
SKS	0 0	0.0	0.0	0.0	0.0	0.0	0.0	
PP	6 12	52.59	9.16	12.1	19.2	0.67	0.16	
SS	6 21	45.25	16.53	6.7	20.0	1.21	0.27	
P-P	6 11	17.65	7.64	14.5	16.0	0.35	0.15	
S-P	6 11	30.27	7.54	14.7	15.7	0.35	0.15	
PCP	6 12	0.01	3.72	29.9	7.7	0.42	0.15	
PCP2	6 19	44.56	2.29	48.6	4.7	1.11	0.15	
SCP	6 15	45.71	4.35	25.6	9.0	0.58	0.15	
PCS	6 15	57.24	4.30	25.9	5.1	0.58	0.26	
PS	6 14	13.14	0.0	0.0	0.0	0.62	0.26	
SP	6 19	2.01	14.31	7.8	31.0	0.62	0.17	
P-S	6 7	3.61	0.0	0.0	0.0	0.62	0.26	
S-S	6 18	53.88	13.65	8.1	16.4	0.62	0.27	
SCS	6 20	26.19	6.97	16.0	8.3	0.75	0.26	
SCS2	6 34	30.40	4.25	26.2	5.0	2.01	0.26	



Figure 3.1

Some seismic phases from a deep (top) and a shallow (bottom) earthquake. The numbers to the left are the distances in km from the earth's center.





period Z (vertical) was read, and all readings were given an estimated reading error. From the observed travel times, the residuals were calculated.

Unfortunately many records were of poor quality with either no core reflected phase or a poor direct phase. Differential residuals from only 42 different rays were obtained for the PcP or ScS phase and none for PcP2 and ScS2. The data base obtained was augmented by results in the published literature.

Data from the VASA array (figure 3.2), operated by the University of Alberta, was used. The array consists of up to 7 stations each having two horizontal (NS and EW) and one vertical seismometer (Z). The stations have been relocated in each running season, thereby making it possible to examine the effect of varying aperture and crustal structure. The field data, recorded digitally at each station, was edited and transferred to a master tape. This master tape contains all the data from each event together with information about the earthquake. Thus the master tape very conveniently contains all relevant data for processing. For more detailed information about the VASA array see Kanaswich et al (1974) and and Bates (1976).

#### Calculation of p-Az

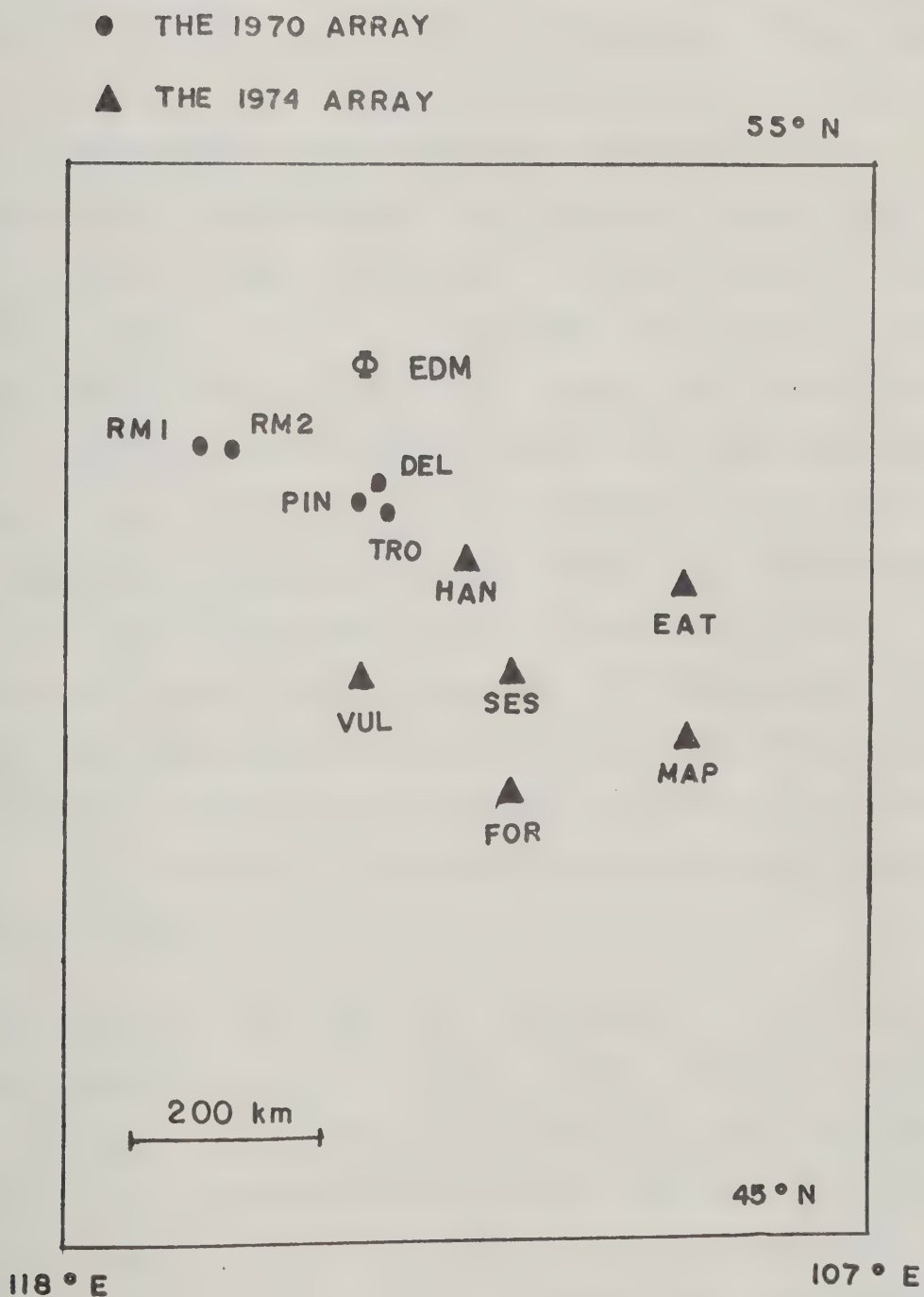
Assuming that the array is located in a 2 dimensional cartesian coordinate system, the arrival time,  $t(x,y)$  of a





Figure 3.2

The location of the VASA arrays in Alberta. The Edmonton station EDM was part of both the 1970 and 1974 array.





plane wave at each seismometer can be written as

$$t(x,y)=t_0 + p_1 * x + p_2 * y \quad (1.1)$$

where  $t_0$  is the arrival time at the origin and  $p_1$  and  $p_2$  are the  $x$  and  $y$  components of the ray parameter  $p$ . From the arrival times for at least 3 stations a unique but not necessarily correct  $p$  and  $Az$  can be determined. With more than 3 stations no unique solution can be obtained since local inhomogeneities will introduce inconsistent delays at the individual seismometers. The arrival times must be fitted to (1.1) to find  $(p_1, p_2)$  in a least squares sense (Husebye (1969)), and the resulting  $p$ - $Az$  will be a more reliable average for the area. The effect of small scale random inhomogeneities is then averaged out. The success of this operation is a function of the number of stations and the geometry of the array (Bates (1976)). For reducing the effect of crustal inhomogeneities a large array, with an aperture of at least 150 km (like the 1974 VASA array), will be best for the study of teleseismic arrivals since delays in the arrival times, caused by local structure then give smaller relative error in the travel time difference between pairs of stations.

A superior technique for determining  $p$ - $Az$  is by a velocity spectral analysis. The so called VESPA technique used by Davies et al (1971) involves the formation of a beam by delay and summation of the seismic traces of an array, and the determination of the power in the beam over a specified time window, which is stepped down the record.



Using a fixed azimuth a two dimensional plot (called a Vespagram), of power as a function of  $p$  and time, can be made. A further improvement of the VESPA technique is the so called COVESPA technique designed by Gutowski and Kanasewich (1974). Instead of power, a coherency,  $CC$ , is calculated as a function of slowness,  $p$ , and time  $t$ ;

$$CC(Az, p, t) = \frac{2}{M*(M-1)*T} \sum_t \sum_k \sum_i \frac{f_{i,t} * f_{i+k,t}}{\sqrt{\sum_t f_{i,t}^2 * \sum_t f_{i+k,t}^2}}$$

where  $M$  is the number of stations,  $k$  is an incremental integer on channel  $i$  ( $i \neq k$ ),  $T$  is the length of the time window and  $f_{i,t}$  is the amplitude of the signal at  $i$ 'th channel at time  $t$ . The computation starts by inserting time delays into the signals from each station corresponding to the chosen  $p$  and  $Az$ . Then for each time along the records, the zero lag cross correlation of all combinations of two stations, within the time window  $T$ , is computed, normalized to unity and summed. The coherency is one if, at a given  $p$ ,  $Az$  and  $t$ , the phases and wave forms of the signals, within the window, are identical at all stations. A contour plot (COVESPAGRAM) similar to the VESPAGRAM can be plotted with  $CC$  as a function of  $p$  and  $t$ , see fig 3.3. A difficulty with the COVESPAGRAM is that, the azimuth is fixed and since it is really a function of time,  $p$  will only be correct at a time where the azimuth has the assumed value. For instance

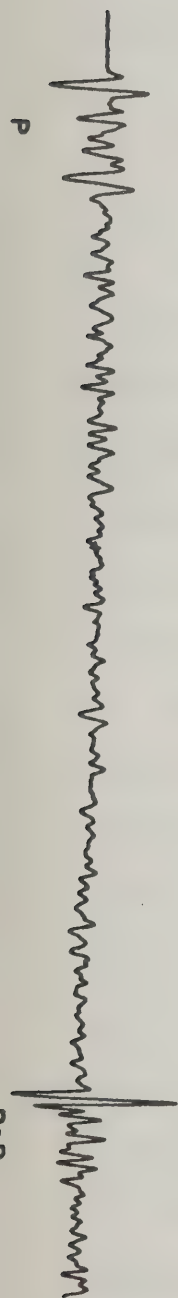
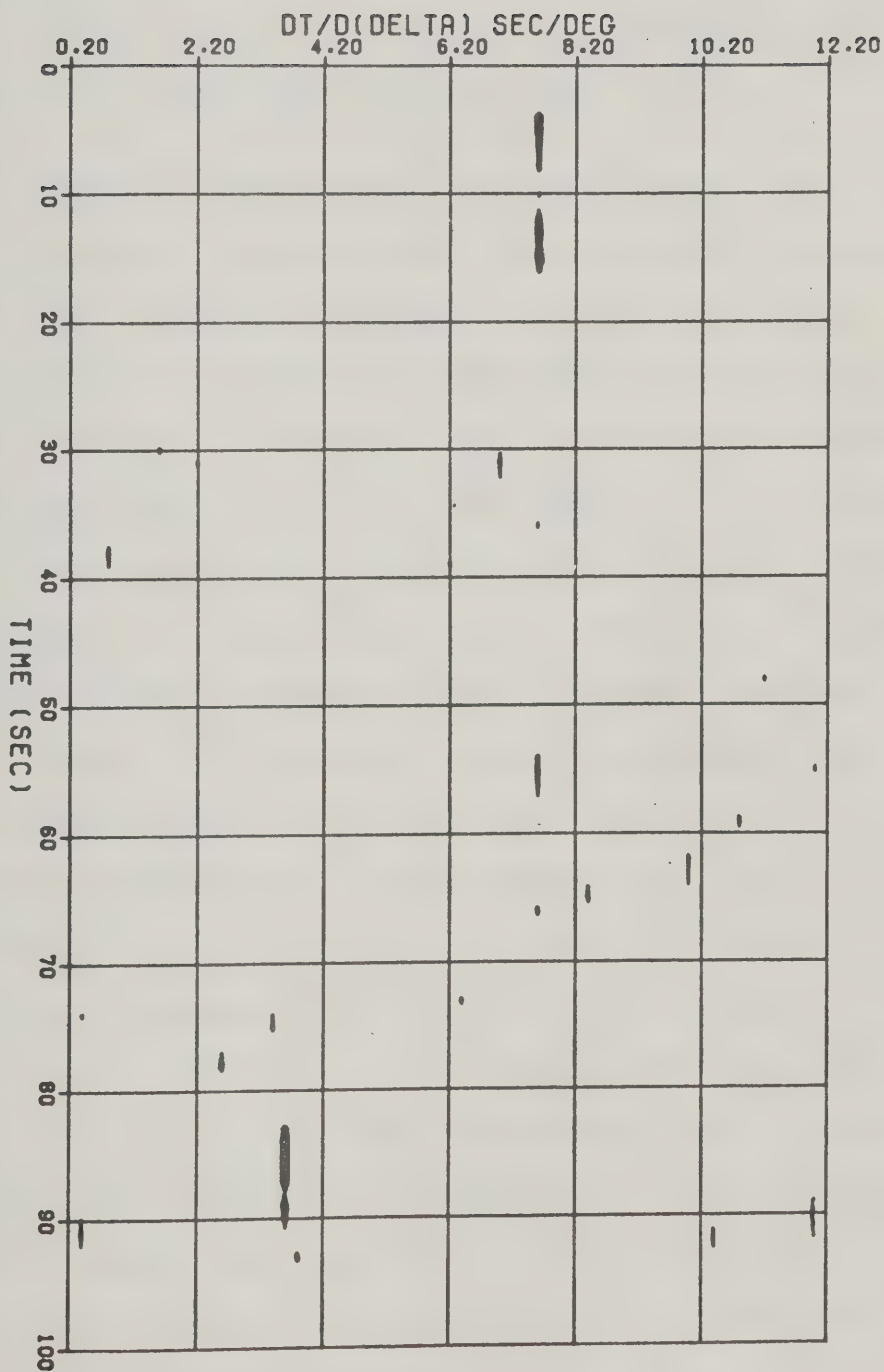






### Figure 3.3

A covespagram showing the arrival of both the P and PcP phases. Below the covespagram is shown one of the corresponding seismograms (same time scale) recorded on the vertical channel at station VUL. The event is from Panama arriving at an azimuthal direction of  $130^{\circ}$ . The magnitude of the event is 5.9 and the depth is 15 km.





if P and PcP do not arrive from the same direction, the p value of either P or PcP will be incorrect. Gutowski showed that the COVESPA technique was superior to the VESPA technique in terms of resolving power, sidelobe leakage and sensitivity to amplitude variation over the array.

The COVESPA technique is especially useful for an array with few stations, since the data is used more efficiently, and it was therefore decided to use this method for determining p and Az for the P and PcP phases. The original program written by Gutowski was modified as follows. To determine the best p and Az at each time, t, the original program calculated and printed out a whole series of Covespagrams for different Az. By fitting a parabolic surface to values of coherency near a maximum the best p and Az was found at discrete times. The Az value which best represented the whole wave train was chosen to make the Covespagram. Since Az (and p) changes with time, it seems more natural to look at CC as a function of p and Az at each time t. Thus for each discrete t the current program prints out CC as a function of p and Az (see table 3.2). The response of the array was calibrated in a computer simulation for each event by using a test signal. This was achieved by giving each station a mixture of up to 3 time signals with delays corresponding to 3 specified p-Az values. The signals had the form

$$A * \sin(2\pi t/T1) * (1 - t/T2) \quad (3.2)$$

where A is the amplitude, T1 the period of the signal and T2



Table 3.2

Typical covespagrams for the PcP and P phases. The covepagram is calculated for an event in the Panama area using the stations EAT, HAN and SES. The top matrix shows the covespagram for the P phase and the bottom one for PcP. Using an arbitrary value for time = 0, P arrives at time T = 3 seconds and PcP at T = 68 seconds. The numbers in the matrix are the coherencies (multiplied by one hundred) as a function of azimuth (first column) in degrees and slowness (first row) in sec/deg. Zeroes indicate negative coherencies

## The P phase.

T= 3	6.50	6.80	7.10	7.40						
130.0	0	0	0	0	0	0	0	0	6	0
131.0	0	0	0	0	0	0	0	0	0	0
132.0	0	4	5	10	9	0	0	0	0	0
133.0	0	59	52	68	73	40	0	0	0	0
134.0	0	8	78	92	99	87	56	1	0	0
135.0	0	0	53	86	91	95	79	27	0	0
136.0	0	0	0	43	77	73	77	56	8	0
137.0	0	0	0	0	13	22	0	15	23	0
138.0	0	0	0	0	0	0	0	0	0	1
139.0	0	0	0	0	0	0	0	31	40	57
140.0	0	0	0	0	0	0	0	48	79	82

## The PcP phase.

T= 68	3.20	3.50	3.80	4.10						
130.0	0	0	0	0	0	0	0	0	0	0
131.0	0	0	0	9	15	0	0	0	0	0
132.0	0	0	0	19	15	24	9	0	0	0
133.0	0	0	9	28	40	35	30	0	0	0
134.0	0	0	21	50	53	59	42	23	0	0
135.0	0	1	26	59	73	77	63	34	16	0
136.0	0	0	25	61	75	92	80	51	32	0
137.0	0	0	15	54	80	88	84	61	29	2
138.0	0	0	11	40	67	88	83	65	26	0
139.0	0	0	0	20	49	64	62	53	26	8
140.0	0	0	0	0	28	43	45	36	25	0





the duration of the signal. Calculating the array response makes it possible to see the effect of period, array geometry, and having a mixture of signals with different p-Az values. An example is shown in table 3.3. A station elevation correction was made to reduce the values of p-Az to corresponding values at sea level. Thus errors due to differences in station elevation were eliminated (the maximum was 0.03 sec/deg. in p and  $0.5^\circ$  in Az). A bandpass filter was included in the program to improve the signal to noise ratio. A significantly better determination of p-Az was then possible with signals contaminated by noise. In the original program it was assumed that the wave front was a straight line (along a great circle), but that is only true if the epicentral distance is  $90^\circ$ . A correction was made by calculating the additional distance, the wave front has to travel from one station to another assuming a curved wave front (small circle on the earth's surface). For a medium sized array (aperture  $< 75$  km), the correction is insignificant, but for the largest possible configuration with the VASA array, the error in p and Az could be as much as 0.2 sec/deg and  $2^\circ$ . Typical errors in this study were 0.05 sec/deg and  $0.5^\circ$ .

#### Testing and using the Covespa program

Numerical experiments were performed to determine the best values for the parameters in the algorithm. The time window was set equal to 1 second (comparable to the periods of the signals) and a p-Az value was read at a time close to



the start of the phase where the highest coherency was found. Usually a value of  $CC > 0.8$  existed within the two first cycles of arrival of P or PcP. The P-Az grid size was decreased until the p-Az values were determined to an accuracy approaching a maximum of 0.02 sec/deg. and  $0.5^\circ$ . The number of stations and the station configuration was very important. Since local inhomogeneities will introduce different time delays for each station it is only to be expected that the coherency will decrease with a larger number of stations, and greater station separation. The 1975 VASA array was large (see fig 3.2) with 6 portable stations in Southern Alberta plus the Edmonton station. By using different combinations of the stations it was found that different combinations of the portable stations gave reasonably consistent results. Different 3 - station combinations gave maximum differences in p and Az of 0.2 sec/deg and  $3^\circ$ , while a simultaneous solution using 4 or more stations reduced the differences to 0.05 sec/deg and  $0.5^\circ$ . Including the station EDM greatly reduced the coherency and stability of the results. This is probably because EDM is relatively far away from the group of portable stations, thus making the difference in crustal structure more significant. Also the array is less symmetric with EDM, and Bates (1976) showed theoretically that the most stable results are obtained by using a symmetric array. Elongating the array will have the effect of making the determination of p and Az less reliable, see the example in



table 3.4. Consequently the EDM station was not used in the 1974 data. Another important result, arising from comparing p-Az values from different station combinations, was that, although different combinations gave different values of p-Az, the difference in p-Az between the phases PcP and P remained constant for different combinations. Thus the effect of local inhomogeneities seems to be the same on p-Az for P and PcP, and therefore a difference will cancel out the effect. In the 1970 array, the array was smaller and closer to EDM so that all stations could be used. The coherency, in general was higher than for the 1974 array, because the array was smaller, but that also had the effect of reducing the resolution, see table 3.3.

Theoretical travel times, p and Az were calculated for all the phases mentioned in table 3.1. The seismograms (plots of the digital data) were searched for PcP, and if at least 2 stations had a good PcP phase, p and Az were measured for P and PcP, using as many stations as possible. If PcP could be identified in the covespagram, the grid size was reduced to the resolution limit, and the value for p and Az read. The error assigned to p and Az would then be the grid size. Also the arrival time of P and PcP were read from all stations, and the average calculated. Finally the travel time and p-Az residuals were calculated for P, PcP and PcP-P using the J-B predicted values. A total of 37 events from South and Central America were available and 9 were found to have PcP phases of reasonable quality.





Table 3.3

An example on the array response for the 1974 and 1970 arrays. The first set of numbers give the slowness (sec/deg), azimuth (degrees) and amplitude of the test signal used to generate the covespagram. The period of the signals is 1 second and the duration is 6 seconds. The second set of numbers are the coherencies (multiplied by one hundred) as a function of azimuth (first column) and slowness (first row).

## ARRAY RESPONSE FOR THE 1974 ARRAY.

SLOWNESS      AZIMUTH      AMPLITUDE  
6.00            140.0            1.00

	5.50				5.80				6.10				6.40			
135.0	0	0	20	30	0	0	0	18	73	89	46					
136.0	0	26	81	82	14	0	0	21	66	59	18					
137.0	2	54	84	52	5	0	0	0	0	0	0					
138.0	0	12	3	0	0	0	0	0	0	0	4					
139.0	0	0	0	0	0	50	39	23	0	0	20					
140.0	0	0	0	0	55	96	80	20	0	0	3					
141.0	23	5	0	4	33	57	48	6	0	0	0					
142.0	17	0	0	0	0	1	0	0	4	5	0					
143.0	0	0	0	0	0	0	0	3	27	29	3					
144.0	0	0	0	20	4	0	0	0	20	33	29					
145.0	0	0	0	0	0	0	0	0	0	20	29					

## ARRAY RESPONSE FOR THE 1970 ARRAY.

SLOWNESS      AZIMUTH      AMPLITUDE  
6.00            140.0            1.00

	5.50				5.80				6.10				6.40			
135.0	47	18	0	0	0	0	21	45	65	77	83					
136.0	36	6	0	0	0	10	38	65	96	96	83					
137.0	2	0	0	0	0	35	69	96	96	83	61					
138.0	0	0	0	0	19	65	87	96	89	70	30					
139.0	0	0	0	3	65	87	96	89	70	44	16					
140.0	0	0	3	35	87	96	89	70	44	16	0					
141.0	0	3	35	65	92	89	70	44	16	0	0					
142.0	0	8	53	76	83	70	47	4	0	0	0					
143.0	8	39	64	81	74	47	18	0	0	0	0					
144.0	23	64	81	83	58	33	0	0	0	0	2					
145.0	50	55	70	56	32	0	0	0	0	0	0					





Table 3.4

Comparison between a symmetric and an elongated array. The first set of numbers give the slowness (sec/deg), azimuth (degrees) and amplitude of the test signal used to generate the covespagram. The period of the signals is 1 second and the duration is 6 seconds. The second set of numbers are the coherencies (multiplied by one hundred) as a function of azimuth (first column) and slowness (first row).

## AN ELONGATED ARRAY

## ARRAY RESPONSE FOR STATIONS FOR SES MAP

SLOWNESS	AZIMUTH			AMPLITUDE		
6.00	140.00			1.00		
	5.50	5.80			6.10	6.40
135.0	0	0	0	0	0	7 15 19 0
136.0	0	0	0	0	0	5 33 30 0 0
137.0	0	0	0	0	21 47 61	1 0 0
138.0	0	0	0	18 57 70 42	0	0 4
139.0	0	0	0	30 83 77 39	0	0 5
140.0	0	0	0 33 79 96 55	0	0	0 0
141.0	0	0	0 58 92 76 23	0	0	0 0
142.0	0	0	30 74 91 50	0	0	0 0
143.0	0	0	48 80 69 19	0	0	0 0
144.0	0	6	44 65 39	0	0	0 0
145.0	0	6	39 23	0	0	0 0

## A SYMMETRIC ARRAY

## ARRAY RESPONSE FOR STATIONS FOR HAN SES

SLOWNESS	AZIMUTH			AMPLITUDE		
6.00	140.00			1.00		
	5.50	5.80			6.10	6.40
135.0	0	0	0	0	0	0 0 8
136.0	0	0	0	0	0	0 0 5
137.0	0	0	0	0	5 2	0 0 5
138.0	0	0	0 33 45 44 44 10	0	0	0
139.0	0	0	17 45 57 61 58 35	6	0	0
140.0	0	0	6 40 77 96 96 77 41	1	0	
141.0	0	0	0 20 39 65 80 76 39	7	0	
142.0	0	0	0 0 3 23 35 19	9	0	0
143.0	17	0	0 0 0	0	0	0
144.0	66	30	0 0 0	0	0	0
145.0	85	60	20 0	0	0	6 2 7



## CHAPTER 4

### DETERMINATION OF THE DIP ON THE MOHO BY COVESPA ANALYSIS

It has been shown that small scale inhomogeneities do not effect the array results seriously but there is the possibility of large scale structure. The most serious effect occurs if the base of the crust at the Mohorovicic discontinuity (MOHO) to be a dipping surface. There are other dipping interfaces in the crust but the Moho is the best defined with the largest velocity contrast. Niazi (1966) showed how corrections for the effect of a dipping plane could be calculated and made a series of correction tables. In general the depth, strike and dip of the Moho can be found by refraction or reflection studies. This is no minor undertaking and has never been done completely for each location of any array. A method which could use the available data from the array itself to determine the dip and strike of the Moho would be desirable. One such technique is presented here.

It was noticed in some of the covespagrams that after the first P arrival the coda of the coherency peak shifted consistently by a small amount in the p-AZ plane. The magnitude of the shift was about 0.1 sec/deg and  $1^\circ$  and it was seen a few seconds after the initial P phase. An explanation could be that P waves were converted to S waves (hereafter called PS) at a sloping interface in the crust.



It was decided to search for similar changes in the covespagram for PS conversions from the Moho. An unconverted P wave shows a smaller change in p-Az as a function of dip angle than a converted (PS) phase. In principle it should be possible to calculate the slope of the Moho given slowness and azimuth for both P and PS arrivals.

The PS will arrive about 4-5 seconds after P, and since P converts to SV waves horizontal seismograms were examined and rotated to yield the radial and transverse components of motion. The converted arrivals are vertically polarized shear waves (SV) and should only appear on the radial component. At an epicentral distance of about  $60^\circ$  the angle of incidence at the base of the crust is  $30^\circ$ . A typical ratio for P velocities above and below the Moho, in Western Canada (see fig 4.1), is 0.9. For these parameters the amplitude transmission coefficient for PS is 0.12 (Larry Marks, personel communication). The amplitude of P as observed on the radial component was, in general, half the P amplitude as observed on the vertical component, so the amplitude ratio of P to PS on the radial component would be about 4. A series of covespagrams were made using data, from the 1974 array, with high signal to noise ratio. On several, a second coherency peak was found 4-5 seconds after the P arrival (table 4.1). Some tests were made with covespagrams calculated from theoretical seismograms to see if it was possible to separate out two phases arriving at nearly the same time but with slightly different p-Az. Using 3 and 4





Figure 4.1 From Cumming and Kanasewich (1966).

# CRUSTAL THICKNESS IN WESTERN CANADA

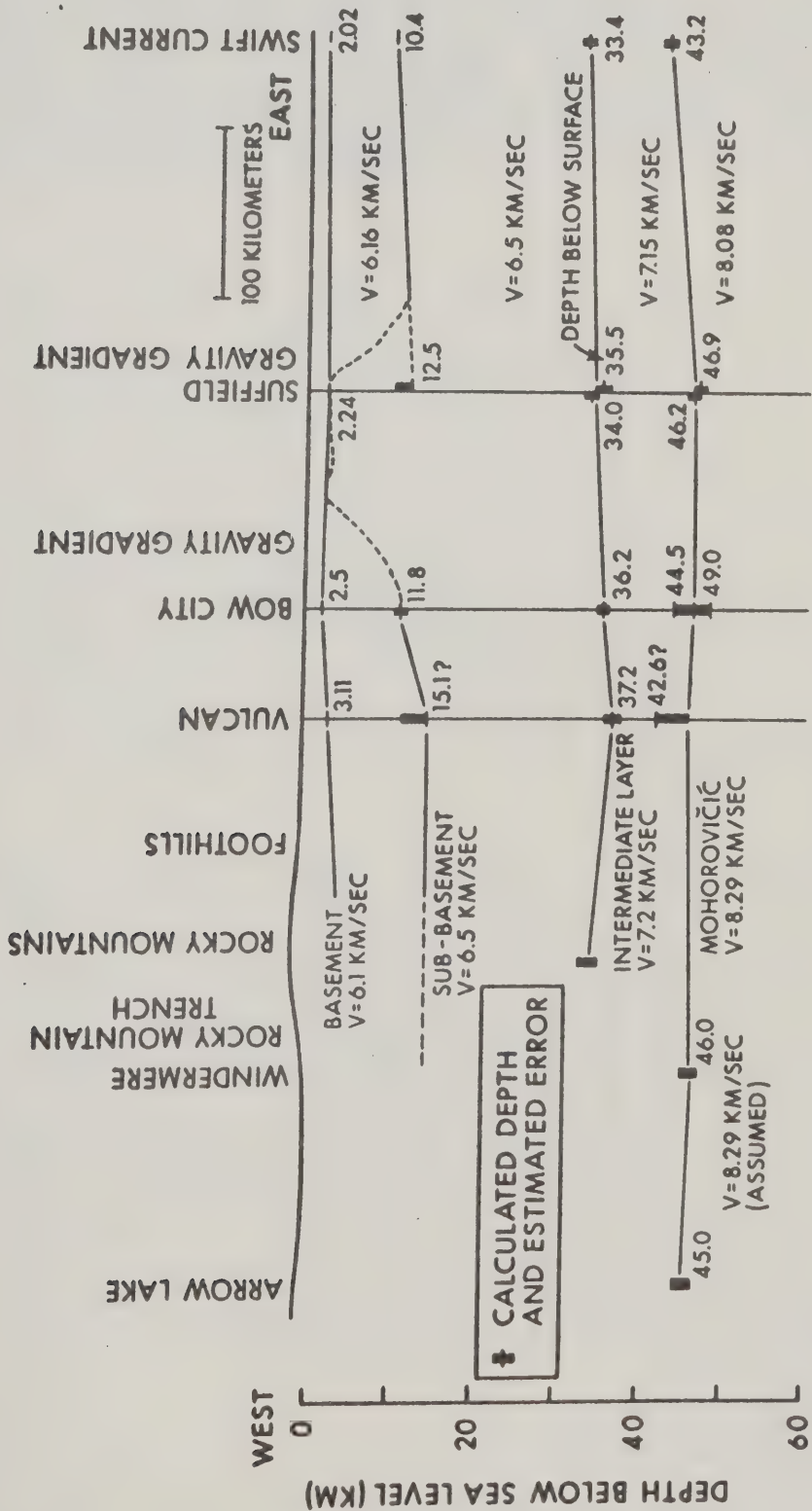




Table 4.1

An example of the covespagrams for the P and converted PS phases. The calculations are made for an event from the Caribbean Sea and using the stations EAT, MAP, SES and VUL. The first covespagram (top) shows the arrival of the P phase (8.2 sec/deg, 136°) at time = 4 seconds and the second (bottom) the arrival of PS (7.8 sec/deg, 129°) at time = 8 seconds. The numbers in the matrix are the coherencies (multiplied by one hundred) as a function of azimuth (first column) in degrees and slowness (first row) in sec/deg. Zeroes indicate negative coherencies

T= 4	7.50	7.80				8.10			8.40			8.70	
126.0	0	0	0	0	2	18	27	1	0	0	0	0	0
127.0	0	0	0	0	0	10	38	47	19	0	0	0	0
128.0	0	4	21	12	0	0	9	46	44	15	0	0	0
129.0	0	0	2	6	21	26	3	0	13	20	4	0	0
130.0	0	0	2	8	1	2	15	6	0	0	0	0	2
131.0	0	0	0	9	9	0	0	0	0	0	0	0	0
132.0	10	0	0	0	1	0	0	0	0	0	0	3	1
133.0	23	4	0	0	0	0	0	0	0	0	0	0	0
134.0	0	0	0	0	2	16	32	8	0	0	0	0	0
135.0	0	0	0	0	7	44	74	82	54	14	0	0	0
136.0	12	0	0	0	0	4	56	92	79	46	0	0	0
137.0	0	0	7	16	34	12	8	25	40	34	17	0	0
138.0	0	0	10	6	6	3	5	0	0	0	0	0	0
139.0	0	0	11	16	7	0	0	0	0	0	0	4	0
140.0	0	1	8	13	6	0	0	0	0	0	0	0	0

T= 8	7.50	7.80	8.10	8.40	8.70								
126.0	0	0	0	0	0	0	0	3	20	5	0	4	36
127.0	17	0	0	0	2	13	0	0	0	0	0	0	0
128.0	9	26	37	6	0	16	39	13	0	0	0	0	0
129.0	0	0	31	77	72	10	3	18	33	7	0	0	0
130.0	15	12	0	23	64	72	31	0	0	3	15	21	0
131.0	0	20	21	13	13	31	33	25	16	7	0	0	5
132.0	3	0	7	0	2	15	16	11	0	8	0	0	0
133.0	54	16	0	0	0	5	26	40	26	2	0	0	0
134.0	30	34	37	33	25	2	0	9	22	30	25	2	0
135.0	0	0	0	12	43	45	22	0	0	0	1	23	30
136.0	25	13	0	0	0	0	8	4	0	0	0	0	2
137.0	5	0	0	1	0	0	0	0	0	0	0	0	0
138.0	23	11	3	0	0	0	0	0	0	0	0	0	0
139.0	0	11	14	15	4	0	0	0	0	0	0	0	0
140.0	0	0	0	0	20	25	18	0	0	0	0	0	0



stations the model covespagrams were calculated for different amplitude ratios and a mixture of two phases similar to what is expected for P and PS. Some examples are shown in table 4.2 and 4.3. It is seen in the example in table 4.2, that excellent separation is obtained while for the example in table 4.3 the response pattern is such, that a P side lobe exists at almost the same  $p\text{-Az}$ , as expected for PS. Thus separation is impossible, and consulting the array response is absolutely necessary before picking a PS phase from the covespagram.

Searching all the data with a reasonably good signal to noise ratio, 7 PS phases were found in the covespagrams, and used for model calculations. The results are plotted as a function of azimuth for elastic waves arriving from earthquakes distributed in widely different directions (figure 4.2). These values had to be compared with theoretical values, and Niazi's tables could not be used, since they do not cover the velocity ratios found in the P to S conversion. Instead of following Niazi's method of calculation a novel method was derived leading to a simpler algorithm.

Define a ray vector  $\underline{B}$  parallel to the ray as in figure 4.3

$$\begin{aligned}\underline{B} &= 1/V * (\sin(I) * \cos(E), \sin(I) * \sin(E), \cos(I)) & (4.1) \\ &= (B_x, B_y, B_z)\end{aligned}$$

The magnitude of  $\underline{B}$  is  $1/V$ , where  $V$  is the seismic wave



Table 4.2

The array response for a single and a mixture of two phases using the 4 stations EAT MAP SES VUL. First is shown the response for the single arrival and below the response for a mixture of two arrivals with different p-Az and an amplitude ratio of 0.2. The numbers in the matrix are the coherencies (multiplied by one hundred) as a function of azimuth (first column) in degrees and slowness (first row) in sec/deg. Zeroes indicate negative coherencies.

SLOWNESS AZIMUTH AMPLITUDE  
4.40 272.00 1.00

	4.00			4.30			4.60			4.90		
260.0	0	0	0	0	0	0	8	0	0	0	0	0
261.0	0	0	0	0	0	0	8	0	0	0	0	0
262.0	0	0	0	0	0	0	6	0	0	0	0	0
263.0	0	0	8	1	0	4	0	0	0	0	0	0
264.0	0	0	6	3	5	1	0	0	0	0	0	0
265.0	0	0	6	10	9	25	7	0	0	0	0	0
266.0	0	0	0	6	24	17	10	0	0	0	0	0
267.0	0	0	0	11	24	14	2	0	0	0	0	0
268.0	0	0	0	29	35	6	0	0	0	0	0	0
269.0	0	0	0	33	46	0	0	0	0	0	0	0
270.0	17	0	1	66	80	18	0	0	0	0	0	0
271.0	13	0	3	64	85	27	0	0	0	3	7	
272.0	19	0	0	60	96	41	0	0	0	0	5	
273.0	13	0	0	47	80	46	0	0	0	0	0	
274.0	3	0	0	22	60	26	0	0	0	0	0	
275.0	0	0	0	11	37	18	0	0	0	0	0	
276.0	0	0	0	0	10	0	0	0	0	0	0	

SLOWNESS AZIMUTH AMPLITUDE  
4.40 272.00 1.00  
4.60 264.00 0.20

	4.00			4.30			4.60			4.90		
260.0	0	0	5	0	0	13	50	17	0	0	0	
261.0	0	0	7	0	0	33	56	15	0	0	0	
262.0	0	0	12	0	0	40	63	17	0	0	0	
263.0	0	0	23	0	0	30	54	12	0	0	0	
264.0	0	0	12	0	3	36	50	18	0	0	0	
265.0	0	0	7	3	7	31	27	0	0	0	0	
266.0	0	0	0	0	21	19	13	0	0	0	0	
267.0	0	0	0	3	18	12	0	0	0	0	0	
268.0	0	0	0	23	29	2	0	0	0	0	0	
269.0	0	0	0	26	39	0	0	0	0	0	0	
270.0	21	0	0	63	76	10	0	13	4	0	5	
271.0	18	0	4	61	80	20	0	1	12	0	18	
272.0	25	0	0	59	94	34	0	0	10	0	9	
273.0	19	0	0	48	78	42	0	0	5	0	5	
274.0	9	0	0	23	60	24	0	0	0	0	0	
275.0	0	0	0	11	38	18	0	0	0	0	0	
276.0	0	0	0	0	10	0	0	0	0	0	2	





Table 4.3

The array response for a single and a mixture of two phases using the 3 stations EAT FOR MAP. First is shown the response for the single arrival and below the response for a mixture of two arrivals with different p-Az and an amplitude ratio of 0.2. The numbers in the matrix are the coherencies (multiplied by one hundred) as a function of azimuth (first column) in degrees and slowness (first row) in sec/deg. Zeroes indicate negative coherencies.

SLOWNESS AZIMUTH AMPLITUDE  
7.00 142.00 1.00

	6.50			6.80			7.10			7.40		
134.0	0	0	0	7	0	14	0	0	0	0	0	0
135.0	22	60	85	85	80	52	17	0	0	0	0	0
136.0	32	49	73	58	43	12	0	0	0	0	0	0
137.0	0	0	0	0	0	0	0	1	30	53	77	
138.0	0	0	0	0	0	0	14	46	74	80	84	
139.0	48	18	0	0	0	0	0	0	0	1	0	
140.0	35	7	0	0	0	0	0	0	0	0	0	
141.0	2	0	0	0	8	23	39	51	30	21	0	
142.0	0	0	0	50	76	100	92	70	30	0	0	
143.0	0	0	20	44	48	43	20	0	0	0	0	
144.0	0	0	0	0	0	0	0	0	0	0	0	
145.0	0	0	0	0	0	0	0	0	0	0	0	
146.0	5	12	27	29	8	0	0	0	0	0	0	
147.0	18	33	29	8	0	0	0	0	0	0	0	

SLOWNESS AZIMUTH AMPLITUDE  
7.00 142.00 1.00  
6.70 138.00 0.20

	6.50			6.80			7.10			7.40		
134.0	0	0	9	26	20	37	5	0	0	0	0	
135.0	12	54	84	94	92	71	33	0	0	0	0	
136.0	6	20	48	38	34	11	0	0	0	0	0	
137.0	0	0	0	0	0	0	0	2	36	63	85	
138.0	0	0	0	0	0	0	4	35	63	73	79	
139.0	70	41	0	0	0	0	0	0	0	0	0	
140.0	46	16	0	0	0	0	0	0	0	0	0	
141.0	0	0	0	0	7	23	40	51	30	21	0	
142.0	0	0	0	45	72	100	92	70	30	0	0	
143.0	0	0	14	39	47	43	20	0	0	0	0	
144.0	0	0	0	0	0	0	0	0	0	0	0	
145.0	0	0	0	1	0	0	0	0	0	0	0	
146.0	5	13	30	30	8	0	0	0	0	0	0	
147.0	15	33	30	8	0	0	0	0	0	0	0	



Figure 4.2

The observed differences in slowness and azimuth between the P and PS arrivals. On top is seen the difference in slowness between the P and the converted PS wave at the Moho as a function of azimuth. Below are the corresponding azimuthal observations.

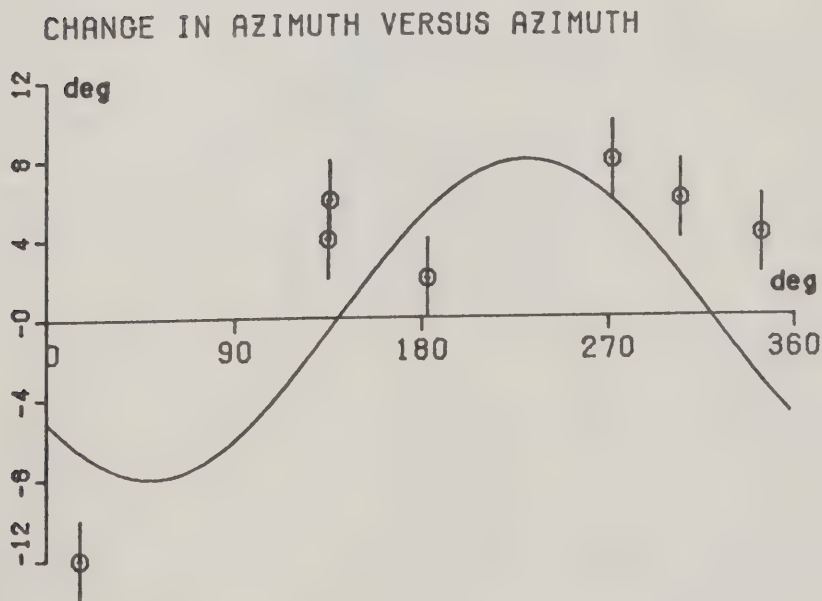
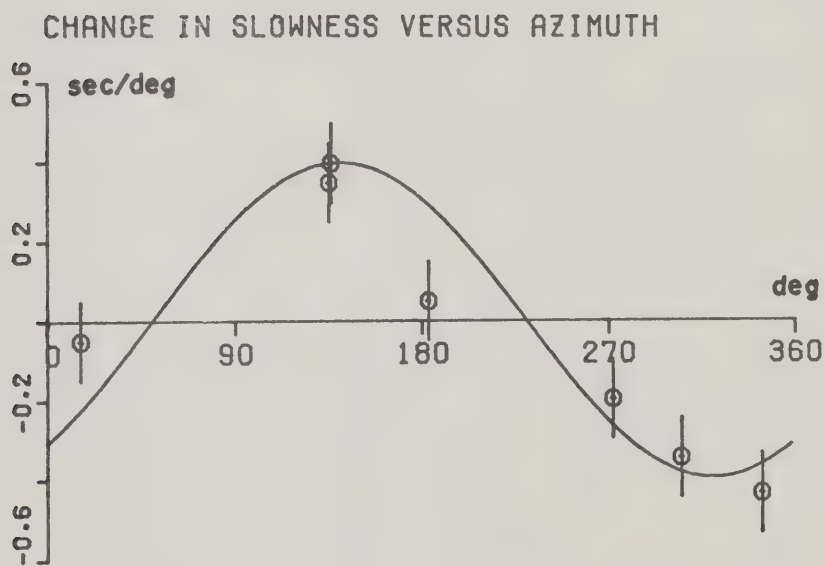
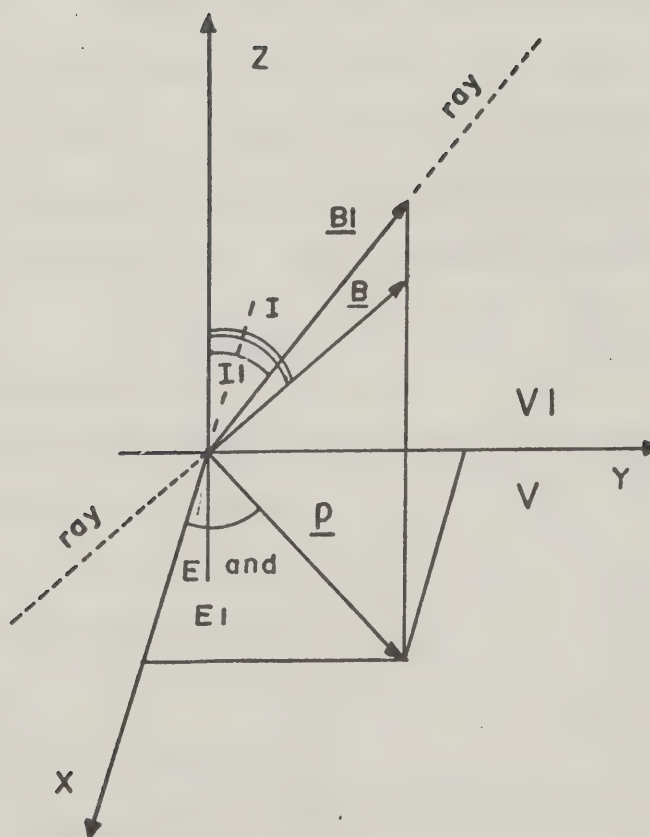




Figure 4.3

The coordinate system in which the ray vector  $\underline{B}$  is defined. The x-y plane is an interface with seismic velocity  $V$  below and  $V_1$  above and the incoming ray approaches the interface from below.







velocity, and the ray parameter  $p$  is  $(B_x, B_y)$  when measured in the  $x$ - $y$  plane. If the  $x$ - $y$  plane is an interface between two layers with velocity  $V_1$ , above and  $V$  below, the ray vector  $\underline{B}_1$  above will be

$$\underline{B}_1 = 1/V_1 * (\sin(I_1) * \cos(E_1), \sin(I_1) * \sin(E_1), \cos(I_1))$$

Using Snell's law and noting that  $E_1 = E$ ,  $\underline{B}_1$  can be written

$$\underline{B}_1 = (B_x, B_y, \cos(I_1)/V_1) \quad (4.1)$$

where  $\cos(I_1)$  can be calculated from  $\cos^2(I_1) = 1 - (V_1 * \sin(I)/V)^2$ .  $\underline{B}$  and  $p$  will depend on the coordinate system in which they are measured and only if the planes in which  $p$  is measured are parallel, will  $p$  remain the same. To find the change in  $p$ , for a ray passing a non parallel interface, some transformations must take place (see fig 4.4). Below the interface the ray vector is  $\underline{B}$  in the unmarked coordinate system,  $\underline{B}'$  in the primed system and  $\underline{B}_1'$  above the interface in the marked and  $\underline{B}_1$  in the unmarked system. The relationships are

$$\underline{B}' = \underline{M} * \underline{B} = (B_x', B_y', B_z')$$

where  $\underline{M}$  is the transformation matrix between the primed and original system. Using (4.1) gives

$$\underline{B}_1' = (B_x', B_y', 1/V * \cos(I_1'))$$

$$\cos^2(I_1') = 1 - (V_1 * \sin(I')/V)^2$$

and  $I'$  is found from

$$\cos(I') = B_z' / |\underline{B}'| = B_z' * V$$

Using the inverse transformation matrix  $\underline{M}^{-1} = \underline{M}^T$  gives

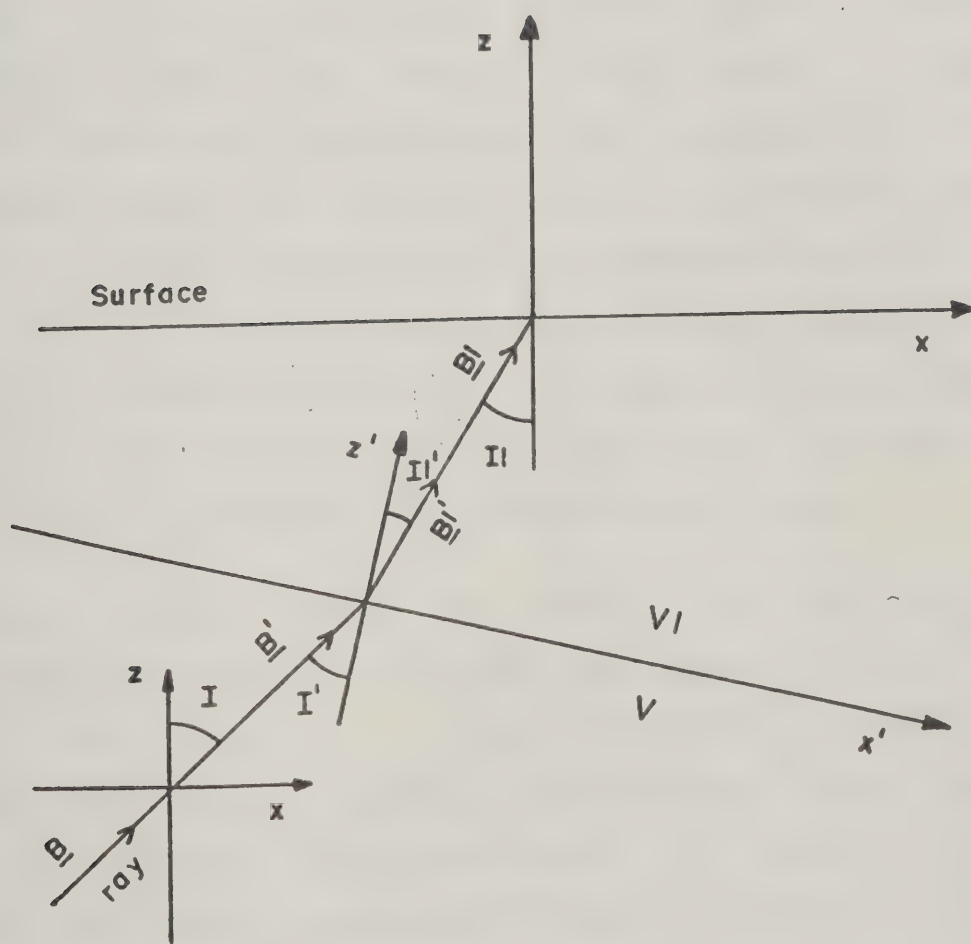
$$\underline{B}_1 = \underline{M}^T * \underline{B}_1' \text{ and } p_1 = (B_{1x}, B_{1y})$$

This analysis can easily be extended to any number of non



Figure 4.4

Dipping interface coordinate system. The standard coordinate system is  $x$ - $z$  while the system for the dipping interface is  $x'$ - $z'$ . The  $z$  and  $z'$  axes are assumed parallel for simplicity.





parallel layers with any orientation.

Using the above formulation a program was written to find the change in  $p$  and  $Az$  for a ray passing an interface which is not parallel with the earth's sea level surface. The orientation of the interface is defined by its strike and dip, and in general, two rotations, one around the  $z$ -axis and one around the  $x$  or  $y$  axis, will give  $\underline{M}$ . These two rotations are most easily combined into one Euler rotation (see appendix 3) with axis of rotation along the strike.

Tabulations of the change in  $p$  and  $Az$  as a function of  $p$ ,  $Az$ ,  $V$ ,  $V_1$ , strike and dip are given in appendix 2. Where possible, results were checked against those of Niazi (1966). The essential features are that increasing dip gives increased change in  $p$  and  $Az$ ; changing  $p$  (and thereby the angle of incidence) only affects the interface change in  $p$  slightly, while the  $Az$  change increases with decreasing  $p$  (decreasing angle of incidence). The  $p$ - $Az$  correction changes cyclically with direction of strike, however the correction to  $p$  is  $90^\circ$  out of phase with the correction to  $Az$ .

The results shown in figure 4.2 were fitted simultaneously (by eye) to two sine functions,  $90^\circ$  out of phase. The  $p$  data fit a sine curve better than the  $Az$  results. That is to be expected (see discussion above) since rays with different  $P$  values were used. By consulting the tables the dip was found from the amplitude of the  $p$  curve and the strike was found from the crossover points. For the



1974 array centered on Suffield, Alberta, the Moho dips down  $2^{\circ} \pm 0.5^{\circ}$  towards the southeast ( $Az = 140^{\circ} \pm 15^{\circ}$ ). These figures are in reasonable agreement with crustal refraction results in Alberta and Montana (Kanasewich (1966), Berry et al (1971) and Ganley and Cumming (1974)).

In conclusion this new technique involving a covespagram of array data appears to be very promising in determining the strike and dip of a major first-order discontinuity. If the velocities are known then it may also be possible to find the depth.





## CHAPTER 5

### MANTLE INHOMOGENEITIES

An interactive program was written which would search for individual or pairs of seismic phases satisfying a given set of parameters. The parameters specified the selection of desired events; seismic stations; short period or long period components; reading of differential times from peak to peak or initial onset to initial onset; maximum allowable reading error; desired anomaly range; depth and distance range for earthquakes and grid location of the ray center. The output can be a numerical print-out or in graphical form as a correlation matrix or map of anomalies. The maps include the continents to help identify the locations and may also include the stations, events, bottoming points of the rays, and all or the central portion of the ray path. An analysis of travel time residuals as a function of some of the parameters must be made first to evaluate their relevance.

It is a common practice to read the differential travel times from peak to peak (written as  $p(\text{ScS-S})$  and  $p(\text{PcP-P})$ ) instead the ideal which would be from individual to individual onsets ( $o(\text{ScS-S})$  and  $o(\text{PcP-P})$ ). If the spectral characteristics of two phases such as P and PcP are not similar, reading  $p(\text{PcP-P})$  instead of  $o(\text{PcP-P})$  could



introduce an error. A comparison is made of residuals from  $p(\text{PcP-P})$ ,  $o(\text{PcP-P})$ ,  $p(\text{ScS-S})$  and  $o(\text{ScS-S})$  in figure 5.1. It is evident that  $p(\text{PcP-P})$  residuals are smaller than those from  $o(\text{PcP-P})$  indicating more high frequency content in PcP than in P. A similar result is obtained for the ScS phase, although much more scatter is present. The average difference between  $o(\text{PcP-P})$  and  $p(\text{PcP-P})$  is 1.0 second and between  $o(\text{ScS-S})$  and  $p(\text{ScS-S})$  is 0.3 second. Kanamori (1967) compared the pulse widths for short period P and PcP phases and found PcP to be shorter than P. He explained the difference in terms of a lower attenuation (high Q) in the lower mantle as compared to the upper mantle. That is, PcP was less damped than P. A similar explanation is plausible for the ScS and S residuals. Fortunately, the differences due to methods of measuring differential residuals are small compared to the actual residuals and the choice is not critical to our interpretation. The  $o(\text{PcP-P})$  and  $o(\text{ScS-S})$  do give the best value and they will be used whenever possible.

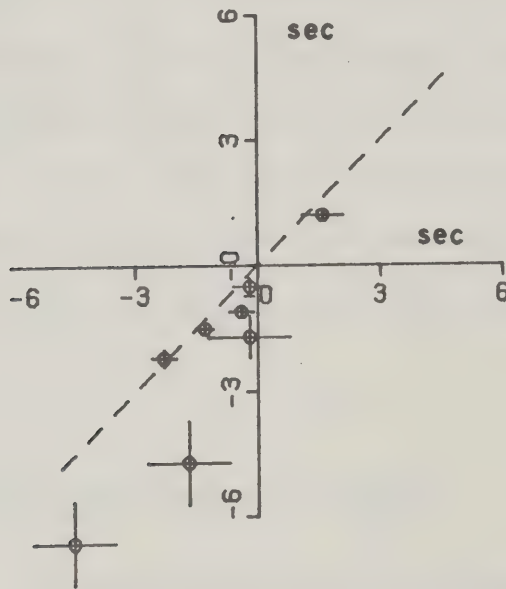
Mitchell and Helmberger (1973) observed that the long period horizontal polarized (SH) ScS arrived earlier than the long period radially polarized (SV) ScS for epicentral distances larger than 60 to 70 degrees. Their interpretation was that precursors to ScS, generated as reflections off a proposed high velocity layer just above the core-mantle boundary, arrived slightly before ScS and would be in phase with the SH ScS and out of phase with the SV ScS. It would then appear as if the SH ScS would arrive earlier than the



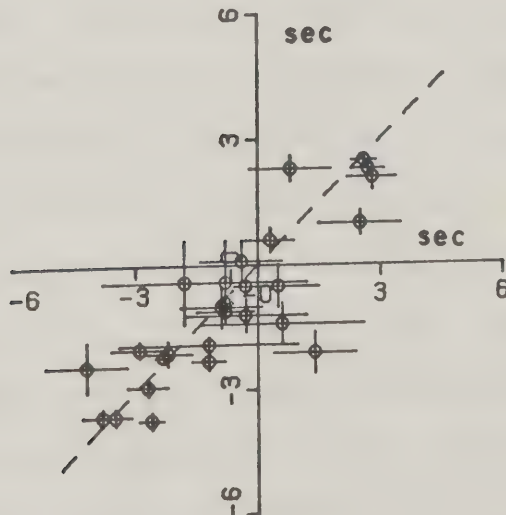
Figure 5.1

Comparison of differential travel times read from peak to peak and onset to onset. The differential travel times read from peak to peak,  $p(\text{ScS-S})$  and  $p(\text{PcP-P})$ , are plotted as a function of the differential travel times read from onset to onset,  $o(\text{ScS-S})$  and  $o(\text{PcP-P})$ .

P(PCP-P) VERSUS O(PCP-P) RESIDUALS



P(SCS-S) VERSUS O(SCS-S) RESIDUALS







SV ScS. The difference in arrival time was, in general, about one second. Both our short and long period data was examined for a similar tendency. Data with ray paths having approximately north or south trajectories were used. Results are shown in table 5.1. If Mitchell and Helmberger's hypothesis is correct then the the sign in the first and third column should be negative and increase with distance. It is not possible to draw any conclusions from our data regarding a high velocity layer. It should be noted that Mitchell and Helmberger's estimated average reading errors were twice the size of the mean of the anomaly they were interpreting (figure 5.2). From the table it is concluded that the choice of using SV or SH waves for studying ScS is not critical.

#### Analysis of the travel time and p-Az data.

The average observed travel time residuals in seconds were found to be 0.1 for P, 2.1 for S, -1.1 for PcP and 0.7 for ScS. Since the average P residual, representing the largest number of observations, is close to zero, a travel time will be considered "normal" if it is within  $\pm 1.0$  second of the J-B tabulation. S wave residuals are defined as normal if the residual is less than 1.7 second. Slowness is "normal" if the anomaly is within  $\pm 0.1$  sec/deg. These limits exclude reading errors. Thus a P wave residual of  $1.3 \pm 0.5$  seconds will be considered normal. All the data used in this study are shown in figure 5.3. The observed



Table 5.1

Comparison between the differential travel times ScS-S read on the east-west and the north-south components. The numbers listed in the first column under the heading o(ScS-S) are the differences between the o(ScS-S) residuals read on the east-west and the north-south components. The second column is the reading error. Numbers under the p(ScS-S) heading are the corresponding differences in the p(ScS-S) residuals. Units are seconds. Distance is the epicentral distance in degrees.

o(ScS-S)		p(ScS-S)		Distance	
0.3	0.7	0.0	0.4	77	
0.1	0.8	0.1	0.4	76	
-1.5	1.7	-1.0	0.4	69	Short period residuals
-0.1	0.7	-0.2	0.2	61	
-2.0	1.2	-	-	54	
0.7	1.1	-0.3	0.4	33	
1.0	4.0	0.0	2.0	57	Long period residuals.
-	-	-1.0	1.0	47	
-0.5	2.0	-1.1	1.0	46	



Figure 5.2

Difference in the travel time residuals of ScS-S between the radially polarized components and the transversely polarized components. The figure is from Mitchell and Helmberger (1973). The solid lines are smoothed differences measured from theoretical seismograms for a model having a 60 km thick transition zone above the core-mantle boundary with a velocity increase of 0.5 km/sec. The symbols identify different events.

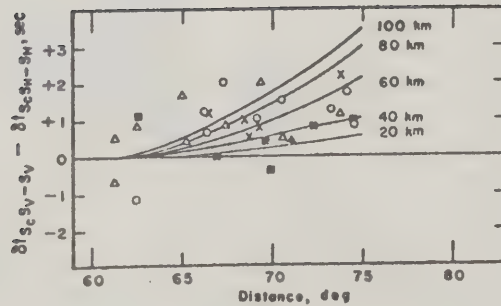
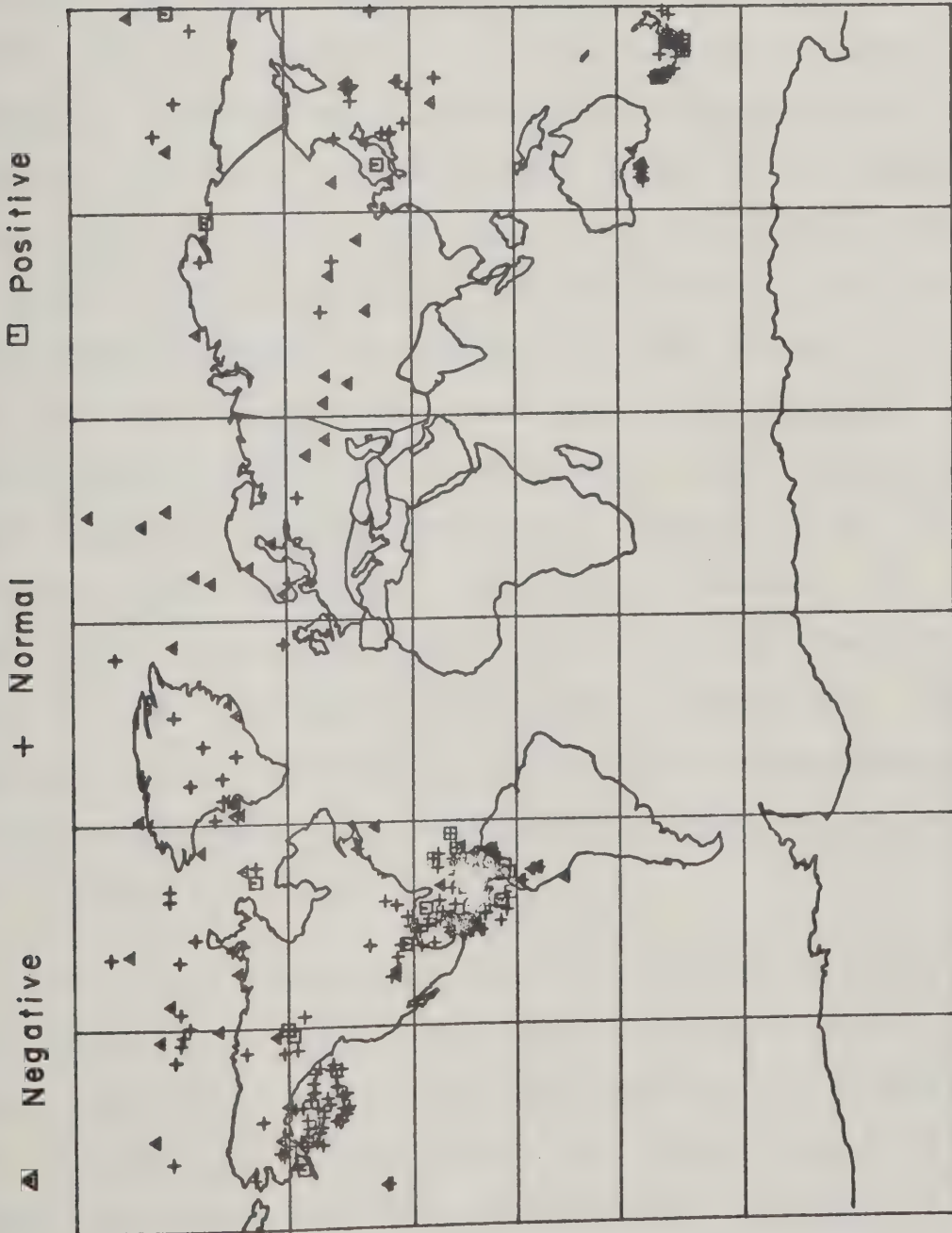




Figure 5.3

All the travel time data used in this study. The symbols indicate the surface projections of the deepest points of the rays. The differential residuals are marked as either positive, normal or negative as defined in the text.







differential travel times and p-Az data from the Caribbean are shown in figures 5.4 and 5.5. The projection of each ray together with its deepest point is plotted. A symbol is indicating if the corresponding differential residual is normal or significantly positive or negative. In these plots all the differential travel time and slowness data are shown including  $o(ScS-S)$ ,  $p(ScS-S)$ ,  $o(PcP-P)$  and  $p(PcP-P)$  for either the two horizontal or the vertical component, as available. Inconsistencies, showing up as superpositions of symbols, are few in number. Lateral change in the anomalies shows up most clearly in the plot of the p-Az differentials. Two sets of rays (X and Y in figure 5.5) having anomalies in differential slowness and azimuth are very close to rays with no such anomalies. Since the p-Az anomalies are differential and the rays in the groups X and Y are very close together at the array, the source of the p-Az anomalies cannot be close to the array. Previously it has been shown that an azimuthal anomaly is not likely to be close to the earthquake and using differential p-Az residuals greatly reduces any effect due to inhomogeneities in the source region. Therefore lateral velocity gradients must exist in the deeper mantle.

The use of differential residuals has the disadvantage that the source of the residual can be either along the direct, reflected, or both rays. One possible way of solving that problem is to correlate the differential p, Az or travel time residual ( $R - D$ ) with either the direct ray



Figure 5.4

All the observed differential travel time residuals from the Caribbean area including both body and shear wave data. Shown are the surface projections of the entire rays together with a symbol marking the deepest points of the rays. The differential residuals are marked positive, normal or negative according to the defination set up in the text.

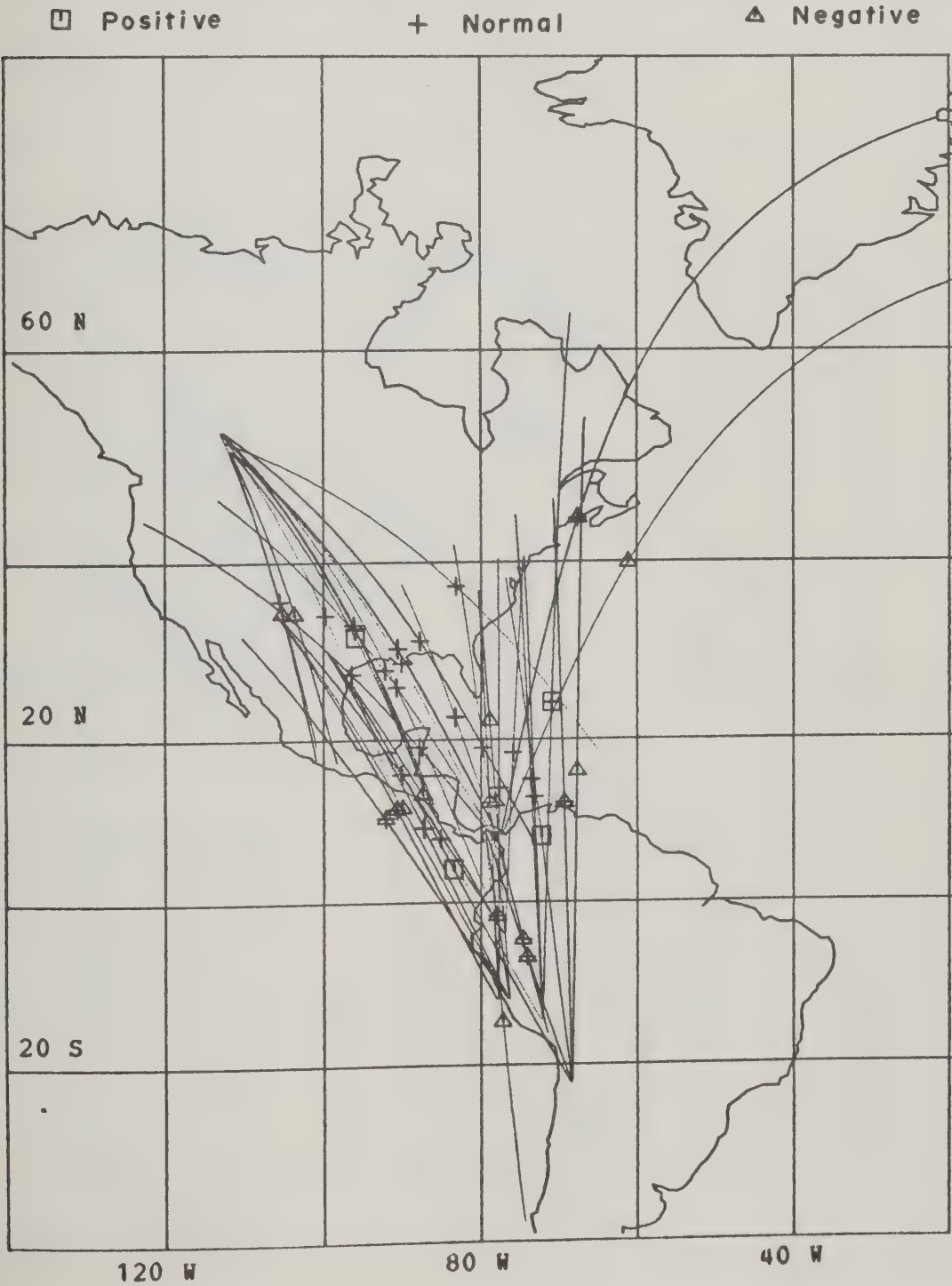
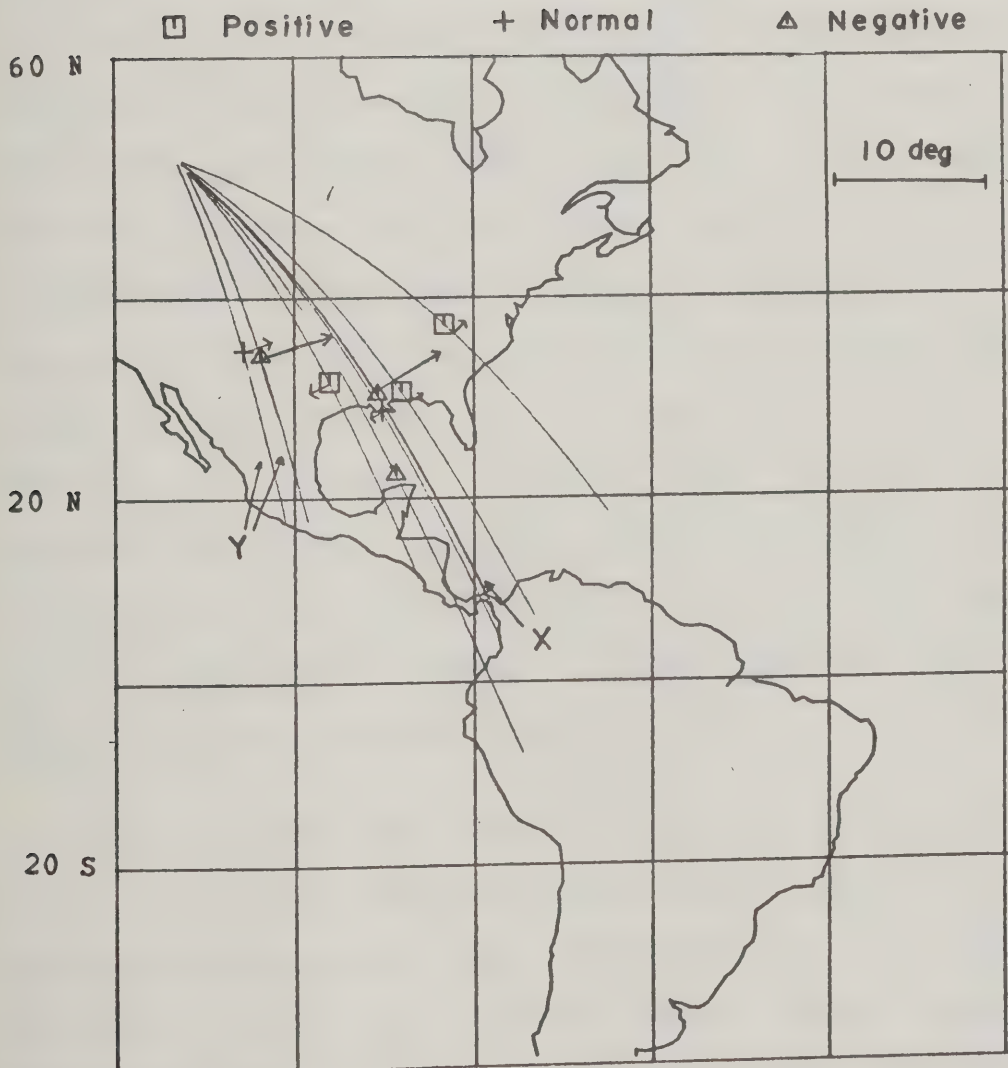




Figure 5.5

The array data for rays passing under the Caribbean. The surface projections of the entire rays together with a symbol marking the midpoints of the rays. The symbols indicate if the differential slowness residuals are significantly positive, negative or normal as defined in the text. Arrows drawn perpendicular to the rays give the size of the differential azimuthal residuals (degrees) and the directions show which way the rays are displaced.







residual, D, or the reflected ray residual R. Assuming the upper mantle is normal (where the direct and reflected rays are close together) the following relationships would hold:

$$(R - D) = 1 * R \quad (5.1)$$

for the velocity anomaly being only along the reflected ray and

$$(R - D) = -1 * D \quad (5.2)$$

for the velocity anomaly being only along the direct ray. If there are velocity anomalies along both the direct and reflected rays the above correlations do not occur. Jordan and Lynn (1974) found that relationship (5.2) held for a large part of their SCS-S data from the Caribbean and therefore concluded that the velocity anomaly was along the S rays. Since our data from the Caribbean covers a much larger area than that of Jordan and Lynn it was not possible to fit any one of the above equations to all the data. Therefore an analysis was made to classify each anomalous differential residual as originating either along the direct or reflected ray or being undefined. By plotting all the thereby identified residuals it was hoped that they would group in a simple geographical pattern.

The principles for classifying the residuals are given below. If only travel times were available, normal differential residuals were discarded. Of the remaining residuals, those which fitted either of the correlation equations within 0.5 second (excluding reading errors), were used. A negative residual was considered a indication of an



high velocity region close to the ray center. If both p-Az and travel time residuals were available, the p residuals had priority in determining the origin of the anomaly. Anomalous differential p residuals were used if they fitted either one of the correlation equations within 0.05 sec/deg excluding reading errors. A negative residual in p was interpreted in terms of a high velocity anomaly. In ambiguous cases (fit to both correlation equations) the travel time and azimuth residuals were consulted. Assuming that the source of the azimuthal anomaly was close to the center of the ray a first order correction to the corresponding travel time residuals was made. If the travel time residuals, according to the above rule, gave a clear indication of which ray was the main source of the anomaly, and in agreement with the interpretation of the slowness anomaly, the data was used.

In several cases there was excellent agreement between the interpretation using the p-Az and travel time data. The results from the Caribbean area are plotted in figures 5.6 and 5.7. It is seen that the majority of reflected ray residuals are located in the southern part of the Caribbean, Central America and the northern portion of South America. Most of the direct ray residuals are north of  $30^{\circ}$  latitude in the USA. It is interesting to examine the correlation plots for all the residuals related to these two areas. More specifically, the northern area was chosen to be between latitude  $30^{\circ}$  to  $40^{\circ}$  north and  $65^{\circ}$  to  $95^{\circ}$  east. The southern



Figure 5.6

Velocity anomalies along the reflected rays. The central  $10^\circ$  of the surface projections of the entire rays are marked to indicate if the velocity anomalies are positive or negative. The results on the map to the left are obtained from observational data (this study) while the results on the map to the right are derived from the published data.

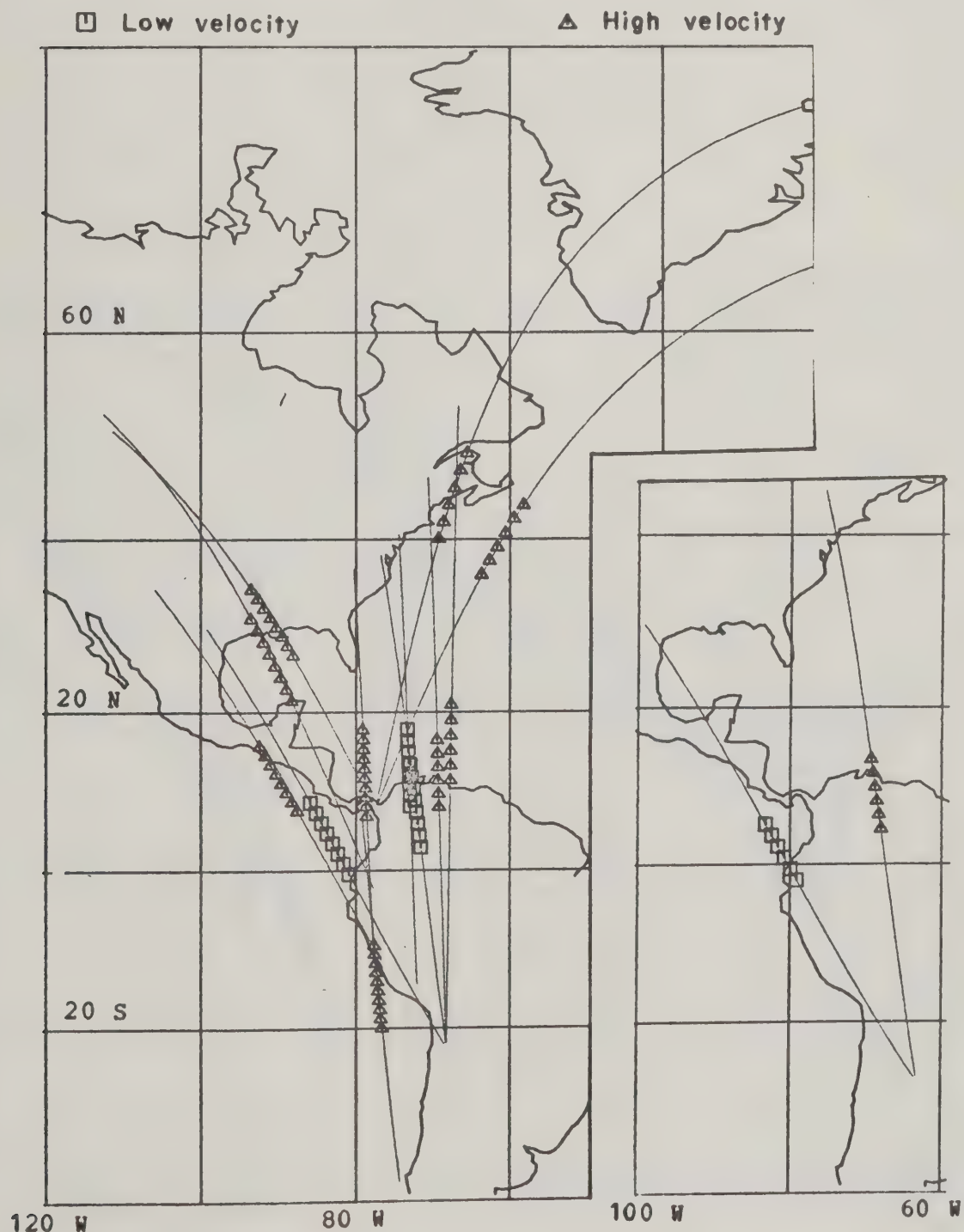
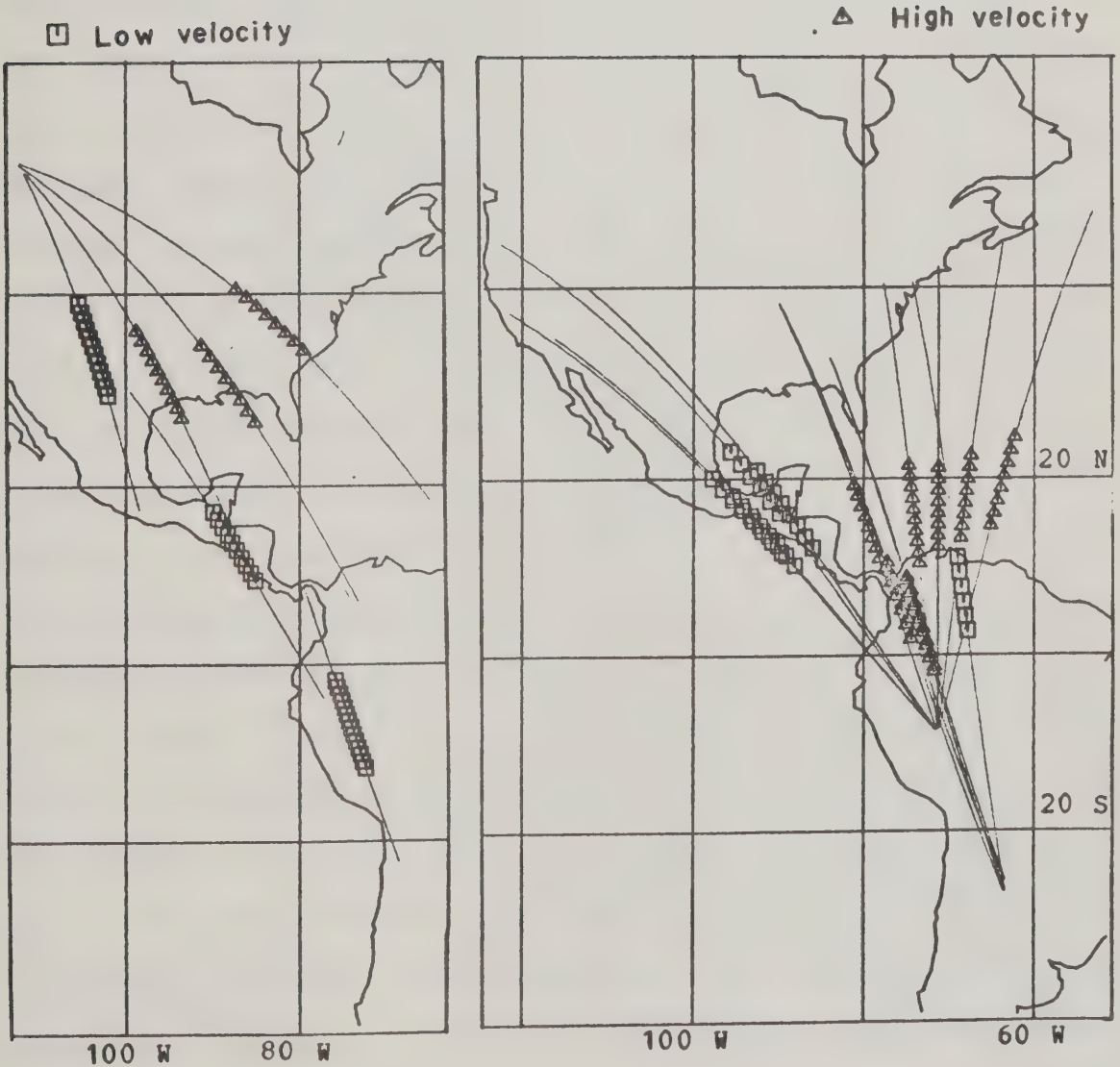






Figure 5.7

Velocity anomalies along the direct rays. The central  $10^\circ$  of the surface projections of the entire rays are marked to indicate if the velocity anomalies are positive or negative. The results on the map to the left are obtained from observational data (this study) while the results on the map to the right are derived from the published data.







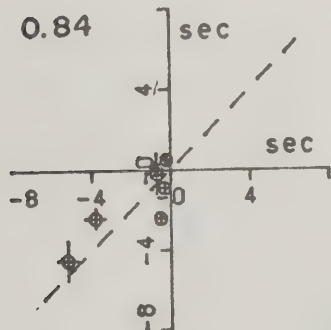
area was between  $5^{\circ}$  to  $20^{\circ}$  north and  $65^{\circ}$  to  $95^{\circ}$  east. The correlation plots for the southern area is shown in figure 5.8 together with the corresponding sample correlation coefficients. The figures indicate that the residuals are most likely due to anomalies along the reflected ray. For the shear waves the sample correlation coefficients are 0.78 versus -0.03 and for the compressional waves 0.84 versus -0.08. This result is in contradiction with the study of Jordan and Lynn (1974) for the same area. Their ScS-S differential travel time results (figure 5.9) indicate that the anomalies were along the direct ray (sample correlation coefficient of -0.86 versus -0.11). The main difference between the two studies is that Jordan and Lynn used long period seismic waves while this study uses predominantly short period data. Therefore it seems possible that the higher resolution, obtained using short period data, makes it possible to detect smaller scale anomalies unnoticed with the long period waves. From the northern area both p-Az and travel time residuals are available (figure 5.10). The sample correlation coefficient for the slowness indicates that the anomalies are predominantly along the direct ray (-0.97 versus 0.78). Note that although the coefficient of 0.78 is relatively high the slope of the line is not  $45^{\circ}$  as it should be. In fact, the PcP residuals are negligible. All the rest of the sample correlation coefficients favor the reflected ray. The S wave residuals are insignificant as compared to the size of the measured errors and correlation



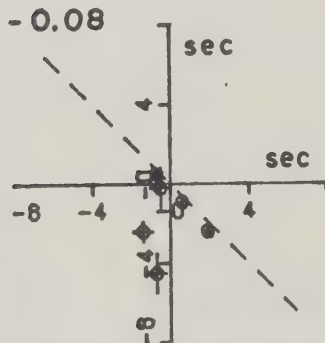
Figure 5.8

Correlation plots for the southern Caribbean area. PCP-P, ScS-S, PCP, ScS, P and S are travel time residuals in seconds. The number shown on each figure is the sample correlation coefficient. The dotted line gives the ideal relationship between the residuals.

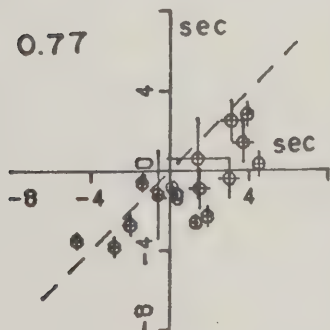
PCP-P VERSUS PCP RESIDUALS



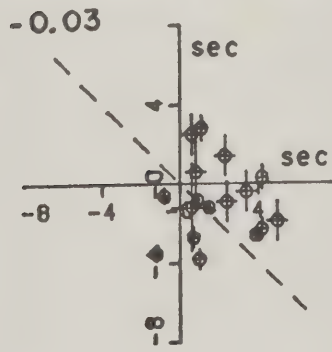
PCP-P VERSUS P RESIDUALS



SCS-S VERSUS SCS RESIDUALS



SCS-S VERSUS S RESIDUALS



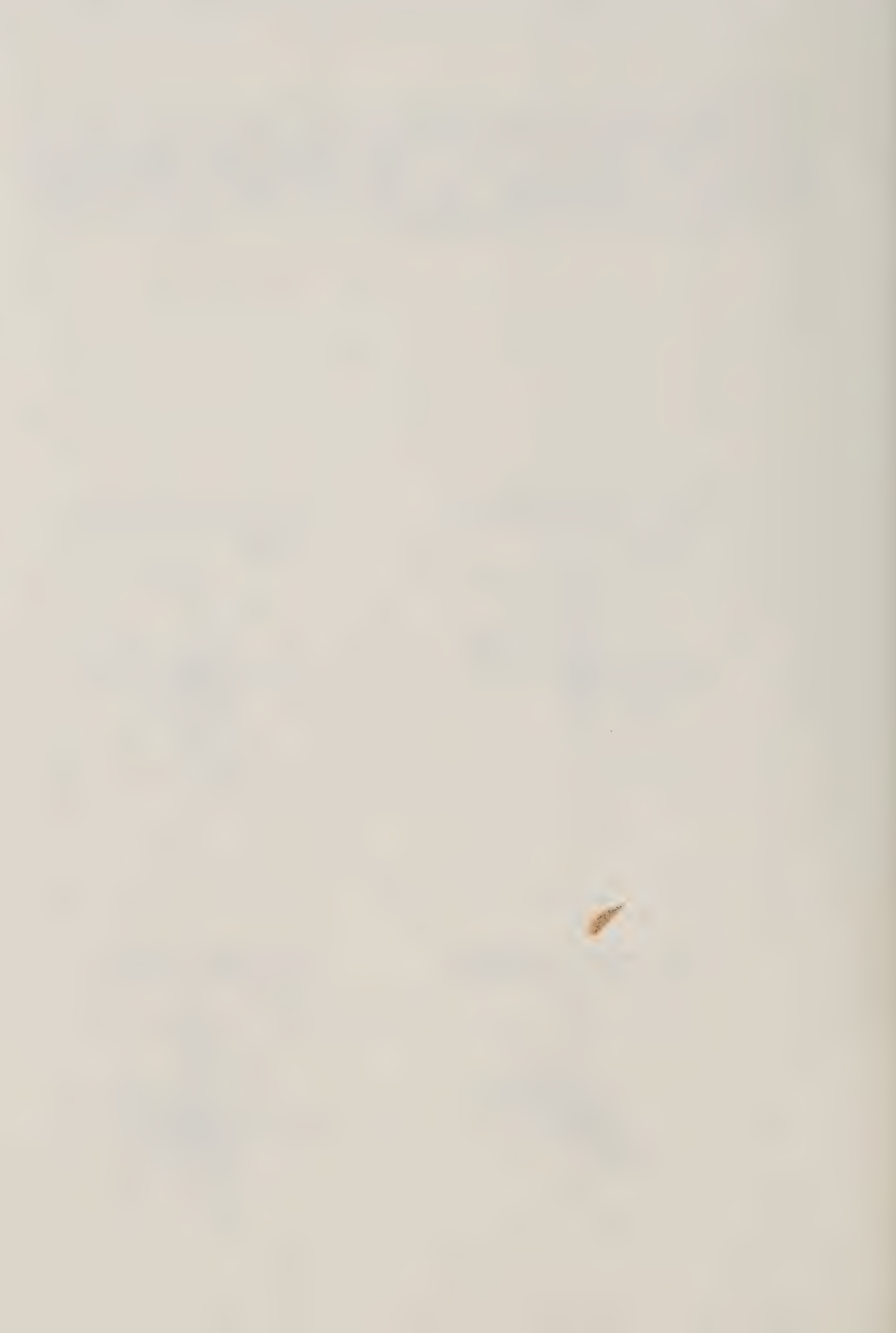


Figure 5.9

Correlation plots of shear wave residuals from Mitchell and Helmberger (1973). On top is shown the S versus ScS-S residuals and below the ScS versus ScS-S residuals. Circles and squares denote times from two different events. The sample correlation coefficients are  $r_S$  and  $r_{ScS}$ .



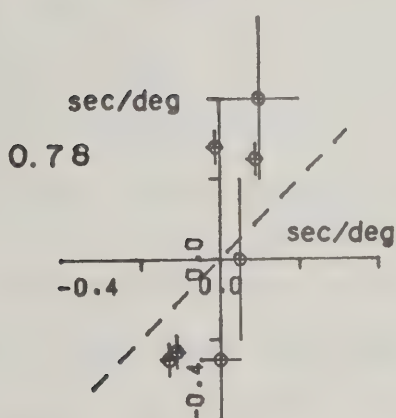




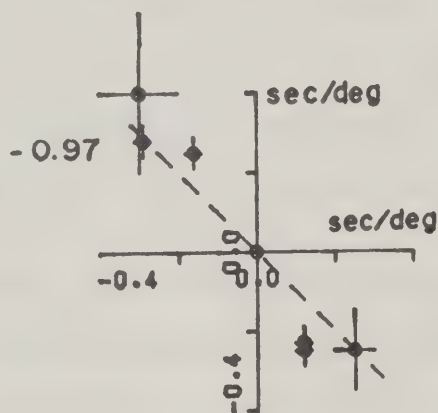
Figure 5.10

Correlation plots for the southern United States. The slowness residuals (sec/deg) for PcP-P, PcP and P are  $p(\text{PcP-P})$ ,  $p(\text{PcP})$  and  $p(\text{P})$  and the azimuthal residuals (degrees) of the corresponding phases are  $\text{Az}(\text{PcP-P})$ ,  $\text{Az}(\text{PcP})$  and  $\text{Az}(\text{P})$ . PcP-P, PcP and P are travel time residuals (seconds). The numbers shown on each figure are the sample correlation coefficients. The dotted line gives the ideal relationship between the residuals.

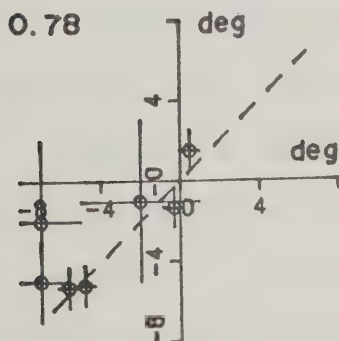
$p(\text{PcP-P})$  versus  $p(\text{PcP})$   
residuals



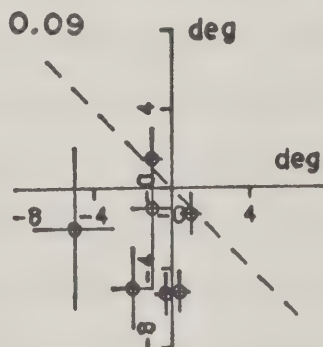
$p(\text{PcP-P})$  versus  $p(\text{P})$   
residuals



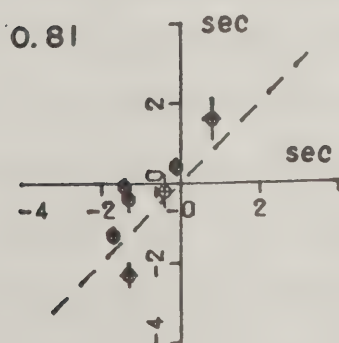
$\text{AZ}(\text{PcP-P})$  VERSUS  $\text{AZ}(\text{PcP})$  RESIDUALS



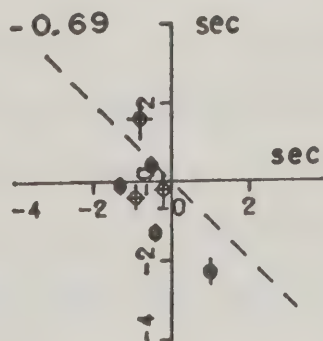
$\text{AZ}(\text{PcP-P})$  VERSUS  $\text{AZ}(\text{P})$  RESIDUALS



$\text{PcP-P}$  VERSUS  $\text{PcP}$  RESIDUALS



$\text{PcP-P}$  VERSUS  $\text{P}$  RESIDUALS





was meaningless. Among the P wave residuals only two are large but since the same rays have slowness residuals these are used predominantly in the interpretation. The azimuth residuals clearly originate along the reflected ray (0.78 versus 0.09), and since the residuals are consistently negative, they might indicate a wide spread horizontal velocity gradient perpendicular to the reflected ray path. Thus there are velocity anomalies both along the direct and reflected rays and that might explain why the sample correlation coefficients are not significantly different for the travel time residuals for the direct and reflected rays.

Data from two other studies are available for rays passing under the Caribbean. Mitchell and Helmberger (1973) published 35 ScS-S observed travel times and the corresponding S residuals. The ScS residuals are calculated here and interpreted for the first time. Jordan and Lynn (1974) used 45 ScS-S, ScS and S residuals in their study of velocity anomalies under the Caribbean. Both studies give the residuals relative to the Jeffreys and Bullen tables, and are directly comparable to our results. The data were required to have a minimum ScS-S residual of 1.7 second and to have a good correlation (within 1 second) between ScS-S and ScS or S residuals. Thus all residuals with uncertain origin of the anomalies and normal data were rejected. The results are plotted in figures 5.6 and 5.7 and it is seen that there is a reasonable agreement between our observations and the published residuals in the few cases



where they overlap.

### Interpretation of the residuals

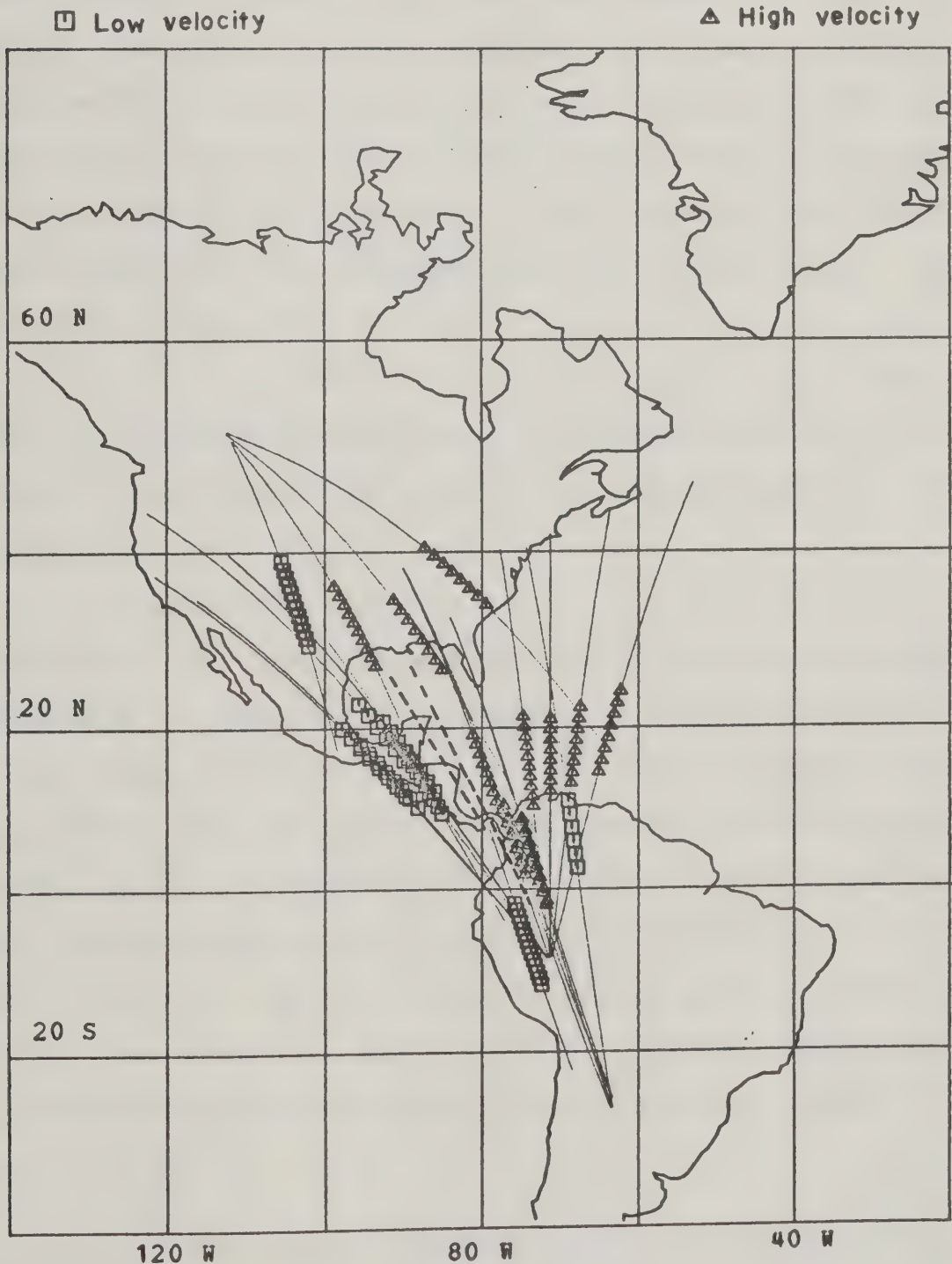
A summary has been made in figure 5.11 showing the central 10° of all direct rays having a significant anomaly. Results from some other studies are indicated as well. The two dashed lines mark bottoming points and direction of P rays having a negative azimuthal residual (Bates (1976), Wright (1973)). A downgoing PcP ray from this study also shows a strong negative azimuthal residual for a trace coinciding with Wright's result. Davies and Sheppard (1972) showed that low values of slowness for P rays exist for rays bottoming under the eastern part of the Caribbean. Similarly Bates (1976) found low slowness values for rays bottoming under the north-eastern part of the Caribbean. The simplest interpretation is that there is a high velocity anomaly along the deepest points of the rays. Combining all the data, it seems that the mantle sampled by the direct rays under the Caribbean is relatively simple. To the east there is a high velocity region, which over a short distance, changes laterally to a low velocity zone under Central America. Both the low and high velocity regions seem to extend well into the southern United States. Such a lateral velocity gradient will also explain the observed azimuth residuals. The depth of the anomalous zone is about 1000 - 2000 km and the horizontal dimensions seems to be about 2000 km. The azimuth residuals of Bates and Wright are about 4°.





**Figure 5.11**

A summary of all the velocity anomalies along the direct rays from the Caribbean area. The central 10° of the surface projection of the ray paths are marked to indicate whether the velocity anomaly is positive or negative. The dotted lines mark strong azimuthal anomalies, which displaces the rays to the east.







An attempt will be made to estimate the velocity contrast required between the areas with high and normal velocity. The radius of curvature,  $R$ , perpendicular to a velocity gradient  $dV/dx$  in the direction of the  $x$ -axis, is  $R=V*dx/dV$ , where  $V$  is the velocity. If the ray length through the region with the velocity gradient, is  $D$ , then to a first approximation, the angular deviation of the ray is  $D/R$  and the azimuth deviation,  $A$ , as seen by the receiver is  $A=D/2R$ . Assuming the velocity perturbation,  $\Delta V$ , measured in percent, occurs linearly over a distance  $L$  in the  $x$ -direction, the azimuth deviation is

$$A = 0.5 * D * \Delta V / L \quad (5.3)$$

The ray acquires an anomalous travel time, measured as the residual  $T_{res}$ , given by  $T_{res}=D*\Delta V/V$ . Combining the two equations gives

$$D * \Delta V = T_{res} * V = 2A * L \quad (5.4)$$

Since  $T_{res}$ ,  $V$ , and  $A$  are known, it is possible to get an estimate of  $L$ . Using  $T_{res}=3$  seconds,  $V=6.7$  km/sec and  $Az=4^\circ$  it is found that  $L=150$  km. From the above equation it is seen that  $D$  and  $\Delta V$  cannot be determined simultaneously. However  $D$  can be estimated to be about 1500 km from fig 5.11. Therefore the velocity perturbation must be about 1.3%. Since a positive velocity anomaly would give a similar travel time residual the velocity contrast between the Central Caribbean region and the Central America region is about 2 to 3%.

Since there is a reasonable amount of seismic data



from direct P and S phases to depths of 2000 km it will be assumed that anomalous PcP or ScS travel times indicate possible velocity anomalies at depths of 2000 to 2900 km. The type of velocity anomaly is indicated on the central 10° of the ray path (figure 5.12) and this corresponds to a 700 km path length extending to about 300 km above the core-mantle boundary. A projection of the entire ray path is shown since the anomalies may not be restricted to the central part. The intersection of several anomalous rays serve as a method for defining the location of the anomalies. The results appear to indicate that in the lower mantle the anomalies have shorter wavelengths than in the upper mantle. As mentioned earlier, bumps on the core-mantle boundary cannot be larger than 5 to 10 km. Since the maximum scatter in the ScS-S residuals is about 7 seconds, variations in the elevations of the core cannot explain the results. It must be concluded for the results presented here that lateral velocity anomalies seem to exist in the lower mantle. Assuming that the anomalous region in the Caribbean has wavelengths of about 700 km and using a typical ScS-S residual of 3 seconds, the corresponding velocity perturbation would be 3%.

#### Data from other parts of the world

Data contained in 4 published papers were found to be of value in this study. None of them had previously been

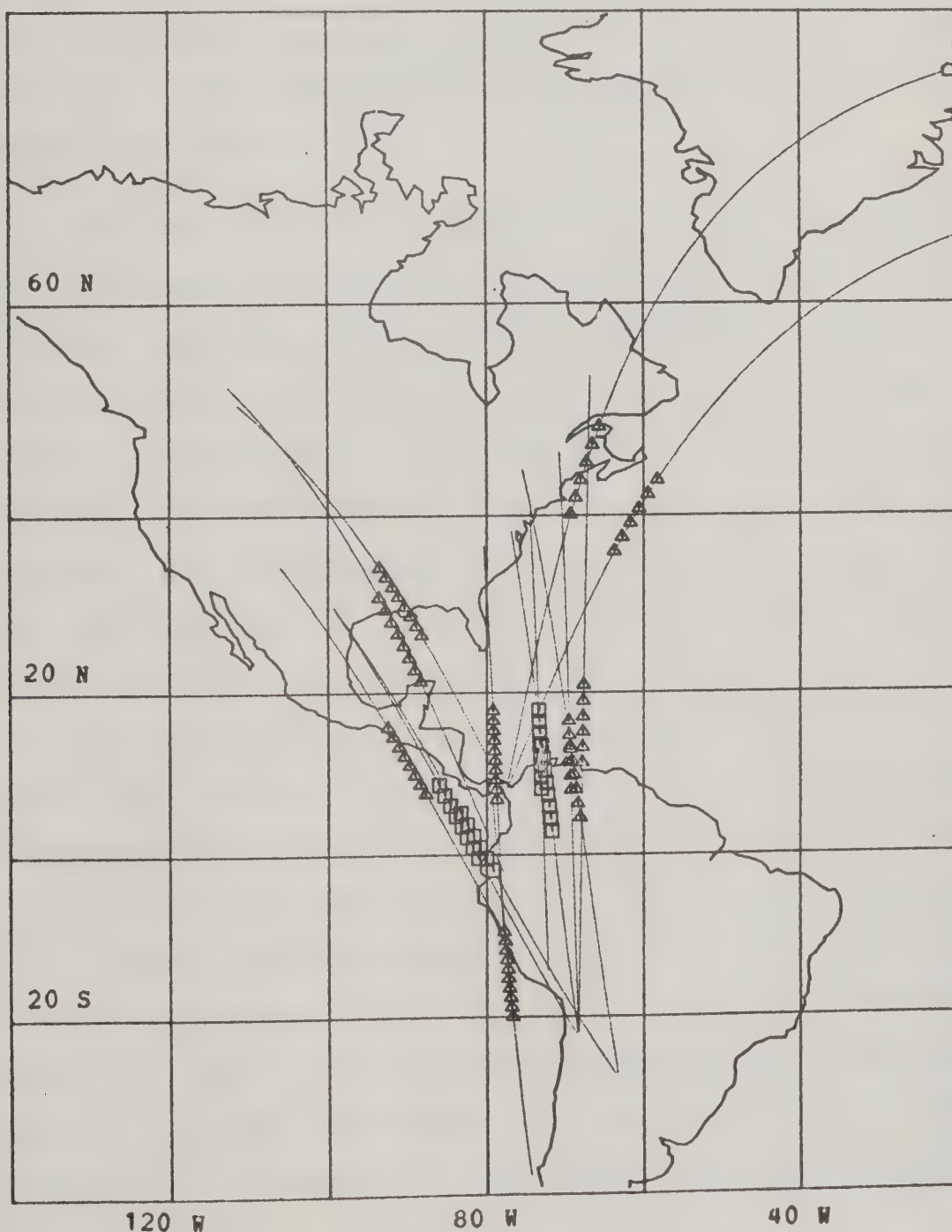


Figure 5.12

A summary of all the velocity anomalies along the reflected rays passing under the Caribbean area. The central  $10^\circ$  of the surface projection of the ray paths are marked to indicate whether the velocity anomalies are positive or negative.

□ Low velocity

△ High velocity







used for research in lateral inhomogeneities in the lower mantle. Listed in table 5.2 are the phases given, the number of differential residuals  $N$ , the travel time table relative to which the residuals were calculated and the authors. The first 3 studies covers a large part of the northern hemisphere while the fourth one focuses on a relatively small area in the Southeast Pacific. The map in figure 5.13 shows ray paths projected on the surface of the earth for all the data in table 5.2.

Buchbinder and Popinet used two nuclear explosions listed in table 5.3 together with the average travel time residuals. The Novaya Zemlya event has dominantly positive P residuals while the Amchitka event has negative residuals for both P and PcP which may indicate a source anomaly. Mitchell and Helmberger's data for a Sea of Okhotsk earthquake has predominantly positive S and ScS residuals, also probably due to a source anomaly. In all cases the average differential residuals are significantly closer to zero than those for the corresponding direct phase. The area covered by the data involve major portions of the northern hemisphere and, as expected, sample correlation coefficients are low and do not allow one to place the anomaly uniquely along either the direct or reflected ray. Consequently only differential residuals will be used to identify anomalous regions anywhere in the middle and lower mantle. Since the data is fairly well distributed geographically the average differential residual for each group will be considered



Table 5.2

The world-wide data. The travel time residuals are given for the phases shown under "Phase". N is the number of differential residuals.

Phase	N	Travel time base	Authors
PcP-P	102	Modified Herrin	Engdahl and Johnson (1974)
PcP,P	86	Herrin	Buchbinder and Popinet (1973)
ScS-S,S	11	J-B	Mitchell and Helmberger (1973)
ScS,S,P	67	J-B	Choudhury et al (1975)



Figure 5.13

All the rays from the world wide travel time data. The entire surface projection of the ray traces together with a symbol marking the deepest part of the rays are shown. The differential residuals are marked as positive, negative or normal according to the definition in the text.

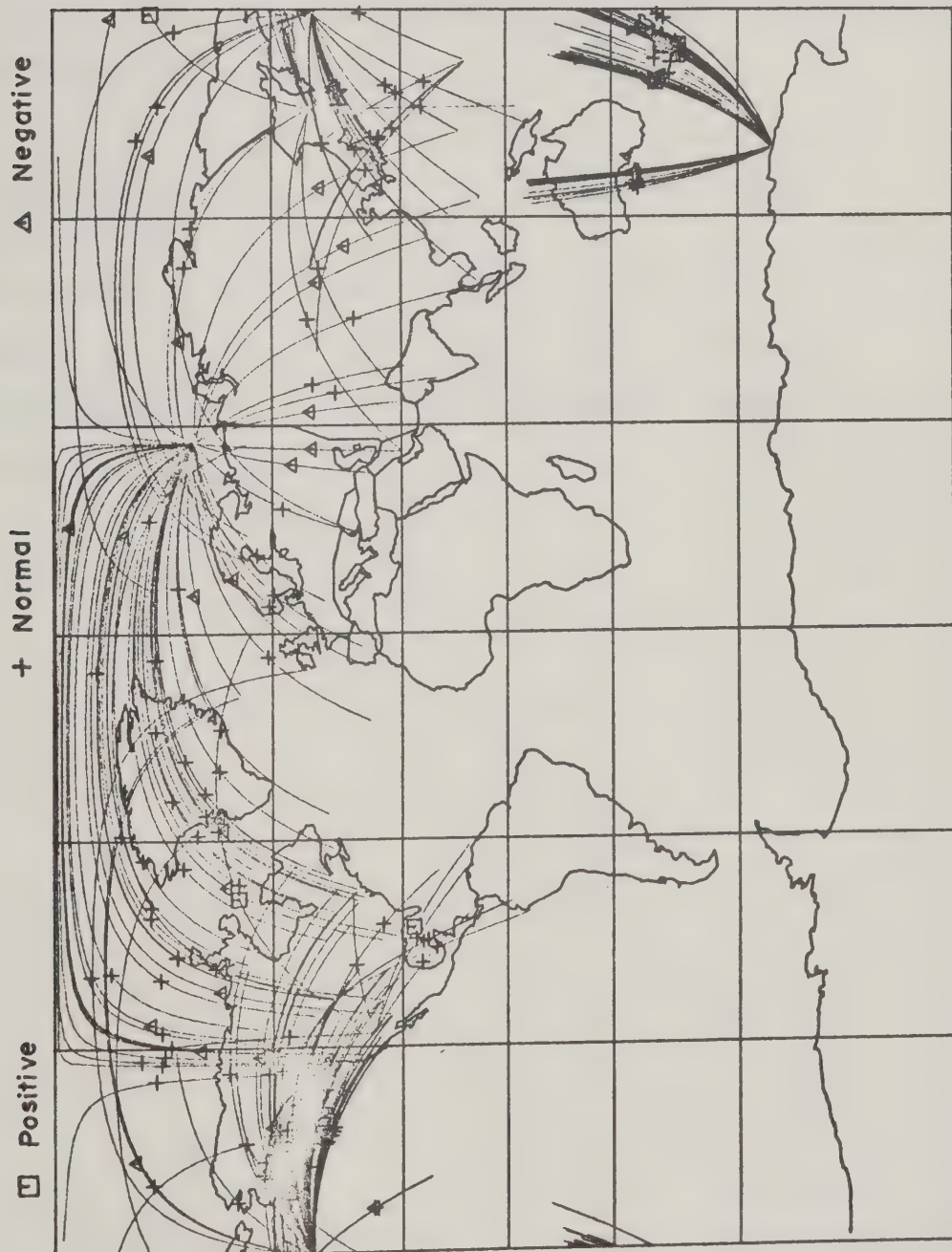




Table 5.3

The average travel time residuals (seconds) for the world-wide data from the northern hemisphere. The residuals given are for PCP (SCS), P (S) and PCP-P (SCS-S), values in parenthesis are for shear waves. N is the number of residuals. Note that the Engdahl and Johnson data give only the differential residuals.

Location of the event or the auther.	N	P	PCP	PCP-P
Novaya Zemlya	52	2.1	0.8	-1.3
Amchitka	32	-1.9	-2.5	-0.6
Sea of Okhotsk	10	(3.7)	(4.3)	(0.6)
Engdahl and Johnson	112	-	-	0.0





"normal" and only data differing significantly (1.4 second for EcP-P and 2.3 seconds for ScS-S) from the average are replotted on the map in figure 5.14. There does not seem to be any obvious correlation between the anomalous rays and surface features. The differential residuals indicate that lateral velocity perturbations exist as a world wide phenomenon in the middle and lower mantle. It is also clear that much more data is necessary to resolve the details of the anomalous regions.

Choudhury et al (1975) used short period ScS-P travel time arrivals from events at widely varying depths to show the existence of lateral inhomogeneities in the upper 250 km of the mantle. A calculation is made here of the ScS-S residuals from the published data to see if this gives any indication of lower mantle inhomogeneities. The data consists of three groups of events all recorded at the station DRV in Antarctica, (figure 5.15). The bottoming points of the rays, in each group, are separated up to 300 km. Choudhury et al showed the existence of S velocity anomalies in the source region by correlating the depths of the events with ScS-P residuals. Events below a certain depth for each group did not show such a correlation and these are used for differential residual computations to search for lower mantle anomalies. The average residuals for the 3 groups are listed in table 5.4. The P travel time residuals for both depth groups show no significant differences between the 3 ray groups indicating that there



Figure 5.14

The anomalous world-wide ray paths.

The entire surface projection of the anomalous ray paths are shown. The central  $10^\circ$  is marked to indicate if the differential travel time residual is significantly larger (positive) or smaller (negative) than the average differential residual.

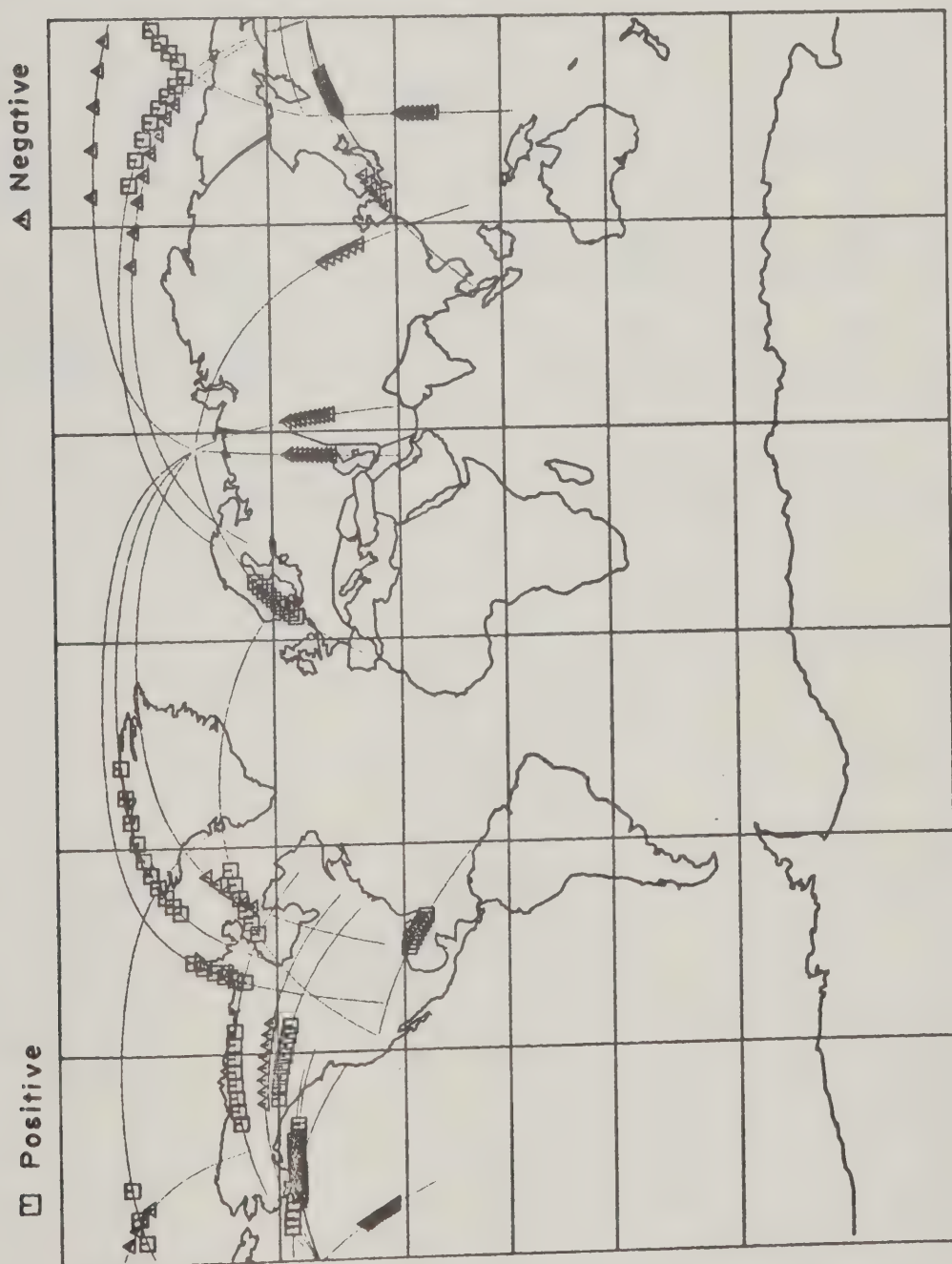




Table 5.4

Average travel time residuals for rays in the southeast Pacific. Residuals (seconds) for P, S, ScS and ScS-S are given as a function of depth,  $h$ , (km) and location of the earthquake.

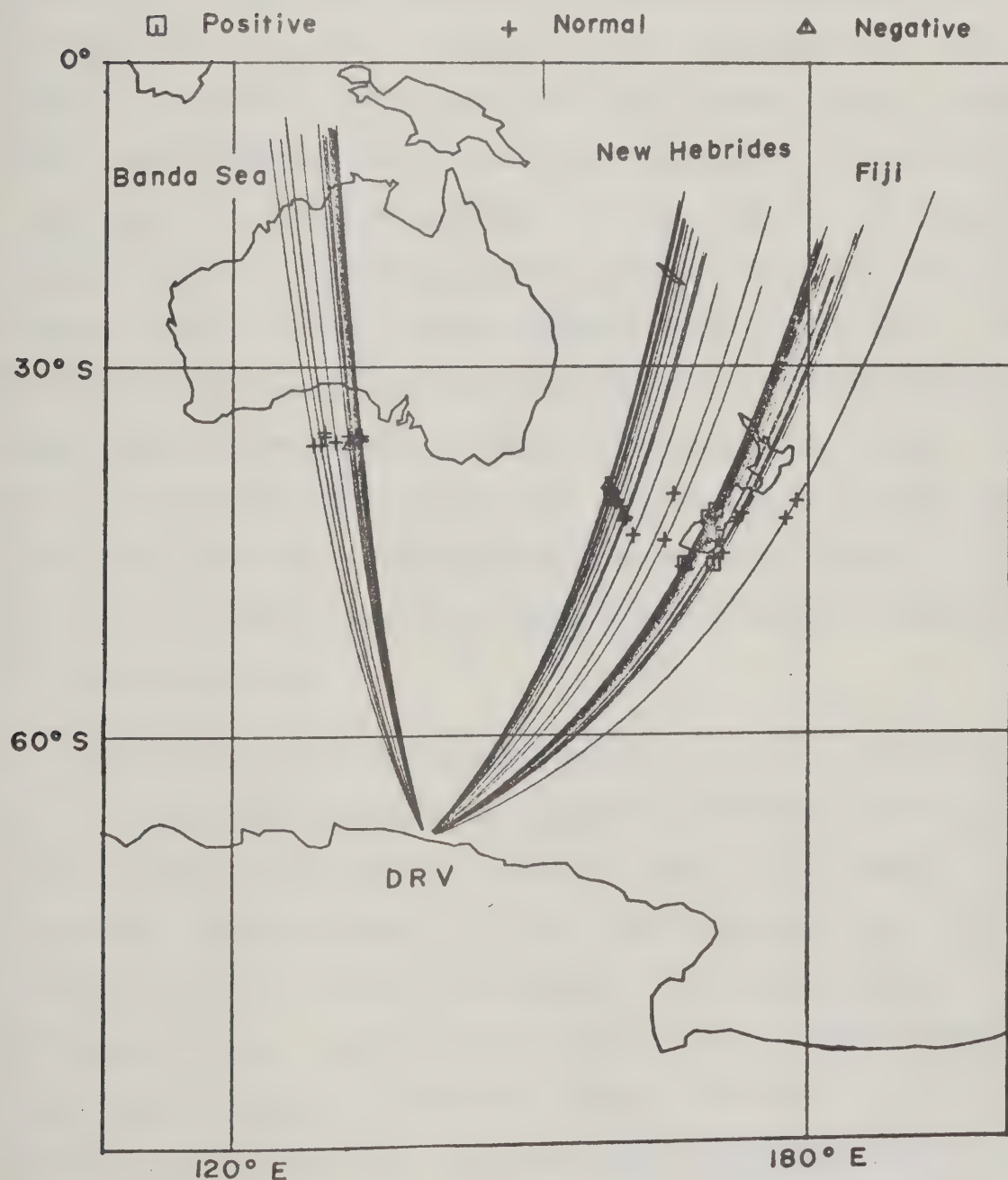
Location	Depth range	Number	P	S	ScS	ScS-S
Banda Sea	$h < 500$	14	-0.6	-1.1	-2.6	-1.5
Banda Sea	$h > 500$	5	-1.1	-2.2	-1.4	0.8
Fiji	$h < 500$	6	-0.3	0.9	1.7	0.8
Fiji	$h > 500$	22	-1.0	-2.0	-1.3	0.8
New Hebrides	$h < 150$	11	-0.7	3.3	3.7	0.5
New hebrides	$h > 150$	9	-0.6	0.5	-0.2	-0.7





Figure 5.15

All the rays originating in the Banda Sea, New Hebrides and Fiji regions are shown. The surface projections of the entire rays together with a symbol marking the deepest point of the ray are plotted. The symbol indicates if the differential SCS-S residual is significantly positive, negative or normal according to the definition in the text.





are no large scale lateral variations in the P velocities of the elastic waves. The shear wave data is much more significant because we can interpret differential travel time anomalies of ScS and S. The average ScS and S residuals for the Fiji and Banda Sea group of events are almost identical for the deeper events. Thus, no large scale middle or lower mantle shear velocity heterogeneities are evident. Choudhury et al found a region of low S velocities to a depth of 150 km under the New Hebrides source region, which also show up clearly in the S and ScS residuals. Compared to rays from the two other regions the S, and to a lesser extent the ScS, phases are slow. This is also true for the deepest events in this group (maximum depth is 246 km). So the low S velocity zone must extend well below the seismic zone. The difference in the ScS-S residuals, for events in the deeper group, between the New Hebrides data and the two other data sets must originate at a depth where the S and ScS rays are well separated. This must be below the Benioff or subduction zone.

For an error in focal depth of 10 km for an earthquake at a depth of 350 km and an epicentral distance of  $50^\circ$  the error in ScS-S differential times is only 0.3 second. An epicentral mislocation of  $0.1^\circ$  would change the ScS-S residual by 0.7 second (J-B tables). Since these values of mislocation are typical upper limits the largest possible difference in ScS-S residuals should be  $\pm(0.3 + 0.7 + 0.4(\text{reading error})) = \pm 1.4$  seconds. Table 5.5 shows the



Table 5.5

Maximum absolute range of the ScS-S travel time residuals (seconds) for events in the southeast Pacific given as a function of the depth,  $h$ , (km) and location of the earthquakes.

Location	Depth range	$ \max(\text{ScS-S}) - \min(\text{ScS-S}) $
Banda Sea	$h < 500$	3.4
banda Sea	$h > 500$	1.1
Fiji	$h > 500$	7.4
Fiji	$h < 500$	6.2
New Hebrides	$h < 150$	10.1
New Hebrides	$h > 150$	4.3



maximum absolute range of the SCS-S residuals within the different ray groups and figure 5.16 shows the residuals of the rays in the deeper ray groups as a function of depth and longitude of the earthquake. No obvious correlation is seen of the residuals with the earthquake location, but table 5.5 shows that in all cases do the scatter in the residuals decrease using deeper events. This indicates that the fluctuations are source related. The Fiji and New Hebrides data show much more scatter (figure 5.16) than the Banda Sea data and in all cases the scatter is larger than  $\pm 1.4$  seconds. This means that small scale inhomogeneities must exist below the seismic zones at Fiji and New Hebrides, but possibly not below Banda Sea. Since the rays for that area are leaving the seismic zone at a right angle to the strike of the descending plate the Banda Sea data will be less sensitive to source inhomogeneities than the rays from the two other regions where the strike of the downgoing plate is at an angle or nearly parallel to the rays. Once again it must be concluded that the most likely location for these anomalies is along the downgoing rays close to the subduction zone where the rays with extreme values have the greatest separation.

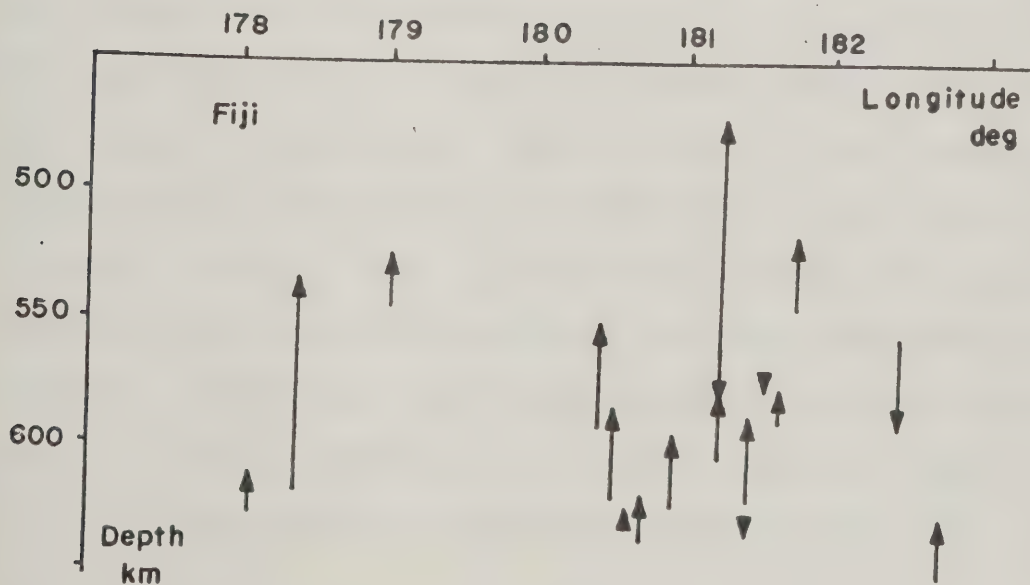
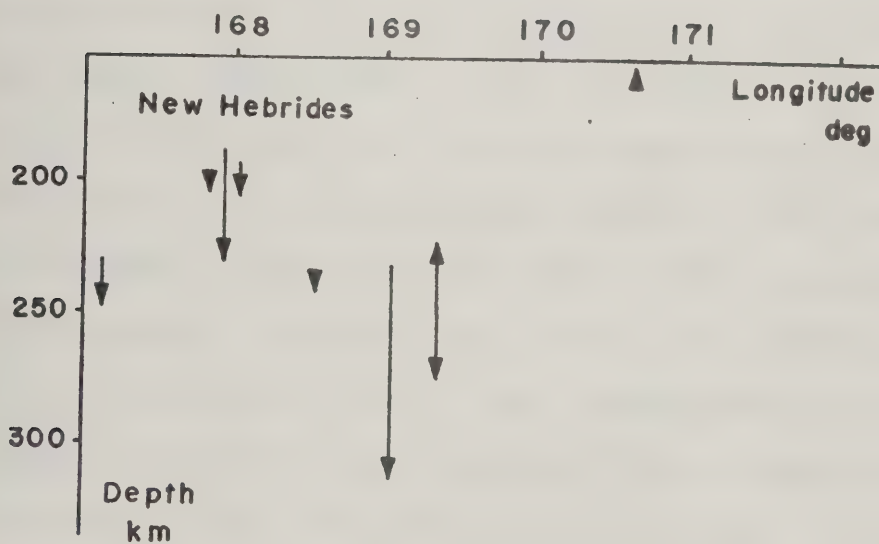
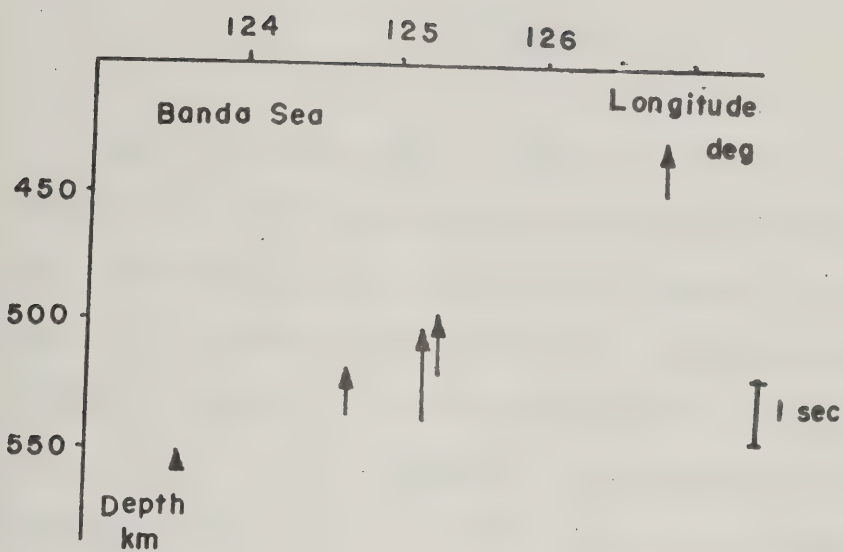






Figure 5.16

ScS-S travel time residuals for the deepest events from Fiji, Banda Sea and New Hebrides plotted as a function of depth and longitude of the earthquakes. Depths are plotted versus longitude (positive east) at the tails of the arrows. The length of the arrow is the size (sec) of the residual, positive if the arrow points up and negative down.





## CONCLUSION

The continental segments, and therefore the lithosphere, have been shown to be highly organized in time and space for the entire Phanerozoic . Only 6 to 9 major plates are necessary to describe satisfactorily the main geological events in the paleomagnetic reconstruction of the continents. It is difficult to conceive of an upper mantle convective system, or another driving mechanism, which will produce plates with dimensions of 60 to 180 degrees which are stable over a time scale of several hundred million years. Therefore the evidence seems to be irrefutable that mantle-wide convection was present. The order of the convective system varied very little during the entire Phanerozoic . A third order system was present during the Lower Paleozoic Era . The intense world-wide Caledonian Orogeny appears to have resulted from a change in convective pattern to a second order system. This was responsible for the formation of the super continent Pangaea . The close of the Mesozoic Era was marked by a second transition from a 2nd order convective system to a 3rd order one. Geologically, this was also accompanied by an increase in tectonic activity on a world-wide basis. Finally, it is concluded that the ten principles for plate tectonics are a valuable guide for the reconstruction of the geological past. If further observational evidence supports them, they may be of assistance in modelling the Precambrian Era .





Numerous publications have indicated the existence of mantle wide lateral inhomogeneities which, all taken together, are difficult to explain without assuming movement in the mantle. This study has presented further evidence from seismology for lower mantle inhomogeneities of both large and small scale. A method of using not only differential travel times but also differential slowness and azimuth residual for core reflected phases proved useful in determining the location of the anomalies. On a global scale lateral inhomogeneities in the mantle do exist but only in areas with a large number of rays sampling the mantle was it possible to estimate the location of the anomalies. Since both large and small scale seismic anomalies exist under the Caribbean and the anomalies in the Southeast Pacific seem to indicate the continuation of subduction well below the Benioff zone the hypothesis of mantle wide convection must be considered seriously. Many more studies with new station and array locations are necessary to establish if a world wide pattern of seismic inhomogeneities in the mantle is consistent with the hypothesis of mantle-wide convection.

The value of seismic array studies has been established in two new directions. The first is the use of differential slowness and azimuth residuals for PcP and P phases. The second is the use of a covespa analysis on both vertical and horizontal detectors to measure the slowness and azimuth of



the direct P wave and the PS conversion at prominent first order discontinuities. As a specific application it was possible to compute the dip and strike of the Moho discontinuity in Southern Alberta.



## REFERENCES

- Aki, K., Huebye, E., Christofferson, A. and Powell, C. 1974. Three dimensional seismic velocity anomalies in the crust and upper mantle under the U.S.G.S. California seismic array. Transactions, American Geophysical Union 56, pp. 1145.
- Al-Khafaji, S.A. and Vincenz, S.A. 1971. Magnetization of the Cambrian Lamotte Formation in Missouri. Geophysical Journal of the Royal Astronomical Society, 24, 175-202.
- Alexander, S.S. and Phinney, R.A. 1966. A study of the core mantle boundary using P waves diffracted by the earth's core. Journal of Geophysical Research, 71, 5943-5958.
- Anonymous. 1964. Geological Society Phanerozoic time scale 1964. Geological Society of London Quarterly Journal, 120, pp. 260-262.
- Athavale, R.N., Hansraj, A. and Verma, R.K. 1972. Palaeomagnetism and age of Bhandar and Rewa sandstones from India. Geophysical Journal of the Royal Astronomical Society, 28, pp. 499-509.
- Atwater, T. 1970 Implications of plate tectonics for the Cenozoic tectonic evolution of Eastern North America. Geological Society of America Bulletin, 81, pp. 3513-3536.
- Atwater, T. and Molnar, P. 1973. Relative motion of the Pacific and North American plates deduced from sea-floor spreading in the Atlantic, Indian and South Pacific Oceans. Proceedings of conference on tectonic problems of San Andreas fault systems (ed. Kovach, R.L. and Nur, A.). Stanford University, pp. 136-148.
- Au, C.Y.D. 1977. Lower mantle P wave travel time under Asia. Thesis, the University of Alberta, Edmonton.
- Barron, E.J., Harrison, C.G.A. and Hay, W. 1977. Positions of Southern Continents revised. American Geophysical Union, Transactions, 58, pp. 502.
- Bates, A.C. 1976. Slowness-Azimuth measurements and P wave velocity distributions. A thesis at the University of Alberta.
- Baumgardt, D.R. and Alexander, S.S. 1976. Evidence for lateral heterogeneity in the lower mantle beneath





- continents and oceans from PcP-P residual anomalies. Transactions, American Geophysical Union, 57, pp. 283.
- Berry, M.J., Jacobic, W.R., Niblett, E.R. and Stacey, R.A. 1971. A review of geophysical studies in the Canadian cordillera. Canadian Journal of Earth Sciences, 8, pp. 788-801.
- Berteussen, K.A. 1975. Array analysis of lateral inhomogeneities in the deep mantle. Earth and Planetary Science Letters, 28, pp. 212-216.
- Best, W.J. and Johnson, L.R. 1974. SCS and the mantle beneath Hawaii. Transactions, American Geophysical Union, 55, pp. 1147.
- Briden, J.C. and Irving, E. 1964. Palaeoclimatic spectra of sedimentary palaeoclimatic indicators. In Nairn, A.E.M., ed., Problems in palaeoclimatology. Interscience, N.Y., pp. 199-250.
- Briden, J.C., Smith, A. Gilbert, and Sallomy, J.T. 1970. The geomagnetic field in Permo-Triassic time. Geophysical Journal of the Royal Astronomical Society, 23, pp. 101-117.
- Brown, R.J. 1973. Azimuthally varying P-wave travel-time residuals in Fennoscandia and lateral inhomogeneity. Pure and applied geophysics, 105, pp. 741-758.
- Buchbinder, G.G.R. 1968. Amplitude spectra of PcP and P phases. Bulletin of the Seismological Society of America, 58pp. 1797-1819.
- Buchbinder, G.G.R. and Popinet, G. 1973. Problems related to PcP and the core-mantle boundary illustrated by two nuclear events. Bulletin of the Seismological Society of America, 63, pp. 2047-2070.
- Bugayevskiy, G.N., Nersesov, I.L. and Rogozhiha V.A. 1970. Horizontal inhomogeneities of the upper mantle in central Asia. Akademia Nauk SSSR Izvestia Physics of the Solid Earth. pp. 103.
- Bullard, E.C., Everett, J.E. and Smith, A.G. 1965. The fit of the continents around the Atlantic. In Symposium on continental drift. Philosophical Transactions of the Royal Society, London, A258, pp. 41-51.
- Bullen, K.E. 1965. An introduction to seismology. Cambridge at the university press.
- Chamalaun, T. and Roberts, P.H. 1962. The theory of convection in spherical shells and its application to





- the problem of thermal convection in the earth's mantle. In *Continental Drift* (ed., S.K. Runcorn). Academic Press, New York, pp. 177-194.
- Chandrasekhar, S. 1961. Hydrodynamic and hydromagnetic stability. Oxford Univ. Press, pp. 220-271.
- Chinnery, M.A. 1969. Velocity anomalies in the lower mantle. *Physics of the Earth and Planetary Interiors*, 2, pp. 1-10.
- Choudhury, M.A., Popinet, G. and Perrier, G. 1975. Shear velocity from differential travel times of short period SCS-P in New Hebrides, Fui-Tonga, and Banda Sea Regions. *Bulletin of the Seismological Society of America*, 65, pp. 1787-1796.
- Churkin, M. Jr. 1969. Palaeozoic tectonic history of the Arctic Basin north of Alaska. *Science*, 165, pp. 549-555.
- Churkin, M. Jr. 1972. Western boundary of the North American continental plate in Asia. *Geological Society of America Bulletin*, 83, pp. 1027-1036.
- Cooper, A.K., School, D.W. and Marlow, M.S. 1976. Plate tectonic model for the evolution of the eastern Bering Sea Basin. *Geological Society of America Bulletin*, 87, pp. 1119-1126.
- Cumming, G.L. and Kanasewich, E.R. 1966 Crustal structure in western Canada. Report, Department of Physics, The University of Alberta, Edmonton.
- Davies, G.F. 1977. Whole-mantle convection and plate tectonics. *Geophysical Journal of the Royal Astronomical Society*, 49, pp. 459-486.
- Davies, D., Kelly, E.J. And Filson, J.R. 1971. Vespa process for analysis of seismic signals. *Nature*, 232, pp. 8-13.
- Davies, D. and Sheppard, R.M. 1972. Lateral heterogeneity in the earth's mantle. *Nature*, 239, pp. 318-323.
- Deutsch, E.R. and Rao, K.V. 1977. New palaeomagnetic evidence fails to support rotation of western Newfoundland. *Nature*, 266, pp. 314-318.
- Dewey, J.F. and Bird, J.M. 1970. Mountain belts and the new global tectonics. *Journal of Geophysical Research*, 75, pp. 2625-2647.
- Doornbos, D.J. 1976. Characteristics of lower mantle



- inhomogeneities from scattered waves. *Geophysical Journal Royal Astronomical Society*, 44, pp. 447-470.
- Dziewonski, A.M., Hager, B.H. and O'Connell R.J. 1977. Large scale heterogeneities in the lower mantle. *Journal of Geophysical Research*, 82, pp. 239-255.
- Dziewonski, A.M., Hales, A.L. and Lapwood, E.R. 1975. Parametrically simple earth models consistent with geophysical data. *Physics of the earth and planetary interiors*, 10, pp. 12-48.
- Elsasser, W.M. 1969. Convection and stress propagation in the upper mantle, *In The Application of Modern Physics to the Earth and Planetary Interiors* (ed. Runcorn, S.K.). pp. 223-246, Wiley, New York.
- Engdahl, E.R. 1975. Effects of plate structure and dilatancy on relative teleseismic P-wave residuals. *Geophysical Research Letters*, 2, pp. 420-422.
- Engdahl, E.R. and Johnson, E.J. 1974. Differential PcP travel times and the radius of the core. *Geophysical Journal Royal Astronomical Society*, 39, pp. 435-456.
- Evans, M.E. 1976. Test of the dipolar nature of the geomagnetic field throughout the Phanerozoic time. *Nature*, 262, pp. 276-277.
- Faller, A.M., Briden, J.C. and Morris, W.A. 1977. Palaeomagnetic results from the Borrowdale Volcanic Group, English Lake District. *Geophysical Journal of the Royal Astronomical Society*, 48, pp. 111-121.
- Fisher, R.A. 1953. Dispersion on a sphere. *Proceedings of the Royal Society of London*, A217, pp. 295-305.
- Fisher, R.L., Sclater, J.G. and McKenzie, D.P. 1971. Evolution of the Central Indian Ridge, Western Indian Ocean. *Geological Society of America Bulletin*, 82, pp. 553-562.
- French, R.B., Alexander, D.H. and Van der Voo, R. 1977. Paleomagnetism of Cambrian intrusives from Colorado, submitted to *Geological Society of America Bulletin*.
- Ganley, D.C. and Cumming, G.L. 1974. A seismic reflection model of the crust near Edmonton, Alberta. *The Canadian Journal of Earth Sciences*, 11 pp. 101-109.
- Gutowski, P.R.H. 1974. Seismic array investigation of the upper and lower mantle. Ph. D. thesis. The University of Alberta.





- Gutowski, P.R. and Kanasewich E.R. 1974. Velocity spectral evidence of upper mantle discontinuities. *Geophysical Journal Royal Astronomical socieity*, 36, pp. 21-32.
- Hales, A.L., Cleary, J.R. and Roberts, J.L. 1968. Velocity distribution in the lower mantle. *Bulletin of the Seismological Society of America*, 58, pp. 1975-1989.
- Hales, A.L. and Roberts, J.L. 1970. Shear velocities in the lower mantle and the radius of the core. *Bulletin of the Seismological Society of America*, 60, pp. 1427-1436.
- Hailwood, E.A. 1974. Palaeomagnetism of the Msissi Norite (Morocco) and the Palaeozoic reconstruction of Gondwanaland. *Earth and Planetary Science Letters*, 23, pp. 376-386.
- Harrington, H.J. 1962. Palaeogeographic development of South America. *American Association of Petroleum Geologists Bulletin*, 46, pp. 1773-1814.
- Heirtzler, J.R., Dickson, G.O., Herron, E.M., Pitman, W.C. and Le Pichon, X. 1968. Marine anomalies, geomagnetic field reversals and motions of the ocean floor and continents. *Journal of Geophysical Research*, 73, pp. 2119-2136.
- Herrin, E. and Taggart J. 1968. Regional varriations in P travel times. *Bulletin of Seismological Society of America*, 58, pp. 1325-1337.
- Herrin, E. and Taggart, J. 1968. Source bias in epicenter determination. *Bulletin of the Seismological Society of America*, 58, pp. 1791-1796.
- Herron, E.M. 1972. Sea-floor spreading and the Cenozoic history of the East-Central Pacific. *Geological Society of America Bulletin*, 83, pp. 1671-1692.
- Hess, H.H. 1962. History of ocean basins. In *Petrologic studies*: (ed. Engel, A.J., James, H.L. and Leonard, B.F.). *Geological Society of America, Buddington Volume*, pp. 599-620.
- Husebye, E.S. 1969. Direct measurement of  $dT/d$ , *Bulletin of the Seismological Society of America*, 59, 717-727.
- Husebye, E.S., Kanestrom, R. and Rud, R. 1971. Observations of vertical and lateral P-velocity anomalies in the earth's mantle using the Fennoscandian continental array. *Geophysical Journal Royal Astronomical Society*, 25, pp. 3-16.





- Husebye, E.S. and King, D.W. 1976. Precursors to PKiKP and seismic wave scattering near the core mantle boundary. *Journal of Geophysical Research*, 81, pp. 1870-1882.
- Irving, E. 1960a. Palaeomagnetic pole positions, Part I. *Geophysical Journal of the Royal Astronomical Society*, 3, pp. 96-111.
- Irving, E. 1960b. Part II. *Ibid.*, 3, pp. 444-449.
- Irving, E. 1961. Part III. *Ibid.*, 5, pp. 70-79.
- Irving, E. 1962a. Part IV. *Ibid.*, 6, pp. 263-267.
- Irving, E. 1962b. Part V. *Ibid.*, 7, pp. 263-274.
- Irving, E. 1965. Part VII. *Ibid.*, 9, pp. 185-194.
- Irving, E. 1964. Palaeomagnetism and its application to geological and geophysical problems. John Wiley and Sons Inc., New York, 399 pp.
- Irving, E. and Scott, P.M. 1963. Palaeomagnetic directions and pole positions, Part VI, *Geophysical Journal of the Royal Astronomical Society*, 8, pp. 249-257.
- Isacks, B., Oliver, J. and Sykes, L.R. 1968. Seismology and the new global tectonics. *Journal of Geophysical Research*, 73, pp. 5855-5899.
- Jacob, K.H. 1972. Global implications of anomalous seismic P travel times from the nuclear explosion Longshot. *Journal of Geophysical Research*, 77, pp. 2556-2573.
- Jeffreys, H. and Jeffreys, B.S. 1946. *Methods of mathematical physics*. Cambridge at the University Press.
- Jeffreys H. and Bullen, K.E. 1967. *Seismological tables*. British Association, London.
- Johnson, L.R. 1967. Array measurements of P velocities in the upper mantle. *Journal of Geophysical Research*, 72, pp. 6309-6325.
- Johnson, L.R. 1969. Array measurements of P velocities in the lower mantle. *Bulletin of the Seismological Society of America*, 59 pp. 973-1008.
- Jordan, T.H. 1975. Lateral heterogeneity and mantle dynamics. *Nature*, 257, pp. 745-750.
- Jordan, T.H. and Lynn W.S. 1974. A velocity anomaly in the lower mantle. *Journal of Geophysical Research*, 79, pp.



2679-2685.

- Julian, B.R. and Sengupta M.K. 1973. Seismic travel time evidence for lateral inhomogeneity in the deep mantle. *Nature*, 242, pp. 443-447.
- Kanamori, H. 1967. Spectrum of P and PcP in relation to the mantle-core boundary and attenuation in the mantle. *Journal of Geophysical Research*, 72, pp. 559-571.
- Kanasewich, E.R. 1966. Deep crustal structure under the plains and rocky mountains. *Canadian Journal of earth sciences*, 3, pp. 937-945.
- Kanasewich, E.R. 1976. Plate tectonics and planetary convection. *Canadian Journal of Earth Sciences* 13, pp. 331-340.
- Kanasewich, E.R., Ellis, R.M. Chapman, C.H. and Gutowski, P.R. 1972. Teleseismic array evidence for inhomogeneities in the lower mantle and the origin of the Hawaiian Islands. *Nature*, 239 pp. 99-100.
- Kanasewich, E.R., Ellis, R.M., Chapman, C.H. and Gutowski, P.R. 1973. Seismic array evidence of a core boundary source for the Hawaiian linear volcanic chain. *Journal of Geophysical Research*, 78, pp. 1361-1371.
- Kanasewich, E.R., Ellis, R.M., Chapman, C.H. and Gutowski, P.R. 1975. Reply. *Journal of Geophysical Research*, 80, pp. 1920-1922.
- Kanasewich, E.R. and Gutowski, P.R. 1975. Detailed seismic analysis of a lateral mantle inhomogeneity. *Earth and Planetary Science Letters*, 25, pp. 379-384.
- Kanasewich, E.R., Siewert, W.P., Burke, M.D., McCloughan, C.H. and Ramsdell, L. 1974. Gain-ranging analog or digital seismic system. *Bulletin of the Seismological Society of America*, 64 pp. 103-113.
- Kaula, W.M. 1975. Absolute plate motions by boundary velocity minimizations. *Journal of Geophysical Research*, 80, pp. 244-248.
- Khramov, A.N. and Sholpo L.Ye. 1967. Synoptic labels of U.S.S.R. paleomagnetic data. Appendix I of *Paleomagnetism*. Nedra Press, Leningrad, 213-233 (Translated by E.R. Hope, Directorate of Scientific Information Service, DRB, Canada T510R, 1970) (129,212,282)
- King, P.B. 1970. Tectonics and Geophysics of Eastern North America. In *The megatectonics of continents and*



- oceans. (ed.: Johnson, H. and Smith, B.L.). Rutgers University Press, New Brunswick, New Jersey, pp. 74-112.
- Kulhanek, O. and Brown, R.J. 1974. P-Wave velocity anomalies in the earth's mantle from the Uppsala array observations. *Pure and Applied Geophysics*, 112, pp. 597-617.
- Kummell, B. 1970. *History of the Earth*. Freeman, 2nd ed. San Francisco, 707 pp.
- Ladd, J.W. 1976. Relative motion of South America with respect to North American and Caribbean tectonics. *Geological Society of America Bulletin*, 87, pp. 969-976.
- Lambert, R. St. J. 1974. Global tectonics and the Canadian Arctic Continental Shelf. *Proceedings of the Symposium on the Geology of the Canadian Arctic*, (ed. Aitken, J.D. and Glass, D.J.). G.A.C. special publication, pp. 5-22.
- Larson, R.L. and Chase, C.G. 1972. Late Mesozoic evolution of the western Pacific Ocean. *Geological Society of America Bulletin*, 83, pp. 3627-3644.
- Larson, R.L. and Pitman, W.C. 1972. World-wide correlation of Mesozoic magnetic anomalies and its implications. *Geological Society of America Bulletin*, 83, pp. 3645-3662.
- Le Pichon, X. 1968. Sea-floor spreading and continental drift. *Journal of Geophysical Research*, 73, pp. 3661-3697.
- McBirney, A.R. and Bass, M.N. 1969. Structural relations of pre-Mesozoic rocks of northern Central America. *American Association of Petrology and Geology, Memoir* 11, pp. 269-280.
- McElhinny, M.W. 1964. Statistical significance of the fold test in palaeomagnetism. *Geophysical Journal of the Royal Astronomical Society*, 8, pp. 338-340.
- McElhinny, M.W. 1968a. Notes on progress in geophysics. Palaeomagnetic directions and pole positions, Part VIII. *Geophysical Journal of the Royal Astronomical Society*, 15, pp. 409-430.
- McElhinny, M.W. 1968b. Part IX. *Ibid.*, 16, pp. 207-224.
- McElhinny, M.W. 1969. Part X. *Ibid.*, 19, 305-327.





- McElhinny, M.W. 1970. Part XI. Ibid., 20, pp. 417-429.
- McElhinny, M.W. 1972a. Part XII. Ibid., 27, pp. 237-257.
- McElhinny, M.W. 1972b. Part XIII. Ibid., 30, pp. 281-293.
- McElhinny, M.W. 1973. Palaeomagnetism and Plate Tectonics. Cambridge University Press.
- McElhinny, M.W. and Cowley, J.A. 1977. Palaeomagnetic directions and pole positions, Part XIV. Geophysical Journal of the Royal Astronomical Society, 49, pp. 313-356.
- McElhinny, M.W. and Embleton, B.J.J. 1974. Australian Palaeomagnetism and the Phanerozoic plate tectonics of Eastern Gondwanaland. Tectonophysics, 22, pp. 1-29.
- McElhinny, M.W. and Merrill, R.T. 1975. Geomagnetic secular variations over the past 5m.y. Reviews of Geophysics and Space Physics, 13, pp. 687-708.
- McKenzie, D.P. 1969. Speculations on the consequences and causes of plate motions. Geophysical Journal of the Royal Astronomical Society, 18, pp. 1-32.
- McKenzie, D.P. and Morgan, W.J. 1969. The evolution of triple junctions. Nature, 224, pp. 125-133.
- McKenzie, D.P. and Parker, R.L. 1967. The north Pacific: An example of tectonics on a sphere. Nature, 216, pp. 1276-1280.
- McKenzie, D.P. and Sclater, J.G. 1971. The evolution of the Indian Ocean since the Late Cretaceous. Geophysical Journal of the Royal Astronomical Society, 24, pp. 437-528.
- Minster, J.B., Jordan, T.H., Molnar, P. and Haines, E. 1974. Numerical modelling of instantaneous plate tectonics. Geophysical Journal of the Royal Astronomical Society, 36, pp. 541-576.
- Mitchell, B.J. and Helmberger, D.V. 1973. Shear velocities at the base of the mantle from observations of S and ScS. Journal of Geophysical Research, 78, pp. 6009-6020.
- Molnar, P., Atwater, T., Mannerickx, J. and Smith, S.M. 1975. Magnetic Anomalies, Bathymetry and the Tectonic Evolution of the South Pacific since the late Cretaceous. Geophysical Journal of the Royal Astronomical Society, 40, pp. 383-420.





- Morgan, W.J. 1968. Rises, trenches, great faults, and crustal blocks. *Journal of Geophysical Research*, 73, pp. 1952-1982.
- Needham, R.E. and Davies, D. 1973. Lateral heterogeneity in the deep mantle from seismic body wave amplitudes. *Nature*, 244, pp. 152-153.
- Nersesov, I.L., Nikolayev A.V. and Sedova Y.N. 1972. Horizontal inhomogeneities of the earth's mantle as derived from seismic data. *Akademiia Nauk SSSR Izvestia Physics of the solid earth*. 207 pp. 29.
- Niazi, M. 1966. Corrections to apparent Azimuths and travel-time gradients for a dipping Mohorovicic discontinuity. *Bulletin of the Seismological Society of America*, 56, pp. 491-509.
- Niazi, M. 1973. SH travel times and lateral heterogeneities in the lower mantle. *Bulletin of the Seismological Society of America*, 63, pp. 2035-2046.
- Noponen, I. 1974. Seismic ray direction anomalies caused by deep structure in Fennoscandia. *Bulletin of the Seismological Society of America*, 64, pp. 1931-1941.
- Okal, E.A. and Anderson D.L. 1975. A study of lateral inhomogeneities in the upper mantle by multiple SCS travel time residuals. *Geophysical Research Letters*, 2, pp. 313-316.
- Okal, E. and Kuster, G. 1975. A teleseismic array study in French Polynesia; implications for distant and local structure. *Geophysical Research Letters* 2, pp. 5-8.
- Oliver, J. and Isacks, B. 1967. Deep earthquake zones, anomalous structures in the upper mantle, and the lithosphere. *Journal of Geophysical Research*, 72, pp. 4259-4275.
- Peltier, W.R. 1973. Penetrative convections in the planetary mantle. *Geophysical Fluid Dynamic*, 5, pp. 47-88.
- Phinney, R.A. and Alexander, S.S. 1969. The effect of a velocity gradient at the base of the mantle on diffracted P waves in the shadow. *Journal of Geophysical Research*, 74, pp. 4967-4971.
- Pitman, W.C. and Talwani, M. 1972. Sea-floor spreading in the North Atlantic. *Geological Society of America Bulletin*, 83, pp. 619-646.
- Pitman, W.C., Larson, R.L. and Herron, E.M. 1974. The age of the Ocean Basins. *Geological Society of America*,



Boulder, Colorado.

- Pospelova, G.A., Larionova, G. Ya, and Anuchin, A.V. 1968. Paleomagnetic investigations of Jurassic and Lower Cretaceous sedimentary rocks of Siberia. *International Geological Review*, 10, pp. 1108-18.
- Powell, C. 1976. Array evidence for lower mantle heterogeneity beneath subduction zones. *Transactions, American Geophysical Union*, 57, pp. 284.
- Robinson, R. and Kovac, R.L. 1972. Shear wave velocities in the earth's mantle. *Physics of the Earth and Planetary Interiors*, 5, 30-44.
- Sacks, I.S. 1967. Diffracted P-wave studies of the earth's core., 2 lower mantle velocity, core size, lower mantle structure. *Journal of Geophysical Research*, 72, pp. 2589-2594.
- Sacks, J.S. and Snoke, A. 1976. Heterogeneous velocity structure at the base of the mantle. *Transactions, American Geophysical Union*, 57, pp. 284.
- Schmidt, P.W. 1976. The non-uniqueness of the Australian Mesozoic palaeomagnetic pole position. *Geophysical Journal of the Royal Astronomical Society*, 47, pp. 285-300.
- Sclater, J.G. and Fisher, R.L. 1974. Evolution of the East Central Indian Ocean. *Geological Society of America Bulletin*, 85, pp. 683-702.
- Sengupta, M.K. and Toksoz, M.N. 1976. Three dimensional model of seismic velocity variation in the earth's mantle. *Geophysical Research Letters*, 3, pp. 84-86.
- Sipkin, S.A. and Jordan, T.H. 1975. Lateral heterogeneity of the upper mantle determined from travel times of SCS. *Journal of Geophysical Research*, 80, 1474-1484.
- Sipkin, S.A. and Jordan, T.H. 1976. Lateral heterogeneity of the upper mantle from multiple SCS travel times. *Transactions, American Geophysical Union*, 57, pp. 283.
- Smith, A.G. and Hallam, A. 1970. The fit of the southern continents. *Nature*, 225, pp. 139-144.
- Smith, A.G., Briden, J.C. and Drewry, G.E. 1973. Phanerozoic world maps; Special papers in palaeontology, No. 12, pp. 1-42.
- Spall, H. 1970. Paleomagnetism of basement granities in southern Oklahoma; Final report, Okla. Geol. Notes, 30





, pp. 136-150.

- Stewart, I.C.F. 1977. Travel-time anomalies in the lower mantle under the North Atlantic. *Geophysical Journal Royal Astronomical Society*, 49, pp. 487-497.
- Takeuchi, H. and Sakata, S. 1970. Convection in a mantle with variable viscosity. *Journal of Geophysical Research*, 75, pp. 921-927.
- Thompson, R. 1972. Palaeomagnetic results from the Paganzo Basin of North-west Argentina. *Earth and Planetary Science Letters*, 15, pp. 145-156.
- Thompson, R. 1973. South American Palaeozoic palaeomagnetic results and the welding of Pangaea. *Earth and Planetary Science Letters*, 18, pp. 266-278.
- Toksoz, M.N., Arkani-Hamed, J. and Knight, C.A. 1969. Geophysical data and long-wave heterogeneities of the earth's mantle. *Journal of Geophysical Research*, 74, pp. 3751-3770.
- Toksoz, M.N. Chinnery, M.A. and Anderson D.L. 1967. Inhomogeneities in the Earth's mantle. *Geophysical Journal Royal Astronomical Society*, 13, pp. 31-59.
- Vinik, L.P., Lukk, A.A. and Nikolaev, A.V. 1972. Inhomogeneities in the lower mantle. *Physics of the Earth and Planetary Interiors*, 5, pp. 328-331.
- Vine, F.J. and Matthews, D.H. 1963. Magnetic anomalies over oceanic ridges. *Nature*, 199, pp. 947-949.
- Torreson, O.W., Murphy, T. and Graham, J.W. 1949. Magnetic polarization of sedimentary rocks and the Earth's magnetic history. *Journal of Geophysical Research*, 54, pp. 111-129.
- Van der Voo, R., French, R.B. and Williams, D.W. 1976. Palaeomagnetism of the Wilberns Formations (Texas) and the Late Cambrian Palaeomagnetic Field for North America. *Journal of Geophysical Research*, 81, pp. 5633-5638.
- Wegener, A.L. 1929. The origin of Continents and Oceans. (1966 English translation of fourth revised edition, 1929, of "Die Entstehung der Kontinente und Ozeane"). Dover Publications, New York.
- Wensink, H. 1972. A note on the palaeomagnetism of the Lower Siwaliks near Saiden Shah, Pakistan. *Pakistan Journal of Scientific and Industrial Research*, 1, pp. 89-91.





- Wensink, H. 1975. The structural history of the India-Pakistan subcontinent during the Phanerozoic. In Progress in Geodynamics (ed. Borradaile, G.J., Ritsema, A.R., Rondeel, H.E. and Simon, O.J.). North-Holland Publishing Co., pp. 190-207.
- Wensink, H. and Klootwijk, C.T. 1971. Paleomagnetism of the Deccan Traps in the Western Ghats near Poona (India), Tectonophysics, 11, pp. 175-190.
- Wiechert, D.H. 1972. Anomalous azimuths of P: evidence for lateral variations in the deep mantle. Earth and Planetary Science Letters, 17, pp. 181-188.
- Wilson, J.T. 1965. A new class of faults and their bearing on continental drift. Nature, 207, pp. 343-347.
- Wilson, J.T. 1966. Did the Atlantic close and then re-open? Nature, 211, pp. 676-681.
- Wright, C. 1973. Array studies of P phases and the structure of D" Region of the mantle. Journal of Geophysical Research, 78, pp. 4965 - 4982.
- Wright, C. 1975. The origin of short-period precursors to PKP. Transactions, the American Geophysical Union, 56, pp. 395.
- Wright, C. 1975. Comments on 'Seismic array evidence of a core boundary source for the Hawaiian linear chain' by E.R. Kanasewich et al. Journal of Geophysical Research, 80, pp. 1915-1919.
- Wright, C. and Lyons, J.A. 1975. Seismology,  $dT/d\Delta$  and deep mantle convection. Geophysical Journal Royal Astronomical Society, 40, pp. 115-138.



## APPENDIX 1

### PALAEOMAGNETIC DATA AND CONTINENTAL MOVEMENT

Table A1.1

Rotation data and average unrotated palaeomagnetic poles for the different geological periods. The abbreviations are: RLAT and RLON: Latitude (positive north) and longitude (positive east) in degrees of the Euler pole; RROT: Angle of rotation in degrees, positive anticlockwise; VEL1 and VEL2: Maximum and minimum velocity (cm/year) of the continental segment going forwards in time from the relevant reconstruction to the succeeding one; LAT,LON: Latitude (positive north) and longitude (positive east) in degrees of the average pole; R: The length of the vector resultant of the poles treated as unit vectors; K: Fisher's K, see text; A95: Radius in degrees of a small circle centered on (LAT,LON), and within which the mean lies 95 % confidence.



## TERTIARY

CONTINENT	RLAT	RLON	RROT	VEL1	VEL2	LAT	LON	A95	K	N
N. AMERICA TPA-TO	52.2	81.6	15.5	4.6	3.3	-87	19	7	38	11
KOLYMA	7.9	88.6	9.4	....	....	...	....	...	...	..
W. EUROPE TE-TM	7.9	88.6	9.4	2.8	1.7	-76	-19	4	76	17
RUSS. PLT. TPA-TO	7.9	88.6	9.4	....	....	-68	12	14	44	4
SPAIN TPA-TE	7.9	88.6	9.4	....	....	-75	19	9	76	5
GREENLAND KU-TE	52.2	81.6	15.5	3.9	2.9	-62	14	17	55	3
SIBERIA T	7.9	88.6	9.4	2.6	0.4	-85	-157	5	84	12
CHINA TE-TM	7.9	88.6	9.4	....	....	-75	-142	...	...	1
S. AMERICA T-QP	51.1	55.7	8.2	2.4	1.3	-77	-122	18	26	4
ANTARCTICA TM-TP	-53.8	81.8	6.7	1.6	0.5	-81	-86	...	...	1
AFRICA TE-TM	-22.1	107.6	11.3	3.3	2.6	-82	-65	9	51	6
AUSTRALIA TO	-39.4	-163.3	24.1	6.6	4.5	-69	92	...	...	1
NEW ZEALAND	-39.4	-163.3	24.1	....	....	...	....	...	...	..
MADAGASCAR	-22.1	107.6	11.3	2.8	2.7	...	....	...	...	..
ARABIA KU-TE	-32.1	133.3	13.9	....	....	-69	84	18	47	3
INDIA KU-TM	-25.3	-147.3	37.4	8.6	5.9	-56	89	...	...	2

## CRETACEOUS

CONTINENT	RLAT	RLON	RROT	VEL1	VEL2	LAT	LON	A95	K	N
N. AMERICA JU-KU	53.5	107.6	34.4	3.1	1.8	-67	6	7	40	12
KOLYMA KL-KU	53.5	107.6	34.4	....	....	-60	-14	10	43	6
W. EUROPE KL-KU	-25.9	129.6	22.5	2.6	0.7	-86	-93	12	56	4
RUSS. PLT. KL	-25.9	129.6	22.5	....	....	-66	-14	...	...	2
SPAIN KU	-25.9	129.6	22.5	....	....	-76	-6	...	...	1
GREENLAND	21.7	111.8	27.5	2.7	2.2	...	....	...	...	..
SIBERIA KL-KU	-25.9	129.6	22.5	2.8	2.1	-77	-4	18	15	6
CHINA K	-25.9	129.6	22.5	....	....	-69	2	19	44	3
S. AMERICA JU-TPA	51.7	-3.4	29.3	3.6	2.8	-84	19	12	62	4
ANTARCTICA	-13.2	-41.7	33.2	5.4	5.0	...	....	...	...	..
AFRICA JU-KL	-19.7	141.3	27.7	2.8	0.3	-57	77	11	41	6
AUSTRALIA KL	-19.8	-91.7	41.4	4.5	1.6	-53	152	12	114	3
NEW ZEALAND	-19.9	-82.7	48.4	....	....	...	....	...	...	..
MADAGASCAR	-41.9	159.2	16.5	1.6	1.5	...	....	...	...	..
ARABIA KL-KU	-22.1	150.2	31.8	....	....	-46	98	13	28	6
INDIA KL	-20.5	-161.5	71.6	5.5	4.8	-15	117	18	48	3



## TRIASSIC, BULLARD ET AL MODEL

CONTINENT	RLAT	RLON	RROT	VEL1	VEL2	LAT	LON	A95	K	N
N. AMERICA TRU	58.6	40.3	57.1	4.8	2.0	-67	-90	6	43	16
KOLYMA TR	58.6	40.3	57.1	....	....	-63	57	13	35	5
W. EUROPE TRL-U	22.6	59.6	30.1	2.7	0.1	-46	-37	7	108	5
RUSS. PLT. TRL-U	22.6	59.6	30.1	....	....	-51	-26	7	52	10
SPAIN TR	-7.2	112.7	25.4	....	....	-59	8	...	...	2
GREENLAND TRU	45.2	57.1	46.3	2.8	1.8	-34	-77	...	...	1
SIBERIA TRL-M	22.6	59.6	30.1	4.9	2.1	-47	-29	7	31	16
S. AMERICA TRU-JM	44.4	5.5	30.2	0.7	0.6	-78	-102	8	111	4
ANTARCTICA J	-26.0	-36.7	33.3	0.7	0.0	-55	-145	9	77	5
AFRICA TRU-JM	-26.0	129.7	32.3	1.1	0.6	-68	74	4	80	18
AUSTRALIA TRU-JM	-30.6	-94.1	39.6	0.7	0.1	-47	176	9	75	5
NEW ZEALAND	-30.2	-90.5	48.8	....	....	...	....	...	...	..
MADAGASCAR TRU-JL	-49.0	136.2	21.8	0.7	0.6	-74	97	...	...	1
ARABIA	-27.6	138.9	35.8	....	....	...	....	...	...	..
INDIA TRU	-22.9	-168.2	71.4	0.7	0.4	-20	128	...	...	2

## TRIASSIC, OUR PREFERRED MODEL

CONTINENT	RLAT	RLON	RROT	VEL1	VEL2	LAT	LON	A95	K	N
N. AMERICA TRU	59.6	48.9	53.9	4.1	1.8	-67	-90	6	43	16
KOLYMA TR	55.9	167.8	49.3	3.6	2.8	-63	57	13	35	5
W. EUROPE TRL-U	19.7	68.6	27.2	2.2	0.2	-46	-37	7	108	5
RUSS. PLT. TRL-U	19.7	68.6	27.2	....	....	-51	-26	7	52	10
SPAIN TR	-11.8	122.4	27.5	....	....	-59	8	...	...	2
GREENLAND TRU	44.4	65.0	43.3	2.3	1.6	-34	-77	...	...	1
SIBERIA TRL-M	19.7	68.6	27.2	4.2	1.6	-47	-29	7	31	16
S. AMERICA TRU-JM	35.9	2.9	32.7	1.3	0.8	-78	-102	8	111	4
ANTARCTICA J	-27.8	-31.2	37.6	0.8	0.1	-55	-145	9	77	5
AFRICA TRU-JM	-28.9	119.6	31.2	1.6	0.4	-68	74	4	80	18
AUSTRALIA TRU-JM	-35.8	-87.3	40.1	1.4	0.7	-47	176	9	75	5
NEW ZEALAND	-34.7	-85.3	49.5	....	....	...	....	...	...	..
MADAGASCAR TRU-JL	-55.0	115.5	21.9	0.5	0.3	-74	97	...	...	1
ARABIA	-30.8	130.1	34.2	....	....	...	....	...	...	..
INDIA TRU	-25.8	-170.1	67.8	0.7	0.3	-20	128	...	...	2





## PERMO CARBONIFEROUS

CONTINENT	RLAT	RLON	RROT	VEL1	VEL2	LAT	LON	A95	K	N
N. AMERICA CL-PL	39.1	52.5	48.3	2.2	0.1	-39	-55	4	94	16
KOLYMA	39.1	52.5	48.3	....	....	...	....	...	...	..
W. EUROPE CU-PL	-9.6	72.4	36.7	2.3	1.6	-39	-14	3	81	24
RUSS. PLT. CL	-9.6	72.4	36.7	....	....	-43	-12	4	106	12
SPAIN CU-P	-25.3	111.7	43.1	....	....	-46	33	8	74	6
GREENLAND	19.9	66.3	44.5	1.8	1.4	...	....	...	...	..
SIBERIA CL-TR	-11.1	75.0	34.3	2.2	1.3	-34	-36	9	25	11
S. AMERICA C-PU	64.9	88.1	41.9	2.8	0.2	-70	-15	6	47	12
ANTARCTICA	36.3	-63.7	11.0	4.1	2.1	...	....	...	...	..
AFRICA CU-PL	2.8	151.8	50.9	3.8	0.5	-40	64	...	...	2
AUSTRALIA CU-PU	9.8	-122.9	35.1	4.4	4.1	-48	137	6	178	5
NEW ZEALAND	6.0	-108.0	36.7	....	....	...	....	...	...	..
MADAGASCAR	3.6	159.7	37.1	2.9	2.7	...	....	...	...	..
ARABIA P	0.7	157.0	54.3	....	....	-18	102	...	...	1
INDIA CU-PU	-1.9	-164.6	86.3	3.7	2.9	4	130	27	9	5

## DEVONIAN

CONTINENT	RLAT	RLON	RROT	VEL1	VEL2	LAT	LON	A95	K	N
N. AMERICA SM-DU	22.1	50.9	64.6	2.8	1.8	-33	-53	11	20	10
KOLYMA	22.1	50.9	64.6	....	....	...	....	...	...	..
W. EUROPE DL-CL	-9.8	70.4	59.3	2.8	1.9	-19	-26	8	26	13
RUSS. PLT. DL-DU	-9.8	70.4	59.3	....	....	-36	-18	4	162	10
SPAIN SU	-16.6	98.1	61.5	....	....	-29	36	...	...	2
GREENLAND	9.0	62.1	64.8	2.8	2.8	...	....	...	...	..
SIBERIA DL-DU	17.3	71.8	65.3	3.8	0.1	-28	-29	8	65	7
S. AMERICA DL-CU	29.4	74.0	69.5	5.3	4.0	-43	-29	26	24	3
ANTARCTICA	3.1	78.1	35.3	5.3	4.6	...	....	...	...	..
AFRICA DU	12.6	122.1	79.0	5.3	3.3	-1	25	...	...	1
AUSTRALIA SU-DU	25.3	137.2	22.1	5.2	4.1	-72	-6	20	23	4
NEW ZEALAND	21.6	136.6	12.6	....	....	...	....	...	...	..
MADAGASCAR	11.6	119.5	64.3	4.8	4.7	...	....	...	...	..
ARABIA	12.6	126.9	79.5	....	....	...	....	...	...	..
INDIA	17.7	169.7	82.5	4.8	3.8	...	....	...	...	..



## ORDOVICIAN

CONTINENT	RLAT	RLON	RROT	VEL1	VEL2	LAT	LON	A95	K	N
N. AMERICA C-OU	25.6	43.0	67.8	0.9	0.2	-32	-57	4	181	7
KOLYMA	25.6	43.0	67.8	.....	.....	...	.....	...	...	..
W. EUROPE OL-OU	-4.8	62.3	59.6	0.8	0.0	-8	9	9	37	9
RUSS. PLT. OL-SL	-4.8	62.3	59.6	.....	.....	-28	-31	16	25	5
SPAIN	-13.0	90.0	57.5	.....	.....	...	.....	...	...	..
GREENLAND	13.6	54.8	66.4	0.3	0.1	...	.....	...	...	..
SIBERIA OL-OU	23.3	83.6	133.4	7.2	0.4	25	-49	6	49	15
S. AMERICA C-O	7.7	84.1	107.8	5.6	3.6	16	-29	37	7	4
ANTARCTICA OL	-6.2	99.9	80.7	5.6	4.1	-28	10	...	...	1
AFRICA O	9.6	115.7	127.9	5.6	4.3	50	-11	...	...	1
AUSTRALIA OL-OM	9.5	117.9	69.5	4.7	2.7	-15	36	30	18	3
NEW ZEALAND	5.0	117.5	61.3	.....	.....	...	.....	...	...	..
MADAGASCAR	7.2	114.5	113.6	5.1	5.0	...	.....	...	...	..
ARABIA	11.0	118.7	128.0	.....	.....	...	.....	...	...	..
INDIA	27.4	145.3	116.5	4.9	4.0	...	.....	...	...	..

## CAMBRIAN

CONTINENT	RLAT	RLON	RROT	VEL1	VEL2	LAT	LON	A95	K	N
N. AMERICA PC-CU	2.3	73.1	86.1	4.6	0.3	-4	-19	6	99	7
KOLYMA	2.3	73.1	86.1	.....	.....	...	.....	...	...	..
W. EUROPE CL	-4.2	75.8	75.2	3.0	2.4	-22	-13	...	...	2
RUSS. PLT. CL	-4.2	75.8	75.2	.....	.....	-8	-9	15	38	4
SPAIN	-8.3	100.9	77.4	.....	.....	...	.....	...	...	..
GREENLAND	-6.2	81.8	92.2	4.1	2.9	...	.....	...	...	..
SIBERIA CM	10.3	92.3	138.6	4.1	2.8	44	-23	12	61	4
S. AMERICA C	24.4	83.7	124.1	3.9	1.3	38	22	41	4	5
ANTARCTICA OL-CU	-7.5	108.3	109.9	4.4	2.9	-2	28	...	...	1
AFRICA PC-OL	27.3	118.9	130.5	3.9	0.1	15	-23	21	19	4
AUSTRALIA CL-M	7.9	118.9	101.2	3.4	1.4	15	28	...	...	2
NEW ZEALAND	4.8	119.6	93.0	.....	.....	...	.....	...	...	..
MADAGASCAR	26.4	115.2	116.8	1.9	1.6	...	.....	...	...	..
ARABIA C-O	28.8	122.2	129.7	.....	.....	37	-37	...	...	1
INDIA PC-CU	45.8	152.7	114.2	2.9	1.8	-34	32	11	52	5





Table A1.2

Comparable statistics for all solutions using paleomagnetic data.

The abbreviations are: N,LAT,LON,R,K,A95: As in table A1.1; F%: Test of the significance level in percent using the ratio of two K values in an F distribution. The third table gives the increase in precision for the ratio  $K(\text{preferred})/K(\text{alternate})$ .



## STATISTICS FOR OUR SOLUTIONS

	BEFORE ROTATION						AFTER ROT.				
TIME PERIOD	N	LAT	Lon	R	K	A95	R	K	A95	F%	
TERTIARY	13	-83.8	38.0	12.4	21	9	12.6	30	8	80.0	
CRETACEOUS	12	-76.4	59.0	10.5	7	17	11.5	21	10	99.5	
TRIASSIC	13	-82.7	-42.6	10.3	4	24	12.4	21	9	99.9	
FERMO CARB.	10	-62.5	33.0	6.5	3	38	9.5	18	12	99.9	
DEVONIAN	8	-36.0	-12.0	6.9	6	24	7.8	41	9	99.9	
ORDOVICIAN	7	-2.9	-19.0	5.2	3	39	6.8	33	11	99.9	
CAMBRIAN	9	4.9	-3.0	7.5	5	25	8.7	26	10	99.5	
CAMBRIAN ALTERNATE	9	4.9	-3.0	7.5	5	25	8.3	12	16	95.0	

## STATISTICS FOR THE BULLARD SOLUTION COMPARED TO OUR SOLUTION.

BULLARD							OURS			
TIME PERIOD	N	LAT	LON	R	K	A95	R	K	A95	F%
TRIAS. EXCL. KOL.	12	-90.0	.....	11.6	28	8	11.4	19	10	....
PERMO CARB.	10	-67.4	52.0	9.4	15	13	9.5	18	12	65.0
DEVONIAN	8	-50.0	3.0	7.7	25	11	7.8	41	9	80.0
ORDOVICIAN	7	-9.7	-7.0	5.8	5	31	6.8	33	11	99.8
CAMBRIAN	9	0.9	-5.0	7.2	4	28	8.7	26	10	99.9

## STATISTICS FOR OURS AND BARRON ET AL'S ALTERNATE GONDWANALAND SOLUTION COMPARED TO OUR PREFERRED SOLUTION.

		OURS									
		ALTERNATE				PREFERRED			BARRON		
TIME PERIOD	N	R	K	A95	R	K	A95	R	K	A95	F%
TRIASSIC	13	12.3	17	10	12.4	21	9	12.3	18	10	65.0
PERMO CARB.	10	9.5	19	12	9.5	18	12	9.4	16	13	50.0
DEVONIAN	8	7.7	21	12	7.8	41	9	7.8	31	10	90.0
ORDOVICIAN	7	6.7	22	13	6.8	33	11	6.7	19	14	75.0
CAMBRIAN	9	8.6	21	12	8.7	26	10	8.3	11	16	60.0





Table A1.3  
Paleomagnetic data used in reconstructions.

The poles used are listed her by age and continent. Most poles are identified by the number (or group of numbers for combined entries) given them in the lists published in the Geophysical Journal of The Royal Astronomical Society. Thus the number 8.33 refers to pole 33 of list 8. Russian data are taken from the list published by Khramov and Sholpo (1967) and are prefixed by the letter R. Other poles taken from the recent litterature are referenced individually.

TERTIARY

N. America	9.29; 10.46; 11.25; 11.30-31; 12.45; 13.20; 14.120; 14,133; 14.138; 14.146; 14.148:
Greenland	9.27; 14.157; 14.177:
W. Europe	1.31; 1.32; 1.33; 1.34; 2.13; 2.14; 2.15; 6.11-13; 8.23; 8.33; 11.28; 12.49; 14.128; 14.143; 14.144; 14.145; Irving 1964 pole 11.024:
Spain	10.42; 10.43; 11.29; 13.19; 14.142:
Russian Platform	R.65; R.68; R.69; R.70:
Siberia	Ottawa list - poles 11-349; 472; 473; 474; 480; 481; 482; 486; 487; 488; 553; 738:
China	10.36-38,44:
S. America	10. 48; 11.15; 12.51; 14.136:
Africa	8.36; 12.46; 14.125; 14.127; 14.129; 14.135:
Arabia	10.41; 10.49; R.71:
Australia	14.126:
India	Two poles are averaged - Siwalik Beds, Wensink 1972; Deccan Traps, 13.21-24, 14.178-181, 183- 185, and Wensink & Klootwijk 1971:
Antarctica	2.11:



CRETACEOUS

N. America	7.25; 8.48; 8.52; 9.42; 9.43; 11.35; 11.36; 11.37, 14.191; 14.212; 14.213; 14.214:
W. Europe	5.15-16; 8.46; 8.51; 14.211:
Spain	11.32:
Russian Platform	R.76; 8.53:
Siberia	8.45; R.73; R.73 subdivided into 3 poles (see McElhinny, 1973, p. 299); 1 pole from Pospelova et al 1968 (see McElhinny 1973):
Kolyma	12.55; 12.66,70; 12.68; 12.69; 12.76; 12.77:
China	8.49; 10.55; 10.51-2, 10.57-61:
S. America	6.35; 14.190; 14.215; 14.227:
Africa	7.21; 9.40; 13.32; 14.224; 14.225; 14.226:
Arabia	9.41; 10.56; 10.62; 12.67; 12.71; 14.223:
Australia	6.31; 7.23; 15.035:
India	7.31; 12.73; 13.30:





TRIASSIC

N. America	1.67; 5.34; 5.35; 8.68; 8.69; 9.49; 9.50; 10.88; 10.89; 10.90; 11.44; 13.39; 14.278; 14.279; 14.280; 14.285:
Greenland	14.275:
W. Europe	1.63+4.7; 1.64; 10.91; 14.292; Irving 1964 pole 8.07:
Spain	9.61; 11.54:
Russian Platform	R.89; R.91; R.92; R.105; R.106; R.107; R.109; R.110; R.111; R.112:
Siberia	R.93; R.94; R.95; R.96; R.97; R.98; R.99; R.100; R.101; R.102; R.103; R.115; R.116; R.117; R.118; R.119:
Kolyma	12.97; 12.98; 12.99; 12.103; 12.104:
S. America	11.46; 12.102; 14.241; 14.274:
Africa	6.40-43; 8.59; 8.63; 8.67; 8.72; 10.77; 12.93; 13.35; 13.36; 13.40; 14.248; 14.249; 14.250; 14.288; 14.290; 14.693; 15.087; 15.088:
India	11.43; 11.45:
Madagascar	14.269:
Antarctica	2.26; 2.27; 6.63; 10.70; 14.239:



CARBONIFEROUS

N. America	1.106-7; 8.95-7; 8.99; 8.100; 8.101; 8.113; 8.117; 9.98; 10.115; 10.119; 10.120; 11.76; 11.78; 13.50; 13.51; 13.52:
W. Europe	1.96; 2.36; 10.107; 10.108; 10.109; 10.111; 10.112; 10.113; 11.71; 11.77; 12.119; 13.53; 14.310; 14.311; 14.312; 14.313; 14.314; 14.315; 14.316; 14.317; 14.318; 14.334; 14.338; 14.350:
Spain	7.36; 9.78-9; 9.80; 11.72; 11.73; 11.74:
Russian Platform	9.92; 9.93; 9.94; 9.111; 9.112; 9.113; R.149; R.151; R.153; R.155; R.156; R.189:
Siberia	9.85; 9.100; 9.114; 10.100; 10.116; 10.123; 10.124; R.120; R.145; R.178; R.192:
S. America	14.305; 14.309; 14.332; 14.333; 14.345; 14.346:
Australia	7.39; 8.103; 8.104; 8.105:
Africa	8.91; 8.92:
Arabia	8.84:
India	9.66; 10.144; 11.64; 14.329; 1 pole from Athavale et al 1972 (see Wensink 1975):



DEVONIAN

N. America	1.117; 8.120; 8.121; 8.123; 9.120; 9.125; 10.126; 14.364; 14.365; 14.366:
W. Europe	1.97; 1.99-101; 1.102; 8.118; 8.124; 12.134; 13.63; 14.358; 14.359; 14.362; 14.363; 14.373; 14.374:
Spain	9.126; 9.127:
Russian Platform	R.204; R.205; R.206; R.207; R.224; R.226; R.227; R.228; R.229; R.230:
Siberia	10.127; 10.128; R.208; R.213; R.214; R.219; R.225:
S. America	12.124; 12.127; 12.135:
Africa	14.361:
Australia	8.127; 14.360; 14.368; 14.369:





ORDOVICIAN

N. America	14.392; 14.394; 14.396 poles N1,N3,N4 and M2 reported by Deutsch and Rao 1977:
W. Europe	poles A,B,C,E,M,V,W,X and Y reported by Fallier et al 1977:
Russian Platform	R.237; R.249,51; R.250: R.253: R.254-5:
Siberia	10.131; 10.132; 10.133; 10.134; 10.135; 10.136; 10.137; 10.138; 10.139; R.239; R.247; R.248; R.256; R.259; R.260:
S. America	12.140; 12.144; 12.145; 14.406:
Antarctica	10.140:
Africa	4.32:
Australia	14.393; 14.395; 14.405:



CAMBRIAN

N. America	13.77; 13.78; 13.85; 15.142; 1 pole from Spall 1970; 1 pole from Al-Khafaji and Vincenz 1971; 1 pole from French et al 1977: (These seven poles constitute the "preferred" group fo Van der Voo et al 1976) .
W. Europe	5.83; 13.66:
Russian Platform	R.282; R.283; R.284; R.285:
Siberia	R.273; R.274; R.275; R.276:
S. America	14.417; 14.418; 14.419; 14.420; 14.421:
Antarctica	14.408:
Africa	9.132; 9.137; 12.149; 1 pole from Creer and Snape 1973 (see Hailwood 174):
Arabia	12.147:
Australia	14.413; 14.415:
India	11.85; 14.414; 14.424; 14.514; 14.515:



## APPENDIX 2

### TABLES GIVING THE CHANGE IN SLOWNESS AND AZIMUTH FOR A PLANE WAVE PASSING A DIPPING INTERFACE

Table A2.1

The first set of tables give the corrections to the P wave and the second set of tables the difference in slowness and azimuth for the P and the converted PS wave. The abbreviations are: P: The slowness (sec/deg) of the incoming wave; Az: The azimuth (degrees) of the incoming wave; V: The seismic velocity (km/sec) of the medium before the interface; V1: The seismic velocity (km/sec) of the medium after the interface; VS1: The seismic velocity (km/sec) of the converted phase after the interface. Strike and dip are measured in degrees. The first column of numbers in each dip column is the correction to the slowness and the second the correction to the azimuth.

The change in slowness and azimuth for the P phase.

P= 3.00    AZ= 180.0    V= 8.00    V1= 7.00    VS1= 0.0

STRIKE	DIP=0.5		1.0		1.5		2.0	
0.0	-0.00	-0.3	-0.00	-0.7	-0.00	-1.0	-0.00	-1.4
30.0	0.01	-0.3	0.02	-0.6	0.03	-0.9	0.03	-1.2
60.0	0.02	-0.2	0.03	-0.3	0.05	-0.5	0.06	-0.7
90.0	0.02	0.0	0.04	0.0	0.05	0.0	0.07	0.0
120.0	0.02	0.2	0.03	0.3	0.05	0.5	0.06	0.7
150.0	0.01	0.3	0.02	0.6	0.03	0.9	0.03	1.2
180.0	-0.00	0.3	-0.00	0.7	-0.00	1.0	-0.00	1.4
210.0	-0.01	0.3	-0.02	0.6	-0.03	0.9	-0.04	1.2
240.0	-0.02	0.2	-0.03	0.3	-0.05	0.5	-0.06	0.7
270.0	-0.02	0.0	-0.04	0.0	-0.05	0.0	-0.07	0.0
300.0	-0.02	-0.2	-0.03	-0.3	-0.05	-0.5	-0.06	-0.7
330.0	-0.01	-0.3	-0.02	-0.6	-0.03	-0.9	-0.04	-1.2
360.0	-0.00	-0.3	-0.00	-0.7	-0.00	-1.0	-0.00	-1.4



P= 4.00 AZ= 180.0 V= 8.00 V1= 7.00 VS1= 0.0

STRIKE	DIP=0.5	1.0	1.5	2.0
0.0	-0.00 -0.3	-0.00 -0.5	-0.00 -0.8	-0.00 -1.0
30.0	0.01 -0.2	0.02 -0.4	0.03 -0.7	0.04 -0.9
60.0	0.02 -0.1	0.03 -0.3	0.05 -0.4	0.06 -0.5
90.0	0.02 0.0	0.04 0.0	0.05 0.0	0.07 0.0
120.0	0.02 0.1	0.03 0.3	0.05 0.4	0.06 0.5
150.0	0.01 0.2	0.02 0.4	0.03 0.7	0.04 0.9
180.0	-0.00 0.3	-0.00 0.5	-0.00 0.8	-0.00 1.0
210.0	-0.01 0.2	-0.02 0.4	-0.03 0.7	-0.04 0.9
240.0	-0.02 0.1	-0.03 0.3	-0.05 0.4	-0.06 0.5
270.0	-0.02 0.0	-0.04 0.0	-0.05 0.0	-0.07 0.0
300.0	-0.02 -0.1	-0.03 -0.3	-0.05 -0.4	-0.06 -0.5
330.0	-0.01 -0.2	-0.02 -0.4	-0.03 -0.7	-0.04 -0.9
360.0	-0.00 -0.3	-0.00 -0.5	-0.00 -0.8	-0.00 -1.0

P= 5.00 AZ= 180.0 V= 8.00 V1= 7.00 VS1= 0.0

STRIKE	DIP=0.5	1.0	1.5	2.0
0.0	-0.00 -0.2	-0.00 -0.4	-0.00 -0.6	-0.00 -0.8
30.0	0.01 -0.2	0.02 -0.4	0.03 -0.6	0.04 -0.7
60.0	0.02 -0.1	0.03 -0.2	0.05 -0.3	0.06 -0.4
90.0	0.02 0.0	0.04 0.0	0.06 0.0	0.07 0.0
120.0	0.02 0.1	0.03 0.2	0.05 0.3	0.06 0.4
150.0	0.01 0.2	0.02 0.4	0.03 0.6	0.04 0.7
180.0	-0.00 0.2	-0.00 0.4	-0.00 0.6	-0.00 0.8
210.0	-0.01 0.2	-0.02 0.4	-0.03 0.5	-0.04 0.7
240.0	-0.02 0.1	-0.03 0.2	-0.05 0.3	-0.06 0.4
270.0	-0.02 0.0	-0.04 0.0	-0.05 0.0	-0.07 0.0
300.0	-0.02 -0.1	-0.03 -0.2	-0.05 -0.3	-0.06 -0.4
330.0	-0.01 -0.2	-0.02 -0.4	-0.03 -0.5	-0.04 -0.7
360.0	-0.00 -0.2	-0.00 -0.4	-0.00 -0.6	-0.00 -0.8

P= 6.00 AZ= 180.0 V= 8.00 V1= 7.00 VS1= 0.0

STRIKE	DIP=0.5	1.0	1.5	2.0
0.0	-0.00 -0.2	-0.00 -0.4	-0.00 -0.5	-0.00 -0.7
30.0	0.01 -0.2	0.02 -0.3	0.03 -0.5	0.04 -0.6
60.0	0.02 -0.1	0.03 -0.2	0.05 -0.3	0.07 -0.4
90.0	0.02 0.0	0.04 0.0	0.06 0.0	0.08 0.0
120.0	0.02 0.1	0.03 0.2	0.05 0.3	0.07 0.4
150.0	0.01 0.2	0.02 0.3	0.03 0.5	0.04 0.6
180.0	-0.00 0.2	-0.00 0.4	-0.00 0.5	-0.00 0.7
210.0	-0.01 0.2	-0.02 0.3	-0.03 0.5	-0.04 0.6
240.0	-0.02 0.1	-0.03 0.2	-0.05 0.3	-0.06 0.4
270.0	-0.02 0.0	-0.04 0.0	-0.06 0.0	-0.07 0.0
300.0	-0.02 -0.1	-0.03 -0.2	-0.05 -0.3	-0.06 -0.4
330.0	-0.01 -0.2	-0.02 -0.3	-0.03 -0.5	-0.04 -0.6
360.0	-0.00 -0.2	-0.00 -0.4	-0.00 -0.5	-0.00 -0.7





P= 7.00 AZ= 180.0 V= 8.00 V1= 7.00 VS1= 0.0

STRIKE	DIP=0.5	1.0		1.5		2.0	
0.0	-0.00 -0.2	-0.00	-0.3	-0.00	-0.5	-0.00	-0.6
30.0	0.01 -0.1	0.02	-0.3	0.03	-0.4	0.04	-0.6
60.0	0.02 -0.1	0.03	-0.2	0.05	-0.2	0.07	-0.3
90.0	0.02 0.0	0.04	0.0	0.06	0.0	0.08	0.0
120.0	0.02 0.1	0.03	0.2	0.05	0.2	0.07	0.3
150.0	0.01 0.1	0.02	0.3	0.03	0.4	0.04	0.6
180.0	-0.00 0.2	-0.00	0.3	-0.00	0.5	-0.00	0.6
210.0	-0.01 0.1	-0.02	0.3	-0.03	0.4	-0.04	0.5
240.0	-0.02 0.1	-0.03	0.2	-0.05	0.2	-0.07	0.3
270.0	-0.02 0.0	-0.04	0.0	-0.06	0.0	-0.08	0.0
300.0	-0.02 -0.1	-0.03	-0.2	-0.05	-0.2	-0.07	-0.3
330.0	-0.01 -0.1	-0.02	-0.3	-0.03	-0.4	-0.04	-0.5
360.0	-0.00 -0.2	-0.00	-0.3	-0.00	-0.5	-0.00	-0.6

P= 8.00 AZ= 180.0 V= 8.00 V1= 7.00 VS1= 0.0

STRIKE	DIP=0.5	1.0		1.5		2.0	
0.0	-0.00 -0.1	-0.00	-0.3	-0.00	-0.4	-0.00	-0.6
30.0	0.01 -0.1	0.02	-0.3	0.03	-0.4	0.04	-0.5
60.0	0.02 -0.1	0.04	-0.1	0.05	-0.2	0.07	-0.3
90.0	0.02 0.0	0.04	0.0	0.06	0.0	0.08	0.0
120.0	0.02 0.1	0.04	0.1	0.05	0.2	0.07	0.3
150.0	0.01 0.1	0.02	0.3	0.03	0.4	0.04	0.5
180.0	-0.00 0.1	-0.00	0.3	-0.00	0.4	-0.00	0.6
210.0	-0.01 0.1	-0.02	0.3	-0.03	0.4	-0.04	0.5
240.0	-0.02 0.1	-0.04	0.1	-0.05	0.2	-0.07	0.3
270.0	-0.02 0.0	-0.04	0.0	-0.06	0.0	-0.08	0.0
300.0	-0.02 -0.1	-0.04	-0.1	-0.05	-0.2	-0.07	-0.3
330.0	-0.01 -0.1	-0.02	-0.3	-0.03	-0.4	-0.04	-0.5
360.0	-0.00 -0.1	-0.00	-0.3	-0.00	-0.4	-0.00	-0.6



The difference in slowness and azimuth between the P and the converted PS phases.

P= 3.00 AZ= 180.0 V= 8.00 V1= 7.00 VS1= 4.00

STRIKE	DIP=0.5		1.0		1.5		2.0	
0.0	-0.00	2.0	-0.01	4.0	-0.02	6.0	-0.04	7.9
30.0	0.05	1.8	0.10	3.6	0.14	5.6	0.18	7.6
60.0	0.09	1.0	0.18	2.2	0.27	3.4	0.35	4.8
90.0	0.11	0.0	0.21	0.0	0.32	-0.0	0.42	-0.0
120.0	0.09	-1.0	0.18	-2.2	0.27	-3.4	0.35	-4.8
150.0	0.05	-1.8	0.10	-3.6	0.14	-5.6	0.18	-7.6
180.0	-0.00	-2.0	-0.01	-4.0	-0.02	-6.0	-0.04	-7.9
210.0	-0.05	-1.7	-0.11	-3.3	-0.17	-4.8	-0.24	-6.3
240.0	-0.09	-1.0	-0.18	-1.9	-0.28	-2.7	-0.37	-3.4
270.0	-0.10	0.0	-0.21	0.0	-0.31	0.0	-0.42	0.0
300.0	-0.09	1.0	-0.18	1.9	-0.28	2.7	-0.37	3.4
330.0	-0.05	1.7	-0.11	3.3	-0.17	4.8	-0.24	6.3
360.0	-0.00	2.0	-0.01	4.0	-0.02	6.0	-0.04	7.9

P= 4.00 AZ= 180.0 V= 8.00 V1= 7.00 VS1= 4.00

STRIKE	DIP=0.5		1.0		1.5		2.0	
0.0	-0.00	1.5	-0.01	3.0	-0.02	4.5	-0.03	6.0
30.0	0.05	1.3	0.10	2.7	0.15	4.2	0.19	5.6
60.0	0.09	0.8	0.18	1.6	0.27	2.5	0.36	3.5
90.0	0.11	0.0	0.21	0.0	0.32	-0.0	0.43	-0.0
120.0	0.09	-0.8	0.18	-1.6	0.27	-2.5	0.36	-3.5
150.0	0.05	-1.3	0.10	-2.7	0.15	-4.2	0.19	-5.6
180.0	-0.00	-1.5	-0.01	-3.0	-0.02	-4.5	-0.03	-6.0
210.0	-0.05	-1.3	-0.11	-2.5	-0.17	-3.7	-0.23	-4.9
240.0	-0.09	-0.7	-0.18	-1.4	-0.28	-2.1	-0.37	-2.7
270.0	-0.11	0.0	-0.21	0.0	-0.32	0.0	-0.42	0.0
300.0	-0.09	0.7	-0.18	1.4	-0.28	2.1	-0.37	2.7
330.0	-0.05	1.3	-0.11	2.5	-0.17	3.7	-0.23	4.9
360.0	-0.00	1.5	-0.01	3.0	-0.02	4.5	-0.03	6.0



P= 5.00 AZ= 180.0 V= 8.00 V1= 7.00 VS1= 4.00

STRIKE	DIP=0.5	1.0	1.5	2.0
0.0	-0.00 1.2	-0.01 2.5	-0.01 3.7	-0.02 4.9
30.0	0.05 1.1	0.10 2.2	0.15 3.3	0.20 4.5
60.0	0.09 0.6	0.18 1.3	0.28 2.0	0.37 2.7
90.0	0.11 0.0	0.21 0.0	0.32 0.0	0.43 -0.0
120.0	0.09 -0.6	0.18 -1.3	0.28 -2.0	0.37 -2.7
150.0	0.05 -1.1	0.10 -2.2	0.15 -3.3	0.20 -4.5
180.0	-0.00 -1.2	-0.01 -2.5	-0.01 -3.7	-0.02 -4.9
210.0	-0.05 -1.0	-0.11 -2.1	-0.17 -3.0	-0.23 -4.0
240.0	-0.09 -0.6	-0.19 -1.2	-0.28 -1.7	-0.37 -2.2
270.0	-0.11 0.0	-0.21 0.0	-0.32 0.0	-0.43 0.0
300.0	-0.09 0.6	-0.19 1.2	-0.28 1.7	-0.37 2.2
330.0	-0.05 1.0	-0.11 2.1	-0.17 3.0	-0.23 4.0
360.0	-0.00 1.2	-0.01 2.5	-0.01 3.7	-0.02 4.9

P= 6.00 AZ= 180.0 V= 8.00 V1= 7.00 VS1= 4.00

STRIKE	DIP=0.5	1.0	1.5	2.0
0.0	-0.00 1.0	-0.01 2.1	-0.01 3.1	-0.02 4.1
30.0	0.05 0.9	0.10 1.8	0.15 2.8	0.20 3.8
60.0	0.09 0.5	0.19 1.1	0.28 1.7	0.37 2.3
90.0	0.11 0.0	0.22 0.0	0.33 0.0	0.44 0.0
120.0	0.09 -0.5	0.19 -1.1	0.28 -1.7	0.37 -2.3
150.0	0.05 -0.9	0.10 -1.8	0.15 -2.8	0.20 -3.8
180.0	-0.00 -1.0	-0.01 -2.1	-0.01 -3.1	-0.02 -4.1
210.0	-0.06 -0.9	-0.11 -1.7	-0.17 -2.6	-0.23 -3.4
240.0	-0.09 -0.5	-0.19 -1.0	-0.28 -1.5	-0.38 -1.9
270.0	-0.11 0.0	-0.22 0.0	-0.32 0.0	-0.43 0.0
300.0	-0.09 0.5	-0.19 1.0	-0.28 1.5	-0.38 1.9
330.0	-0.06 0.9	-0.11 1.7	-0.17 2.6	-0.23 3.4
360.0	-0.00 1.0	-0.01 2.1	-0.01 3.1	-0.02 4.1

P= 7.00 AZ= 180.0 V= 8.00 V1= 7.00 VS1= 4.00

STRIKE	DIP=0.5	1.0	1.5	2.0
0.0	-0.00 0.9	-0.00 1.8	-0.01 2.7	-0.02 3.6
30.0	0.05 0.8	0.11 1.6	0.16 2.4	0.21 3.3
60.0	0.10 0.5	0.19 0.9	0.29 1.4	0.38 2.0
90.0	0.11 0.0	0.22 0.0	0.33 0.0	0.44 0.0
120.0	0.10 -0.5	0.19 -0.9	0.29 -1.4	0.38 -2.0
150.0	0.05 -0.8	0.11 -1.6	0.16 -2.4	0.21 -3.3
180.0	-0.00 -0.9	-0.00 -1.8	-0.01 -2.7	-0.02 -3.6
210.0	-0.06 -0.8	-0.11 -1.5	-0.17 -2.3	-0.23 -3.0
240.0	-0.10 -0.4	-0.19 -0.9	-0.29 -1.3	-0.38 -1.7
270.0	-0.11 0.0	-0.22 0.0	-0.33 0.0	-0.44 0.0
300.0	-0.10 0.4	-0.19 0.9	-0.29 1.3	-0.38 1.7
330.0	-0.06 0.8	-0.11 1.5	-0.17 2.3	-0.23 3.0
360.0	-0.00 0.9	-0.00 1.8	-0.01 2.7	-0.02 3.6





P= 8.00    AZ= 180.0    V= 8.00    V1= 7.00    VS1= 4.00

STRIKE	DIP=0.5		1.0		1.5		2.0	
0.0	-0.00	0.8	-0.00	1.6	-0.01	2.4	-0.02	3.2
30.0	0.06	0.7	0.11	1.4	0.16	2.2	0.21	2.9
60.0	0.10	0.4	0.19	0.8	0.29	1.3	0.39	1.7
90.0	0.11	0.0	0.23	0.0	0.34	0.0	0.45	0.0
120.0	0.10	-0.4	0.19	-0.8	0.29	-1.3	0.39	-1.7
150.0	0.06	-0.7	0.11	-1.4	0.16	-2.2	0.21	-2.9
180.0	-0.00	-0.8	-0.00	-1.6	-0.01	-2.4	-0.02	-3.2
210.0	-0.06	-0.7	-0.12	-1.4	-0.18	-2.0	-0.24	-2.7
240.0	-0.10	-0.4	-0.20	-0.8	-0.29	-1.1	-0.39	-1.5
270.0	-0.11	0.0	-0.22	0.0	-0.34	0.0	-0.45	0.0
300.0	-0.10	0.4	-0.20	0.8	-0.29	1.1	-0.39	1.5
330.0	-0.06	0.7	-0.12	1.4	-0.18	2.0	-0.24	2.7
360.0	-0.00	0.8	-0.00	1.6	-0.01	2.4	-0.02	3.2



## APPENDIX 3

### THE EULER ROTATION

Euler's theorem states that a general displacement of a rigid body with one point fixed is a rotation around some axis through that point. In the case of the earth the fixed point is the center. The vector  $\underline{R}$  around which the rotation  $ROT$  degrees is performed intersects the surface at a point (LAT, LON) (latitude and longitude in degrees, positive north and east) called the Euler pole. Using a cartesian coordinate system and setting the earth's radius to one, a point on the surface with radius vector  $\underline{x} = (x_1, x_2, x_3)$  can be written

$$\begin{aligned} x_1 &= \sin(90-xlat) * \cos(xlon) \\ x_2 &= \sin(90-xlat) * \sin(xlon) \\ x_3 &= \cos(90-xlat) \end{aligned} \tag{A3.1}$$

where  $xlat$  and  $xlon$  are the latitude and longitude of the point. The Euler rotation of the point can then be written

$$\underline{y} = \underline{A} * \underline{x} \tag{A3.2}$$

where  $\underline{y}$  is the new vector of  $\underline{x}$  and  $\underline{A}$  is the transformation matrix. In terms of (LAT, LON, ROT)  $\underline{A}$  is given by (Jeffreys and Jeffreys (1946))

$$\begin{array}{lll} C+n_1^2*(1-C) & n_1*n_2*(1-C)-n_3*S & n_1*n_3*(1-C)+n_2*S \\ n_1*n_2*(1-C)+n_3*S & C+n_2^2*(1-C) & n_2*n_3*(1-C)-n_1*S \\ n_3*n_1*(1-C)-n_2*S & n_2*n_3*(1-C)+n_1*S & C+n_3^2*(1-C) \end{array} \tag{A3.3}$$

where  $\underline{R} = (n_1, n_2, n_3)$ ,  $C = \cos(ROT)$  and  $S = \sin(ROT)$ . The



direction cosines  $n_1, n_2$  and  $n_3$  are determined from (LAT, LON). Rotations were performed using the above formulation for  $\underline{A}$  and equation (A3.2). When several subsequent rotations take place the resultant transformation matrix is calculated by multiplying together the individual matrices. It is also necessary to be able to invert the resultant matrix  $\underline{A}$  in terms of (LAT, LON, ROT). From equation (A3.3) it is seen that the trace of  $\underline{A}$  is  $1 + 2 * \cos(\text{ROT})$  and the angle of rotation can therefore be determined as  $\text{ROT} = \arccos((a_{11} + a_{22} + a_{33})/2)$ . The sign depends on the hemisphere chosen for the pole. Since  $\underline{R}$  is fixed the following must hold

$$\underline{A} * \underline{R} = \underline{R}$$

$$(\underline{A} - \underline{E}) * \underline{R} = \underline{0}$$

where  $\underline{E}$  is the unit matrix. The system of linear equation to find  $\underline{R}$  are

$$\begin{aligned} (a_{11} - 1) * n_1 + a_{12} * n_2 + a_{13} * n_3 &= 0 \\ a_{21} * n_1 + (a_{22} - 1) * n_2 + a_{23} * n_3 &= 0 \quad (\text{A3.4}) \\ a_{31} * n_1 + a_{32} * n_2 + (a_{33} - 1) * n_3 &= 0 \end{aligned}$$

where  $a_{ij}$ , ( $i = 1, 2, 3$  and  $j = 1, 2, 3$ ) are the elements of  $\underline{A}$

This homogeneous system can only be solved for ratios of  $n_1, n_2$  and  $n_3$ . The system

$$\begin{aligned} (a_{11} - 1) * (n_1/n_3) + a_{12} * (n_2/n_3) &= -a_{13} \\ a_{21} * (n_1/n_3) + (a_{22} - 1) * (n_2/n_3) &= -a_{23} \quad (\text{A3.5}) \end{aligned}$$

will give  $n_1/n_3$  and  $n_2/n_3$  as

$$n_1/n_3 = A_1/A_3 \text{ and } n_2/n_3 = A_2/A_3 \quad (\text{A3.6})$$



where  $A_1$ ,  $A_2$  and  $A_3$  are the determinants of (A3.5). From (A3.1) and (A3.6) it is seen that

$$(n_2/n_3)/(n_1/n_3) = A_2/A_1$$

$$LON = \text{artan}(n_2/n_1) \quad (A3.7)$$

and  $COLAT = (90 - LAT)$  is

$$\begin{aligned} COLAT &= \arctan \left( (n_1/n_3)^2 + (n_2/n_3)^2 \right) \\ &= \arctan \left( (A_1^2 + A_2^2) / A_3^2 \right) \end{aligned} \quad (A3.8)$$

There are two possible poles of rotation; One in the northern and one in the southern hemisphere. A usefull FORTRAN function is  $ATAN2(x,y) = \arctan(y/x)$  which determines which quadrant the point  $(x,y)$  is in. Thus (A3.7) can be written

$$LON = ATAN2(A_2/A_3, A_1/A_3) \quad (A3.9)$$

and the pole can now be either in the northern or southern hemisphere. By chosing  $ROT$  to be positive it is then possible to fix  $(LAT, LON)$  to either hemisphere by calculating an  $\underline{A}$  from the inverted values of  $(LAT, LON, ROT)$  and compare to the original  $\underline{A}$ . In the actual calculations other considerations must be taken. If  $ROT = 0$  then  $\underline{A} = \underline{E}$ ,  $A_1 = A_2 = A_3 = 0$ , and  $(LAT, LON)$  are undefined.  $COLAT = 90^\circ$  also gives  $A_1 = A_2 = A_3 = 0$  and  $LON$  must be calculated differently. Using

$$a_{11} = (\cos(LON))^2 * (1 - \cos(ROT)) + \cos(ROT)$$

gives

$$LON = \arccos \left( (a_{11} - \cos(ROT)) / (1 - \cos(ROT)) \right)$$

The sign of  $LON$  can be determined from

$$\begin{aligned} a_{12} &= n_1 * n_2 * (1 - \cos(ROT)) + n * \sin(ROT) \\ &= (\sin(COLAT))^2 * \sin(LON) * \cos(LON) \end{aligned}$$





$$= \sin(\text{LON}) * \cos(\text{LON})$$

Thus  $a_{12}$  and LON have the same sign. The last complication which can arise is when COLAT = 0 giving  $A_1 = A_2 = 0$ . Since the pole is at the North Pole, LON can be given any arbitrary value.



#### APPENDIX 4

##### MINIMIZING THE CONTINENTAL MOVEMENT

The present day map of landmasses (bounded by 500 fathom lines) were divided into a number of equal area segments, each represented by one point. A total of 625 points were used. To calculate the minimum movement for a continental segment from period A to period B, the Euler rotation (pole and angle of rotation(LAT,LON,ROT)) was found from the Euler rotations from the present to A and the present to B. The movement from A to B for a continental segment is then carried out by rotating it by an angle ROT around the point (LAT,LON). Each point belonging to the continental segment is then moving along a small circle with radius D calculated as the distance from the point to (LAT,LON). The displacement along the small circle is  $ROT * \sin(D)$  degrees. Continent B could then be moved a specified number of degrees of longitude. The new resultant movement (LAT,LCN,ROT) for each segment is calculated and the sum of the squares of the distances found for each equal area point. A minimum in the sum of the squares of the distances as a function of longitudinal movement was found and the corresponding minimum and maximum velocity of the continental segment was calculated.



APPENDIX 5  
THE PROGRAMS

The main programs are listed first and at the end all the subroutines are given in alphabetical order.

```
C  CALCULATION OF TRAVEL TIMES, DISTANCES, APPARENT
C  VELOCITIES FOR FOR ANY NUMBER OF STATION
C  EVENT COMBINATIONS AND FOR UP TO 39 DIFFERENT SEISMIC
C  PHASES. THE INPUT IS MADE EASY BY HAVING 3 LIBRARIES OF:
C      1: STANDARD STATION COORDINATES
C      2: EVENTS
C      3 TRAVEL TIME TABLES
C  INPUT IS ONLY THE PHASE NAME, THE STATION IDENTIFIER AND
C  AND AN ASSIGNED EVENT IDENTIFIER.
C  THE OTHER INPUT AND OUTPUTS ARE:
C      4: INPUT OF STATION AND EVENT IDENTIFIERS
C      5: CHOSEN PHASES AND PROGRAM PARAMETERS
C      6: OUTPUT OF ALL THE CALCULATIONS ARRANGED AS THEY
C          PROCEED, THAT IS FOR ONE PHASE AT A TIME.
C      7: OUTPUT OF THE DATA IN CONCENTRATED FORM AND
C          SORTED OUT SO ALL RELEVANT DATA FOR ONE STATION-
C          EVENT COMBINATION IS TOGETHER. OUTPUT IS FORMATTED
C          TO FIT 2 LIBRARY CARDS.
C
C      8: A SCRATCH FILE
C
C  1: STATION LIBRARY: INFORMATION ABOUT THE STATIONS USED. ONE
C  STATION FOR EACH LINE. THE INFORMATION IS STATION
C  IDENTIFIER, LATITUDE IN DECIMAL DEGREES(+NORTH),
C  LONGITUDE IN DECIMAL DEGREES(+EAST), ELEVATION IN KM AND
C  ALPHA NUMERICAL STATION INFORMATION. A BLANK LINE
C  INDICATES END OF DATA.
C  FORMAT(2X,A4,4X,3F10.0,12A4)
C
C  2: EVENT LIBRARY: INFORMATION ABOUT THE EVENTS, ONE EVENT
C  FOR EACH LINE. THE INFORMATION IS DAY, MONTH, YEAR, HOUR,
C  MINUTE, SECOND, LATITUDE(+NORTH), LONGITUDE(+EAST), DEPTH
C  (KM), MAGNETUDE, COMMENT, EVENT IDENTIFIER, EVENT NUMBER,
C  EVENT LOCATION.
C  FORMAT(5I3,3F10.3,F4.0,F4.1,6A1,1X,A4,2X,A4,12A4)
C
C  3: TRAVEL TIME LIBRARY: CONTAINS TRAVEL TIME TABLES WITH
C  J-B ELLIPTICITY CORRECTION TABLES, AND CORRESPONDING
C  SURFACE VELOCITIES (KM/SEC).
C  1. LINE: NAME OF PHASE AND NUMBER OF REFLECTIONS, E.G.
```





C                    PPP     3            FORMAT(2X,A4,2X,I1)  
 C    2. LINE: DDEL AND I. FORMAT(F5.2,I4)  
 C                    DDEL: INCREMENT IN EPICENTRAL DISTANCE(DEGREES)  
 C                                IN TRAVEL TIME TABLE.  
 C                    L:        INITIAL DISTANCE IN TRAVEL TIME TABLE.  
 C    3. LINE: A GROUP OF LINES GIVING THE TRAVEL TIMES.  
 C                    EACH LINE CONTAINS TRAVEL TIMES FOR ONE  
 C                    DISTANCE AND 14 DEPHTS. INPUT COME IN ORDER  
 C                    OF INCREASING DISTANCE AND THE TRAVEL TIMES  
 C                    ARE GIVEN IN MINUTES AND TENS OF SECONDS.  
 C                    FORMAT(14(I2,I3))  
 C                    A BLANK LINE INDICATES END OF TRAVEL TIME  
 C                    DATA.  
 C    4 GROUP OF LINES: 2 LINES GIVING THE J-B ELLIPTICITY  
 C                    CORRECTIONS FOR THE FUNCTION F(DISTANCE) FOR THE  
 C                    DISTANCES 0,10,20.....180 DEGREES.  
 C                    FORMAT(10F6.3)

C    NEXT LINE: NEAR SURFACE VELOCITY OF THE CORRESPONDING  
 C                    PHASE.  
 C                    FORMAT(F6.3)

C    THE ABOVE GROUPS OF CARDS CAN BE REPEATED FOR ANY  
 C    NUMBER OF PHASES. THE ORDER DOES NOT MATTER. THE  
 C    LAST LINE IN THE FILE MUST BE THE WORD SLUT,  
 C    FORMAT(2XA4). THIS IS TO ENSURE THAT IF A CHOSEN PHASE  
 C    IS NOT FOUND AT THE END OF THE TABLE, THE READING  
 C    WILL START FROM THE BEGINNING AGAIN, THUS READING  
 C    THE WHOLE TABLE.

C    4: INPUT OF STATION AND EVENT COMBINATIONS FOR  
 C    THE DISIRED CALCULATIONS. THE REASON THAT THIS  
 C    INFORMATION IS READ FROM A SEPARATE FILE IS  
 C    THAT THE SAME SET OF STATION-EVENTS THEN CAN  
 C    BE USED FOR ALL THE DIFFERENT PHASE CALCULATIONS  
 C    BY REWINDING THE FILE. 4 CAN BE A TERMINAL OR  
 C    CARDS WHEN VERSION "CHEAP" IS USED. SEE BELOW.

#### C    VERSION "CHEAP":

C    1. GROUP OF LINES: EACH LINE CONTAINS A CHOSEN  
 C    STATION IDENTIFIER AND THE CORRESPONDING  
 C    SURFACE VELOCITY. IF THE VELOCITY IS ZERO  
 C    THE DEFAULT SURFACE VELOCITY FOR THE  
 C    CORRESPONDING PHASE (READ FROM INPUT 3)  
 C    IS USED. A BLANK LINE INDICATES END OF  
 C    STATIONS.

C                    FORMAT(A4,F10.0)

C    2. GROUP OF LINES: ONE LINE GIVING THE EVENT  
 C    IDENTIFIER AND EVENT NUMBER.

C                    FORMAT(A4,1X,A4)

C    IN VERSION "CHEAP" CALCULATIONS ARE ONLY MADE  
 C    FOR ONE EVENT AND A NUMBER OF STATIONS AND  
 C    PHASES. THIS VERSION IS CONSIDERABLE CHEAPER



IN TERMS OF CPU TIME THAN THE STANDARD  
VERSION, WHICH CAN CALCULATE THE TRAVEL TIMES  
FOR ANY COMBINATION OF A NUMBER OF PHASES,  
STATIONS AND EVENTS. THIS INVOLVES READING  
FILE 1, 2 AND 3 FOR EACH NEW EVENT USED.

#### STANDARD VERSION:

1. GROUP OF CARDS: AS IN VERSION "CHEAP".
2. GROUP OF LINES: ANY NUMBER OF LINES  
SPECIFYING THE EVENT IDENTIFIERS.  
SAME FORMAT AS IN VERSION "CHEAP" A BLANK  
LINE INDICATES END OF EVENTS.
3. GROUP OF LINES: ANOTHER SET OF STATIONS AND  
EVENTS CAN BE READ IN. 2 BLANK LINES  
INDICATES END OF INPUT OF STATIONS-EVENTS  
COMBINATIONS.

#### 5: 1. LINE: CHEAP,NL

CHEAP: VERSION "CHEAP" IS USED IF THE  
INPUT IS THE WORD 'CHEAP'

NL: IF DIFFERENT FROM ZERO DATA IS  
WRITTEN OUT ON UNIT 6.

FORMAT(A8,I10)

2. AND 3. LINE: PHASES FOR WHICH TRAVEL TIMES  
ARE CALCULATED. UP TO 39 DIFFERENT  
PHASES CAN BE USED. 4 BLANKS INDICATE  
END OF PHASES.

FORMAT(20A4)

IF VERSION "CHEAP" IS USED THE PHASES MUST  
BE READ IN IN THE SAME ORDER AS THEY  
APPEAR IN THE TRAVEL TIME TABLE (INPUT 3).  
IN THE STANDARD VERSION THE ORDER DOES NOT  
MATTER, BUT THE RUNNING COST CAN INCREASE  
UP TO 100% IF THEY ARE NOT IN ORDER.

#### 4. LINE : JCODE:

JCODE=1: GEOCENTRIC LATITUDE IS USED TO  
COMPUTE DISTANCES.

JCODE=0: BULLEN'S SEISMOLOGICAL LATITUDE  
IS USED TO COMPUTE DISTANCES.

#### 6: OUTPUT: SELF EXPLANATORY.

- 7: CONTAINS ALMOST THE SAME OUTPUT DATA AS 6, BUT  
IN A FORMAT SUITABLE FOR PRINTING ON LIBRARY  
FOR PRINTING LIBRARY CARDS USE THE FOLLOWING  
COMMANDS:

SIGNON XXXX FORM=IK RIBBON=SC

SET LINECNT=66

COPY FILE7 TO \*PRINT\*



NOTE ABOUT THE OUTPUT: IF THE EPICENTRAL DISTANCE EXCEEDS THE DISTANCE IN THE TRAVEL TIME TABLE, ZERO'S WILL BE INSERTED FOR ALL CUTPUT VALUES CALCULATED USING THE TRAVEL TIME TABLE.

8: SCRATCH FILE.

AN EXAMPLE OF A RUN DECK

```

C SIGNON HAVS PRIO=D TIME=25S P=800 RETURN=PHYS
C CRE -P SIZE=80P
C RUN TR+LIB 1=STATION 6=-PK 2=EVENT 3=T 4=-ST 7=CARD1 8=-P
C CHEAP
C P PKP S SKS PP SS P-P S-P PCP PCP2SCP PCS PS SP P-S S-S SCS

    DIMENSION FT(200),FG(200), TSUR(200)
    DIMENSION DEL(200),AZ(200),AZE(200)
    INTEGER ZERO/' ',ST,STA(200)
    DIMENSION SLDEL(200),TP(200),DT(200),ELEVA(200),VELOC(
*200)
    DIMENSION FLT(2),FLG(2)
    DIMENSION FLAT(2),FLONG(2),GLAT(2),CLAT(2),SLONG(2),CL
*ONG(2)
    DIMENSION A(2),B(2),C(2),COSZ(2),SINZ(2),Z(2)
    1,LT(2),GLT(2),LG(2),GLG(2),
    2SGLAT(200),CDEI(200),XMIN(14),XSEC(14),RECORD(20)
    DIMENSION BLAT(2),AS(2),BS(2),CS(2),CLAS(2)
    DIMENSION ELLIP(19),TCELL(200)
    REAL LAT(500),LON(500),HI(500)
    DIMENSION SLOC(300,12),SSLOC(300,12)
    COMMON TA(14,201),IDEP(14)
    INTEGER PHAS(40),NSTA(500),PPHA,SLUT/'SLUT'/',CHO,NCOUN
*T(50)
    REAL*8 CHEAPP,CHEAP/'CHEAP '
702 FORMAT(2X,A4,2X,I1)
703 FORMAT(2X,A4,4X,3F10.0,12A4)
704 FORMAT('0',1X,A4,' LAT=',F10.2,' DEG ', 'LONG=',F10.
*2,' DEG
1', 'ELEV.=',F5.3,' KM. VEL.=',F5.3,' KM./SEC. ',6A
*4)
705 FORMAT(5I3,3F10.3,F4.0,F4.1,6A1,1X,12A4)
706 FORMAT('/0', ' EVENT',I3,' DAY,MON.,YR.=',3I3,' TIME=
*',I3,' HR. '
1,I3,' MIN. ',F5.2,' SEC. LAT.=',F6.2,' DEG. LONG.
*= '
1F7.2,' DEG.')
707 FORMAT('0', ' DEPTH=',F5.0,' KM. MAG.=',F4.1,3X,6A1
*,3X,12A4)
708 FORMAT('0', ' STATION SEISMIC DIST.(DEG) GEOC.
*DIST.(DEG)

```





```

1GEOC. DIST.(KM) GEOC AZ.(EP) GEOC. AZ.(ST)')
709 FORMAT('0',10X,A4,9X,F8.3,8X,F8.3,6X,F9.2,6X,F7.2,5X,F
*7.2)
711 FORMAT(F5.2,3I4)
712 FORMAT(14I4)
713 FORMAT(14(F2.0,F3.1),A4,F4.1,A2)
714 FORMAT(I3)
715 FORMAT('0',' BULLEN SEISMOLOGICAL LATITUDE USED TO COM
*PUTE TIMES')
716 FORMAT('0',' GEOCENTRIC DISTANCES USED TO CALCULATE TR
*AVEL TIMES')
717 FORMAT(10F6.3)
718 FORMAT('0',1X,'STATION DAY HR. MIN SEC. PHASE TIME
*ELLIP. CORR
1. SURF. CORR. DT D DEL(SEC/DEG) APP. VEL(KM/SEC) ANG.
*OF INC. :
*PHASE,CP,CS')
719 FORMAT('0',2X,A4,2X,I3,1X,I3,1X,I3,2X,F6.2,1X,F8.2,4X,
*F6.2,8X,F6.2
1,8X,F6.2,10X,F6.2,2X,4F7.1)
720 FORMAT('0',' TRAVEL TIMES IN ERROR')
721 FORMAT(F2.0,F3.1,13F5.1,A4,F4.1,A2)
722 FORMAT('0','DDEL= ',F5.2,' L= ',I4,' MODE= ',I4)
724 FORMAT(///2X,A4,' TRAVELTIMES'//)
725 FORMAT(//'PHASE ',A4,' NOT IN TRAVEL TIME TABLE'//)
728 FORMAT(///'NUMBER OF PHASES FOR WHICH TRAVELTIMES ARE'
*,
*' CALCULATED',I5,/'NUMBER OF TRAVELTIMES CALCULATED FO
*R',
*' EACH PHASE',I5//)
735 FORMAT(A4,F10.0)
750 FORMAT(20(A4))
755 FORMAT(A8,I10)
760 FORMAT('STATION ',A4,' NOT FOUND IN LIBRARY')
751 FORMAT(60X,A4,2X,A4)
752 FORMAT('EVENT WITH SOURCE ',A4,' AND NUMBER ',A4,' NOT
*FOUND IN EVENT LIBRARY')
753 FORMAT('NUMBER OF STATIONS IN LIBRARY',I5)
MDE = 0

```

```

C
C INPUT OF PHASES PHAS(-) FOR TRAVEL TIME CALCULATION.
C
C III COUNTS THE NUMBER OF PHASES SEARCHED FOR THE TRAVEL
C TIME TABLE
C
C MINUS CHO IS NUMBER OF PHASES NOT FOUND IN TRAVEL
C TIME TABLE
C

```

```

CHO=0
ISLUT=0
III=0
READ(5,755)CHEAPP,NL
READ(5,750)(PHAS(I),I=1,40)
READ(5,714)JCODE

```





```

      GO TO 401
402  REWIND 3
      ISLUT=ISLUT+1
      IF (ISLUT.EQ.2) GO TO 415
      GO TO 400
415  WRITE(6,725) PHAS(III)
      ISLUT=0
      CHO=CHO-1
401  III=III+1
      REWIND 4

C
C  END OF PHASES
C
      IF (PHAS(III).EQ.ZERC) GO TO 930
      NNN=0
      KEPIC=1

C
C  INPUT OF TRAVEL TIME TABLE
C
400  READ(3,702) PPHA
      IF (PPHA.EQ.SLUT) GO TO 402
      IF (PPHA.NE.PHAS(III)) GO TO 400
      WRITE(6,724) PPHA
      BACKSPACE 3
      READ(3,702) PPHA,NMN
      READ(3,711) DDEL,L
      MDE=0.0
      MODE=0
      IF (NL.NE.0) WRITE(6,722) DDEL,L,MODE
      READ(3,712) (IDEP(IZK),IZK=1,14)
811  IF (MODE) 830,812,830
812  READ(3,713) (XMIN(I),XSEC(I),I=1,14),PHASE,DEG,JB
      DO 814 I=1,14
      TA(I,1)=XSEC(I)+XMIN(I)*60.
814  CONTINUE
      J=1
815  READ(3,713) (XMIN(I),XSEC(I),I=1,14),PHA,DE,JC

C
C  CHECK IF CARD IS BLANK SIGNALLING END OF PHASE DATA.
C
      IF (XSEC(1)+XMIN(1)) 813,840,813
813  J=J+1
      JMAX=J
818  DO 819 I=1,14
      TA(I,J)=XSEC(I)+XMIN(I)*60.
819  CONTINUE
      GO TO 815
830  READ(3,721) XMIN(1),XSEC(1), (XSEC(I),I=2,14),PHASE,DEG,
      *JB
      TA(1,1)=XSEC(1)+XMIN(1)*60.
      DO 831 I=2,14
      TA(I,1)=TA(1,1)-XSEC(I)
831  CONTINUE
      J=1

```



```

832 READ(3,721) XMIN(1),XSEC(1),(XSEC(I),I=2,14),PHA,DE,JC
    IF(XSEC(1)+XMIN(1)) 833,840,833
833 J=J+1
    JMAX=J
836 TA(1,J)=XSEC(1)+XMIN(1)*60.
    DO 839 I=2,14
C
C   IF PHASE DEPTH CORRECTION IS ZERO, PHASE DOES NOT
C   EXIST, SET TA=0.
C
    IF(XSEC(I)) 837,837,838
837 TA(I,J)=0.0
    GO TO 839
838 TA(I,J)=TA(1,J-XSEC(I))
839 CONTINUE
    GO TO 832
840 CONTINUE
C
C   READ ELLIPTICITY CORRECTION IN SEC/KM AT 10 DEG
C   INTERVALS FROM 0 180 DEGREES.
C
    READ(3,717) (ELLIP(I),I=1,19)
C
C   READ SOUFACE CORRECTION VELOCITY FROM TRAVEL TIME TABLE
C
    READ(3,717) VVELO
    IF((III+CHO).GT.1) GO TO 75
    I=0
70   I=I+1
C
C   INPUT OF STATION LIST
C
    READ(1,703) NSTA(I),LAT(I),LON(I),HI(I),(SLOC(I,J),J=1,
    *12)
    IF(NSTA(I).EQ.ZERO) GO TO 71
    NNST=I
    GO TO 70
71   WRITE(6,753) NNST
    GO TO 2003
75   CONTINUE
    IF(CHEAPP.EQ.CHEAP) GO TO 303
2003 N=0
4    READ(4,735) ST,VELO
    IF(ST.EQ.ZERO) GO TO 206
C
C   FINDING THE CHOSEN STATION IN THE LIST
C
    CALL LOOK1(NNST,ST,NSTA,INDEX)
    IF(INDEX.EQ.0) GO TO 20
    N=N+1
    FT(N)=LAT(INDEX)
    FG(N)=LON(INDEX)
    STA(N)=NSTA(INDEX)
    ELEVA(N)=HI(INDEX)

```



```

DO 277 J=1,12
277 SSLOC(N,J)=SLOC(INDEX,J)
   IF(VELO.EQ.0.) VELO=VVELO
   IF ( MDE .EQ. 1 ) VELO = VELO * 0.576
   VELOC(N)=VELO
   IF(NL.NE.0) WRITE(6,704) STA(N),FT(N),FG(N),ELEVA(N),VEL
   *O
   GO TO 4
20  WRITE(6,760) ST
   GO TO 4
206 CONTINUE
C    M IS CURRENT NUMBER OF OBSERVATORY FOR WHICH DISTANCES
C    ARE BEING COMPUTED.
207 M=1
   REWIND 2
C
C    INPUT OF EVENT FROM FILE, NSO AND NNO ARE THE IDENTIFIERS
C
   READ(4,765) NSO,NNO
765  FORMAT(A4,1X,A4)
   IF(NSO.EQ.ZERO) GO TO 305
310  READ(2,751) ISO,INO
   IF(ISO.EQ.ZERO) GO TO 300
   IF(ISO.NE.NSO) GO TO 310
   IF(INO.NE.NNO) GO TO 310
   BACKSPACE 2
   READ(2,705) ID,IM,IY,IH,IN,RSEC,FLT(1),FLG(1),RDP,RMG,S
   *1,S2,S3,S4,S
15,S6,(RECORD(I),I=1,12)
   GO TO 303
305  CONTINUE
   IF(CHEAPP.EQ.CHEAP) GO TO 401
   READ(4,750) NSO
   IF(NSO.EQ.ZERO) GO TO 401
   BACKSPACE 4
   GO TO 2003
300  WRITE(6,752) NSC,NNO
   GO TO 207
303  CONTINUE
   IF(NL.NE.0) WRITE(6,706) KEPIC,ID,IM,IY,IH,IN,RSEC,FLT(1
   *),FLG(1)
   IF(NL.NE.0) WRITE(6,707) RDP,RMG,S1,S2,S3,S4,S5,S6
   *,(RECORD(I),I=1,12)
302  FLAT(1)=FLT(1)/57.295778
   FLONG(1)=FLG(1)/57.295778
C
C    COMPUTE GEOCENTRIC LATITUDE OF EARTHQUAKE
C
   GLAT(1)=ATAN(0.993277*(SIN(FLAT(1))/COS(FLAT(1))))
   EGLAT=GLAT(1)
   CLAT(1)=COS(GLAT(1))
   SLONG(1)=SIN(FLONG(1))
   CLONG(1)=COS(FLONG(1))
   A(1)=CLAT(1)*CLONG(1)

```





```

      B(1)=CLAT(1)*SLONG(1)
5  C(1)=SIN(GLAT(1))

```

```

C
C      CALCULATE SEISMOLOGICAL LATITUDE OF EARTHQUAKE
C      FOLLOWING BULLEN.
C

```

```

      BLAT(1)=1.1*GLAT(1)-0.1*FLAT(1)
      CLAS(1)=COS(BLAT(1))
      AS(1)=CLAS(1)*CLONG(1)
      BS(1)=CLAS(1)*SLONG(1)
      CS(1)=SIN(BLAT(1))
203 IF(M-N) 204,204,301
204 FLT(2)=FT(M)
      FLG(2)=FG(M)
      ST=STA(M)
205 FLAT(2)=FLT(2)/57.295778
      FLONG(2)=FLG(2)/57.295778

```

```

C
C      COMPUTE GEOCENTRIC LATITUDE OF STATION FROM GEOGRAPHIC
C      LATITUDE
C

```

```

      GLAT(2)=ATAN(0.993277*(SIN(FLAT(2))/COS(FLAT(2))))
      CLAT(2)=COS(GLAT(2))
      SLONG(2)=SIN(FLONG(2))
      CLONG(2)=COS(FLONG(2))

```

```

C
C      COMPUTE EPICENTRAL DISTANCE, DELTA.
C

```

```

      A(2)=CLAT(2)*CLONG(2)
      B(2)=CLAT(2)*SLONG(2)
      C(2)=SIN(GLAT(2))

```

```

C
C      COMPUTE BULLENS SEISMOLOGICAL LATITUDE OF STATION, BLAT(2).
C

```

```

      BLAT(2)=1.1*GLAT(2)-0.1*FLAT(2)
      CLAS(2)=COS(BLAT(2))
      AS(2)=CLAS(2)*CLONG(2)
      BS(2)=CLAS(2)*SLONG(2)
      CS(2)=SIN(BLAT(2))
      SCOSD=AS(1)*AS(2)+BS(1)*BS(2)+CS(1)*CS(2)
      SSIND=SQRT(1.-SCOSD**2)
      SDEL=57.295778*ATAN(SSIND/SCOSD)
      IF(SDEL) 66,77,77
66 SDEL=SDEL+180.
77 COSDT=A(1)*A(2)+B(1)*B(2)+C(1)*C(2)
      SINDT=SQRT(1.-COSDT**2)
      DELTA=57.295778*ATAN(SINDT/COSDT)
      IF(DELTA) 6,7,7
6 DELTA=DELTA+180.

```

```

C
C      CALCULATE AZIMUTH, AZ, AND BACK AZIMUTH, AZE.
C

```

```

7 XI=B(1)*C(2)-B(2)*C(1)
  XJ=A(1)*C(2)-A(2)*C(1)

```



```

      XK=A (1) *B (2-A (2) *B (1)
      DO 8 I=1,2
      COSZ (I) =- (XI*SLONG (I) +XJ*CLONG (I) ) / ( (-1.) **I*SINDT)
      SINZ (I) =- ( (-1.) **I/CLAT (I) ) *XK) /SINDT
      Z (I) =57.295778*ATAN (SINZ (I) /COSZ (I) )
      IF (COSZ (I) ) 9,10,10
    9  Z (I) =Z (I) +180.
   10  IF (Z (I) ) 11,8,8
   11  Z (I) =Z (I) +360.
    8  CONTINUE
      IF (FLT (2) .EQ. -90.00) GO TO 500
      GO TO 208
500  DELTA=57.295778*ATAN ( (SQRT (1.-C (I) **2) ) / (-C (I) ) )
      IF (DELTA) 501,502,502
501  DELTA=DELTA+180.
502  Z (I) =180.
      IF (FLG (1) ) 503,504,504
503  Z (2) =360. +FLG (1)
      GO TO 208
504  Z (2) =FLG (1)
      IF (NL.NE.0) WRITE (6,555)
555  FORMAT (///)
208  DEL (M) =DELTA
      SLDEL (M) =SDEL

C
C      DEL (M) =GEOCENTRIC EPICENTRAL DISTANCE IN DEGREES.
C      SLDEL (M) = SEISMIC LATITUDE EPICENTRAL DISTANCE IN DEGREES.
C

      AZ (M) =Z (1)
      AZE (M) =Z (2)
      SGLAT (M) =GLAT (2)

C
C      CHOOSE NEXT STATION AND CALCULATE DISTANCE AGAIN.
C

      M=M+1
      GO TO 203
301  CALL DEGKM (N, EGLAT, SGLAT, DEL, CDEL)

C
C      SUBROUTINE DEGKM COMPUTES GEOCENTRIC DISTANCE, CDEL, IN KM.
C

      IF (NL.NE.0) WRITE (6,708)
      DO 17 I=1,N
      IF (CHEAPP.EQ.CHEAP) VELOC (I) =VVELO
      IF (NL.NE.0) WRITE (6,709) STA (I) ,SLDEL (I) ,DEL (I) ,CDEL (I) ,
      *AZ (I) ,AZE (I)
      IF (III.GT.1) GO TO 17

C
C      OUTPUT OF DATA TO LIBRARY CARDS
C

      WRITE (8,774) STA (I) ,ISO,INO
      WRITE (8,771) (SSLOC (I,J) ,J=1,12) ,FT (I) ,FG (I) ,ELEVA (I)
771  FORMAT (1X,12A4,/, ' STATION DATA: LAT,LON (DEG) ,ELEV (KM)
      * ,/,
      *1X,2 (F8.3,1X) ,F5.3,1X,F5.2)

```



```

WRITE(8,772) (RECORD(J),J=1,12),FLT(1),FLG(1),RDP,RMG,
*ID,IM,IY,IH,IN,RSEC
772 FORMAT(1X,'EVENT DATA: ID AND LOCATION.',/,1X,12A4,/,
*' LAT,LON(DEG): ',1X,2F8.2,/,1X,'DEPH(KM) AND MAG. ',
*F6.1,1X,F4.1,/, ' ORIGIN TIME: ',5(I3),1X,F5.2)
WRITE(8,773) SLDEL(I),DEL(I),CDEL(I),AZ(I),AZE(I)
773 FORMAT(1X,'DISTANCES AND AZIMUTHS:',/, ' SEISM DIST(DEG
*) : ',
*1X,F7.2,/,1X,'GEOC DIST(DEG): ',F7.2,/, ' GEOC DIST(KM)
*: ',
*F8.1,/, ' GEOC AZM(DEG) EV: ',
*F7.2,/,1X,'GEOC AZM(DEG) ST: ',F7.2)
WRITE(8,775)
775 FORMAT(' THE FOLLWCING CARD HAS PHASE ARR. TIM',
*'E(HR,MIN, ',/, ' SEC), RAY PARAMETER P(SEC/DEG), APPAREN
*T VELOCITY',
*/, ' APPV(KM/SEC), ANGLE OF INCIDENCE AINC(DEG) ',/
*' ELLIPTICITY CORRECTION CELL(SEC) AND STATION',
*/, ' ELEVATION CORRECTION CSUR(SEC) ')
WRITE(7,774) STA(I),ISO,INO
774 FORMAT(1X,A4,20X,A4,1X,A4)
17 CONTINUE
IF(III.GT.1) GO TO 780
DO 779 I=1,N
WRITE(7,778)
778 FORMAT(' PHA ARR TIME P APPV AINC CELL CS
*UR')
779 CONTINUE
780 CONTINUE
IF(JCODE-1) 910,911,911

C
C CALCULATION OF TRAVEL TIMES AND VELOCITIES
C
910 CALL TIMEP(N,JMAX,L,DDEL,RDP,SLDEL,TP,DT)
IF(NL.NE.0) WRITE(6,715)
GO TO 912
911 CALL TIMEP(N,JMAX,L,DDEL,RDP,DEL,TP,DT)
IF(NL.NE.0) WRITE(6,716)
912 IF(NL.NE.0) WRITE(6,718)
R=6371.

C
C CALCULATE ELLIPTICITY CORRECTION FOR EARTHQUAKE.
C CALCULATE SURFACE CORRECTIONS AND ABSOLUTE TIMES FOR
C N STATIONS.
C
DO 920 I=1,N

C
C IF TRAVEL TIME OR VELOCITY IS NON EXCISTENT, THE AFFECTED
C OUTPUT VARIABLES ARE ZERO.
C
IF(TP(I).EQ.0.) GO TO 1009
FGFG=FG(I)/57.295778
CALL MELIP(NMN,GLAT(1),FLONG(1),SGLAT(I),FGFG,ELLIP,RD
*P,DEL(I)

```



\*, TCELL(I) )

C  
C COMPUTE ANGLE OF INCIDENCE ,AINC, AT SURFACE AND FIND SURFACE  
C CORRECTION AT OBSERVATORY STATION, TSUR.  
C

AINC=ARSIN(VELOC(I)\*57.3\*DT(I)/R)  
TSUR(I)=ELEVA(I)/(VELOC(I)\*COS(AINC))  
VANG=(VELOC(I)\*DT(I)\*57.3/R)  
IF (ABS(VANG).GE.1.0) VANG=0.  
VANG=ARSIN(VANG)\*57.3  
CVANG=13.64\*DT(I)\*57.3/2898.  
IF (ABS(CVANG).GE.1.0) CVANG=0.  
CVANG=ARSIN(CVANG)\*57.3  
CSANG=7.30\*DT(I)\*57.3/2898  
IF (ABS(CSANG).GE.1.0) CSANG=0.  
CSANG=ARSIN(CSANG)\*57.3

C  
C TP = PREDICTED ARRIVAL TIME FULLY CORRECTED.  
C ORIGIN TIME OF EVENT IS ID DAYS, IH HOURS, IN MINUTES,  
C RSEC SECONDS.  
C

TP(I) = TP(I) + TCELL(I) +TSUR(I)  
MINI=TP(I)/60.  
GM = MINI  
IHR=GM/60.  
TSEC = TP(I) - GM \* 60.0

C  
C COMPUTE ABSOLUTE TIME OF ARRIVAL OF PHASE.  
C

TSEC=RSEC+TSEC  
IF (TSEC-60.) 1002,1001,1001  
1001 TSEC=TSEC-60.0  
MINI = MINI + 1  
1002 IMIN = MINI + IN  
IF (IMIN-60) 1004,1003,1003  
1003 IHR=IHR+1  
IMIN=IMIN-60  
1004 IHR=IH+IHR  
IDR=ID  
IF (IHR-24) 1006,1005,1005  
1005 IHR=IHR-24  
IDR=ID+1  
IDN = 1  
1006 IF (DT(I)) 1007,1008,1007  
1007 SCA=2.\*3.14159\*R/360.  
APPV=SCA/DT(I)  
GO TO 1010  
1008 APPV=0.0  
GO TO 1010  
1009 CONTINUE  
IDR=0  
IHR=0  
IMIN=0  
TSEC=0.





```

      TP(I)=0.
      TCELL(I)=0.
      TSUR(I)=0.
      VANG=0.
      SANG=0.
      CVANG=0.
      CSANG=0.
      APPV=0.
1010 IF(NL.NE.0) WRITE(6,719) STA(I),IDR,IHR,IMIN,TSEC,TP(I),
      *TCELL(I)
      *,TSUR(I),DT(I),
      1APPV,VANG,CVANG,CSANG
      WRITE(7,742) PHAS(III),IHR,IMIN,TSEC,DT(I),APPV,VANG,TC
      *ELL(I),
      *TSUR(I)
742  FORMAT(1X,A4,1X,2(I2,1X),2(F5.2,1X),2X,F5.1,1X,F4.1,1X
      *,2(F5.2,1X))
      NNN=NNN+1
920  CONTINUE
      NCOUNT(KEPIC)=N
      KEPIC=KEPIC+1
      IF(CHEAPP.EQ.CHEAP) GO TO 401
      GO TO 207
930  CONTINUE
C
C  USING SUBROUTINES SHUF AND SPT, THE FILES ARE NOW
C  REARRANGED TO GET THE PHASES IN THE RIGHT ORDER, AND
C  TO FIT THE LIBRARY CARD FORMAT.
C
      III=III-1-CHO
      WRITE(6,728) III,NNN
      KEPIC=KEPIC-1
      IF(CHEAPP.NE.CHEAP) CALL SHUF(7,KEPIC,NCOUNT)
      III=III+2
      LIII=20-III
      IF(LIII) 410,411,412
412  CONTINUE
      READ(7,450,END=417)
      GO TO 412
417  CONTINUE
      DO 413 L=1,NNN
      DO 413 K=1,LIII
413  WRITE(7,450)
450  FORMAT(/)
      III=20
      GO TO 411
410  WRITE(6,451)
451  FORMAT(/,'TOO MANY LINES TO PRINT CARDS',/)
411  CONTINUE
      CALL SPT(7,8,III,NNN)
      STOP
      END

```



THIS PROGRAM IS A GENERAL VELOCITY - AZIMUTH SPECTRAL  
ANALYSIS PRODUCED BY P. R. H. GUTOWSKI AT THE U. OF ALBERTA

THE PROGRAM HAS BEEN CHANGED SUBSTANCIALY BY JENS HAVSKOV  
LATEST UPDATE IS FROM JUNE 1976.

THE MOST IMPORTANT CHANGES ARE:

CORRECTION FOR STATION ELEVATION.

CORRECTION FOR EARTH CURVATURE AT THE ARRAY SITE. THIS  
CORRECTION IS ONLY IMPORTANT FOR LARGER ARRAYS.

OUTPUT OF COVESPAGRAMS ON A P-AZ GRID INSTEAD OF A  
TIME-P GRID.

CALCULATION OF THE ARRAY RESPONSE FOR EACH RUN.

ORIGINAL VELOCITY SPECTRAL ANALYZER GIVEN BY  
D. DAVIES AT AL, NATURE 1970 WHICH FEATURED  
BEAMFORMING FOR EACH VELOCITY (DELAY AND SUM)  
TAKING THE POWER OF ONE SECOND OF BEAM AT 1 SEC  
INCREMENTS DOWN THE RECORD. THE RESULTANT VELOCITY  
VERSUS TIME MATRIX WAS THEN CONTOURED AND PLOTTED.  
THIS METHOD HAS SINCE BEEN SHOWN TO BE RATHER  
DEPENDENT ON AMPLITUDE VARIATION ACROSS THE ARRAY  
WITH DISTINCT SIDE LOBES APPEARING EVEN FOR LARGE  
NUMBER OF SENSORS. THE VELOCITY - AZIMUTH  
SPECTRAL ANALYSIS METHOD (VESPA) DOES NOT SUFFER  
FROM THIS DRAWBACK AS IT INVOLVES A COHERENCY  
FUNCTION GENERATED BY CROSS MULTIPLICATION OF  
TRACES IN COMBINATIONS OF TWO STATIONS. THE SIMPLE  
SUMMATION OF SENSORS I.E. FOR 5 SENSORS BEAMFORM  
WOULD LEAD TO THE SUM OF 5 TRACES WHEREAS VESPA  
WOULD CROSS MULTIPLY 10 TIMES AND THUS MAKES MUCH  
MORE EFFICIENT USE OF THE AVAILABLE DATA REDUNDANCY.  
IN ADDITION VESPA SWEEPS NOT ONLY THROUGH VELOCITY  
AND TIME , BUT ALSO THROUGH AZIMUTH THUS EMPLOYING  
THE MAXIMUM INFORMATION INHERENT IN ARRAY DATA.  
FOR A MODERATE NUMBER OF SENSORS THEREFORE, THERE  
WILL BE VIRTUALLY NO SIDE LOBE PROBLEM.

INPUT

INPUT 1:

CARD 1 TO CARD 7: A FILE CONTAINING A LIST OF STATION  
IDENTIFIERS, LATITUDES, LONGITUDES (DEG) AND  
ELEVATIONS (KM).

FORMAT (2X, A4, 4X, 3F10.4)

FROM THIS FILE THE STATIONS NEEDED FOR A PARTICULAR  
RUN IS CHOSEN. THE STATIONS DO NOT HAVE TO BE IN  
ANY ORDER.

INPUT 5:



CARD 1: NS,IREL,LL (3I5)

NS: NUMBER OF STATION IN THE ARRAY.

IREL: STATION NUMBER RELATIVE TO WHICH P AND AZ IS MEASURED. THE ORDER IS DETERMINED THE ORDER OF INPUT TO CARD 2.

IL: COMPONENT TO BE USED FOR CORRELATION, 0,1,2 ARE Z, NS, AND EW.

CARD 2: KEITBL(I) (7(A4))

STATION IDENTIFIERS, E.G. 'EDM '.

CARD 3: NOEV,NCOMB (2I5)

NOEV: NUMBER OF RUNS WITH A NEW SET OF PARAMETERS TO BE SPECIFIED (SEE CARD 4-9).

NCOMB: NUMBER OF RUNS WITH SAME PARAMETERS (CARD 4-9), EXCEPT A NEW STATION COMBINATION HAS TO BE READ IN (CARD 7). THUS CARD 4-9 FOR THE FOLLOWING RUNS ARE REPLACED BY CARD 7.

CARD 4: NSTAT,ITSPAN,NPOP,NEND,F1,F2 (4I5,2F6.2)

NSTAT: NUMBER OF STATIONS USED IN A PARTICULAR RUN.

ITSPAN: A COVESPAGRAM IS CALCULATED FOR EACH SECOND ITSPAN SECONDS.

NPOP: OVER THE TIME SPAN ITSPAN THE PROGRAM WILL FIND THE POINT (P,AZ) WITH THE HIGHEST CORRELATION. NEND=2 WILL MAKE THE PROGRAM RECALCULATE THE COVESPAGRAM CENTERED ON (P,AZ), AND WITH P AND AZ STEPS 5 TIMES SMALLER, THUS GIVING A BETTER ESTIMATE OF THE MAXIMUM. IN GENERAL THE PROGRAM GOES THROUGH THE LOOP NPOP TIMES, EACH TIME DECREASING THE P AND AZ STEP. IF NPOP=0, ONLY THE ARRAY RESPONSE WILL BE CALCULATED, AND INPUT 8 DOES NOT HAVE TO BE CONNECTED.

NEND: NUMBER OF DATA POINTS OVER WHICH THE THE CORRELATION IS PERFORMED. E.G. NEND=25 GIVES A TIME SPAN OF 2 SEC, AS THE SAMPLING RATE IS 12.5.

F1,F2: LOWER AND UPPER FREQUENCY(HZ) FOR BANDPASS FILTERING THE DATA. NO FILTERING IS DONE IF BOTH F1 AND F2 ARE ZERO.

CARD 5: VL1,VU1,VDIV1,CORLIM (4F10.0)

VL1,VU1: LOWER AND UPPER P LIMET(DEG/SEC) FOR THE COVESPAGRAM.

VDIV1: INCREMENT OF P, MUST BE SUCH THAT ONLY 31 VALUES OF P RESULTS.

CORLIM: CORRELATIONS ARE NORMALIZED TO 1.0, AND CORRELATIONS BELOW CORLIM ARE EQUATED TO 0.

CARD 6: AZML1,AZMU1,AZDIV1 (3F10.0)

AZML1,AZMU1: LOWER AND UPPER AZIMUTH LIMITS OF COVESPAGRAM.

AZMDIV1: INCREMENT OF AZIMUTH, MUST BE SUCH THAT ONLY 21 VALUES OF AZ RESULTS.

CARD 7: NFILE,STATNS(I) (I3,7A4)

NFILE: FILE NUMBER ON THE DATA TAPE OF THE FIRST STATION IN A PARTICULAR RUN. THE NUMBER IS FOR THE TAPE HEADER.





STATNS: STATION IDENTIFIERS OF NSTAT STATIONS USED,  
STATION MUST COME IN SAME ORDER AS ON TH TAPE.

CARD 8: TTSTART,T1,T2 (3F10.0)  
TTSTART: CORRELATION START TIME. TTSTART=0 IMPLIES  
THAT CORRELATION WILL START 3 SEC BEFORE  
THE PREDICTED P-WAVE ARRIVAL TIME.

T1: PERIOD (SEC) OF THE ANALYZED SIGNAL, USED FOR  
CALCULATION THE ARRAY RESPONSE.

T2: TIMESPEAN OF GENERATED TEST SIGNAL WITH PERIOD  
T1.

CARD 9: VVV (I),AZZ (I),AMP (I) (9F6.1)  
VVV,AZZ,AMP: F,AZ AND AMPLITUDE OF ABOVE TEST SIGNAL  
USED FOR CALCULATION OF ARRAY RESPONSE.  
UP TO 3 DIFFERENT PULSES CAN BE USED.

# EXAMPLE OF A RUN DECK:

```
RUN CO 1=VASASTATION 8=*T*
6,2,
EDM DEL FIN TRO RM1 RM2
1,1,
3,11,1,25,0.1,1.3,
7,8,0.05,-1,
103,120,1,
145PIN TRO RM2
0,1,6,
7.55,113,1,
3,10,1,25,0.1,1.3,
2.2,3.2,0.05,-1,
103,120,1,
145PIN TRO RM2
74,1,6,
3.7,113,1,
```

THE PROGRAM WILL NOW SEARCH OVER THE SPECIFIED VELOCITY,  
TIME AND AZIMUTH RANGES GENERATING A SERIES OF VESPAGRAMS  
FOR EACH TIME WINDOW PRINTING THESE OUT AND PICKING THE  
SUCCESSIVE MAXIMA OVER THE TIME WINDOW INCREMENTED AT  
1 SECOND INTERVALS AND THUS PRODUCING A SERIES OF  
VELOCITY TIME AND AZIMUTH ESTIMATED BY PARABOLA FITTING.

```
DIMENSION CZ (10),AZ (7,7),D (7,7),V (7,2300),CC (7,7)
DIMENSION CCOR (20,31,31),AZM (7),DELTA (7,7)
DIMENSION XVEE (31),AT (21),IA (7),L (21),M (21),ITD (7)
DIMENSION W (2300),DD (8)
DIMENSION NCCOR (50),XXVEL (3),XXAZ (3)
```



```

DIMENSION HEIGHT(7),NTD(3,10),AMP(3),VVV(3),AZZ(3)
INTEGER*2 IDAT(8192)
DOUBLE PRECISION DOUB1,DOUB2
DOUBLE PRECISION TIMES(7),TMAX,TSTRT,TDEL
DIMENSION FFQ(24)
REAL KEYTBL(10),LAT(10),LON(10)
INTEGER*4 TD(7,7)
REAL*4 STATNS(7)
NFLST=1
READ(5,115) NS,IREL,LL
READ(5,116) (KEYTBL(I),I=1,NS)
116  FORMAT(10A4)
DO 62 I=1,NS
51  CONTINUE
    READ(1,103) ST
    IF(ST.NE.KEYTBL(I)) GO TO 51
    BACKSPACE 1
    READ(1,103) ST,LAT(I),LON(I),HEIGHT(I)
62  CONTINUE
103  FORMAT(2X,A4,4X,3F10.4)
C
C  ALL COMBINATIONS OF AZIMUTHS AND DISTANCES BETWEEN ANY TWO
C  STATIONS IS CALCULATED.
C
    DO 22 J=1,NS
    DO 22 I=1,NS
    CALL DELAZG(LAT(J),LCN(J),LAT(I),LON(I),DI,SKM,AZI)
    AZ(J,I)=AZI/57.29578
    D(J,I)=SKM
22  CONTINUE
C
C  AZIMUTH CORRECTION FOR NON FLAT EARTH.
C
    CALL CAZM(NS,IREL,LAT,LON,CZ)
    READ(5,115) NOEV,NCCMB
115  FORMAT(16I5)
101  FORMAT(7F10.6)
    DO 10 IEV=1,NOEV
    DO 1010 KCOM=1,NCOMB
    NREAD=1
    IF(KCOM.EQ.1) NREAD=0
    IF(NREAD.EQ.0) READ(5,70) NSTAT,ITSPAN,NPOP,NEND,F1,F2
70  FORMAT(4I5,2F7.2)
    NPOP=NPOP+1
    IF(NEND.EQ.0) NEND=50
    NUM=(NSTAT*(NSTAT-1))/2
    IRDIM=ITSPAN+108
    WRITE(6,129) KEYTBL(IREL)
129  FORMAT('1','REFERENCE STATION IS',1X,A4)
    WRITE(6,126) LL
126  FORMAT('CHANNEL NUMBER',I3)
    WRITE(6,179) NEND
    WRITE(6,187) F1,F2
187  FORMAT('CORNER FREQUENCES ',2F7.2)

```



```

179  FORMAT('NEND=',I3)
      RDIM=IRDIM
      IRDIM=RDIM*12.5
      LORNA=ITSPAN+1
      IF(NREAD.EQ.0) READ(5,80) VL1,VU1,VDIV1,CORLIM
      VU=VU1
      VL=VL1
      VDIV=VDIV1
      IF(NREAD.EQ.0) READ(5,80) AZML1,AZMU1,AZDIV1
      AZML=AZML1
      AZMU=AZMU1
      AZMDIV=AZDIV1
80    FORMAT(4F10.0)
      NAZM=(AZMU-AZML)/AZMDIV +2
      NVELS=1
      DO 27 J2=1,35
      VIND=VL+J2*VDIV
      IF(VIND.GT.(VU+0.0001)) GO TO 13
      GO TO 14
13    CONTINUE
      WRITE(6,200) NVELS
200   FORMAT(1H,'NVELS=',I5)
      GO TO 21
14    CONTINUE
      NVELS=NVELS+1
27    CONTINUE
21    CONTINUE
      PSTART=(VL+VU)/2.0
      RAD=3.14159/180.
      READ(5,100) NFILE,STATNS
100   FORMAT(I3,7A4)
102   FORMAT(7F10.0)
      IF(NREAD.EQ.0) READ(5,102) TTSTRT,T1,T2
      IF(NREAD.EQ.0) READ(5,113) (VVV(I),AZZ(I),AMP(I),I=1,3)
113   FORMAT(9F6.1)
      WRITE(6,122) T1,T2
      DO 176 J=1,10
      DO 176 K=1,3
      XXVEL(K)=0.0
      XXAZ(K)=0.0
176   NTD(K,J)=0.0
122   FORMAT('PERIOD=',F3.1,5X,'TIME WINDOW=',F3.1)
      TSTRT=TTSTRT/60.0
      IF(NPOP.EQ.1) GO TO 402
      IF(NFILE.NE.NFLST) GO TO 401

C
C    IDENTIFY STATIONS
C
402   DO 71 I=1,NSTAT
      DO 72 J=1,NS
      IF(STATNS(I).NE.KEYTBL(J)) GO TO 72
      IA(I)=J
      GO TO 71
72   CONTINUE

```



```

71 CONTINUE
  NSTOP=0
  IF(NPOP.EQ.1) GO TO 1200
C
C   FIND START TIMES FROM TAPE
C
  DIST=0.0
  NBACK=0
  DO 2333 I=1,NSTAT
    IQ=IA(I)
2335 CONTINUE
    READ(8) IEVENT,STAT,DEL,AZIM,IH,IM,DOUB1,MODE,NWB,IHS,I
    *MS,DOUB2,
    1ID,IMON,IYEAR,IHOU,IMIN,ESEC,ELAT,ELON,EDEP,EMAG,NP,(F
    *FQ(IXX),
    *IXX=1,5)
    IF(STAT.EQ.KEYTBI(IQ)) GO TO 2334
    CALL SKIP(2,0,8)
    NBACK=NBACK+2
    GO TO 2335
2334 CONTINUE
    DIST=DEL/NSTAT+DIST
    TIMES(I)=DOUB2+60*IMS+3600*IHS
    CALL SKIP(2,0,8)
    NBACK=NBACK+2
2333 CONTINUE
    NBACK=NBACK+1
    IF(NFILE.EQ.1) GO TO 74
    CALL SKIP(-NBACK,0,8)
    CALL SKIP(1,0,8)
    GO TO 75
74 REWIND 8
75 CONTINUE
C
C   CORRECTION FOR ALTITUDE
C
  STH=PSTART*6.2*57.3/6371.
  STH=SQRT(1-STH**2)
  DO 1133 I=1,NSTAT
    TIMES(I)=TIMES(I-HEIGHT(IA(I)))/(STH*6.2)
1133 CONTINUE
  WRITE(6,141) IYEAR,IEVENT
1200 CONTINUE
  IF(NPOP.EQ.1) DIST=50.0
141  FORMAT(//,'EVENT  VA',I2,2X,I3,//)
C
C   GENERATE ALL POSSIBLE COMBINATIONS OF TWO STATIONS
C
  AN=NSTAT
  J=1
  K=1
  DO 19 I=1,NUM
    K=K+1
    IF(K.LE.NSTAT) GO TO 11

```





```

      J=J+1
      K=J+1
11  L(I)=J
19  M(I)=K
      IF(NPOP.EQ.1) GO TO 1101
C
C      FIND AMOUNT OF DATA TO TAKE FROM TAPE AND WHERE TO START
C
      TMAX=TIMES(1)
      IMAX=1
      DO 20 I=2,NSTAT
      IF(TMAX.GT. TIMES(I)) GO TO 20
      TMAX=TIMES(I)
      IMAX=I
20  CONTINUE
      TSTRT=(63.0-(TMAX-TIMES(1)))/60.0+TSTRT
      WRITE(6,6565) TTSTRT,(TIMES(I),I=1,NSTAT)
6565  FORMAT(1H,'TSTRT=',F10.2,2X,'TIMES=',7F10.3)
1212  FORMAT('TDEL=',F7.1,'IS TOO BIG')
      DO 17 I=1,NSTAT
      TDEL=TMAX-TIMES(I)
      IF(DABS(TDEL).GT.150.) WRITE(6,1212) TDEL
      IDELAY=12.5*TDEL+0.5
17  ITD(I)=4*IDELAY
      BLK=TSTRT/2.73067
      MBLK=BLK
      XBLK=MBLK
      TREM=2.73067*(BLK-XBLK)
      IREM=4*IFIX(TREM*750.)
      ITSPAN=ITSPAN+108
      TSPAN=ITSPAN
      ISPAN=12.5*TSPAN
      WRITE(6,814) (ITD(IX2),IX2=1,NSTAT)
C
814  FORMAT(5X,'ITD...',5I10)
      WRITE(6,818) BLK,XBLK,TREM,IREM,ISPAN
818  FORMAT(5X,'...',3F10.4,3I10)
      DO 210 I=1,NSTAT
      IQ=IA(I)
2000  CONTINUE
      READ(8) IEVNT,STAT,(FFQ(IXX),IXX=1,4),DOUB1,(FFQ(IXX),
      *IXX=5,8),DOU
      1B2,(FFQ(IXX),IXX=9,24)
      IF(STAT.EQ.KEYTBL(IQ)) GO TO 2001
      CALL SKIP(2,0,8)
      NFLST=NFLST+2
      GO TO 2000
2001  CONTINUE
      CALL SKIP(1,0,8)
C
C      SKIP TO STATION DATA FOR THIS EVENT
C
220  CALL SKIP(0,MBLK,8)
      ICOR=0

```



```

      READ(8) IDAT
      WRITE(6,820) I
820  FORMAT(5X,'STATN...I',I10)
C
C      PICK OFF DATA FOR EACH STATION SO THAT ALL TRACES ARE
C      ALIGNED IN TIME.
C
      DO 230 J=1,ISPAN
      I4=4*J
      K=I4+IREM+ITD(I-3+LI+ICOR
      V(I,J)=IDAT(K)
      IF(K.LT. 8189+LL) GO TO 230
      WRITE(6,820) K
      WRITE(6,820) I4
      READ(8) IDAT
      ICOR=-IREM-ITD(I-I4
230  CONTINUE
C
C      REMOVE DC LEVEL
C
      DC=0.0
      DO 233 J=1,ISPAN
233  DC=DC+V(I,J)
      DC=DC/FLOAT(ISPAN)
      DO 234 J=1,ISPAN
234  V(I,J)=V(I,J-DC
      WRITE(6,900) IEVNT,STAT
900  FORMAT(1H,I5,A4)
      WRITE(6,821) DC
821  FORMAT(5X,'DC...',F10.3)
      CALL SKIP(1,0,8)
210  NFLST=NFLST+2
      ITSPAN=ITSPAN-54
      NSTOP=0
C
C      FILTERING THE TRACES
C
      IF((F1+F2).LT.0.0001) GO TO 65
      CALL BNDPAS(F1,F2,80.0,DD)
      DO 60 KS=1,NSTAT
      DO 61 I=1,IRDIM
61  W(I)=V(KS,I)
      CALL FILTER(W,IRDIM,DD)
      DO 79 I=1,IRDIM
79  V(KS,I)=W(I)
60  CONTINUE
65  CONTINUE
1100 CONTINUE
      NSTOP=NSTOP+1
      IF(NSTOP.LE.1) GO TO 1101
      IF(NSTOP.EQ.NPOP) GO TO 1155
C
C      FIND VELOCITY AND AZIMUTH FOR NEXT CALCULATION
C

```



```

ITSPAN=ITSPAN+54
VDIV=VDIV/5
VL=VELMAX-((IVLIM-1)*VDIV)/2
VU=VELMAX+((IVLIM-1)*VDIV)/2
AZMDIV=AZMDIV/5
AZML=AZMAX-(NIZ-1)*AZMDIV/2
AZMU=AZMAX+(NIZ-1)*AZMDIV/2
1101 CONTINUE
IVL=VL*100. + 0.2
IVU=VU*100. + 0.2
IVDIV=VDIV*100. + 0.2
IAZML=AZML*100.
IAZMU=AZMU*100.
IZDIV=AZMDIV*100
IZ=0
GO TO 1143
1155 CONTINUE
IZ=0
IF(NPOP.EQ.1) NSTOP=1
C
C CALCULATE TIMESERIES FOR ARRAY RESPONSE
C
NTD(1,1)=0.0
NTD(2,1)=0.0
NTD(3,1)=0.0
ITSPAN=54
DO 1134 I=1,IRDIM
DO 1134 J=1,NSTAT
1134 V(J,I)=0.0
DO 1135 KLM=1,3
DO 1135 J=1,NSTAT
KL1=-NTD(KLM,J)+675
KL2=KL1+T2*12.5
DO 1135 I=KL1,KL2,1
V(J,I)=(FLOAT(KL2-I)/FLOAT(KL2-KL1))*SIN((I-KL1)*0.502
*65/T1)
**AMP(KLM)+V(J,I)
1135 CONTINUE
1143 CONTINUE
DO 107 IAZM=IAZML,IAZMU,IZDIV
IZ=IZ+1
AT(IZ)=FLOAT(IAZM)/100.
A=AT(IZ)
DO 281 IJ=1,NS
AZM(IJ)=A+CZ(IJ)
281 CONTINUE
C
C CALCULATE DISTANCES FROM STATION TO STATION WAVEFRONT
C HAS TO TRAVEL FOR EACH AZIMUTH.
C
DO 250 I=1,NUM
DELTA(L(I),M(I))=D(IA(L(I)),IA(M(I)))*COS(RAD*(AZM(IA(
*L(I)))-
1AZ(IA(L(I)),IA(M(I))))

```





```

C
C   DISTANCE CORRECTION FOR EARTH CURVATURE
C
      CALL CURVE(D(3,IA(L(I))),D(3,IA(M(I))), (1/RAD)*AZ(3,IA
      *(L(I))),
      *(1/RAD)*AZ(3,IA(M(I))),AZM(3),DIST,X)
      IF(DELTA(L(I),M(I)).LT.0.) X=-X
      DELTA(L(I),M(I))=DELTA(L(I),M(I))+X
250  CONTINUE
C
C   FOR THIS AZIMUTH CALCULATE VESPAGRAM
C
      IV=0
      DO 306 IVEL=IVL,IVU,IVDIV
      IT=0
      IV=IV+1
      VEX=FLOAT(IVEL)/100.
      IVLIM=IV
      VEE=111.2/VEX
      XVEE(IV)=VEX
C
C   CALCULATE DELAY TIMES FOR EACH 2 STN COMBO FOR EACH VELOCITY
C
      DO 301 I=1,NUM
301  TD(L(I),M(I))=12.5*(DELTA(L(I),M(I))/VEE)+0.5
      IF(NPOP-1.NE.NSTOP) GO TO 1188
C
C   FIND DELAY TIMES FOR CALCULATION OF ARRAY RESPONSE
C
      DO 1187 KN=1,3
      IK1=ABS(VVV(KN)*100-IVEL)
      IK2=ABS(AZZ(KN)*100-IAZM)
      IF(IK1.LE.IVDIV/2.AND.IK2.LE.IZDIV/2) GO TO 1177
      GO TO 1187
1177  CONTINUE
      XXVEL(KN)=IVEL/100.
      XXAZ(KN)=IAZM/100.
      NUM1=NSTAT-1
      DO 1178 I=1,NUM1
      NTD(KN,I+1)=TD(L(I),M(I))
1178  CONTINUE
1187  CONTINUE
1188  CONTINUE
C
C   STEP DOWN IN TIME ALONG THE RECORDS DELAYED FOR THIS VELOCITY
C
      IF(NPOP.EQ.1.AND.NSTOP.EQ.0) GO TO 306
      DO 305 ITOR=54,ITSPAN
      IOR=12.5*FLOAT(ITOR)
      TCC=0.0
      IT=IT+1
      IOR1=IOR
      K=1

```



```

C
C   CROSS MULTIPLY NEND POINTS OF DATA FOR ALL COMBOS AND
C   SUM THESE AT THIS TIME.
C
      DO 302 I=1,NUM
      TTCC=0.0
      ANORM1=0.0
      ANORM2=0.0
      DO 303 JJ=1,NEND
      J=JJ-1
      TTCC=TTCC+V(L(I),IOR1+J)*V(M(I),IOR1+J-TD(L(I),M(I)))
      ANORM1=ANORM1+V(L(I),IOR1+J)**2
303  ANORM2=ANORM2+V(M(I),IOR1+J-TD(L(I),M(I)))**2
      IF((ANORM1*ANORM2).EQ.0.0) GO TO 7676
      CC(L(I),M(I))=TTCC/(ANORM1*ANORM2)**0.5
      GO TO 7677
7676 CC(L(I),M(I))=0.0
7677 CONTINUE
      TCC=TCC+CC(L(I),M(I))
C
C   ENTER THIS VALUE INTO MATRIX
C
      CCOR(IT,IV,IZ)=TCC*2./(AN*(AN-1.))
      IF(I.EQ.NUM) GO TO 302
      IF(L(I+1).EQ.L(I)) GO TO 302
      IOR1=IOR-TD(L(K),M(K))
      K=K+1
302  CONTINUE
305  CONTINUE
C
C
306  CONTINUE
      IT=1
      NIZ=IZ
      NNIZ=NIZ-1
107  CONTINUE
      IF(NSTOP.EQ.NPOP) GO TO 999
      IF(NPOP.EQ.1.AND.NSTOP.EQ.0) GO TO 1155
      ITSPAN=ITSPAN-54
C
C   STEP DOWN MATRICES IN TIME AND PICK MAXIMA ABOVE LOWER LIMIT
C
      WRITE(6,455)
455  FORMAT(/)
      CLMAX=0.0
      J=0
692  J=J+1
      IF(J.EQ.(ITSPAN+2)) GO TO 999
      CMAX=-2.0
      IT=J
      DO 91 IZ=1,NIZ
      DO 91 IV=1,IVLIM
      IF(CCOR(IT,IV,IZ).LE.CMAX) GO TO 91

```



```

      CMAX=CCOR(IT,IV,IZ)
      ITBIB=IT
      IVBIB=IV
      IZBIB=IZ
91    CONTINUE
      IT=ITBIB
      IV=IVBIB
      IZ=IZBIB
      IF(CMAX .GE. CORLIM) GO TO 93
      WRITE(6,952) CMAX
952  FORMAT(5X,'CORREL LESS THAN LIMIT, CMAX= ',F10.3)
      GO TO 691
93    CONTINUE
3    CONTINUE
      IF(IV .LE. IVLIM-1 .AND. IV .GE. 2) GO TO 694
      WRITE(6,701) IV,IZ,IT
701  FORMAT(5X,'MAX. CORREL AT MATRIX EDGE,IV,IZ,IT= ',3I5)
      GO TO 691
694  IF(IZ .LE. NNIZ .AND. IZ .GE. 2) GO TO 693
      WRITE(6,701) IV,IZ,IT
      GO TO 691
693  CONTINUE

C
C    FIT PARABOLAS IN TIME, VELOCITY, AND AZIMUTH
C
C
      TWOA=CCOR(IT,IV+1,IZ)+CCOR(IT,IV-1,IZ-2.*CCOR(IT,IV,I
      *Z)
      B=(CCOR(IT,IV+1,IZ-CCOR(IT,IV-1,IZ))/2. - TWOA*FLOAT(
      *IV)
      FP=-B/TWOA
      IFP=FP
      APPVEE=XVEE(IFP)+(FP-FLOAT(IFP))*(XVEE(IFP+1-XVEE(IFP
      *)))

C
C
      TWOA=CCOR(IT,IV,IZ+1)+CCOR(IT,IV,IZ-1-2.*CCOR(IT,IV,I
      *Z)
      B=(CCOR(IT,IV,IZ+1-CCOR(IT,IV,IZ-1))/2. - TWOA*FLOAT(
      *IZ)
      FP=-B/TWOA
      IFP=FP
      APPAZM=AT(IFP)+(FP-FLOAT(IFP))*(AT(IFP+1-AT(IFP))

C
      WRITE(6,560) CMAX
560  FORMAT(5X,'MAX. CORREL.= ',F10.3)

C
C    WRITE TIME AZIMUTH VELOCITY
C
      IF(CMAX.GT.CLMAX) GO TO 1021
      GO TO 1022
1021 VELMAX=APPVEE
      AZMAX=APPAZM
      CLMAX=CMAX

```



```

1022 CONTINUE
      WRITE(6,550) APPVEE,IT,APPAZM
550  FORMAT(5X,'APP. VEL= ',F10.2,' TIME= ',   I5,' APP. AZ
      *M= ',F10.2/)
691  GO TO 692
C
C
C
401  CALL SKIP(NFILE-NFLST,0,8)
      IF(NFILE-NFLST .LT. 0) GO TO 501
      NFLST=NFILE
      GO TO 402
501  CALL SKIP(-1,0,8)
      CALL SKIP(1,0,8)
      NFLST=NFILE
      WRITE(6,4775)
4775  FORMAT(1H ,'SKIPPED A NEG. NO. OF FILES')
      GO TO 402
999  CONTINUE
      LORNA1=LORNA
      IF(NSTOP.EQ.NPOP) LCRNA1=1
      IF(NSTOP.EQ.NPOP) WRITE(6,937)
937  FORMAT(/,'ARRAY RESPONSE')
      IF(NSTOP.EQ.NPOP) WRITE(6,938) (XXVEL(I),XXAZ(I),AMP(I)
      *,I=1,3)
938  FORMAT(/'VELOCITY  AZIMUTH  AMPLITUDE ',/,3(3F9.2/))
      DO 450 IT=1,LORNA1
      WRITE(6,903) IT, (XVEE(I),I=1,IVLIM,3)
903  FORMAT(/1X,'T=',I2,5X,27(F4.2,5X))
      DO 450 IZ=1,NIZ
      DO 451 IV=1,IVLIM
      IF(CCOR(IT,IV,IZ) .LT. CORLIM) CCOR(IT,IV,IZ)=0.0
      NCCOR(IV)=(CCOR(IT,IV,IZ)+0.005)*100
451  CONTINUE
      WRITE(6,901) AT(IZ), (NCCOR(IV),IV=1,IVLIM)
901  FORMAT(1X,F7.1,2X,40I3)
450  CONTINUE
      IF(NSTOP.LT.NPOP) GO TO 1100
1010 CONTINUE
10  CONTINUE
      STOP
      END

```





```

C
C PROGRAM PERFORMS EULER ROTATIONS ON COORDINATES
C LOCATED IN UP TO 4 DIFFERENT FILES. INPUT IS
C FROM 1-4 AND THE CORRESPONDING OUTPUT IN 11-14
C
      REAL LAT(3000),LON(3000)
      DIMENSION A(3,3),TEXT(6),B(10),C(10),D(10),BB(10)
      DIMENSION NF(4),CC(10),DD(10)
      READ(5,102)M,KJU,NF
      NF1=0
      DO 20 I=1,4
20    NF1=NF1+NF(I)
      IF(KJU.EQ.0) KJU=3
C
C M IS NUMBER OF DIFFERENT ROTATIONS
C KJU IS NUBER OF FILES TO BE ROTATED. THESE
C FILES ARE ALL ROTATED THE SAME AMOUNT, THE
C FIRST ONE CONTAINING MORE BLOCKS THAN THE
C NEXT ONE ETC.
C IF KJU IS ZERO ROTATION IS PERFORMED ON 3
C FILES. A CHOISE OF FILE CAN BE MADE BY
C ASSIGNING VARIOUS VALUES TO NF(I), I=1,4.
C IF ALL NF(I) ARE ZERO ROTATION IS PERFORMED
C ON AS MANY FILES AS SPECIFIED BY KJU. IF
C ONE NF(I) IS DIFFERENT FROM ZERO ROTATION
C IS ONLY PERFORMED ON THOSE FILES WHERE
C NF(I)=I, I=1,4. A FILE MUST ALWAYS BE
C CONNECTED TO 1, AS THE IDENTIFIERS NCONT
C ARE READ FROM INPUT 1.
C
102  FORMAT(6I5)
      WRITE(6,202) M
      DO 2 K=1,M
202  FORMAT(//'NUMBER OF DIFFERENT ROTATIONS',I6//)
101  FORMAT(2I5,6A4)
100  FORMAT(3F10.0,2I10)
      READ(5,100)B(1),C(1),D(1),NSEC,NROT
C
C B,C,D ARE EULER LATITUDE(+NORTH), LONGITUDE(+EAST)
C AND ANGLE OF ROTATION(+ANTICLOCKWISE).
C NSEC IS NUMBER OF BLOCKS ROTATED THE SAME AMOUNT
C NROT IS NUMBER OF ROTATIONS TO BE READ IN FOR
C THESE PARTICULAR BLCKKS.
C
      IF(NROT.EQ.0) NROT=1
      IF(NSEC.EQ.0) NSEC=1
      BACKSPACE 5
      READ(5,105) (B(I),C(I),D(I),I=1,NROT)
105  FORMAT(3F10.0)
      DO 2 LL=1,NSEC
      READ(1,101) N,NCONT,(TEXT(I),I=1,6)
      READ(1,103) (LAT(I),LON(I),I=1,N)
C
C ANGLE OF ROTATION ZERO IMPLIES OUTPUT OF

```



C DATA WITHOUT ROTATION.

C

IF(D(1).EQ.0.) GO TO 7

C

C THE NROT NUMBER OF ROTATIONS ARE COMBINED TO  
C CNE ROTATION, AND THE TRANSFORMATION MATRIX A  
C IS FOUND USING SUBROUTINE MUL.

C

DO 6 L=1,NROT

NRO=NROT

BB(L)=B(L)

CC(L)=C(L)

6 DD(L)=D(L)

CALL MUL(NRO,BB,CC,DD,A)

103 FORMAT(5(2F8.0))

7 CONTINUE

C

C THE DIFFERENT FILES ARE READ IN. EACH BLOCK  
C IS CHARACTERIZED BY THE NUMBER NCONT(FILE 1)  
C AND NC(FILE 2-4). IF NCONT IS THE SAME AS  
C NC, THE SAME ROTATION IS PERFORMED ON THAT  
C PARTICULAR BLOCK(FILE 2-4) AS THE ROTATION FOR THE  
C CORRESPONDING BLOCK IN FILE 1.

C

DO 2 KJ=1,KJU

IF(NF1.NE.0.AND.KJ.EQ.1) GO TO 2

IF(NF1.NE.0.AND.NF(KJ).NE.KJ) GO TO 2

IN=KJ

NOUT=KJ+10

C

C ANGLE OF ROTATION ZERO IMPLIES OUTPUT OF  
C DATA WITHOUT ROTATION.

C

IF(KJ.EQ.1.AND.D(1).EQ.0.) GO TO 5

IF(KJ.EQ.1) GO TO 13

READ(IN,101,END=2)N,NC,TEXT

IF(NC.EQ.NCONT) GO TO 14

BACKSPACE IN

GO TO 2

14 READ(IN,103)(LAT(I),LON(I),I=1,N)

IF(D(1).EQ.0.) GO TO 5

13 CONTINUE

C

C TRANSFORMATION OF COORDINATES.

C

DO 1 I=1,N

1 CALL ROT(LAT(I),LCN(I),A)

5 CONTINUE

WRITE(NOUT,101)N,NCONT,(TEXT(I),I=1,6)

WRITE(NOUT,201)((LAT(I),LON(I)),I=1,N)

201 FORMAT(5(2F8.2))

2 CONTINUE

STOP

END



```

C
C CALCULATION OF THE RESULTANT EULER ROTATION FROM
C UP TO 10 DIFFERENT EULER ROTATIONS (LAT,LON,ROT)
C LATITUDE AND LONGITUDE (DEGREES, POSITIVE NORTH
C AND EAST) AND ANGLE OF ROTATION (POSITIVE ANTICLOCK-
C WISE) .
      DIMENSION A(3,3),B(3,3),C(3,3),U(3,3),R(20,30,3,3),TEXT(5)
      REAL LAT(10),LON(10),ROT(10),LLAT,LLON
C
C NFILE: NUMBER OF DIFFERENT FILES CONTAINING AT SET
C OF ROTATIONS FOR DIFFERENT CONTINENTAL
C SEGMENTS.
C
      READ(5,100) NFILE
      DO 10 I=1,3
      DO 10 J=1,3
      IF(I.EQ.J) U(I,J)=1.
      IF(I.NE.J) U(I,J)=0.
10  CONTINUE
      DO 1 K=1,NFILE
      MMM=0
      NF=10 + K
C
C NF: INPUT OF ROTATIONS FROM A FILE CONNECTED TO NF.
C
      READ(NF,100) N
      DO 1 J=1,N
C
C M: NOT USED IN THIS PROGRAM, BUT USED IN ROTATING
C THE CONTINENTAL SEGMENTS.
C NROT: NUMBER OF ROTATIONS FOR ANY ONE CONTINENTAL
C SEGMENT.
C
      READ(NF,101) LAT(1),LON(1),ROT(1),M,NROT
      IF(NROT.EQ.0) NROT=1
      IF(M.EQ.0) M=1
      MM=MMM+1
      MMM=M+MM-1
      BACKSPACE NF
      READ(NF,103) (LAT(I),LON(I),ROT(I),I=1,NROT)
C
C MUL COMBINES UP TO 10 DIFFERENT EULER ROTATIONS TO ONE.
C
      CALL MUL(NROT,LAT,LCN,ROT,A)
      DO 1 I=MM,MMM
      DO 1 L=1,3
      DO 1 LL=1,3
      R(K,I,L,LI)=A(L,LL)
1  CONTINUE
      WRITE(7,100) MMM
      DO 2 I=1,MMM
      CALL MATRIX(B,U,U)
      DO 3 K=1,NFILE
      DO 4 L=1,3

```





```

      DO 4 LL=1,3
      C(L,LL)=R(K,I,L,LL)
4      CONTINUE
      CALL MATRIX(A,C,B)
      CALL MATRIX(B,A,U)
3      CONTINUE
C
C      INVEUL CALCUTES (LAT,LON,ROT) FROM THE RESULTANT
C      TRANSFORMATION MATRIX.
C
      CALL INVEUL(B,LLAT,LLON,RROT)
C
C      TEXT CONTAINS THE NAMES OF THE CONTINENTAL SEGMENTS
C
      READ(1,102) (TEXT(J),J=1,5)
C
C      OUTPUT OF THE FINAL EULER ROTATIONS, IN FILE 6
C      WITH THE CORRESPONDING NAMES FOR THE CONTINENTAL
C      SEGMENTS, AND IN 7 IN A FORMAT SUITABLE FOR
C      PERFORMING ROTATIONS OF CONTINENTAL SEGMENTS
C      USING THE ROTATION PROGRAM.
C
      WRITE(6,200) (TEXT(J),J=1,5),LLAT,LLON,RROT
      WRITE(7,201) LLAT,LLON,RROT
2      CONTINUE
100     FORMAT(16I5)
101     FORMAT(3F10.0,2I10)
102     FORMAT(5A4)
103     FORMAT(3F10.0)
200     FORMAT(5A4,5X,3F10.2)
201     FORMAT(3F10.2)
      STOP
      END

```



C  
C CALCULATION OF THE SUM OF THE SQUARES OF THE MOVEMENTS  
C OF POINTS ON A SPHERE FROM ONE GEOLOGICAL PERIOD TO  
C ANOTHER. IT IS ASSUMED THAT THE MOVEMENT IS PERFORMED  
C AS AN EULER ROTATION, THUS GOING ALONG THE SMALLEST POSSIBLE  
C DISTANCE AS MEASURED ALONG A SMALL CIRCLE.

C  
C REAL LXAT(15,200),LXON(15,200)  
C REAL LAT1(100),LON1(100),ROT1(100),LAT2(100),LON2(100)  
C DIMENSION ROT2(100)  
C DIMENSION A(3,3),NC(15),D(50),DX(50)  
C DIMENSION SMIN(50),SLMIN(50),SLOMIN(50)  
C DIMENSION SMAX(50),SLMAX(50),SLOMAX(50)  
C DIMENSION CLMAX(15),CLOMAX(15),CLMIN(15),CLOMIN(15),  
C \*CX(15),CY(15),CZ(15)  
C REAL LAND(25,5),LAT(15),LON(15),ROS(15)  
C REAL MAXD(15),MIND(15)  
C DIMENSION NN(25),XLAT(15),XLON(15),XROT(15),N1(25)  
C DATA NN/3\*1,5\*0,2\*1,4\*0,4\*1,4\*0,1,0,1/  
C READ(4,105)((LAND(I,J),J=1,5),I=1,25)  
105 FORMAT(5A4)  
C READ(5,102) XMIL

C  
C XMIL: NUMBER OF MILLION YEARS BETWEEN THE TWO  
C GEOLOGICAL PERIODS. DEFAULT IS ONE HUNDRED.

C  
C IF(XMIL.EQ.0.) XMIL=100.  
C WRITE(6,210) XMIL  
210 FORMAT(/,'TIMESPAN IS',F6.0,2X,'MILL. YEARS',/)

C  
C NC: CODE NUMBERS FOR THE CONTINENTAL SEGMENTS.  
C CALCULATIONS ARE ONLY PERFORMED FOR THE SEGMENT WHICH  
C HAVE THE CORRECT NUMBER. 11 NUMBERS MUST BE READ IN.  
C THE CODES ARE: 1: NORTH AMERICA  
C 2: KOLYMA  
C 3: EUROPE  
C 4: GREENLAND  
C 5: ASIA  
C 6: SOUTH AMERICA  
C 7: ANTARTICA  
C 8: AFRICA  
C 9: AUSTRALIA  
C 10: MADAGASCAR  
C 11: INDIA

C  
C READ(5,100)(NC(I),I=1,11)

C  
C 1: INPUT EULER ANGLES AND POLES OF ROTATION FOR PERIOD 1,  
C MOVEMENT IS RELATIVE TO 1. THERE ARE 25 DATA SETS.  
C THESE ARE IN ORDER: NORTH AMERICA, KOLYMA, N. EUROPE,  
C CASPIAN, IRELAND, ENGLAND, S. EUROPE, SPAIN, GREENLAND,  
C ASIA(5 ELEMENTS), S. AMERICA, ANTARCTICA, AFRICA,  
C AUSTRALIA, NEW GUINEA, N. CALEDONIA, NEW ZEALAND(2  
C ELEMENTS), MADAGASCAR, ARABIA, INDIA.



```

C
C 2: INPUT OF EULER ANGLES AND ANGLES OF ROTATION FOR PERIOD 2.
C
C ALL ROTATIONS ARE FROM THE PRESENT.
C
      READ(1,102) (LAT1(I),LON1(I),ROT1(I),I=1,25)
      READ(2,102) (LAT2(I),LON2(I),ROT2(I),I=1,25)
102  FORMAT(3F10.2)
      L=0
C
C CALCULATION OF EULER ANGLES AND ANGLE OF ROTATION
C FROM PERIOD 1 TO 2.
C
      DO 20 I=1,25
      IF(NN(I).NE.1) GO TO 20
      L=L+1
      NN(L)=I
      LAT1(L)=LAT1(I)
      LON1(L)=LON1(I)
      ROT1(L)=-ROT1(I)
      LAT2(L)=LAT2(I)
      LON2(L)=LON2(I)
      ROT2(L)=ROT2(I)
20   CONTINUE
      DO 25 J=1,11
C
C INPUT OF THE COORDIANATES(LATITUDE(+NORTH),LONGITUDE(+EAST))
C FOR THE POINTS TO BE ROTATED.
C N1: THE NUMBER OF POINTS IN EACH CONTINENTAL SEGMENT.
C LXAT,LXON: THE LATITUDES AND LONGITUDES
C
      READ(3,100) N1(J)
      N=N1(J)
      READ(3,101) (LXAT(J,I),LXON(J,I),I=1,N)
25   CONTINUE
      DO 30 J=1,11
      XLAT(1)=LAT1(J)
      XLON(1)=LON1(J)
      XROT(1)=ROT1(J)
      XLAT(2)=LAT2(J)
      XLON(2)=LON2(J)
      XROT(2)=ROT2(J)
      N=2
C
C MUL CALCULATES THE RESULTANT ROTATION FOR SEVERAL
C EULER ROTATIONS.
C
      CALL MUL(N,XLAT,XLON,XROT,A)
      LAT(J)=XLAT(10)
      LON(J)=XLON(10)
      ROS(J)=XROT(10)
30   CONTINUE
C
C ONLY COORDINATES BLOCKS WITH NC(I)=I,I=1,11 ARE

```



```

C   USED IN THE CALCULATIONS.
C
C       DO 35 J=1,11
C
C   ROTATION OF PRESENT COORDINATES TO PERIOD 1.
C
C       IF(J.NE.NC(J)) GO TO 35
C       X=LAT1(J)
C       Y=LON1(J)
C       Z=-ROT1(J)
C       CALL EUL(X,Y,Z,A)
C       N=N1(J)
C       DO 36 I=1,N
C       CALL ROT(LXAT(J,I),LXON(J,I),A)
36  CONTINUE
35  CONTINUE
100  FORMAT(16I5)
101  FORMAT(10F8.2)
C
C   INPUT OF PARAMETERS TC MOVE PERIOD 2 HORIZONTALY
C   RELATIVE TO PERIOD 1.
C   SU TO SL IS THE LONGITUDE(DEGREES) RANGE OF MOVEMENT
C   AND SDEL IS THE INCREMENT.
C
C
C       READ(5,101) SL,SU,SDEL
C       M=(SU-SL)/SDEL+1
C
C   CALCULATION OF SUM OF SQUARES OF MOVEMENTS FROM
C   PERIOD 1 TO 2 ALONG SMALL CIRCELS.
C
C       DO 1 K=1,M
C       D(K)=0
C       SMAX(K)=0.0
C       SMIN(K)=100000.
C       DX(K)=SL+SDEL*(K-1)
C       DO 17 KJ=1,11
C       IF(NC(KJ).NE.KJ) GO TO 17
C       IF(M.NE.1) GO TO 18
C       SMAX(K)=0.0
C       SMIN(K)=100000.
18  CONTINUE
C       CALL SCIR(LAT(KJ),LCN(KJ),RCS(KJ),X,Y,Z,DX(K))
C       I2=N1(KJ)
C       DO 2 L=1,I2
C       CALL LCIR(X,Y,Z,LXAT(KJ,L),LXON(KJ,L),DIST)
C       IF(DIST.LT.SMAX(K)) GO TO 5
C
C   MAX AND MIN VALUES ARE STORED.
C
C       SLMAX(K)=LXAT(KJ,L)
C       SLOMAX(K)=LXON(KJ,L)
C       SMAX(K)=DIST
5  CONTINUE

```





```

      IF(DIST.GT.SMIN(K)) GO TO 2
      SLMIN(K)=LXAT(KJ,L)
      SLOMIN(K)=LXON(KJ,L)
      SMIN(K)=DIST
2     D(K)=D(K)+DIST**2
      IF(M.NE.1) GO TO 17
      CLMAX(KJ)=SLMAX(1)
      CLOMAX(KJ)=SLOMAX(1)
      CLMIN(KJ)=SLMIN(1)
      CLOMIN(KJ)=SLOMIN(1)
      CX(KJ)=X
      CY(KJ)=Y
      CZ(KJ)=Z
      MAXD(KJ)=SMAX(1)*(11.2/XMIL)
      MIND(KJ)=SMIN(1)*(11.2/XMIL)
17    CONTINUE
1     CONTINUE
      IF(M.EQ.1) GO TO 80
      DMAX=0
C
C     CONVERSION OF DISTANCE FROM DEGREES TO CM/Y
C     ASSUMING A TIME SPAN CF XMIL MIL YEARS FROM
C     PERIOD 1 TO 2.
C
      DO 3 I=1,M
      SMAX(I)=SMAX(I)*(11.12/XMIL)
      SMIN(I)=SMIN(I)*(11.12/XMIL)
3     IF(D(I).GT.DMAX) DMAX=D(I)
      DO 4 I=1,M
4     D(I)=D(I)/DMAX
      WRITE(6,200)
      WRITE(6,201) (DX(I),D(I),SMAX(I),SLMAX(I),SLOMAX(I),
      *SMIN(I),SLMIN(I),SLOMIN(I),I=1,M)
200    FORMAT(/,'PARR. MOVE. DIST. SUM MAX MOVE. ',
      *' LAT LON MIN MOVE LAT LON')
201    FORMAT(1X,F7.1,7X,F6.4,5X,F6.2,1X,2F9.1,3X,F6.2,F7.1,F9.1)
80    CONTINUE
C
C     IF CALCULATIONS ARE MADE FOR A RANGE OF LONGITUDES
C     THE PROGRAM STOPS HERE. IF CALCULATIONS ARE ONLY
C     PERFORMED FOR ONE RELATIVE POSITION OF THE
C     CONTINENTS IN THE TWO PERIODS (THE ONE GIVING
C     THE MINIMUM IN THE SQUARE OF THE DISTANCES, IF
C     POSSIBLE), NEXT STEP IS TO CALCULATE THE MINIMUM
C     AND MAXIMUM VELOCITY VECTORS.
C
      IF(M.NE.1) STOP
C
C     CALCULATION OF COORDINATES OF TRACES OF MAX AND
C     MIN MOVEMENT FOR CONTINENTS CHOSEN BY NC(I).
C
      WRITE(6,202)
202    FORMAT(' CONTINENT MAX MOVE LAT LON ',
      *'MIN MOVE LAT LON ')

```



```

DO 75 I=1,11
  IF(NC(I).NE.I) GO TO 75
  WRITE(6,203) (LAND(NN(I),J),J=1,5),MAXD(I),CLMAX(I),
*CLOMAX(I),MIND(I),CLMIN(I),CLOMIN(I)
75  CONTINUE
203  FORMAT(5A4,6F8.1)
DO 60 KJ=1,11
  IF(NC(KJ).NE.KJ) GO TO 60
  ND=MAXD(KJ)*XMIL/10.+1.5
  IF(ND.EQ.1) ND=2
  DO 50 J=1,ND
    X1=CX(KJ)
    Y1=CY(KJ)
    Z1=(CZ(KJ)/(ND-1))*FLOAT(J-1)
    CALL EUL(X1,Y1,Z1,A)
    XX=CLMAX(KJ)
    YY=CLOMAX(KJ)
    CALL ROT(XX,YY,A)
    LAT1(J)=XX
    LON1(J)=YY
50  CONTINUE
    LL=75
C
C  OUTPUT OF POINTS DEFINING THE VELOCITY VECTORS.
C
  WRITE(7,100) ND,LL
  WRITE(7,101) (LAT1(I),LON1(I),I=1,ND)
  ND=MIND(KJ)*XMIL/10.+1.5
  IF(ND.EQ.1) ND=2
  DO 55 J=1,ND
    X1=CX(KJ)
    Y1=CY(KJ)
    XX=CLMIN(KJ)
    YY=CLOMIN(KJ)
    Z1=(CZ(KJ)/(ND-1))*FLOAT(J-1)
    CALL EUL(X1,Y1,Z1,A)
    CALL ROT(XX,YY,A)
    LAT2(J)=XX
    LON2(J)=YY
55  CONTINUE
  WRITE(7,100) ND,LL
  WRITE(7,101) (LAT2(I),LON2(I),I=1,ND)
60  CONTINUE
  STOP
  END

```



```

C
C  CALCULATION OF THE POINTS OF A CIRCLE ON THE
C  SURFACE OF THE EARTH GIVEN THE RADIUS AND THE
C  CENTER. THE PROGRAM IS USED FOR CALCULATING ERROR CIRCLES
C  AROUND PALEOMAGNETIC POLES. THE FILE WITH THE UNROTATED
C  POLES (LAT, LON) (POSITIVE NORTH AND EAST) ALSO CONTAINS
C  THE RADIUS OF THE ERROR CIRCLE R (DEGREES). THE ACTUAL
C  ROTATED POLES ARE READ FROM A SECOND FILE.
C
    DIMENSION T(10), X(100), Y(100)
    REAL LAT(10), LON(10), R(10)
    CON=57.29577951
    M=0
    NP=40
5  CONTINUE
    READ(1,102,END=1) N, (T(I), I=1,10)
C
C  1: COORDINATES OF THE ROTATED POLES OF OF A CONTINENTAL
C  SEGMENT. N: NUMBER OF POLES IN EACH SEGMENT; T:
C  TITLE.
C
    READ(5,100) KZX
C
C  5: COORDINATES OF THE UNROTATED POLES (NOT USED) AND
C  THE RADIUS (DEGREES) OF THE CIRCLE.
C
    READ(5,101) (LAT(I), LON(I), R(I), I=1, N)
    READ(1,101) (LAT(I), LON(I), I=1, N)
    DO 2 K=1, N
    LAT(K)=LAT(K)/CON
    LON(K)=LON(K)/CON
    R(K)=R(K)/CON
C
C  CALCULATION OF THE POINTS OF THE CIRCLE. NP=40
C  POINTS IS USED.
C
    CALL CIRCLE(NP, R(K), LAT(K), LON(K), X, Y)
    DO 3 L=1, NP
    X(L)=X(L)*CON
    Y(L)=Y(L)*CON
3  WRITE(2,102) NP, (T(I), I=1,10)
C
C  2: OUTPUT FILE FOR THE COORDINATES OF THE POINTS
C  OF THE CIRCLE.
C
    WRITE(2,101) (X(I), Y(I), I=1, NP)
    2  M=M+1
    GO TO 5
    1  CONTINUE
C
C  M: THE NUMBER OF GROUPS OF POLES, NORMALLY
C  THERE IS ONLY 1 IN EACH GROUP.
C
    WRITE(6,200) M

```





```
100  FORMAT(16I5)
101  FORMAT(10F8.2)
102  FORMAT(I5,10A4)
200  FORMAT('NUMBER OF POLES',I5/)
      STOP
      END
```



PROGRAM TO SORT OUT TRAVEL TIME RESIDUALS ACCORDING TO A NUMBER OF SPECIFICATIONS. ALSO SURFACE PROJECTIONS OR PART THEREOF CAN BE CALCULATED. THE INPUTS ARE:

- 1: THE RESIDUALS WITH INFORMATION. COMES AS FOLLOWS:  
 EVENT IDENTIFIER, EVENT NUMBER, STATION, PHASE IDENTIFIER, TRAVEL TIME RESIDUAL AND ERROR. FORMAT  
 5(A4,1X),2F6.0.  
 A BLANK LINE INDICATES END OF DATA.
- 2: STATION LIBRARY. IN THE ORDER: STATION IDENTIFIER, LATITUDE IN DEGREES(POSITIVE NORTH), LONGITUDE IN DEGREES(POSITIVE EAST), ELEVATION IN KM AND STATION LOCATION(NOT NESCESSARY FOR THIS PROGRAM).  
 FORMAT(2X,A4,4X,3F10.3,12A4).  
 A BLANK LINE INDICATES END OF DATA.
- 3: EVENT LIBRARY. IN ORDER: DAY, MONTH, YEAR, HOUR, MINUTE, SECONDS, LATITUDE(POSITIVE NORTH), LONGITUDE(POSITIVE EAST), DEPTH IN KM, MAGNETUDE, COMMENTS, EVENT IDENTIFIER EVENT NUMBER AND COMMENTS.  
 FORMAT(5I3,3F10.3,F4.0,F4.1,6A1,1X,A4,2X,A4,12A4)  
 A BLANK LINE INDICATES END OF DATA.
- 4: FILE FOR OUTPUT, CAN BE SPECIFIED DURING THE RUN OF THE PROGRAM.
- 5: INPUT OF PARAMETERS TO CHOOSE THE RESIDUALS AND SORT THEM OUT. THE PROGRAM IS INTERACTIVE AND WILL ASK QUESTIONS. PARAMETERS CAN BE CHOSEN BY DEFAULT BY INPUTTING BLANKS(A RETURN CHARACTER). ANY PARAMETER IN FILE 1 CAN BE CHOSEN THAT WAY, E.G. IF A BLANK IS GIVEN INSTEAD OF A SERIES OF STATION IDENTIFIERS, ALL STATIONS IN THE FILE WILL BE CONSIDERED.  
 IN THE REST OF THE PROGRAM, BLANKS MEANS THAT THE CORRESPONDING OPTION IS BYPASSED, E.G IF THE QUESTION "DEPTHS ? " IS ANSWERED WITH A BLANK, NO CONSIDERATION IS GIVEN TO THE DEPTHS.
- 6: SELF EXPLANATORY.
- 7: OUTPUT OF THE COORDINATES FOR THE STATIONS, EVENTS AND SURFACE PROJECTIONS OF THE DEEPEST POINTS OF THE RAYS AND POINTS MARKING THE CENTRAL PART OF THE RAY. THE COORDINATES ARE SORTED OUT IN DIFFERENT GROUPS ACCORDING TO THE SIZE OF THE RESIDUALS. EACH GROUP HAVE AS A FIRST LINE THE NUMBER OF POINTS IN THE GROUP, THE SYMBOL NUMBER TO BE USED FOR THE POINT(FOR PLOTTING) AND A TITLE. THE NEXT LINES CONTAIN THE COORDINATES OF THE POINTS.  
 FORMAT(2I5,20A4)  
 FORMAT(10F8.1)



```

C
C 8: COORDINATES OF THE POINTS GIVING THE RAY TRACES.
C   THESE ARE ALSO SORTED OUT LIKE THE POINTS IN FILE
C   7, AND GROUPED ACCORDINGLY. THE FORMAT IS THE
C   SAME AS FOR OUTPUT 7.
C
C 11: IF TRAVEL TIMES HAVE BEEN COMPARED, E.G. THE P
C     WITH THE PCP, THE CORRESPONDING RESIDUALS AND
C     ERRORS CAN BE WRITTEN.
C     FORMAT(4F8.2)
C
C
C
C     DIMENSION D(10),INPUT(5),TIME(500),NST(500),SLAT(500),SLON(500)
C     *DATA2(4,500),NNO(500),HLAT(500),HLON(500),M(10,500),KK(10),
C     *ERR(500),X(100),Y(100)
C     INTEGER PAR(5,100),SIGN(20),EMPTY,ZERO/'      '/,DATA1(5,500),
C     *YES/'YES '/
C     INTEGER OK,OK1,OK2,CK3
C     REAL ZERO1/'      '/
C     DIMENSION TITL1(5),NHVS(10),DEL(500),DEPTH(500),DEP(500)
C     INTEGER PAR1(5,1),PAR2(5,1)
C     DATA NHVS/69,85,83,02,03,00,86,87,88,105/
C
C INPUT OF CHOOSING PARAMETERS
C
C     DO 60 I=1,5
C     DO 60 J=1,100
60    PAR(I,J)=ZERO
C     J=0
C     WRITE(6,231)
231    FORMAT('EVENT ID AND NUMBER ?')
C     1    J=J+1
C     READ(5,100) PAR(1,J),PAR(2,J)
C     IF(PAR(1,J).NE.ZERO) GO TO 1
C     J=0
C     WRITE(6,232)
232    FORMAT('STATIONS ?')
C     31    J=J+1
C     READ(5,100) PAR(3,J)
C     IF(PAR(3,J).NE.ZERO) GO TO 31
C     J=0
C     WRITE(6,233)
233    FORMAT('COMPONENTS ?')
C     32    J=J+1
C     READ(5,100) PAR(4,J)
C     IF(PAR(4,J).NE.ZERO) GO TO 32
C     J=0
C     WRITE(6,234)
234    FORMAT('PHASES ?')
C     33    J=J+1
C     READ(5,100) PAR(5,J)
C     IF(PAR(5,J).NE.ZERO) GO TO 33
C

```



```

C
C      NT=1
      XA=0.0
      NREAD=0
C
C      NT: NO OF RESIDUALS CHOSEN.
C
      WRITE(6,251)
251  FORMAT('ERROR AND ANOMALY RANGE EXCLUDED')
      READ(5,106) TO, AMIN, AMAX
      IF(TO.EQ.0.) TO=10.
2    READ(1,100) (INPUT(I), I=1,5), DELT, ER
      IF(INPUT(1).EQ.ZERO) GO TO 4
      CALL LOOK3(PAR, INPUT, OK)
      IF(OK.NE.1) GO TO 2
      IF(ER.GT.TO) GO TO 2
      IF(AMAX.GT.DELT.AND.AMIN.LT.DELT) GO TO 2
      TIME(NT)=DELT
      XA=XA+DELT
      ERR(NT)=ER
      DO 3 I=1,5
3    DATA1(I,NT)=INPUT(I)
      NT=NT+1
      GO TO 2
4    CONTINUE
      NT=NT-1
      XA=XA/NT
      CALL ADIV(NT,XA,TIME,AD)
      WRITE(6,201) NT, XA, AD
201  FORMAT('NUMBER OF RESIDUALS',I5,2X,'AVERAGE',F6.2,
      *2X,'AVERAGE DEVIATION',F5.2)
C
C      COMPARISON OF PARAMETERS. CAN BE DONE EITHER BEFORE
C      DATA HAVE BEEN SELECTED ACCORDING TO DEPTH, DISTANCE,
C      AND GRID OR AFTER. IN THE LATTER CASE, NPR MUST BE
C      SET EQUAL TO 'ZERO' IN THE FIRST RUN.
C
      NCOMP=0
28   CONTINUE
      A1=0.0
      A2=0.0
      NCOMP=NCOMP+1
      WRITE(6,255)
255  FORMAT('INPUT OF COMPARATIVE PARAMETERS COMP, PHASE/COR, LIM ?')
      READ(5,107) NPP, NPR
      IF(NPR.EQ.ZERO) GO TO 1012
      NCOMP=NCOMP+1
      READ(5,108) XCOR, XLIM
C
C      NPP: COMPONENT E.G. SPEW.
C      NPR: PHASE E.G. SCS
C      XCOR: CORRELATION COEFFICIENT.
C      XLIM: ACCEPTED ERROR IN CORRELATION EXCLUDING

```





```

C          READING ERRORS;H.
C
WRITE(6,218) PAR(4,1),PAR(5,1),NPP,NPR
WRITE(6,277)
277  FORMAT('OUTPUT UNIT ?')
READ(5,105) IL
NNEW=0
REWIND 1
DO 70 K=1,NT
NBLOCK=0
OK3=0
DO 71 J=1,5
PAR2(J,1)=DATA1(J,K)
71  PAR1(J,1)=DATA1(J,K)
PAR1(4,1)=ZERO
PAR1(5,1)=ZERO
IF(NPP.NE.ZERO) PAR2(4,1)=NPP
PAR2(5,1)=NPR
72  READ(1,100) (INPUT(I),I=1,5),DELT,ER
IF(INPUT(1).EQ.ZERO) GO TO 76
CALL LOOK(1,PAR1,INPUT,OK1)
CALL LOOK(1,PAR2,INPUT,OK2)
IF(OK3.NE.1) GOTO 75
IF(OK1.EQ.1) GO TO 74
NBLOCK=NBLOCK+1
DO 77 KB=1,NBLOCK
77  BACKSPACE 1
GO TO 70
75  IF(OK1.NE.1) GO TO 72
OK3=1
74  NBLOCK=NBLOCK+1
IF(OK2.NE.1) GO TO 72
IF(ABS(TIME(K-XCOR*DELT).GE.(XLIM+ER+ERR(K))) GO TO 70
IF(IL.NE.0) WRITE(IL,219) (DATA1(I,K),I=1,5), (INPUT(L),L=4,5)
*,TIME(K),ERR(K),DELT,ER
A1=A1+DELT
A2=A2+TIME(K)
WRITE(11,221) TIME(K),ERR(K),DELT,ER
221  FORMAT(4F8.2)
NNEW=NNEW+1
TIME(NNEW)=TIME(K)
ERR(NNEW)=ERR(K)
DO 80 I=1,5
80  DATA1(I,NNEW)=DATA1(I,K)
70  CONTINUE
76  CONTINUE
NT=NNEW
WRITE(6,257) NT
220  FORMAT('INPUT OF COORDIANTES, YES OR NO ?')
C
C  CALCULATION OF AVERAGE RESIDUAL
C
A1=A1/NT
A2=A2/NT

```



```

WRITE(6,223) PAR(5,1),A2,NPR,A1
223  FORMAT(' AVERAGE RESIDUAL FOR ',A4,F5.2,1X,' AND ',A4,F5.2)
1012 CONTINUE
      IF(NREAD.NE.0) GO TO 29
      WRITE(6,220)
      READ(5,104) NO
      IF(NO.NE.YES) STOP
      NREAD=1
      NS=1

C
C  NS: NO OF STATIONS.
C  INPUT OF STATION LIBRARY.
C
5      READ(2,102) NST(NS),SLAT(NS),SLON(NS)
      IF(NST(NS).EQ.ZERO) GO TO 6
      NS=NS+1
      GO TO 5
6      NS=NS-1
      WRITE(6,202) NS

C
C  CHOISE OF STATIONS
C
      DO 8 I=1,NT
      CALL LOOK1(NS,DATA1(3,I),NST,INDEX)
      IF(INDEX.EQ.0) GO TO 7
      DATA2(1,I)=SLAT(INDEX)
      DATA2(2,I)=SLON(INDEX)
      GO TO 8
7      DATA2(1,I)=99.
      WRITE(6,203) DATA1(3,I)
8      CONTINUE

C
C  INPUT OF EVENT LIBRARY.
C
      NE=1

C
C  NE: NO OF EVENTS.
C
9      READ(3,103) SLAT(NE),SLON(NE),DEP(NE),NST(NE),NNO(NE)
      IF(NST(NE).EQ.ZERO) GO TO 10
      NE=NE+1
      GO TO 9
10     NE=NE-1
      WRITE(6,204) NE

C
C  CHOISE OF EVENTS
C
      DO 12 I=1,NT
      CALL LOOK2(NE,DATA1(1,I),DATA1(2,I),NST,NNO,INDEX)
      IF(INDEX.EQ.0) GO TO 11
      DEPTH(I)=DEP(INDEX)
      DATA2(3,I)=SLAT(INDEX)
      DATA2(4,I)=SLON(INDEX)
      GO TO 12

```



```

11  DATA2(3,I)=99.
    WRITE(6,205) DATA1(1,I),DATA1(2,I)
12  CONTINUE
C
C  SORTING OUT RESIDUALS FOR WHICH COORDINATES WERE
C  NOT FOUND.
C
    J=0
    DO 52 I=1,NT
    IF (DATA2(1,I).EQ.99.0.OR.DATA2(3,I).EQ.99.9) GO TO 52
    J=J+1
    TIME(J)=TIME(I)
    ERR(J)=ERR(I)
    DO 53 K=1,4
53  DATA2(K,J)=DATA2(K,I)
    DO 54 K=1,5
54  DATA1(K,J)=DATA1(K,I)
52  CONTINUE
    NT=J
    WRITE(6,252)
252 FORMAT('OUTPUT OF STATION, MIDPOINT OR EVENT COORDINATES , ',
*'YES OR NO ?')
C
C  CHOISE OF OUTPUT COORDINATES: IF YES IS INPUT, THE CORRESPONDING
C  COORDINATES ARE WRITTEN OUT. THE PARAMETERS ARE:
C  NEV: EVENTS.
C  NHA: POINT MIDWAY BETWEEN EVENT AND STATION.
C  NSTA: STATION
C
    READ(5,104) NSTA,NHA,NEV
    IF(NSTA.EQ.YES) WRITE(6,213)
    IF(NHA.EQ.YES) WRITE(6,214)
    IF(NEV.EQ.YES) WRITE(6,215)
    DO 13 I=1,NT
    CALL DIV(1,1,DATA2(1,I),DATA2(2,I),DATA2(3,I),DATA2(4,I),X,Y)
    HLAT(I)=X(1)
    HLON(I)=Y(1)
13  CONTINUE
C
C  SELECTING DATA HAVING DEEPEST POINT OF RAY IN
C  A LAT LON SQUARE X1,X2 AND Y1,Y2.
C
C  CHOISE OF DATA IN DEPTH RANGE H1 TO H2.
C
C  CHOISE OF DATA IN DISTANCE RANGE D1 TO D2
C
    WRITE(6,261)
261  FORMAT('DEPTH RANGE?')
    READ(5,106) H1,H2
    WRITE(6,262)
262  FORMAT('DISTANCE RANGE?')
    READ(5,106) D1,D2
    NT1=0
    WRITE(6,237)

```





```

237  FORMAT('GRID?')
      READ(5,212) X1,X2,Y1,Y2
      DO 73 I=1,NT
      IF((X1+X2).EQ.0.) GO TO 41
      IF(HLAT(I).GE.X1.AND.HLAT(I).LT.X2.AND.HLON(I).
*GE.Y1.AND.HLON(I).LT.Y2) GO TO 41
      GO TO 73
41   CONTINUE
      IF((H1+H2).EQ.0.0) GO TO 42
      IF(DEPTH(I).GE.H1.AND.DEPTH(I).LT.H2) GO TO 42
      GO TO 73
42   CONTINUE
      CALL DELAZG(DATA2(1,I),DATA2(2,I),DATA2(3,I),DATA2(4,I),AD,DUM
      IF((D1+D2).EQ.0.) GO TO 43
      IF(AD.GE.D1.AND.AD.LT.D2) GO TO 43
      GO TO 73
43   CONTINUE
      NT1=NT1+1
      HLAT(NT1)=HLAT(I)
      HLON(NT1)=HLON(I)
      DO 78 K=1,4
78   DATA2(K,NT1)=DATA2(K,I)
      DO 79 K=1,5
79   DATA1(K,NT1)=DATA1(K,I)
      TIME(NT1)=TIME(I)
      ERR(NT1)=ERR(I)
      DEPTH(NT1)=DEPTH(I)
      DEL(NT1)=AD
73   CONTINUE
      NT=NT1
      WRITE(6,257) NT
257  FORMAT('NUMBER OF RESIDUALS ARE NOW',I5)
61   CONTINUE
14   CONTINUE
C    CALCULATION OF AVERAGE RESIDUAL.
C
      XX=0.
C
      DO 15 I=1,NT
15   XX=XX+TIME(I)/NT
      CALL ADIV(NT,XX,TIME,AD)
      WRITE(6,207) XX,AD
      IF(NCOMP.EQ.1) GO TO 28
29   CONTINUE
C
C    CALCULATION OF SURFACE RAY TRACES
C
      IF(NO.NE.YES) GO TO 69
      WRITE(6,235)
235  FORMAT('RAY TRACES?')
      READ(5,100) NTR
      IF(NTR.NE.YES) GO TO 65
      I=100
      DO 66 L=1,NT

```



```

CALL DIV(I,1,DATA2(1,L),DATA2(2,L),DATA2(3,L),DATA2(4,L),X,Y)
WRITE(8,105) I
WRITE(8,212) (X(IJ),Y(IJ),IJ=1,100)
66  CONTINUE
65  CONTINUE

```

```

C
C  THE CHOSEN DATA IS WRITTEN OUT
C

```

```

WRITE(6,253)
253  FORMAT('OUTPUT UNIT ?')
READ(5,105) IL
IF(IL.EQ.0) GO TO 55
WRITE(IL,216)
DO 16 J=1,NT
IDEPTH=DEPTH(J)
16  WRITE(IL,208) (DATA1(I,J),I=1,5), (DATA2(K,J),K=1,4), HLAT(J), HLON
*,DEL(J), IDEPTH, TIME(J), ERR(J)
55  CONTINUE

```

```

C
C  INPUT OF SORTING BOUNDARIES
C

```

```

WRITE(6,254)
254  FORMAT('INPUT OF SORTING BOUNDARIES, HOW MANY ?')
READ(5,105) NSYM
IF(NSYM.EQ.0) GO TO 69
WRITE(6,209)
209  FORMAT('SORTING BOUNDARIES, SMALLEST ONE FIRST ?')
READ(5,106) (D(I),I=1,NSYM)
D(NSYM+1)=10.

```

```

C
C  CORRECTING THE RESIDUALS FOR ERRORS, SO THE RESIDUALS
C  ARE CENTERED AROUND THE MIDDLE TWO SORTING BOUNDARIES.
C

```

```

DO 81 I=1,NT
IF(ERR(I).EQ.0.0) GO TO 81
IF(TIME(I).LT.D(NSYM/2)) TIME(I)=TIME(I)+ERR(I)
IF(TIME(I).GT.D(NSYM/2+1)) TIME(I)=TIME(I)-ERR(I)
81  CONTINUE
DO 17 J=1,10
KK(J)=0
DO 17 I=1,500
17  M(J,I)=0

```

```

C
C  SORTING OF THE RESIDUALS
C

```

```

NSYM=NSYM+1
CALL SORT(NSYM,NT,D,TIME,M,KK)
WRITE(6,211) (KK(I),I=1,NSYM)
N1=1
WRITE(6,306)

```

```

C
C  INPUT OF TITLE
C

```

```

306  FORMAT('TITLE?')

```



```

      READ (5,150) TITL1
150  FORMAT (A4,4A4)
C
C  CALCULATION OF CENTRAL POINTS OF A PARTIAL RAYTRACE.
C
      WRITE (6,110)
110  FORMAT ('CENTRAL RAY POINTS, HOW MANY DEGREES ?')
      READ (5,106) RPOINT
      IF (RPOINT.EQ.0.0) GO TO 67
      DO 85 I=1,NSYM
      K1=KK(I)
      IF (K1.EQ.0) GO TO 85
      DO 68 J=1,K1
      JJ=M(I,J)
C
C  40 POINTS IS USED FOR THE ENTIRE RAY.
C
      NPOINT=40
      CALL DIV (NPOINT,1,DATA2(1,JJ),DATA2(2,JJ),DATA2(3,JJ),
*DATA2(4,JJ),X,Y)
      FRAC=(RPOINT/DEL(JJ))
      ISIDE=40.*(1.-FRAC)/2.
      ICEN=40-2*ISIDE
      I1=ISIDE+1
      I2=ISIDE+ICEN
      WRITE (7,301) ICEN,NHVS(I+3),D(I),TITL1
      WRITE (7,212) (X(IJ),Y(IJ),IJ=I1,I2)
68  CONTINUE
85  CONTINUE
67  CONTINUE
      IF (NEV.NE.YES) GO TO 20
C
C  SORTING OF EVENT COORDINATES.
C
300  FORMAT (2I5,'EV. UPPER LIMIT',F5.1,1X,5A4)
301  FORMAT (2I5,'HV. UPPER LIMIT',F5.1,1X,5A4)
302  FORMAT (2I5,'ST. UPPER LIMIT',F5.1,1X,5A4)
      DO 19 I=1,NSYM
      K1=KK(I)
      IF (K1.EQ.0) GO TO 19
      WRITE (7,300) K1,I,D(I),TITL1
      DO 18 J=1,K1
      JJ=M(I,J)
      SLAT(J)=DATA2(3,JJ)
18  SLON(J)=DATA2(4,JJ)
      WRITE (7,212) (SLAT(L),SLON(L),L=1,K1)
19  CONTINUE
20  CONTINUE
      IF (NHA.NE.YES) GO TO 23
C
C  SORTING OF HALF DISTANCE COORDINATES
C
      DO 22 I=1,NSYM
      K1=KK(I)

```



```

IF(K1.EQ.0) GO TO 22
WRITE(7,301) K1,NHVS(I+3),D(I),TITL1
DO 21 J=1,K1
  JJ=M(I,J)
  SLAT(J)=HLAT(JJ)
21  SLON(J)=HLON(JJ)
  WRITE(7,212) (SLAT(L),SLON(L),L=1,K1)
22  CONTINUE
23  CONTINUE
  IF(NSTA.NE.YES) GO TO 26

```

C  
C  
C

# SORTING OF STATION CCORDINATES

```

DO 25 I=1,NSYM
  K1=KK(I)
  IF(K1.EQ.0) GO TO 25
  ISM=I+112
  WRITE(7,302) K1,I,D(I),TITL1
  DO 24 J=1,K1
    JJ=M(I,J)
    SLAT(J)=DATA2(1,JJ)
24  SLON(J)=DATA2(2,JJ)
    WRITE(7,212) (SLAT(L),SLON(L),L=1,K1)
25  CONTINUE
26  CONTINUE
69  CONTINUE
241 CONTINUE
100 FORMAT(5(A4,1X),2F6.0)
101 FORMAT(20A4)
102 FORMAT(2X,A4,4X,2F10.0)
103 FORMAT(25X,2F10.0,F4.0,11X,A4,2X,A4)
104 FORMAT(3A4)
105 FORMAT(I5)
106 FORMAT(10F10.0)
107 FORMAT(2(A4,1X))
108 FORMAT(2F5.1)
202 FORMAT('NUMBER OF STATIONS IN LIBRARY',I5)
203 FORMAT('STATION ',A4,' NOT FCUND IN TABLE')
204 FORMAT('NUMBER OF EVENTS IN LIBRARY',I5)
205 FORMAT('EVENT WITH SOURCE ',A4,' AND NUMBER ',A4,' NOT
*FOUND IN LIBRARY'/)
207 FORMAT('AVERAGE RESIDUAL AND AVERAGE DEVIATION',2F5.2)
208 FORMAT(A4,1X,4A4,3(F5.1,1X,F6.1,1X),F5.1,1X,I3,1X,F5.1,1X,F3.1)
211 FORMAT('NUMBER OF NUMBERS IN EACH GROUP',10I5)
212 FORMAT(10F8.2)
213 FORMAT('STATION COORDIANATES ARE OUTPUT')
214 FORMAT('HALFWAY COORDINATES ARE OUTPUT')
215 FORMAT('EVENT COORDINATES ARE OUTPUT')
216 FORMAT(' PARAMETERS',11X,' STLA STLO EVLA EVLO HWLA ',
*'HWLO DIST DEPTH RESI ERR')
218 FORMAT('OUTPUT OF RESIDUALS WITH COMPARETIVE',
*' PARAMETERS',4(2X,A4))
219 FORMAT(7(A4,1X),2(2F8.2,2X))
STOP

```





END



```

C  PROGRAM TO CALCULATE THE DIFFERENCE IN P AND AZIMUTH
C  BETWEEN THE P WAVE AND THE CONVERTED PS WAVE, THE
C  CONVERSION TAKING PLACE AT A DIPPING INTERFACE.
C  IF THE S VELOCITY IN THE SECOND MEDIA IS SET TO ZERO
C  ONLY THE CAHNGE IN THE RAY PARAMETER OF THE P WAVE
C  IS CALCULATED.
C
C

```

```

C      DIMENSION DELP(10),DELAZ(10)
C      DIMENSION D(10)
C      WRITE(6,101)
101  FORMAT('NDIP AND NSTRK ?')
C      READ(5,102)NDIP,NSTRK
102  FORMAT(10I5)
C      WRITE(6,104)
104  FORMAT('P,AZ,VO,V1,VS1 ?')
C
C  NDIP: NUMBER OF DIFFERENT DIP'S, START WITH 0.5 AND
C        INCREASES BY 0.5 DEGREES. MAXIMUM NUMBER IS 10.
C  NSTRK: NUMBER OF DIFFERENT STRIKES USED, THE STRIKES
C         USED WILL BE (360/NSTRK)*I,I=1,NSTRK+1.
C  P: RAY PARAMETER(SEC/DEG) OF THE INCOMING RAY.
C  AZ: AZIMUTH(DEGREES POSITIVE CLOCKWISE FROM THE NORTH)
C      OF THE INCOMING RAY.
C  V: VELOCITY(KM/SEC) OF RAY BEFORE THE INTERFACE.
C  V1 P-VELOCITY OF RAY AFTER THE INTERFACE.
C  VS1: S-VELOCITY OF THE CONVERTED P WAVE AFTER THE
C       INTERFACE.
C

```

```

C      READ(5,100)P,AZ,VO,V1,VS1
100  FORMAT(6F8.2)
C      NP=3

```

```

C
C  IF P IS ZERO, 6 DIFFERENT TABLES WILL BE CALCULATED WITH
C  THE P VALUES 3,4,5,6,7 AND 8.
C  IF P IS NOT ZERO, ONLY ONE TABLE WITH THE P VALUE WILL
C  BE CALCULATED.
C

```

```

C      IF(P.EQ.0.0) NP=8
C      DO 10 KP=3,NP
C      IF(NP.NE.3) P=KP
C      WRITE(6,201)P,AZ,VO,V1,VS1
201  FORMAT('/',1X,'P=',F5.2,2X,'AZ=',F6.1,2X,'V=',F5.2,
C      *2X,'V1=',F5.2,2X,'VS1=',F5.2/)
C      DO 3 IS=1,NDIP
C      D(IS)=0.5*IS
3  CONTINUE
C      WRITE(6,202) (D(I),I=1,NDIP)
202  FORMAT('STRIKE',2X,'DIP=',10(F3.1,9X)/)
C      N1=NSTRK+1
C      DO 2 IAZ=1,N1
C      DO 1 IS=1,NDIP
C      AROT=IS*0.5
C      ALON=(IAZ-1)*(360./NSTRK)

```



```
CALL DIP(P,AZ,V0,V1,AROT,ALON,PP,AZP)
IF(VS1.EQ.0.0) GO TC 5
CALL DIP(P,AZ,V0,VS1,AROT,ALON,PS,AZS)
DELP(IS)=PP-PS
DELAZ(IS)=AZS-AZP
GO TO 1
5  DELP(IS)=P-PP
   DELAZ(IS)=AZ-AZP
1  CONTINUE
   WRITE(6,200) ALON, (DELP(I),DELAZ(I),I=1,NDIP)
200 FORMAT(1X,F5.1,3X,10(F5.2,F5.1,2X))
2  CONTINUE
10 CONTINUE
   STOP
   END
```





## SUBROUTINES

SUBROUTINE ADIV(N,AV,X,AD)

C  
C CALCULATION OF THE AVERAGE DEVIATION AD FOR N  
C DATA POINTS WITH AVERAGE AV AND STORED IN THE  
C ARRAY X.  
C  
C

DIMENSION X(N)

AD=0.0

DO 1 I=1,N

1 AD=AD+ABS(X(I-AV))

AD=AD/N

RETURN

END

SUBROUTINE BNDPAS(F1,F2,DELT,D,G)

C  
C SUBROUTINE BY DAVE GANLEY ON MARCH 5, 1977.  
C

C THE PURPOSE OF THIS SUBROUTINE IS TO DESIGN AND APPLY A  
C RECURSIVE BUTTERWORTH BAND PASS FILTER (KANASEWICH, TIME SERIES  
C ANALYSIS IN GEOPHYSICS, UNIVERSITY OF ALBERTA PRESS, 1975; SHANKS,  
C JOHN L, RECURSION FILTERS FOR DIGITAL PROCESSING, GEOPHYSICS, V32,  
C PP 33-5 1, 1967). IN ORDER TO DESIGN THE FILTER A CALL MUST BE  
C MADE TO BNDPAS AND THEN THE FILTER MAY BE APPLIED BY CALLS TO  
C FILTER. THE FILTER WILL HAVE 8 POLES IN THE S PLANE AND IS  
C APPLIED IN FORWARD AND REVERSE DIRECTIONS SO AS TO HAVE ZERO  
C PHASE SHIFT. THE GAIN AT THE TWO FREQUENCIES SPECIFIED AS  
C CUTOFF FREQUENCIES WILL BE -6DB AND THE ROLLOFF WILL BE ABOUT  
C 96 DB PER OCTAVE. A BILINEAR Z TRANSFORM IS USED IN DESIGNING  
C THE FILTER TO PREVENT ALIASING PROBLEMS.  
C

COMPLEX P(4),S(8),Z1,Z2

DIMENSION D(8),X(1),XC(3),XD(3),XE(3)

DATA ISW/C/,TWOPI/6.2831853/

C  
C THIS SECTION CALCULATES THE FILTER AND MUST BE CALLED BEFORE  
C FILTER IS CALLED  
C

F1 = LOW FREQUENCY CUTO FF (6 DB DOWN)

F2 = HIGH FREQUENCY CUTOFF (6 DB DOWN)

DELT = SAMPLE INTERVAL IN MILLISECONDS

D = WILL CONTAIN 8 Z DOMAIN COEFFICIENTS OF RECURSIVE FILTER

G = WILL CONTAIN THE GAIN OF THE FILTER  
C

DT=DELT/1000.0

TDT=2.0/DT

FDT=4.0/DT



```

ISW=1
P(1)=CMPLX(-.3826834,.9238795)
P(2)=CMPLX(-.3826834,-.9238795)
P(3)=CMPLX(-.9238795,.3826834)
P(4)=CMPLX(-.9238795,-.3826834)
W1=TWOPI*F1
W2=TWOPI*F2
W1=TDT*TAN(W1/TDT)
W2=TDT*TAN(W2/TDT)
HWID=(W2-W1)/2.0
WW=W1*W2
DO 19 I=1,4
Z1=P(I)*HWID
Z2=Z1*Z1-WW
Z2=CSQRT(Z2)
S(I)=Z1+Z2
19 S(I+4)=Z1-Z2
G=.5/HWID
G=G*G
G=G*G
DO 29 I=1,7,2
B=-2.0*REAL(S(I))
Z1=S(I)*S(I+1)
C=REAL(Z1)
A=TDT+B+C/TDT
G=G*A
D(I)=(C*DT-FDT)/A
29 D(I+1)=(A-2.0*B)/A
G=G*G
5 FORMAT ('-FILTER GAIN IS ',E12.6)
RETURN
ENTRY FILTER(X,N,D,G,IG)

C
C X = DATA VECTOR OF LENGTH N CONTAINING DATA TO BE FILTERED
C D = FILTER COEFFICIENTS CALCULATED BY BNDPAS
C G = FILTER GAIN
C IG = 1 MEANS TO REMOVE THE FILTER GAIN SO THAT THE GAIN IS
C UNITY.
C
IF (ISW.EQ.1) GO TO 31
WRITE (6,6)
6 FORMAT ('1BNDPAS MUST BE CALLED BEFORE FILTER')
CALL EXIT

C
C APPLY FILTER IN FORWARD DIRECTION
C
31 XM2=X(1)
XM1=X(2)
XM=X(3)
XC(1)=XM2
XC(2)=XM1-D(1)*XC(1)
XC(3)=XM-XM2-D(1)*XC(2-D(2)*XC(1)
XD(1)=XC(1)
XD(2)=XC(2-D(3)*XD(1)

```



```

XD(3)=XC(3-XC(1-D(3)*XD(2-D(4)*XD(1)
XE(1)=XD(1)
XE(2)=XD(2-D(5)*XE(1)
XE(3)=XD(3-XD(1-D(5)*XE(2-D(6)*XE(1)
X(1)=XE(1)
X(2)=XE(2-D(7)*X(1)
X(3)=XE(3-XE(1-D(7)*X(2-D(8)*X(1)
DO 39 I=4,N
XM2=XM1
XM1=XM
XM=X(I)
K=I-((I-1)/3)*3
GO TO (34,35,36),K
34 M=1
M1=3
M2=2
GO TO 37
35 M=2
M1=1
M2=3
GO TO 37
36 M=3
M1=2
M2=1
37 XC(M)=XM-XM2-D(1)*XC(M1-D(2)*XC(M2)
XD(M)=XC(M-XC(M2-D(3)*XD(M1-D(4)*XD(M2)
XE(M)=XD(M-XD(M2-D(5)*XE(M1-D(6)*XE(M2)
39 X(I)=XE(M-XE(M2-D(7)*X(I-1-D(8)*X(I-2)

```

C  
C  
C

FILTER IN REVERSE DIRECTION

```

XM2=X(N)
XM1=X(N-1)
XM=X(N-2)
XC(1)=XM2
XC(2)=XM1-D(1)*XC(1)
XC(3)=XM-XM2-D(1)*XC(2-D(2)*XC(1)
XD(1)=XC(1)
XD(2)=XC(2-D(3)*XD(1)
XD(3)=XC(3-XC(1-D(3)*XD(2-D(4)*XD(1)
XE(1)=XD(1)
XE(2)=XD(2-D(5)*XE(1)
XE(3)=XD(3-XD(1-D(5)*XE(2-D(6)*XE(1)
X(N)=XE(1)
X(N-1)=XE(2-D(7)*X(1)
X(N-2)=XE(3-XE(1-D(7)*X(2-D(8)*X(1)
DO 49 I=4,N
XM2=XM1
XM1=XM
J=N-I+1
XM=X(J)
K=I-((I-1)/3)*3
GO TO (44,45,46),K
44 M=1

```



```

      M1=3
      M2=2
      GO TO 47
45  M=2
      M1=1
      M2=3
      GO TO 47
46  M=3
      M1=2
      M2=1
47  XC(M)=XM-XM2-D(1)*XC(M1-D(2))*XC(M2)
      XD(M)=XC(M-XC(M2-D(3))*XD(M1-D(4))*XD(M2)
      XE(M)=XD(M-XD(M2-D(5))*XE(M1-D(6))*XE(M2)
49  X(J)=XE(M-XE(M2-D(7))*X(J+1-D(8))*X(J+2)
      IF (IG.NE.1) RETURN
      DO 59 I=1,N
59  X(I)=X(I)/G
      RETURN
      END

```

SUBROUTINE CAZM(N,IREL,LAT,LON,CZ)

SUBROUTINE BY JENS HAVSKOV SPRING 77

CALCULATION OF AZIMUTH CORRECTION DUE TO  
 NON PARRALEL LINES OF LONGITUDE AT  
 ANY POSITION NOT ON THE EQUATOR.  
 LAT,LON ARE THE POSITIONS OF THE POINTS, AND  
 ALL CORRECTIONS ARE CALCULATED RELATIVE TO  
 THE POINT LAT(IREL),LCN(IREL)

```

      REAL CZ(10),LAT(10),LON(10)
      CDN=57.295779
      DO 1 I=1,N
      DEL=LON(I-LON(IREL))
      P=(90.-(LAT(I)+LAT(IREL))/2)/CDN
      CZ(I)=DEL*COS(P)
1  CONTINUE
      RETURN
      END

```

SUBROUTINE CIRCLE(N,R,C1,C2,LAT,LON)

A POINT WITH COORDIANITES (C1,C2) ON A SPHERE IS  
 SURROUNDED WITH N POINTS (LAT,LON) IN A DISTANCE  
 R FROM (C1,C2). ALL CCOORDINATES AND DISTANCES  
 ARE IN RADIANES.









```

C      TH1=2*ARSIN(SIN(DD1/2)/SIN(R1))
      TH2=2*ARSIN(SIN(DD2/2)/SIN(R2))
C
C      CALCULATE X
C
      IF(ABS(TH1).LT.0.005) GO TO 1
      A1=ARCOS(COS(R1)*SIN(TH1))
      X1=ARCOS(COTAN(A1)*COTAN(TH1))
      GO TO 4
1     X1=R1
4     CONTINUE
      IF(ABS(TH2).LT.0.005) GO TO 2
      A2=ARCOS(COS(R2)*SIN(TH2))
      X2=ARCOS(COTAN(A2)*COTAN(TH2))
      GO TO 3
2     X2=R2
3     X=(ABS(R1-R2+X2-X1))*(111.2/RAD)
      R1=R1/RAD
      R2=R2/RAD
      TH1=TH1/RAD
      TH2=TH2/RAD
      RETURN
      END

```

SUBROUTINE DEL(LAT1,LON1,LAT2,LON2,AD)

```

C
C      CALCULATION OF THE DISTANCE IN DEGREES D BETWEEN
C      TWO POINTS ON A SPHERICAL EARTH. THE COORDINATES OF
C      THE TWO POINTS ARE LAT1,LON1 AND LAT2,LON2. ALL
C      ANGLES ARE IN DEGREES.
C

```

```

      REAL LAT1,LON1,LAT2,LON2
      CDN=57.295778
      SL1=LAT1/CDN
      SL2=LAT2/CDN
      OL1=LON1/CDN
      OL2=LON2/CDN
      CON=1.57079
      A=LON2-LON1
      A=ABS(A)
      IF(A.GT.180.) A=360.-A
      A=A/CDN
      CD=CON-SL2
      BD=CON-SL1
      AD=COS(CD)*COS(BD)+SIN(CD)*SIN(BD)*COS(A)
      IF(AD.LT.-1.0.AND.AD.GT.-1.02) AD=-1.0
      IF(AD.GT.1.0.AND.AD.LT.1.02) AD=1.0
      AD=ARCOS(AD)*CDN
      RETURN
      END

```



C SUBROUTINE DEGKM(NN,ELAT,SLAT,DLTA,CDLTA)  
 C CONVERTS DISTANCE IN DEGREES TO DISTANCE IN KMS.

```

    DIMENSION SLAT(200),DLTA(200),CDLTA(200)
    XMJ=6378.4
    XMN=6356.9
    SXMJ=XMJ*XMJ
    SXMN=XMN*XMN
    I=0
101 I=I+1
    IF (I.GT.NN) RETURN
    IF (DLTA(I).GT.10.0) GO TO 100
    DFLAT=ELAT-SLAT(I)
    ALAT=ELAT-DFLAT/2.
    SNLAT=SIN(ALAT)
    SNLAT=SNLAT*SNLAT
    CLAT=COS(ALAT)
    CLAT=CLAT*CLAT
    RDSQ=SXMJ*SXMN/(SXMJ*SNLAT+SXMN*CLAT)
    RAD=SQRT(RDSQ)
    CDLTA(I)=RAD*DLTA(I)/57.295778
    GO TO 101
100 CDLTA(I)=111.2*DLTA(I)
    GO TO 101
  END
```

SUBROUTINE DELAZG(LAT1,LON1,LAT2,LON2,AD,KM,AZ)

C  
 C  
 C SUBROUTINE BY JENS HAVSKOV FEB 77  
 C  
 C CALCULATION OF THE GEOCENTRIC DISTANCES D(DEG), KM(KM) AND  
 C AZIMUTH AZ(DEG) BETWEEN TWO POINTS ON A SPHERICAL EARTH.  
 C THE COORDINATES OF THE TWO POINTS ARE LAT1,LON1 AND LAT2,LON2.  
 C ALL ANGLES ARE IN DEGREES AND AZ IS RELATIVE TO (LAT1,LON1).  
 C

```

  REAL KM,LAT1,LON1,LAT2,LON2
  DIMENSION SL(1),DL(1),CDL(1)
  CDN=57.295778
  SL1=LAT1/CDN
  SL2=LAT2/CDN
  SL1=ATAN(0.993277*TAN(SL1))
  SL2=ATAN(0.993277*TAN(SL2))
  CON=1.5707963
  A=LON2-LON1
  A=ABS(A)
  IF(A.GT.180.) A=360.-A
  A=A/CDN
  CD=CON-SL2
  BD=CON-SL1
  AD=COS(CD)*COS(BD)+SIN(CD)*SIN(BD)*COS(A)
  IF(AD.LT.-1.0.AND.AD.GT.-1.02) AD=-1.0
```





```

      IF(AD.GT.1.0.AND.AD.LT.1.02) AD=1.0
      AD=ARCOS(AD)
      IF(AD.LT.0.000001) GO TO 10
      AZ=(COS(CD-COS(BD)*COS(AD))/(SIN(BD)*SIN(AD))
      IF(AZ.LT.-1.0.AND.AZ.GT.-1.02) AZ=-1.0
      IF(AZ.GT.1.0.AND.AZ.LT.1.02) AZ=1.0
      AZ=ARCOS(AZ)*CDN
      AD=AD*CDN
      DL(1)=AD
      SL(1)=SL1
      N=1
      CALL DEGKM(N,SL2,SL,DL,CDL)
      KM=CDL(1)
      IF(LON2.LT.LON1) AZ=360.-AZ
      GO TO 11
10    AZ=0.
      AD=0.
      KM=0.
11    CONTINUE
      RETURN
      END

C    CALCULATION OF THE CHANGE IN THE RAY PARAMETER P
C    (SEC/DEG), AND AZIMUTH(DEG) AZ A RAY UNDERTAKES BY
C    PASSING A DIPPING INTERFACE. THE INTERFACE STRIKES
C    ALONG A LINE WITH AZIMUTH ALON(DEG), AND THE
C    INTERFACE IS DIPPING DCWN AROT DEGREES IN AZIMUTHAL
C    DIRECTION ALON+90 DEGREES. THE RESULTANT RAY
C    PARAMETER AND AZIMUTH IS PO AND AZO.
C
      SUBROUTINE DIP(P,AZ,V0,V1,AROT,ALCN,PO,AZO)
      DIMENSION A(3,3),B(3,3),P1(3),P2(3),P3(3),P4(3)
      PI=3.1415926535
      CON=PI/180.
      AA0=ARSIN(P*(V0/111.19493))
      AAZ=PI-AZ*CON
      SLON=180.-ALON
      ROT=AROT
      SLAT=0.0

C
C    CALCULATION OF TRANSFORMATION MATRIX.
C
      CALL EUL(SLAT,SLON,ROT,A)

C
C    P1 IS THE SO CALLED RAY VECTOR OF THE INCOMING RAY
C    IN THE BASIC COORDINATE SYSTEM, P2 THE RAY VECTOR IN
C    THE COORDINATE SYSTEM OF THE SLOPING INTERFACE
C    BEFORE TRANSMISSION, P3 AFTER TRNASMISSION AND P4
C    IS THE RAY VECTOR OF THE TRANSMITTED RAY IN THE
C    BASIC COORDINATE SYSTEM.
C    (P1(1),P1(2)) IS THE CONVENTIONAL RAY PARAMETER
C    OF THE INCOMING RAY IN THE BASIC COORDINATE SYSTEM.

```



```

C
      P1(1)=SIN(AA0)*COS(AAZ)/V0
      P1(2)=SIN(AA0)*SIN(AAZ)/V0
      P1(3)=COS(AA0)/V0
      DO 10 I=1,3
10     P2(I)=0.0
      DO 1 J=1,3
      DO 1 I=1,3
1     P2(J)=A(J,I)*P1(I)+P2(J)
      COA0=ABS(P2(3)*V0)
      SOA0=SQRT(1-COA0**2)
      P3(1)=P2(1)
      P3(2)=P2(2)
      COA1=SQRT(1-(SOA0*V1/V0)**2)
      P3(3)=COA1/V1
      DO 2 J=1,3
      DO 2 I=1,3

```

```

C
C   THE INVERSE MATRIX.
C

```

```

2     B(I,J)=A(J,I)
      DO 3 J=1,3
      DO 3 I=1,3
3     P4(J)=B(J,I)*P3(I)+P4(J)
      PO=SQRT(P4(1)**2+P4(2)**2)
      AZO=ATAN2(P4(2),P4(1))
      AZO=AZO/CON
      AZO=180.-AZO
      PO=PO*111.19493
      RETURN
      END

```

```

C   CALCULATION OF COORDINATES (LAT,LON), WHICH ARE BETWEEN
C   BETWEEN THE POINTS WITH COORDINATES (LAT1,LON1) AND
C   (LAT2,LON2). THE POINTS ARE CHOSEN ALONG THE GREAT
C   CIRCLE GIVING THE SHORTEST DISTANCE BETWEEN THE TWO
C   GIVEN POINTS, AND THE DISTANCE IS EQUALLY DIVIDED BY N+1.
C   COORDINATES MUST BE GIVEN AS LAT(+NORTH), LON(+EAST).
C   LATITUDES MUST HAVE VALUES -180 TO +180 OR 0 TO 360,
C   BUT NOT MIXED.
C   COORDINATES ARE IN DEGREES IF M=1, AND IN RADIANS IF M=2.
C
C   IF N EQ 0 ONLY THE DISTANCE IS CALCULATED, THE RESULT
C   BEING IN LAT(1).
C

```

```

      SUBROUTINE DIV(N,M,LAT1,LON1,LAT2,LON2,LAT,LON)
      REAL LAT1,LON1,LAT2,LON2,LAT(100),LON(100)
      NCH=N
      IF(N.EQ.0) N=1
      IF(M.NE.1) GO TO 20
      CDN=57.295778

```



```

LAT1=LAT1/CDN
LAT2=LAT2/CDN
LON1=LON1/CDN
LON2=LON2/CDN
20 CONTINUE
CON=1.57079
A=LON2-LON1
IF (A) 1, 1, 2
1 CD=CON-LAT2
BD=CON-LAT1
Y2=LON1
A=-A
GO TO 7
2 CD=CON-LAT1
BD=CON-LAT2
Y2=LON2
7 CONTINUE
DO 10 I=1,N
IF (SIN (BD).EQ.0.) GO TO 3
IF (SIN (CD).EQ.0.) GO TO 4
AD=COS (CD)*COS (BD)+SIN (CD)*SIN (BD)*COS (A)
IF (AD.LT.-1.0.AND.AE.GT.-1.05) AD=-1.0
IF (AD.GT.1.0.AND.AD.LT.1.05) AD=1.0
AD=ARCOS (AD)
IF (NCH.EQ.0) GO TO 40
ADD=AD*I/(N+1)
C=(COS (CD)-COS (BD)*COS (AD))/(SIN (BD)*SIN (AD))
IF (C.LT.-1.0.AND.C.GT.-1.05) C=-1.0
IF (C.GT.1.0.AND.C.LT.1.05) C=1.0
C=ARCOS (C)
D=COS (BD)*COS (ADD)+SIN (BD)*SIN (ADD)*COS (C)
IF (D.LT.-1.0.AND.D.GT.-1.05) D=-1.0
IF (D.GT.1.0.AND.D.LT.1.05) D=1.0
D=ARCOS (D)
AH=SIN (ADD)*SIN (C)/(SIN (D))
IF (AH.LT.-1.0.AND.AH.GT.-1.05) AH=-1.0
IF (AH.GT.1.0.AND.AH.LT.1.05) AH=1.0
AH=ARSIN (AH)
GO TO 6
3 D=(CD/(N+1))*I
IF (NCH.EQ.0) GO TO 38
GO TO 5
4 D=I*BD/(N+1)
IF (NCH.EQ.0) GO TO 38
5 AH=0.
6 CONTINUE
LAT (I)=CON-D
LON (I)=Y2-AH
IF ((A*CDN).GT.180.) LON (I)=Y2+AH
IF (M.EQ.2) GO TO 10
LAT (I)=LAT (I)*CDN
LON (I)=LON (I)*CDN
10 CONTINUE
GO TO 50

```



```

38     AD=CD
      GO TO 40
39     AD=BD
40     LAT(1)=AD
      IF(M.EQ.1) LAT(1)=LAT(1)*CDN
50     CONTINUE
      IF(M.NE.1) GO TO 30
      LAT1=LAT1*CDN
      LON1=LON1*CDN
      LAT2=LAT2*CDN
      LON2=LON2*CDN
30     CONTINUE
      RETURN
      END

```

# SUBROUTINE ELIP(F,H,DEL,T)

```

C
C  CALCULATION OF THE J-B ELLIPTICITY CORRECTION T, WITH
C  INPUT OF THE J-B FUNCTION F(DEL) (DEL IS EPICENTRAL
C  DISTANCE), AND THE SUM OF THE HEIGHTS H=H0+H1 ABOVE
C  THE MEAN SPHERE. H0 IS THE HEIGH OF THE SOURCE AND
C  H1 OF THE RECIEVER, UNIT: METERS.
C  F(DEL) IS THE VALUES CF F FOR DEL=0,10,20....180.
C

```

```

      DIMENSION F(19)
      DO 1 J=1,19
      DI=FLOAT(J-1)*10
      IF(DEL.GT.DI) GO TO 1
      ELL=F(J-(F(J-F(J-1)))*(DI-DEL)/10
      T=H*ELL
      GO TO 2
1     CONTINUE
2     CONTINUE
      RETURN
      END

```

# SUBROUTINE EUL(B,C,D,A)

```

C
C  CALCULATION OF THE TRANSFORMATION MATRIX A FOR AN EULER
C  ROTATION WITH POLE (B,C) (DEGREES, POSITIVE NORTH AND
C  EAST) AND ANGLE OF ROTATION D (DEGREES, POSITIVE
C  ANTICLOCKWISE).
C

```

```

      REAL NX,NY,NZ
      DIMENSION A(3,3)
      B=90.-B
      CC=57.2957795
      O=B/CC
      P=C/CC
      Q=D/CC

```





```

C NX = DIRECTION COSINE WITH RESPECT TO X-AXIS
C NY = DIRECTION COSINE WITH RESPECT TO Y-AXIS
C NZ = DIRECTION COSINE WITH RESPECT TO Z-AXIS

```

```

    NX=SIN(O)*COS(P)

```

```

    NY = SIN(O)*SIN(P)

```

```

    NZ = COS(O)

```

```

    A(1,1) = COS(Q)+NX**2*(1-COS(Q))

```

```

    A(1,2) = NX*NY*(1-COS(Q) - NZ*SIN(Q)

```

```

    A(1,3) = NX*NZ*(1-COS(Q)) + NY*SIN(Q)

```

```

    A(2,1) = NX*NY*(1-COS(Q)) + NZ*SIN(Q)

```

```

    A(2,2) = COS(Q) + NY**2*(1 - COS(Q))

```

```

    A(2,3) = NY*NZ*(1-CCS(Q) -NX*SIN(Q)

```

```

    A(3,1) = NZ*NX*(1-COS(Q) -NY*SIN(Q)

```

```

    A(3,2) = NZ*NY*(1-CCS(Q)) +NX*SIN(Q)

```

```

    A(3,3)=COS(Q)+NZ**2*(1-COS(Q))

```

```

    RETURN

```

```

    END

```

```

    SUBROUTINE INVEUI(A,LAT,LON,ROT)

```

```

C    MATRIX A(3,3) IS GIVEN FOR AN EULER ROTATION,
C    THE CORRESPONDING COORDINATES (LAT,LON) FOR
C    THE EULER POLE, AND THE ANGLE OF ROTATION ROT
C    IS CALCULATED. COORDINATES ARE IN DEGREES AND
C    ARE POSITIVE NORTH AND EAST. ANGLE OF ROTATION
C    IS POSITIVE ANTICLOCKWISE.

```

```

    DIMENSION A(3,3),B(3,3)

```

```

    REAL LAT,LON

```

```

    C=57.29579513

```

```

    ROT=(A(1,1)+A(2,2)+A(3,3)-1)/2

```

```

    ROT=ARCOS(ROT)

```

```

    IF(ROT*C.LT.0.11) GO TO 15

```

```

    X=-A(1,3)*(A(2,2-1)+A(1,2)*A(2,3)

```

```

    Y=-A(2,3)*(A(1,1-1)+A(1,3)*A(2,1)

```

```

    Z=(A(1,1-1)*(A(2,2-1)-A(1,2)*A(2,1)

```

```

    XY=SQRT(X**2+Y**2)

```

```

C    TEST IF COLAT=0

```

```

    IF(ABS(X)+ABS(Y).LT.(10E-10)) GO TO 22

```

```

C    TEST IF COLAT=90. RCUND OFF ERRORS PREVENT Z
C    TO BE ZERO AND THE ERROR INCRESE WITH ROT,
C    THEREFORE MULTIPLY BY COS(ROT)

```

```

    IF(ABS(Z)*COS(ROT).LT.(10E-9)) GO TO 20

```

```

    COLAT=ATAN2(XY,Z)

```

```

    LON=ATAN2(Y,X)

```

```

    GO TO 21

```

```

22  CONTINUE
    COLAT=0.0
    LON=0.0

```



```

      GO TO 21
C
C  ALTERNATIV CALCULATION OF COLAT, WHEN COLAT
C  IS CLOSE TO 90
C
20  COLAT=90./C
    LON=ABS (A (1,1-COS (ROT) ) / (1-COS (ROT) )
C
C  TEST IF LON=90
C
    IF (LON.LT.(10E-6) ) LON=0.
    LON=SQRT (LON)
    LON=ARCOS (LON)
C
C  CHECK IF LON IS POSETIVE OR NEGATIVE.
C
    IF (A (1,2) .LT.0.) LCN=-LON
21  CONTINUE
    ROT=ROT*C
    LON=LON*C
    LAT=90.-COLAT*C
C
C  CHECK IF POLE IS ON NORTHEREN OR SOUTHEREN HEMISPHERE.
C
    CALL TESTEU (LAT,LON,ROT,A)
    GO TO 16
15  CONTINUE
    LAT=0.
    LON=0.
    ROT=0.
16  CONTINUE
    RETURN
    END
    SUBROUTINE TESTEU (LAT,LON,ROT,A)
    REAL LAT,LON
    DIMENSION A (3,3) ,B (3,3)
    CALL EUL (LAT,LON,ROT,B)
    LAT=90.-LAT
    DO 1 I=1,3
    DO 1 J=1,3
    F=ABS (A (I,J)-B (I,J) )
    IF (F.GT.0.01) GO TO 2
1  CONTINUE
    GO TO 3
2  CONTINUE
C
C  FLIP POLE TO THE OPPOSITE HEMISPHERE.
C
    LAT=-LAT
    LCN=LON+180.
    IF (LON.GT.180.) LCN=LON-360
3  CONTINUE
    RETURN
    END

```



SUBROUTINE LCIR(LAT, LON, ROT, SLAT, SLON, DIST)

CALCULATION OF THE DISTANCE DIST ALONG A SMALL  
CIRCLE PATH STARTING IN (SLAT, SLON), AND  
DETERMINED BY AN EULER ROTATION WITH POLE  
(LAT, LON) AND ANGLE OF ROTATION ROT (POSE-  
TIVE ANTICLOCKWISE). ALL ANGLES ARE IN  
DEGREES, POSITIVE NORTH AND EAST.

```

REAL LAT, LON
CDN=57.29578
X1=LAT
X2=SLAT
Y1=LON
Y2=SLON
CALL DEL(X1, Y1, X2, Y2, D)
D=D/CDN
DIST=SIN(D)*ROT
RETURN
END

```

SUBROUTINE LOOK(N, PAR, INPUT, OK)

5 ALPHA NUMERICAL PARAMETERS INPUT(1-5) ARE GIVEN.  
THEY ARE COMPARED TO A SET OF N BY 5 PARAMETERS  
PAR(1-5, 1-N), AND IF ONE OF THE N PARAMETER SETS  
PAR(1-5, I) MATCH WITH INPUT(1-5), THE VARIABLE  
OK IS RETURNED WITH THE VALUE 1, OTHERWISE ZERO.  
BLANKS IN A VALUE OF PAR MEANS THAT THAT ELEMENT  
BY DEFAULT IS MATCHED WITH THE CORRESPONDING VALUE  
OF INPUT.

```

INTEGER PAR(5, 100), INPUT(5), OK, ZERO/'  '/
OK=0
DO 3 J=1, N
DO 1 I=1, 5
IF(PAR(I, J).EQ.ZERO) GO TO 1
IF(PAR(I, J).NE.INPUT(I)) GO TO 2
1 CONTINUE
OK=1
GO TO 4
2 CONTINUE
3 CONTINUE
4 CONTINUE
RETURN
END

```

SUBROUTINE LOOK1(N, NNO, ENO, INDEX)

N ARRAY ELEMENTS ENO(I) (FORMAT(A4)) IS SEARCHED





```

C   FOR THE ELEMENT NNO (FORMAT(A4)). IF FOUND, INDEX
C   RETURNS THE INDEX VALUE FROM ENO(I), IF NOT,
C   INDEX=0.
C

```

```

      INTEGER ENO(500)
      INDEX=0
      DO 1 I=1,N
      IF (ENO(I).NE.NNO) GO TO 1
      INDEX=I
      GO TO 2
1     CONTINUE
2     CONTINUE
      RETURN
      END

```

```

      SUBROUTINE LOOK2(N,NNO,NSO,ENO,ESO,INDEX)

```

```

C
C   N ELEMENTS ENO(I) AND ESO(I) ARE COMPARED TO NNO AND
C   NSO RESPECTIVE. IF BOTH FIT, INDEX IS RETURNED WITH
C   THE CORRESPONDING INDEX VALUE OF ENO AND ESO. OTHER-
C   WISE INDEX IS ZERO.
C

```

```

      INTEGER ENO(500),ESC(500)
      INDEX=0
      DO 1 I=1,N
      IF (ENO(I).NE.NNO) GO TO 1
      IF (ESO(I).NE.NSO) GO TO 1
      INDEX=I
      GO TO 2
1     CONTINUE
2     CONTINUE
      RETURN
      END

```

```

      SUBROUTINE LOOK3(PAR,INPUT,OK)

```

```

C
C   5 ALPHA NUMERIC PARAMETERS INPUT(5) IS COMPARED
C   TO ANY COMBINATION OF 5 PARAMETERS PAR(5,N). IF
C   ONE OF THE N COMBINATIONS MATCH THE INPUT(5)
C   COMBINATION, THE RETURN VALUE OF OK IS 1,
C   OTHERWISE 0. BLANKS IN PAR INDICATES ACCEPTANCE BY
C   DEFAULT EXCEPT IN ELEMENTS PAR(I,1).
C

```

```

      INTEGER PAR(5,20),OK,INPUT(5),ZERO/'    '/
      OK=0
      DO 1 I=1,5
      DO 2 J=1,20
      IF (J.GT.1.AND.PAR(I,J).EQ.ZERO) GO TO 1
      IF (INPUT(I).EQ.PAR(I,J).OR.PAR(I,1).EQ.ZERO) GO TO 3
2     CONTINUE

```



```

3      GO TO 1
1      OK=OK+1
      CONTINUE
      IF (OK.LT.5) OK=0
      IF (OK.EQ.5) OK=1
      RETURN
      END

```

```

      SUBROUTINE MATRIX(A,B,C)
C      MULTIPLICATION OF TWO 3-DIMENSIONAL MATRICES,
C      A=B*C
      DIMENSION A(3,3),B(3,3),C(3,3)
      DO 1 N=1,3
      DO 1 M=1,3
      A(N,M)=0.
      DO 1 J=1,3
1      A(N,M)=B(N,J)*C(J,M)+A(N,M)
      CONTINUE
      RETURN
      END

```

```

      SUBROUTINE MELIP(N,LAT1,LON1,LAT2,LON2,F,RDP,DEL,T)
C
C      CALCULATION OF J-B ELLIPTICITY CORRECTION OF MULTIPLE SURFACE
C      REFLECTED PHASES LIKE PPP OR SCS3.
C
C      N: NUMBER OF SURFACE REFLECTIONS, IS ZERO FOR NO REFLECTION.
C      LAT1,LON1,LAT2,LON2: COORDINATES IN RADIANS OF EPICENTER AND STA
C      F: J-B'S ELLIPTICITY TABLE FOR THE CORRESPONDING NON REFLECTED PH
C      LIKE IN THE CASE OF PPP, THE TABLE FOR P. VALUES OF F ARE GIVEN F
C      THE DISTANCES 0,10,20.....180 DEGREES
C      RDP: THE DEPTH OF THE EARTHQUAKE
C      DEL: EPICENTRAL DISTANCE.
C      T: ELLIPTICITY CORRECTION IN SECS.
C
C      SUBROUTINES DIV AND ELIP ARE CALLED. THE REFLECTION POINTS ARE
C      FOUND USING DIV. NO CORRECTION IS MADE FOR DEPTH OF FOCUS. ERRORS
C      HEREBY INTRODUCED ARE OF THE ORDER 0.1S.
C
C
C      REAL LAT1,LON1,LAT2,LON2,LAT(10),F(19),LON(10)
      IF (N.EQ.0) GO TO 1
      CALL DIV(N,2,LAT1,LON1,LAT2,LON2,LAT,LON)
1      C=1.57079
      R=6371.
      EPSO=0.00337
      EPS1=0.00309
      RQUA=R-RDP
      EPSR=RQUA*(EPSO-RDP*(EPSO-EPS1)/1000.)
      THET=C-LAT1

```



```

      H1=EPSR*(0.3333333-(COS(THET))**2)
      H2=0.
      IF(N.EQ.0) GO TO 3
      EPSR=R*EPSO
      DO 2 J=1,N
      THET=C-LAT(J)
2     H2=H2+2*EPSR*(0.3333333-(COS(THET))**2)
3     CONTINUE
      EPSR=R*EPSO
      THET=C-LAT2
      H3=EPSR*(0.3333333-(COS(THET))**2)
      H=H1+H2+H3
      DDEL=DEL/(N+1)
      CALL ELIP(F,H,DDEL,T)
      RETURN
      END

```

```

      SUBROUTINE MUL(NROT,LAT,LON,ROT,A)
C     CALCULATION OF EULERPOLE AND ANGLE OF ROTATION FOR
C     UP TO 10 SETS OF EULERPOLES (LAT(I),LON(I)), AND
C     ANGLES OF ROTATIONS ROT(I). NUMBER OF ROTATIONS IS
C     NROT, AND FIRST ROTATION VALUES MUST BE IN LAT(1),
C     LON(1),ROT(1). ALSO RESULTANT ROTATION MATRIX A(3,3)
C     IS CALCULATED. RESULTS ARE IN LAT(10),LON(10),ROT(10)
C     AND A. ANGLES ARE IN DEGREES AND POSITIVE NORTH,EAST
C     AND CLOCKWISE.
      DIMENSION A(3,3),B(3,3),C(3,3),U(3,3)
      REAL LAT(10),LON(10),ROT(10)
      DO 10 I=1,3
      DO 10 J=1,3
      IF(I.EQ.J) U(I,J)=1.
      IF(I.NE.J) U(I,J)=0.
10     CONTINUE
      X=LAT(1)
      CALL EUL(X,LON(1),RCT(1),B)
      IF(NROT.EQ.1) GO TO 2
      NROT=NROT-1
      DO 1 I=1,NROT
      CALL EUL(LAT(I+1),LON(I+1),ROT(I+1),C)
      CALL MATRIX(A,C,B)
1     CALL MATRIX(B,A,U)
      CALL INVEUL(A,LAT(10),LON(10),ROT(10))
      GO TO 3
2     CALL MATRIX(A,B,U)
      LAT(10)=LAT(1)
      LON(10)=LON(1)
      ROT(10)=ROT(1)
3     CONTINUE
      RETURN
      END

```



SUBROUTINE ROT(LAT,LCN,A)

THE COORDIANTES LATITUDE AND LONGITUDE (LAT,LON,  
POSITIVE NORTH AND EAST, DEGREES) ARE TRANSFORMED  
TO A NEW SET OF COORDIANTES (LAT,LON) USING THE  
TRANSFORMATION MATRIX A.

REAL LAT,LON  
DIMENSION A(3,3),X(3),XX(3)  
C=57.2958  
LAT=(90.-LAT)/C  
LON=LON/C

THE Z AXIS GOES NORTH FROM THE CENTER OF THE EARTH,  
AND THE X AXIS GOES FRMC THE CENTER TO (0,0). XX  
ARE THE DIRECTION COSINES.

XX(1)=SIN(LAT)\*COS(LON)  
XX(2)=SIN(LAT)\*SIN(LON)  
XX(3)=COS(LAT)  
DO 1 I=1,3  
X(I)=0  
DO 2 J=1,3  
DO 2 I=1,3  
X(J)=X(J)+A(J,I)\*XX(I)  
LON=ATAN2(X(2),X(1))\*C  
SQ=SQRT(X(1)\*\*2+X(2)\*\*2)  
LAT=ATAN2(SQ,X(3))\*C  
LAT=90.-LAT  
RETURN  
END

SUBROUTINE SCIR(LAT,LON,ROT,LAT1,LCN1,ROT1,SDEL)

CALCULATION OF RESULTANT ROTATION OF 2 EULER  
ROTATIONS, ONE BEING LAT,LON,ROT AND THE OTHER  
A ROTATION SDEL AROUND THE NORTH POLE. ALL  
ANGLES ARE IN DEGREES AND ANGLE OF ROTATIONS  
ARE POSETIVE ANTICLOCKWISE. COORDINATES  
POSETIVE NORTH AND EAST

REAL LAT,LON,LAT1,LON1  
DIMENSION X(10),Y(10),Z(10),A(3,3)  
X(1)=LAT  
Y(1)=LON  
X(2)=90.  
Y(2)=0.0  
Z(1)=ROT  
Z(2)=SDEL  
N=2  
CALL MUL(N,X,Y,Z,A)  
LAT1=X(10)





```

LON1=Y(10)
ROT1=Z(10)
RETURN
END

```

```

SUBROUTINE SHUF(NF,NEV,NSTA)

```

```

C
C ROUTINE REARRANGES LINES IN A FILE NF.
C

```

```

        DIMENSION T(1000,12),NSTA(50)
        N2=0
        DO 1 I=1,NEV
1      N2=N2+NSTA(I)*3
        REWIND NF
        READ(NF,100)((T(J,I),I=1,12),J=1,N2)
        REWIND NF
        DO 2 M=1,3
        KF=0
        NS=0
        DO 2 K=1,NEV
        KF=KF+NS*3
        NS=NSTA(K)
        DO 2 L=1,NS
2      WRITE(NF,100)(T(L+KF+(M-1)*NS,I),I=1,12)
100    FORMAT(12A4)
        RETURN
        END

```

```

SUBROUTINE SORT(NSYM,NREC,D,DI,M,K)

```

```

C
C SORTING OF NREC SETS OF NUMBERS AFTER SIZE IN
C NSYM GROUPS. D(I) CONTAINS THE BOUNDARIES BETWEEN
C THE GROUPS, DI(I) THE NUMBERS TO BE SORTED, K(I)
C GIVES THE NUMBER OF NUMBERS FALLING IN EACH GROUP,
C AND M(I,J) GIVES THE VHCORRESPONDING ARRAY ELEMENTS
C E.G. M(3,J=1,K(3)) LISTS THE INDICES OF D(I) FALLING
C IN GROUP 3.
C THE NUMBERS IN D(I) MUST BE INCREASING IN SIZE WITH
C I.
C
C

```

```

        DIMENSION D(10),DI(500),K(10),M(10,500)
        NSYM=NSYM-1
        DO 1 I=1,10
1      K(I)=0
        DO 4 J=1,NREC
        DO 2 I=1,NSYM
        IF(D(I).GT.DI(J)) GO TO 3
        GO TO 5
3      K(I)=K(I)+1

```



```

      K1=K(I)
      M(I,K1)=J
      GO TO 4
5     IF(I-NSYM) 2,6,2
6     K(I+1)=K(I+1)+1
      K1=K(I+1)
      M(I+1,K1)=J
2     CONTINUE
4     CONTINUE
      NSYM=NSYM+1
      RETURN
      END

```

```

      SUBROUTINE SPT(KO,K1,N,M)

```

```

C
C   A LINE FILE CONCISTING OF N GROUPS OF DATA WITH M LINES
C   EACH IS REORGANISED SO THE FIRST LINE FROM GROUP 1 IS
C   FOLLOWED BY THE FIRST LINE FROM GROUP 2 ETC.
C   KO IS THE FILE NUMBER FOR INPUT AND OUTPUT.
C   52 CHARACTERS ARE READ FROM EACH LINE.
C   FROM FILE K1 52 CHARACTERS ARE ALSO RESD AND
C   LISTED IN FILE KO, AND IN THE SAME ORDER AS IN K1
C   STARTING IN LINE 1, FORMAT(60X,12A4). SO THE FORMAT
C   OF THE TOTAL LINE OUTPUT IS (13A4,8X,13A4).
C
      DIMENSION K(4000,13),T(20)
      NM=N*M
      REWIND KO
      REWIND K1
      DO 1 I=1,NM
1     READ(KO,100) (K(I,J),J=1,13)
      REWIND KO
      DO 3 J=1,M
      DO 2 I=1,N
      IF(N.LE.20) READ(K1,100) (T(KK),KK=1,13)
      IF(N.GT.20) WRITE(KO,103) (K(J+M*(I-1),L),L=1,13)
2     IF(N.LE.20) WRITE(KO,102) (T(L),L=1,13), (K(J+M*(I-1),KK),KK=1,13)
      WRITE(KO,101)
3     CONTINUE
100    FORMAT(20A4)
101    FORMAT(///)
102    FORMAT(13A4,8X,13A4)
103    FORMAT(60X,13A4)
      RETURN
      END

```

```

      SUBROUTINE TIMEP(NN,JM,LS,SDEL,RDPS,SSDEL,TPS,DTS)
C   SUBROUTINE CALCULATES TIME AND ITS FIRST DERIVATIVE BY
C   INTERPOLATION OF TRAVEL TIME DATA HELD IN MATRIX T.
C   NN = NUMBER OF STATIONS.

```



```

C      JM = NUMBER OF DISTANCE ENTRIES IN TABLE.
C      LS = INITIAL DISTANCE IN TABLE IN DEGREES.
C      SDDDEL = DISTANCE INCREMENT IN TRAVEL TIME TABLE.
C      RDPS = DEPTH OF FOCUS.
C      SSDEL = ARRAY OF NN DISTANCES IN DEGREES.
C      TPS, DTS = INTERPOLATED TIMES AND DERIVATIVES FOR NN STATIONS
C
      DIMENSION SSDEL(200),TPS(200),DTS(200)
      COMMON T(14,201),IDEPS(14)
      N=0
1     N=N+1
      IF(N.GT.NN) RETURN
2     DIST=SSDEL(N)/SSDEL+1.0-FLOAT(LS)
      J=DIST
      MSDEP=RDPS
C     CHECK IF PHASE EXISTS AT DISTANCE CALCULATED.
      IF(JM-J) 15,15,3
3     IF(SSDEL(N-FLOAT(LS))) 15,4,4
4     IF(IDEPS(14-MSDEP) 15,5,5
5     DO 7 M=2,14
C     FIND DEPTH INDEX, I.
      I=M-1
      IF(IDEPS(M-MSDEP) 7,6,6
6     GO TO 8
7     CONTINUE
8     CONTINUE
      IF(T(I,J).EQ.0.) GO TO 15
      IF(T(I+1,J).EQ.0.) GO TO 15
      IF(T(I,J+1).EQ.0.) GO TO 15
      IF(T(I+1,J+1).EQ.0.) GO TO 15
      TDB=T(I+1,J)-T(I,J)
      TDC=T(I+1,J+1)-T(I,J+1)
      D=FLOAT(MSDEP-IDEPS(I))/(FLOAT(IDEPS(I+1)-IDEPS(I)))
      TB=T(I,J)+TDB*D
      TC=T(I,J+1)+TDC*D
      DJ=SSDEL(N-FLOAT(J-1+LS))*SDDDEL
      DS=DJ/SDDDEL
      TPS(N)=TB+(TC-TB)*DS
C     CALCULATE DERIVATIVE OF TIME WITH RESPECT TO DISTANCE.
      IF(J-1) 16,16,9
9     IF(JM-J-1) 16,16,10
10    IF(T(I,J-1)) 16,16,11
11    IF(T(I+1,J-1)) 16,16,12
12    IF(T(I,J+2)) 16,16,13
13    IF(T(I+1,J+2)) 16,16,14
14    TDA=T(I+1,J-1)-T(I,J-1)
      TDD=T(I+1,J+2)-T(I,J+2)
      TA=T(I,J-1)+TDA*D
      TD=T(I,J+2)+TDD*D
      TPR=TA+(TB-TA)*DS
      TPT=TC+(TD-TC)*DS
      DTS(N) = 0.5 * (TPT-TPR) / SDDDEL
      GO TO 17
15    TPS(N) = 0.0

```





```
16 DTS (N) = 0.0
17 GO TO 1
END
```









# REQUEST FOR DUPLICATION

JENS HAVSKOV (author)  
entitled PLATE TECTONICS - - -

[illegible]





**B30207**